Jörg Patrick-Rene Eichmann, BSc

EXPRESSION OF CYTOCHROME P450 VARIANTS: DESIGN, ENZYME PRODUCTION AND ASSESSMENT OF THE CATALYTIC ACTIVITY

MASTER`S THESIS

to achieve the university degree of

Diplom-Ingenieur

Master`s thesis programme: Biotechnology

submitted to

Graz University of Technology

Supervisor

Dr. Anton Glieder

Institute of Molecular Biotechnology

Graz, July 2016

EIDESSTATTLICHE ERKLÄRUNG

Ich erkläre an Eides statt, dass ich die vorliegende Arbeit selbstständig verfasst, andere als die angegebenen Quellen/Hilfsmittel nicht benutzt, und die den benutzten Quellen wörtlich und inhaltlich entnommenen Stellen als solche kenntlich gemacht habe.

Graz, am …… ……..

(Unterschrift)

STATUTORY DECLARATION

I declare that I have authored this thesis independently, that I have not used other than the declared sources/resources, and that I have explicitly marked all materials which has been quoted either literally or by content from the used sources.

Graz, …….. ……..

(Signature)

DANKSAGUNG

Da meine Masterarbeit und mein Studium nun zu Ende sind, ist es an der Zeit, mich bei einigen Menschen zu bedanken:

Als erstes möchte ich meinem Masterarbeitsbetreuer Ao.Univ.Prof. Mag. Dr.rer.nat Anton Glieder Danke sagen für die Möglichkeit und die Chance, in dieses spannende, faszinierende Thema einzutauchen und eine Menge zu lernen. Die Jahre des Studiums, und besonders die Masterarbeit, waren ein prägender Abschnitt meines Lebens und eine wahrlich gute Schule für meine weitere berufliche Zukunft.

Ich danke der Firma bisy für die Finanzierung meiner Masterarbeit.

Ganz besonders bedanke ich mich bei Dipl.-Ing. Astrid Weninger. Du warst während der gesamten Zeit eine super Betreuerin, warst immer für mich da und hattest immer ein offenes Ohr für alle meine Fragen und Probleme. Danke dass du mir während dieser Zeit so geholfen und mich so unterstützt hast.

Ein riesengroßes Dankeschön geht an die gesamte Glieder-Group. Ohne Ausnahme war jeder für mich da und half mir, besonders in den schwierigen Momenten, mit einem guten Rat oder zumindest einem offenen Ohr und aufbauenden Worten. Wir hatten zusammen wirklich eine Menge Spaß, sei es während der Arbeit oder in den Pausen, und ihr alle seid schuld daran, dass ich mich richtig wohl fühlte und ich euch alle vermissen werde.

Ich möchte auch meinen StudienkollegInnen für die gemeinsame aufregende Zeit während meines Studiums danken.

Weiters möchte ich meinen Freunden danken. Danke dass ihr für mich da wart wann immer ich jemanden gebraucht habe und dass ihr es verstanden habt wenn ich aufgrund meines Studiums keine Zeit für euch hatte.

Der allergrößte Dank kommt zum Schluss und dieser gebührt meiner ganzen Familie. Ich kann nicht in Worte fassen wie dankbar ich bin, das ich euch alle habe. Danke Mama und Papa das ihr mir die Möglichkeit gegeben habt zu studieren und für die finanzielle und seelische Unterstützung während meines gesamten Studiums. Immer wenn ich Stress wegen meines Studiums, meiner Masterarbeit oder egal was hatte und nicht so gut drauf war, habt ihr mich alle aufgefangen, abgelenkt, und mir dadurch gezeigt das, egal was passiert, es wichtigere Dinge im Leben gibt. Wir haben in der ganzen Zeit meines Studiums und darüber hinaus viele Höhen und Tiefen erlebt und gemeinsam bewältigt. Die Liebe, das Verständnis, die Ehrlichkeit und die Unterstützung, die jeder von euch mir in jeder Sekunde meines Lebens gegeben hat und gibt, hält mir in stillen Momenten vor Augen dass ich einfach die besten

Eltern und Geschwister auf der Welt habe. DANKE Walter, Inge, Michael, Katja, Thomas und Teresa dass es euch gibt.

ABSTRACT

In today`s era of biotechnology as well as life sciences, the enzyme cytochrome P450 (CYP450) superfamily take up an significant part. Due to their indispensable role in the human organism, the extraordinary broad range of applications for targeted modification of materials as well as the production of a plurality of substances with unique attributes, CYP450 enzymes are a hotspot of research throughout the last 50 years since their discovery. The possible implementation of eco-friendly processes under milder reaction conditions and the efficient catalysis of challenging chemical reactions as C-H bond hydroxylation, S-oxidation, N-dealkylation, N-hydroxylation or the epoxidation of exogenous and endogenous compounds indicate the capabilities and benefits of CYP450 biocatalysts. Direct evolution and rational protein design are performed to improve the catalytic efficiency, the selectivity, the specificity and the protein yield of CYP450s. Artificial enzyme systems, consisting of a CYP450 monooxygenase and an electron shuttle system, connected in a fused or cooperating manner, are generated as a veritable alternative to natural existing variants.

The aim of this Master`s thesis was to generate novel CYP450 mutants of various prokaryotic and lower eukaryotic CYP450 representatives. Based on their diverse substrate specificities, the bifunctional CYP505X from *Aspergillus fumigatus*, CYP505A1 from *Fusarium oxysporum*, CYP153A6 from *Mycobacterium sp.* strain HXN1500 and CYP154E1 from *Thermobifida fusca TM51* were selected and expressed in various prokaryotic and eukaryotic hosts. Therefore, different *Escherichia coli* and *Pichia pastoris* strains were used. Artificial enzyme fusions, which contain a monooxygenase domain directly fused to a reductase domain from different natural occurring CYP450s, were functionally expressed. By using various model substrates and spectrophotometric assays, the protein level and the catalytic activity of the generated constructs were determined. The produced whole-cell biocatalysts follow the long-term goal of generating enzyme systems with a wide range of applications in modification, production and degradation of substances and raw materials. Moreover, eco-friendly benign and mild reaction conditions and processes may improve the environmental sustainability and the economy of production processes.

KURZFASSUNG

Im heutigen Zeitalter der Biotechnologie und Biowissenschaften nehmen das Enzym Cytochrom P450 (CYP450) und seine zahllosen Vertreter einen bedeutsamen Platz ein. Durch seine unverzichtbare Wirkung im menschlichen Organismus, der außergewöhnlich breiten Palette an Anwendungsmöglichkeiten zur gezielten Modifikation von Materialien sowie der Herstellung einer Vielzahl von Produkten mit einzigartigen Eigenschaften, sind CYP450 Enzyme in den vergangenen 50 Jahren seit seiner Entdeckung in das Zentrum von Forschungsarbeiten gerückt. Die mögliche Implementierung umweltfreundlicher Prozesse mit schonenden Reaktionsbedingungen und die effiziente Katalyse anspruchsvoller chemischer Reaktionen wie zum Beispiel die Hydroxylierung nicht-aktivierter C-H Bindungen, S-Oxidation, N-Dealkylierung, N-Hydroxylierung oder die Epoxidierung exogener und endogener Verbindungen lassen die Möglichkeiten und Vorteile von CYP450 als Biokatalysator erkennen. Methoden der gerichteten Evolution und des rationalen Proteindesigns werden eingesetzt um die katalytische Effizienz, die Selektivität, die Spezifität und die Ausbeute zu steigern. Künstliche Enzymsysteme, bestehend aus der CYP450 Monooxygenase und einem Elektronentransport-System, verbunden durch Fusionierung oder auf kooperativer Ebene, haben in unzähligen Forschungsarbeiten ihre Wirksamkeit und ihren Nutzen als potenzielle Alternative zu natürlich vorkommenden Enzymsystemen bewiesen.

Das Ziel dieser Masterarbeit war die Generierung neuartiger CYP450 Mutanten verschiedener prokaryotischer und niederer eukaryotischer CYP450 Vertreter. Das autonom suffiziente CYP505X von *Aspergillus fumigatus*, CYP505A1 von *Fusarium oxysporum*, CYP153A6 von *Mycobacterium sp.* (Stamm HXN1500) sowie CYP154E1 von *Thermofibida fusca TM5* wurden aufgrund ihrer diversen Substratspezifitäten für die geplanten Modifizierungen ausgewählt und in verschiedenen prokaryotischen und eukaryotischen Wirtssystemen exprimiert. Hierfür wurden unterschiedliche *Escherichia coli* und *Pichia pastoris* Stämme genutzt. Künstlich hergestellte Fusionsenzyme, bestehend aus einer Monooxygenase und einer Reduktase verschiedener, natürlich vorkommender CYP450s, wurden funktionsfähig exprimiert. Durch den Einsatz verschiedener Modellsubstrate und anhand spektrophotometrischer Tests wurden die Expressionsfähigkeit sowie die Reaktivität der einzelnen Konstrukte untersucht. Die in dieser Arbeit erzeugten Ganzzell –Biokatalysatoren folgen dem langfristigen Ziel der Generierung von Enzymsystemen mit einem vielfältigen Einsatz in der Modifizierung sowie in der Herstellung und im Abbau von Substanzen und Rohstoffen. Darüber hinaus können umweltfreundlichere Reaktionsbedingungen und Prozesse

die ökologische Nachhaltigkeit und die Wirtschaftlichkeit von Produktionsprozessen verbessern.

Table of Contents

1. INTRODUCTION

1.1. Dawn of cytochrome P450 research

In the 40`s and 50`s of the last century, the world was in a state of transition, owed by the World War II and subsequent political decisions. These changes brought the field of biosciences to a wider audience. Achievements in physics and the construction of military equipment like atomic bombs and air combats had a catalytic effect on the production of instruments, applicable in newly generated fields of research. A series of reactions was set in motion and led to the formation of science institutions and in collaboration with universities to further deepening researches in more unexplored areas (1).

The first serious steps in research in the field of cytochrome P450s (CYPs) began in the early 1940s with oxygenation studies by investigating the metabolism of carcinogens, drugs and steroids. Researchers detected that the key enzyme for the metabolism of xenobiotic substances is located in liver cells. Further it was identified that oxygen together with the cofactor NADPH and a “particulate fraction” of liver cells was required to metabolize aminoazo dyes (2). The occurrence of CYPs was first observed in the late 1950s. In 1959 Ryan et al. demonstrated the effect of CYPs in the metabolism of steroids. They observed that microsomal fractions of bovine adrenal cortex together with atmospheric oxygen and TPNH, an obsolete term for NADPH, catalize the C-21 hydroxylation of progesterone (3). By gassing out a sample of liver microsomes with carbon monoxide (CO), a CO-binding pigment was detected. This pigment had a large absorbance band with its maximum at 450 nm (4). Because of these findings, it was also the first time when the designation P450 had been considered. In 1963, Cooper et al. demonstrated that adrenocortical microsomes harboured cytochrome b_5 and were able to reduce diverse compounds, when the cofactor NADH (β-Nicotinamide adenine dinucleotide-reduced) or NADPH (β-Nicotinamide adenine dinucleotide phosphate-reduced) was present. They also observed that the CO-binding pigment with an absorption maximum at 450 nm, previously described by Klingenberg et al., was in this microsomal fraction (5). Almost at the same time, Sato and Omura published that the pigment, which was found in liver microsomes, was a heme containing protein and had the ability to bind CO and thus showed an absorbance maximum at 450 nm. They designated this pigment as a new cytochrome (6). In 1963, Estabrook et al. determined the first photochemical action spectrum of steroid hydroxylation by the pigment found in microsomes from the adrenal cortex. This achievement was a cornerstone for the proof of the role of CYPs as terminal oxygenase in the reaction of steroid hydroxylation (7). Omura and Sato provided further remarkable studies

regarding the reaction mechanism of CYPs in mammalian systems (8). In 1965, Cooper and coworkers researched in the field of drug metabolism and reactions, catalyzed by rat liver microsomes, by using a photochemical action spectrum (9). Their findings led to evidence of mammalian CYPs as the key component in multiple reactions for metabolizing drugs and xenobiotic compounds. The first bacterial CYP systems, described as a soluble hydroxylase, discovered by Hedegaard and Gunsalus in 1965 (10). They separated a methylene hydroxylase system from *Pseudomonas putida* into three fractions: a hydroxylase (a soluble CYP, nowadays known as CYP101A1), a putidaredoxin reductase and an iron-sulfur protein named putidaredoxin. Furthermore, the role of putidaredoxin as the electron carrier from the reduced cofactor to the putidaredoxin reductase and from the putidaredoxin reductase to the CYP-substrate complex was demonstrated (11). This article was a major contribution in the understanding of bacterial CYPs. The hemeprotein from soil bacterium *P. putida* became a model enzyme for research in the field of metalloporphyrins and is -to the present day- one among only a few CYPs, whose was characterised by X-ray crystallography (12). The ability to hydroxylate the bicyclic monoterpene camphor, led to the designation $P450_{cam}$ (13). With this specific enzyme multiple mutagenesis studies were performed to obtain improved substrate recognition and thereby oxidize a broader range of organic aliphatic or aromatic molecules like polycyclic aromatic hydrocarbons (PAHs) (14). In the mid-1970, smicrosomal and mitochondrial CYPs were purified for the first time. This work paved the way for characterization and identification of various CYP isoforms from different tissues. The next landmark was the determination of the complete amino acid (aa) sequences of various CYP representatives by a (at that time newly implemented) cDNA cloning technique (15). By the sudden increase in sequencing data and the discovery of new CYPs, a systematic classification was demanded. In 1978, Nebert et al. proposed the symbol “CYP” as a designation and abbreviation for the first time (16). By comparing the decrypted aa sequences of animal, bacteria and plants, Gotoh et al. concluded a single ancestral gene that makes the P450 genes forming one super gene family (15). In the 1980s and 1990s, many mammalian CYPs were characterized regarding their molecular mechanisms as well as the mechanism of regulation and expression. The development of high throughput sequencing methods led to the discovery of several CYP genes in microorganism, plants and animals by elucidating their genomes (15).

1.2. Essential nature of CYPs in the human organism

In the course of the human genome project, an international project with the goal to decode the human genome and to develop new technical applications for data acquisition and processing, 57 human genes encoding for CYPs were identified (16). The human genome includes 18 CYP families split into 41 coding subfamilies encoded by 57 genes (17). A variety of human CYPs are responsible for the metabolization of drugs to treat diseases, which affect humans. Enzymes like the human liver CYP1A2, CYP3A4/5, CYP2C9, CYP2C19 or CYP2D6 are responsible for 80% of all drug conversions (18). Drugs like antihistamines or chemotherapeutics, toxins and other xenobiotic compounds migrate to the liver where they are converted by CYPs to a more soluble state for easier elimination. Others are required for the synthesis of compounds that are essential for the physiological state of humans. CYP disfunction can influence biological processes and lead to the genesis of serious diseases. CYP11A1 is responsible for cleavage of cholesterol side chains. The monooxygenase converts cholesterol to the precursor of all steroid hormones, pregnenolone. A lack of CYP11A1 led to minimal or no serum concentration of different steroids and consequently to severe and lethal endocrine disorders (19). The CYP21A2 is a microsomal monooxygenase necessary for biosynthesis of aldosterone and cortisol. These two steroids control the salt and fluid balance in human body as well as the blood sugar level and stress response. Mutations, which can occur through crossover of the two genes for CYP21A1 and CYP21A2, lead to congenital adrenal hyperplasia (20,21). CYP27A1 is a multifunctional mitochondrial monooxygenase with activities in hydroxylation and degradation of bile acid intermediates to bile acid in the liver, and cholesterol hydroxylation. A decreased production of bile acids, the enhanced production of bile acid alcohol and the formation of cholestanol (by the reduction of cholesterol) are consequences of genetic mutations (21). This causes severe diseases like multiple neurological malfunctions or premature atherosclerosis due to steroid deposition in blood vessels and the brain (19). These are just some examples which illustrate the essential role of the CYP superfamily for an intact human organism and the importance of constantly ongoing research in the field of CYPs.

1.3. Diversity, function and structure of the metalloporphyrin cytochrome P450

CYPs are hemeproteins with enzymatic activity. They belong to the enzyme class of oxidoreductases with its EC number 1.X and are part of the subclass of oxygenases, organized to the group of monooxygenases with EC number 1.14. In this class of enzymes, there exists a

further plurality of subclasses (22). The quantity of CYPs within the biosphere is remarkable and they constitute one of the largest enzyme families, designated as a superfamily. More than 18.000 CYPs were found so far and an end is not assessable (23). They are widely distributed all over the world in every domain and occur in nearly every life form, including prokaryotes like archaea and bacteria, lower eukaryotes like fungi and insects and higher eukaryotes like plants and animals (24).

The name cytochrome P450 is composed of several denominations. “Cyto” indicates microsomal vesicle, “chrome” stands for coloured, “P” for pigment and 450 for the specific spectrophotometric absorption peak at 450 nm by gassing out with CO (25). The absorption maximum at 450 nm can be used to determine if a CYP is folded in a biologically active conformation, because only catalytically active enzymes contain a correctly incorporated heme that is needed to bind CO and exhibit a peak at 450 nm. Catalytically inactive enzymes perform a conformational change due to incorrect folding or denaturation events. This leads to the protonation of the cysteine thiolate, which is required for an active CYP. Thus a neutral thiol is coordinated to the heme iron resulting in a Soret band at 420 nm (26).

CYPs are named and arranged into families and subfamilies on the basis of the aa identity. After the abbreviation CYP stands a number, indicating the family. 40% or more aa identity is required to be in the same family. Followed by a letter, that indicates the subfamily, where 55% or more identity is needed. The last differentiation is made through a further number that gives information about a particular gene (13,27). In the majority of cases, the sequence identity is less than 20% between enzymes of different subfamilies (28), while their overall 3D structures are well conserved.

1.3.1. The catalytic cycle

In a catalytic reaction of CYPs, one oxygen atom from a molecule of oxygen (O_2) is transferred to a substrate to generate a hydroxylated product. Monooxygenases count as mixed-function oxygenases due to their ability to reduce the second remaining oxygen atom to a molecule of water (H_2O). Responsible for the oxygenation process is the presence of an iron (Fe^{3+}) atom, which is located in the middle of heme in the centre of the enzyme. This heme is a complex compound, where a Fe^{3+} atom is centred to a porphyrin molecule, forming a plane. In the axial position, this prosthetic group is attached to the surrounding protein structure through a coordination bond with a single cysteine residue. Oxidation and reduction

of the iron atom enables the enzymatic catalysis of a broad variety of reactions. CYPs are able to catalyze a number of diverse chemical reactions like epoxidations, dealkylations, dehalogenations and hydroxylations. They play an important role in the biotransformation of drugs and in the biosynthesis and metabolism of endogenous compounds like bile acids and steroid hormones as described above, but also many other biochemical such as fatty acids, fat-soluble vitamins and eicosanoids and. Furthermore CYPs are involved in the conversion of aromatic compounds, alkanes, terpenes, in the metabolism of chemical carcinogens and the detoxification of xenobiotics and environmentally contaminating chemicals like PAHs and pesticides and in the synthesis of secondary metabolites in plants and insects like antibiotics, toxins, insecticides and transmitting agents (29,30).

Selective oxidation of C-H bonds, through the use of molecular oxygen, is the most important reaction of CYPs. In Figure 1, a typical hydroxylation reaction, catalyzed by CYPs, is shown.

$$R - H + O_2 + NAD(P)H + H^+ \longrightarrow R - OH + H_2O + NAD(P)^+$$

Figure 1: Scheme of a hydroxylation reaction catalyzed by CYPs.

R – H represents an activated or unactivated bond in the substrate. In the resting state of the enzyme, the iron (Fe) atom in the centre of the enzyme is in a ferric (III+) low-spin and hexacoordinated. In the equatorial plane, it is coordinated with a porphyrin IX ring, through connection to the four nitrogen atoms of the tetrapyrrole ring system (scheme in Figure 2). In the axial plane, the iron atom bonded with a cysteine thiolate group from the enzyme and with a molecule of water in a distal position. The linkage of the iron atom to the thiolate group is responsible for the significant Soret band at 450 nm, when the reduced ferrous (II+) form of the enzyme is saturated with CO. When a substrate molecule binds to the active side, the water molecule is displaced and the Fe becomes pentacoordinated and gets a ferric (III+) high-spin character. This twist in spin is a reason for an increased redox potential. An electron is transferred to the ferric heme via a flavoprotein and/or an iron-sulfur redox protein partner from a cofactor NADH or NADPH that results in the reduction to a ferrous (II+) character of the Fe.

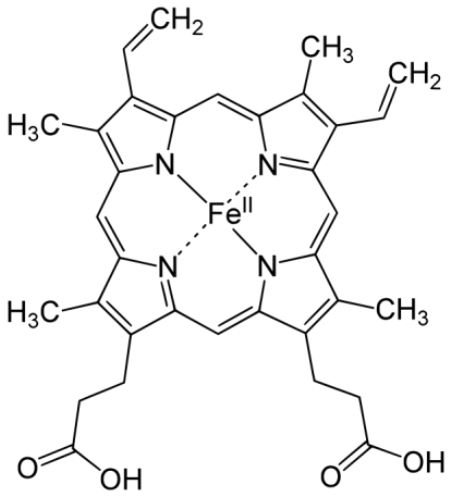

Figure 2: Structure and coordination of a CYP associated heme[1]. The picture shows the arrangement of the heme iron in the equatorial plane.

CYPs cannot receive electrons directly from cofactors and therefore need "shuttle proteins" for the transport of the electrons to the Fe. The use of either NADH or NADPH depends on the nature of the redox system. Through the binding of molecular dioxygen, a ferric (III+) dioxo complex is generated, which is consequently protonated to form a ferric peroxide (III+) complex. However, it may occur that this instable oxy-P450 complex gets separated through the "autoxidation shunt". A reactive superoxide radical (O_2^-) is released with the return of the enzyme to its resting state and the interruption of the catalytic cycle as the consequence (31). A second electron is transferred to the heme and two protons that are necessary for the production of a molecule of water are taken up from bulk solvent via a specific channel in the active site of the enzyme. This leads to the generation of a ferryl-hydroxo (V+) intermediate. The bond between the two oxygen atoms is cleaved, one oxygen is released as a molecule of water and the remaining oxygen atom is incorporated into the R – H bond in the substrate, resulting in the release of a hydroxylated product R – OH and the return of the ferric (III+) hexacoordinated ground state (32). The "peroxide shunt"(S) is an alternative route that skips the conventional catalytic pathway to form directly the ferryl-hydroxo intermediate and oxygenate substrates via a single-oxygen donor e.g. peroxides and hypochlorites (33). The catalytic cycle of a hydroxylation reaction is depicted in Figure 3.

[1] https://en.wikibooks.org/wiki/Structural_Biochemistry/Enzyme/Prosthetic_Group

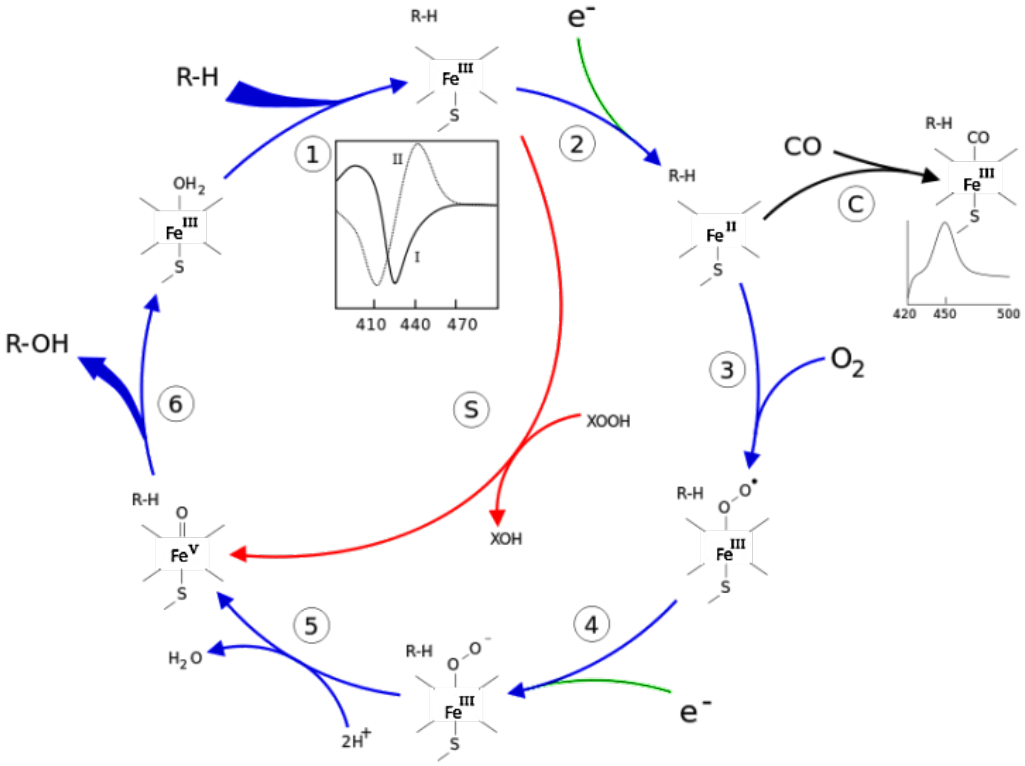

Figure 3: Scheme of the catalytic cycle of a monooxygenase reaction[2]

1.3.2. Structural features of CYPs

CYPs are basically single polypeptides with a size between 40 kDa – 55 kDa. Despite the variability, the basic fold is nearly identical among CYPs, where the primary structure was identified (34). CYPs are made of structural conserved modules, which are essential for function and structure, and more variable areas that determine the individual biochemical properties (35). The ExxR-motif in the K helix is invariant in most CYPs and is involved in structural maintenance, heme binding and stabilization of the core (36). However, unlike initial assumptions that the aa arginine and glutamic acid of the motif are conserved among all domains of life, Rupasinghe et al. revealed that not all CYPs contain this motif. Most probably only the cysteine residue, which connects the prosthetic group to the protein scaffold, is the sole invariant aa (37). A long called I helix runs parallel to the surface of the heme complex and contains residues that interact with substrate and dioxygen. The area around the cysteine (Cys) ligand in the axial plane is highly conserved. This Cys ligand is positioned at the C-terminus of an L helix and is connected to the heme iron through the anionic, thiolate sulphur of the cysteine. This linkage is required to form a responsive redox potential (Figure 4). The conformational flexibility of different helices and loops allows CYPs

[2] http://pfam.xfam.org/family/PF00067

to reshape between a substrate-free (open) and a substrate-bound (close) state. Thus the flexibility is needed to enable structurally dissimilar substrates/products to enter and exit the active site of the enzyme (38).

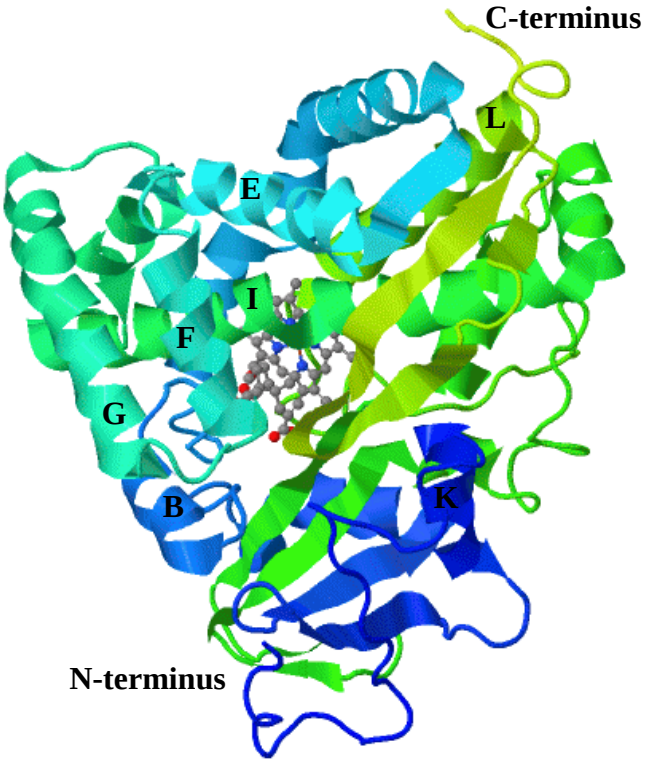

Figure 4: Protein structure of P450cam (taken from PDP (39), accession number: 2CPP). Distal view with secondary structural features labelled according to Asciutto et al. (40)

Significant differences are observed between eukaryotic and prokaryotic CYPs: Eukaryotic CYPs are membrane bound and insoluble, which makes purification more problematic. A nonpolar N-terminal extension anchors eukaryotic CYPs to microsomal or mitochondrial membranes. Whereas some reports state that this N-terminal transmembrane domain has no major impact on the core structure and the enzymatic activity of CYPs (41), other studies indicated the importance of membrane embedded substrate access channel for the acceptance and selectivity for substrate with low solubility in water (42). However, the problems with their purification and expression limit function studies of eukaryotic membrane bound enzymes. Therefore, the first mechanistic, structural and biophysical studies focused on prokaryotic enzymes like CYP101 ($P450_{cam}$) from *P. putida* (34). Prokaryotic CYPs have a major benefit since they are present in a soluble form and located in the cytosol. Nevertheless, it has been shown that it is possible to express also eukaryotic CYP450s in a soluble form: For example the fatty acid hydroxylase CYP505A1 from the fungus *Fusarium oxysporum* (P450foxy) was cloned and expressed in yeast *Saccharomyces cerevisiae* and the recombinant

enzyme was recovered in the soluble portion unlike the native enzyme, which was located in the membrane fraction of the fungal cells (43). In addition human microsomal P450 enzymes can be expressed as enzymatically active soluble enzymes in *E. coli* if their N-terminus is truncated, thereby removing the membrane anchor of these enzymes (44).

Basically, CYPs cannot obtain on their own electrons directly from a cofactor to achieve a reductive activation of dioxygen. One or more partner proteins are needed to shuttle the electrons from the cofactor to the heme centred iron to maintain their catalytic activity. In most of the cases, NADPH serves as the cofactor and reducing agent that supplies electrons. With the discovery of the CYP101 ($P450_{cam}$) in the late 1960s, it was revealed that electrons were transferred from the cofactor NADH via a reductase (putidaredoxin reductase, PdR) containing flavin adenine dinucleotide (FAD) and an iron-sulfur [2Fe-2S] cluster containing protein (putidaredoxin) to the monooxygenase (11). This electron transfer system behaves analogous to a previously discovered mitochondrial adrenal P450 transfer system, consisting of an adrenodoxin reductase (AdR) and an adrenodoxin (Adx) (45).

Hannemann et al. defined ten different classes of CYP systems, consisting of a P450 and its electron transport partner(s), of which class I and class II are the most common (46). Additionally, there exists a variety of unusual CYP systems found in nature (47). Most bacterial three-component systems and most eukaryotic mitochondrial P450 systems, both comprising a P450 monooxygenase, a FAD-containing reductase and an [2Fe-2S] cluster containing ferredoxin, were grouped as class I P450 systems. Electrons are transferred from the cofactor to the ferredoxin via the reductase and the ferredoxin transfers the electrons to the heme complex. Compared to the soluble bacterial systems, in eukaryotic systems only ferredoxin is a soluble protein in the mitochondrial matrix. The reductase and the monooxygenase are bound to the inner mitochondrial membrane. The eukaryotic microsomal CYPs and some bacterial are grouped in class II. These systems have a CPR (Cofactor-cytochrome P450 reductase), containing FAD and flavin mononucleotide (FMN) prosthetic groups, which are responsible to transfer the electrons from the cofactor to the heme. Furthermore, class VIII comprises self-sufficient soluble CYP fusion proteins where a class II-like CPR is fused to the C-terminus of the P450 monooxygenase, making them a single polypeptide. These soluble fusions are expressed as a single protein and act catalytically independent (46). The best known example is CYP102A1 (BM3) from *Bacillus megaterium*. CYP102A1 was the first self-sufficient enzyme that was discovered and is the most

extensively engineered and studied CYP (48). In Figure 5, the most important classes of eukaryotic and prokaryotic CYP systems are summarized.

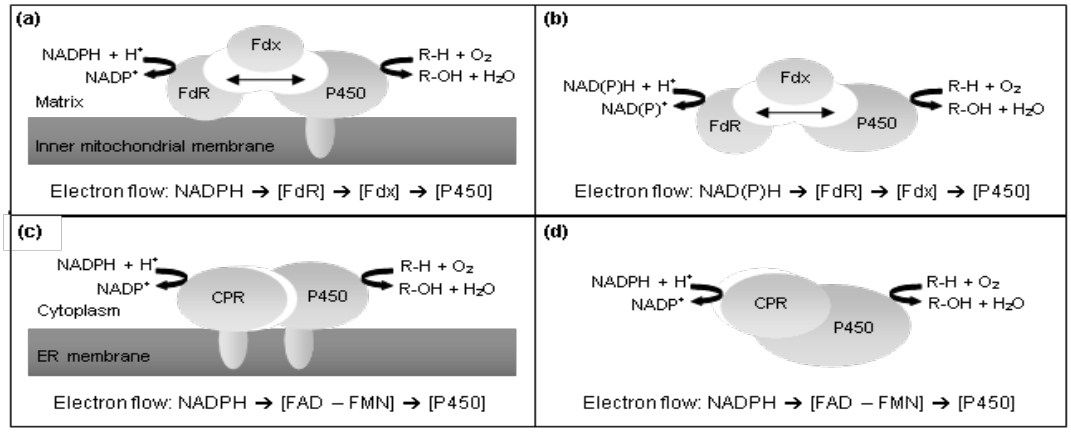

Figure 5: Scheme of the main CYP electron shuttle systems. (a) Eukaryotic mitochondrial class I system, (b) Bacterial soluble class I system, (c) Eukaryotic microsomal class II system, (d) Class VIII system (soluble, catalytically self-sufficient fusion of the Class II system). Taken from (49)

Natural fusion proteins can be discovered and used in various ways. Through protein alignment search by using CYP102A1 (BM3) as a blueprint, Weis et al. discovered nine bacterial and fungal CYPs, where all of them were natural self-sufficient fusion proteins of a monooxygenase and a redox domain. Upon site-directed mutagenesis and selective introduction of mutations based on beneficial positions described for P450 BM3, variants thereof were able to convert the active pharmaceutical ingredients (APIs) diclofenac and chlorzoxazone as observed by human CYPs (50). Self-sufficient natural variants also exist for the bacterial class I type of P450s (51,52). Apart from self-sufficient CYPs, it is feasible to produce fusion proteins artificially to enhance enzyme properties (53,54). In today's biotechnological applications, the fusion of monooxygenase and electron transfer proteins from different organisms is commonly performed. One reason therefore is that the electron transport partners of novel CYP are in many cases not known. Such newly generated artificial systems are often catalytically active and show promising properties. Scheps and coworkers merged the monooxygenase from *Marinobacter aquaeloei* with the reductase domain of CYP102A1 and generated constructs which demonstrated efficient electron coupling, protein expression and conversion of dodecanoic acid with a high regioselectivity (>95%) for the ω-position. Also PFOR from *Rhodococcus ruber* was fused and tested as reductase domain redox partner (55). PFOR is the abbreviation for phthalate family oxygenase reductase and belongs to the phthalate family of oxygenase systems (PFOS). PFOR is named as a member of a novel class of self-sufficient P450s, built by a fusion of a class I monooxygenase with a

PFOR-type (Figure 6). PFOR contains a NADPH-binding domain, a FMN-binding domain and [2Fe-2S] cluster domain (55). Mot and coworkers suggest, that PFOR is the bacterial equivalent to the eukaryotic CPR (51). Furthermore, PFOR displays similarity to the reductase domain of CYP450Rhf from *Rhodococcus sp.* NCIMB 9784. This self-sufficient enzyme comprise an N-terminal P450 domain fused to a reductase domain, containing an FMN-group and a [2Fe-2S] cluster (56). Kulig et al. cloned and expressed 23 CYP450 heme domains from *Rhodococcus jostii* as fusions with the reductase domain of P450Rhf for testing 48 commercially available drugs on hydroxylation and demethylation reactions wherein one recombinant strain catalyzed the N-demethylation of diltiazem and imipramine (57).In spite of the developments in the field of fusion enzymes, the research on multi-component systems is not neglected. Agematu et al. investigated 213 different bacterial CYPs which were co-expressed with PdR and Pdx from *P. putida* for the hydroxylation of testosterone (58). With multi-component systems, the expression ratio of the CYP and its electron transfer partner play an important role to generate highly effective biocatalysts (50). A higher product yield can be obtained by using the CYP in a higher ratio as the redox partner(s) (59). However, it depends entirely which monooxygenase and in particular what type of redox partner system is used.

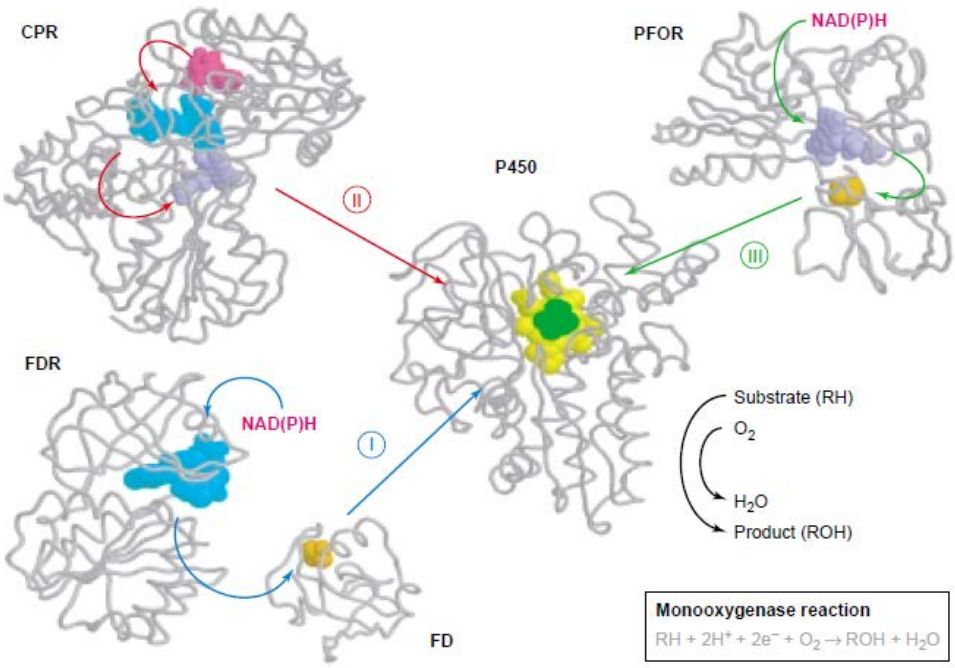

Figure 6: Electron transfer in cytochrome P450 systems. (I) Class I system comprise a monooxygenase, a FAD containing ferredoxin reductase (FDR) and a [2Fe-2S] cluster containing ferredoxin (FD)[NADPH→FAD→[2Fe-2S] →Haem]; (II) Class II system comprise a monooxygenase and a NADPH reductase (CPR)[NADPH→FAD→FMN→Haem]; (III) New (PFOR including) class of self-sufficient CYPs: the monooxygenase domain is fused to PFOR reductase

domain[NADPH→FMN→[2Fe-2S]→Haem]; Haem (yellow), camphor (substrate, green), [2Fe-2S] cluster (orange), FAD (blue), FMN (light purple), NADPH (magenta). Taken from [94]

.

1.4. Introduction to expression hosts and CYPs used in this thesis

1.4.1. Heterologous expression of CYPs

1.4.1.1. *Escherichia coli* BL21 (DE3) and K12 DH5α-T1

CYPs are ubiquitous in each kingdom of life and occur in nearly every organism with relatively few exceptions. One of these is the enteric bacterium *E. coli* (60), which is the best and most studied organism (61). The lack of P450 genes and of homologous CYP expression can be an advantage, when *E. coli* is used as host for heterologous expression of CYP. No background CYP expression facilitates the characterization of the heterologous expressed enzymes (60). Additional advantages for the use of *E. coli* as CYP expression host are its growth on simple and cheap carbon sources, the rapid accumulation of biomass and the possibility to achieve high-cell densities in fermentation processes. Nevertheless, there are also some disadvantages, when using a prokaryotic expression system. *E. coli* lacks post-translational functions, which are needed for recombinant production of eukaryotic proteins. To overcome this restriction, mammalian enzymes e.g. protein acetylases and methylases are co-expressed on the same or separate vectors in *E. coli* (62). Codon bias might cause problems since the available codons are differently utilized in every organism. A heterologous gene with codons that are rarely used in *E. coli* can result in ineffective expression or translation errors (63). Codon optimization and adaption to the bias of the host organism might improve the expression of the heterologous gene. Protein misfolding in the cytoplasm can be reduced by controlling cultivation parameters such as temperature, expression rate or metabolism of the host (63). Furthermore, changing in the growth conditions (C-source, cultivation parameters), the supplementation of heme precursors like biotin or hemin, the co-expression with chaperones or inductive heat/cold shock response could improve expression of CYPs in *E. coli* (30). Using the *E. coli* expression hosts BL21 (DE3) (hereafter called *E. coli* BL21) and K12 DH5α-T1 (hereafter called *E. coli* DH5α-T1) ensures high transformation efficiencies and high-level expression due to lack of intracellular endonucleases and restriction endonucleases (63,64). The genotypic features of the *E. coli* expression hosts BL21 and DH5α-T1 are listed in chapter 3.4.

1.4.1.2. *Pichia pastoris* BSYBG10/BSYBG11 and CBS7435 Wt/MutS

The yeast *P. pastoris* (*Komagataella phaffii*) is one of the main hosts for the production of recombinant proteins (65). The name *P. pastoris* is based on a historic classification. In 2009, through performing rRNA-sequencing, it was enlightened that all biotechnologically used *P.pastoris* strains belong to the closely related yeast species *K. phaffii*. Despite the fact, the established name *P. pastoris* is still used (66). The most commonly used strains for protein expression are derivatives from wild-type strain NRRL-Y11430 (ATCC76273) (67). The *P. pastoris* genome comprises about 9.34 Mbp, including a 35.7 Kbp mitochondrial genome and 5.007 protein coding regions (CDSs) (68). The presence of the strong, methanol-inducible *AOX1* (*alcohol oxidase 1*) promoter made *P. pastoris* a preferred host for heterologous protein expression (65). The enzyme alcohol oxidase 1 (Aox1) catalyzes within the peroxisome the oxidation of methanol to formaldehyde and hydrogen peroxide, the first step in the methanol utilization pathway (MUT, Figure 7). Hydrogen peroxide is degraded to oxygen and water by the enzyme catalase 1 (Cat1, also known as CTA1 in *P. pastoris*). Formaldehyde is processed in two different pathways. In the dissimilative pathway, formaldehyde leaves the peroxisome and is oxidized to carbon dioxide and formate, which is used as energy source for growth on methanol. In the assimilative cyclic pathway, the remaining formaldehyde is used to form cellular constituents (69).

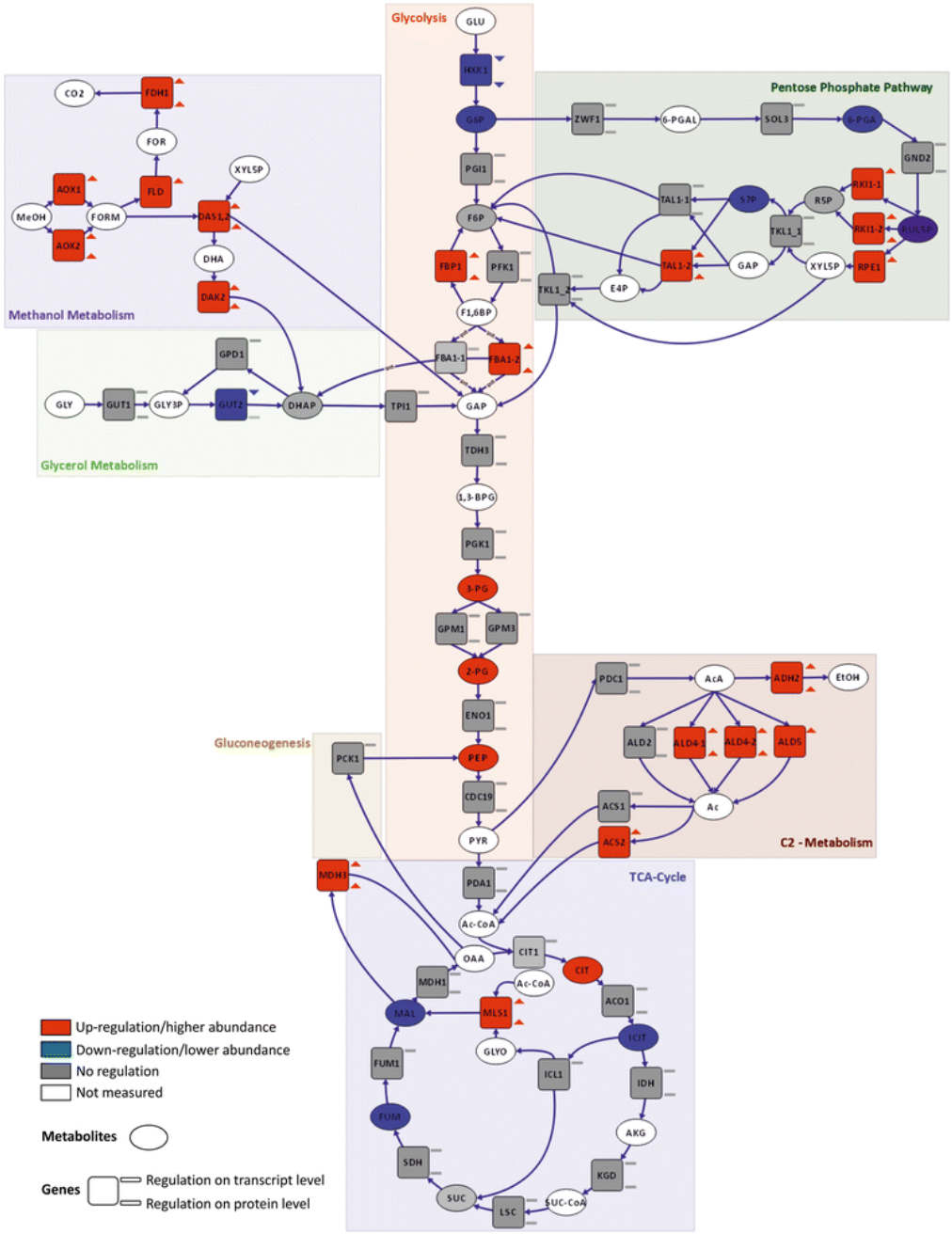

Figure 7: Differential regulation of carbon metabolism. Comparative presentation of methanol- (methanol utilization pathway (MUT)), glycerol- and glucose-grown cells. Description of changes in transcript (square, upper symbol), protein (square, lower symbol), and metabolite (oval) levels. Red: up-regulation on methanol/glycerol; blue: down-regulation on methanol/glycerol; gray: not differentially regulated; white/no symbol: not measured. Taken from (70)

In this thesis, four different *P. pastoris* strains were used for heterologous expression of CYPs. The *P. pastoris* CBS7435 MutS strain is a derivative of the CBS7435 Wt strain. In the MutS strain, the *AOX1* gene is replaced by the full *AOX1* reading frame (71). As a consequence, the Aox2 protein, which is expressed from the weak *AOX2* promoter, is solely responsible for methanol utilization resulting in a reduced growth phenotype on methanol (72). Through weaker methanol utilization, bioprocess management is simplified. Less heat is

produced in a bioreactor and a facilitated cooling system can be used in larger processes. Moreover the slower methanol consumption provides the maintenance of purposeful methanol concentrations for induction. Additional to the CBS7435 strains, *P. pastoris* BSYBG10 (Wt phenotype) and BSYBG11 (MutS) were used which were obtained from BioGrammatics and are owned by bisy e.U. The BSYBG strains are a house strain series from BioGrammatics, Inc., based on BG strains of BioGrammatics. A starting strain BG08 was grown under selective conditions by BioGrammatics to remove cytoplasmic killer plasmids, resulting in BG10 (73). Such killer plasmids are double-stranded plasmid-like particles that code for toxins that are lethal to rivals not carrying the plasmid (74,75). Removal of the killer plasmids resulted in up to 20% less total DNA, facilitating molecular strain engineering and characterization. BG11 was derived from BG10 and similar to the *P. pastoris* CBS7435 MutS strain, the *AOX1* gene was deleted and its enzymatic function taken over by the weaker *AOX2,* resulting in a slower methanol utilization. The BG strains BG20 *pep4Δ*, BG21 *sub2Δ* or BG22Δ *pro1Δ* have deficiencies in the BG10 background, such as the absence of proteases like the vacuolar aspartyl protease or subtilisin that has an impact on the level of posttranslational protein regulation and sporulation (76,77). These strains might further improve heterologous CYP expression (78) but were not tested in this thesis.

1.4.2. CYP102A1 (BM3)

CYP102A1 from *B. megaterium* belongs to the CYP superfamily of heme b-dependent monooxygenases, which exists in al domains of life. The enzyme was discovered at the beginning of the 1970s by Fulco et al. (79). CYP102A1 was the third CYP to be isolated from *B. megaterium*, leading to its characteristic name $P450_{BM3}$. It was identified as a soluble fatty acid hydroxylase (80). Hydroxylation takes place exclusively at sub-terminal positions, a characteristic that is shared with all known natural CYP 102 homologs. Pentadecanoic acids are the preferred saturated straight-chain substrates and the enzyme activity increases or decreases by the chain length (80). The enzyme also converts alcohols, fatty amides and unsaturated fatty acids. CYP102A1 consists of a 55 kDa monooxygenase domain (BMP) fused to a 65 kDa reductase domain (BMR) that exhibits a flavoprotein character by containing FAD and FMN. The size and sequence of the linker, connecting the C-terminal end of the CYP with the N-terminal end of the FMN module within the reductase is very important for the enzymatic function (81). The BMR showed sequence similarity with mammalian CPRs (82). BMP shared sequence and structural similarities with eukaryotic CYPs (83). Besides $P450_{cam}$, CYP102A1 is one of the most studied cytochromes to date and

was the first discovered self-sufficient class VIII CYP (48). Since then, also other self-sufficient CYPs were identified such as the CYP102A1 homolog sub-terminal fatty acid hydroxylase from fungus *F. oxysporum* (84,85). The self-sufficient CYP102A1 was an object for several directed evolution studies and biotechnological applications as alternative redox partner fusions and directed mutagenesis methods (86). Directed mutagenesis comprises the exchange of aa in the P450 sequence to improve the regio- and enantio-selectivity and to increase the selectivity and activity towards new substrates (86). Lewis at el. showed that the conversion of larger substrates including steroids, opiate alkaloids and peralkylated monosaccharides increased upon the combinatorial incorporation of alanine in the enzymes active site (87). Further they demonstrated that the activity, regioselectivity and substrate-specificitiy could be improved by additional rounds of directed evolution (86). Site-directed mutagenesis at positions present in the substrate access channel (R47L, Y51F) enhanced the coupling efficiency and epoxidation rate (88). However, it had been shown that many mutations also led to destabilizing events (Figure 8). This can be disadvantageous, since beneficial mutations might be overseen. In order to prevent this, the previous incorporation of stabilizing mutations into CYP102A1 mutants maintained an efficient folding and ensured its stability leading to an increased success rate in subsequent mutagenesis experiments (86,89).

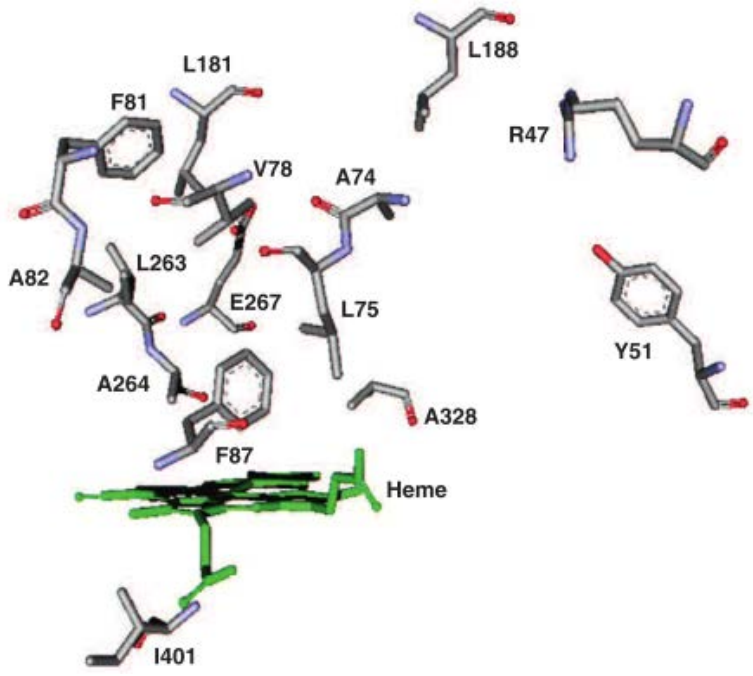

Figure 8: Amino acid residues distal (except I401) to the heme of CYP102A1 (BM3), which influence the substrate specificity and selectivity. Taken from [64]

Countless mutants of CYP102A1 with specific mutations are known and were reported to broaden the substrate specificity (90). It was shown that especially the mutation F87A has an

important influence. By replacement of phenylalanine with alanine at position 87, CYP102A1 turned into a high turnover stereo- and regioselective arachidonic acid epoxigenase. Through its location at the core end of the substrate access channel in direct proximity to the heme above the porphyrin ring, the aa at position 87 has an enormous effect on substrate recognition and on the ability to oxidize fatty acids (91). Furthermore, the performance of the enzyme was increased with multiple mutations e.g. F87V/L188Q, A74G/F87V/L188Q (92) or R47L/Y51F/A264G (93). Engineering BM3 at positions 74, 87 and 188 but also at 47, 51 and 264 led to high active mutants towards PAHs. In addition to the ability of position 87 to influence the substrate affinity of BM3, A74 and L188 form the surface end of the substrate access channel and ensure hydrophobic interaction with the substrates (92). Even R47 and Y51 are positioned at the entrance of the substrate channel and are involved in the recognition of substrates, possible to act as an anchor capable of binding the carboxylate group of substrates. Combining mutations at these positions with mutations at positions at the active side like A264 and F87 resulted in increased activity, NADPH turnover rates and coupling efficiencies toward hazardous PAHs (93).

1.4.3. CYP505X

The fungus *Aspergillus fumigatus* is a life-threatening microorganism through its presence as pathogen as well as allergen. It has a productive conidia formation and thus provides a permanent human health risk. The clinical isolate Af293 contains a 29.4 megabase genome comprising 9.926 genes packed to eight chromosomes (94). The genome, which was sequenced in 2005 (95), comprised 74 CYP genes (96,97). One of these genes codes for the self-sufficient CYP505X.

In 2009 Weis and coworkers described the identification and characterization of a number of bacterial and fungal enzymes including a self-sufficient CYP from *A. fumigatus*. The aa sequence exhibits a 56% similarity and a 36% identity to that of CYP102A1 (BM3). CYP505X turned out to be a class VIII natural self-sufficient enzyme comprising a P450 domain and a CPR domain and to be stable during preparation processes and in presence of higher organic co-solvents (Figure 9). Chaperon coexpression improved the yield of soluble P450 in *E. coli* significantly.

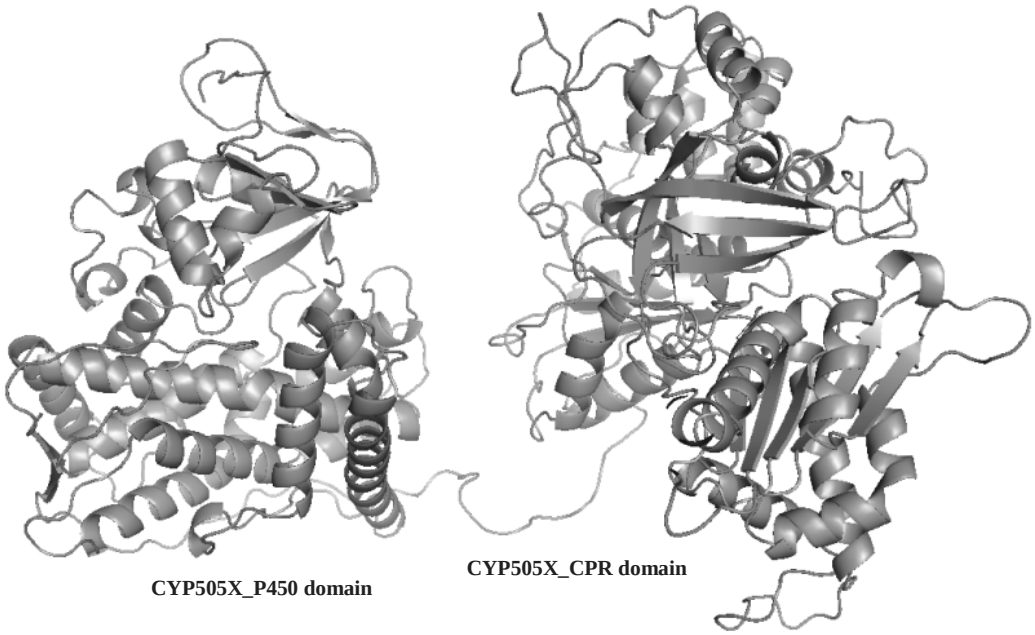

Figure 9: Protein structure model of fusion enzyme CYP505X[3,4]. A linker sequence connects the C-terminal end of the P450 domain with the N-terminal end of the CPR domain.

For the first time, single mutations were embed into the sequence of CYP505X and thus resulting mutants showed a significantly higher catalytic activity towards diclofenac (50). A structure alignment illustrates the structural consistency of BM3 and CYP505X.

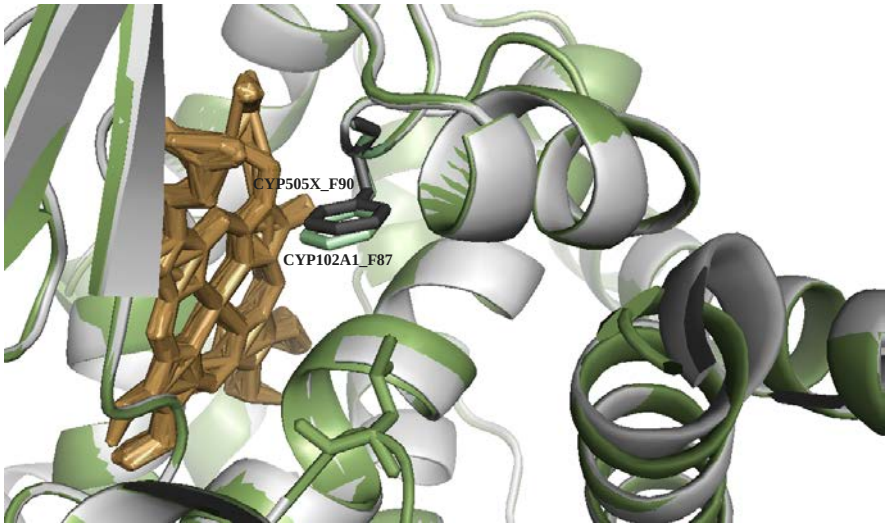

Figure 10: Structure alignment of CYP102A1 (green) and CYP505X (grey) monooxygenase domains[3,4]. Phenylalanine in CYP102A1 (position 87, green) and CYP505X (position 90, Black), Heme complex (brown)

[3] The **PyMOL** Molecular Graphics System

[4] **PHYRE**[2] (Protein structure prediction on the web: a case study using the Phyre server;Kelley LA and Sternberg MJE. Nature Protocols 4, 363 - 371 (2009))

Figure 10 shows that both P450 active sites are equivalent to each other and that the aa positions 87 and 90 in CYP102A1 and *A. fumigatus* CYP505X are located in similar spatial positions.

1.4.4. CYP505A1 (P450foxy)

The filamentous ascomycete *F. oxysporum* belongs to the genus *Fusarium*, whose many different species are one of the most abundant microbes in the soil microflora (98). Some *F. oxysporum* strains are responsible for plant diseases, which is problematic in the agricultural sector, while others have biotechnologically interesting features, e.g. the ability to degrade lignin (99,100). A representative of this genus is *F.oxysporum* MT-811, which harbours a gene that codes for the class II, membrane-bound, fatty acid hydroxylase CYP505A1. It is one of 170 CYP encoding genes found in the species *F. oxysporum* and the first identified self-sufficient fungal P450 (101). CYP505A1 from *F. oxysporum* is also known as P450foxy. The properties of the fungal hydroxylase are similar to the bacterial CYP102A1 from *B. megaterium*. It is a catalytically self-sufficient fusion protein consisting of a monooxygenase and its reductase-domain (85). Like CYP102A1, CYP505A1 is known for sub-terminal hydroxylation of saturated and unsaturated fatty acids (46). CYP505A1 has a 54% similarity and a 36% sequence identity to CYP102A1 (50). It is assumed that CYP fusion proteins have a eukaryotic origin and their presence in prokaryotic genomes is due to horizontal gene transfer (85). Although CYP505A1 is membrane bound in *F. oxysporum*, the enzyme was expressed in a soluble form in the yeast *Saccharomyces cerevisiae*, previously. It was speculated that most probably a post- or co-translational mechanism to bind the protein to the membrane in fungal cells is supressed in yeast cells (43). However, other published data show indicate that at least a significant fraction of the P450 was found in the cell debris and not soluble. Nevertheless, the fact that CYP505A1 is a fusion protein that does not require any additional electron shuttle proteins, makes the enzyme a promising candidate for biotechnological applications employing yeast chassis.

1.4.5. CYP153A6

Mycobacteria are a part of the phylum of actinobacteria and comprise numerous different strains. Severe mammalian diseases like tuberculosis can be triggered by mycobacterial pathogens (102). A mycobacterial representative is the strain HXN1500 from *Mycobacterium*

sp., which harbours an operon in its genome that encodes for the monooxygenase CYP153A6, together with a ferredoxin reductase (FdR) and a ferredoxin (Fdx). CYP153s are soluble monooxygenases, which are able to catalyze a wide range of substrates, including the epoxidation of linear and cyclic compounds and the terminal hydroxylation of alkanes and other alkyl- and alicyclic-substituted substrates (103) unlike most bacterial CYPs that hydroxylate exclusively at sub-terminal positions (83). Such diverse operational possibilities are required in biocatalytic synthesis since these kinds of reactions are difficult or not to handle by organic chemistry. In contrast to BM3, the enzyme CYP153A6 from *Mycobacteria sp.* HXN1500 catalyzes the hydroxylation of medium-length alkanes at the terminal position with an outstanding regiospecificity of more than 95%. A terminal hydroxylation of hydrocarbons is the first step to use these substances as carbon source for cell growth (103,104). Beside medium-chain alkanes CYP153A6 is able to hydroxylate limonene, a monoterpene, to perillyl alcohol, a putative anticancer agent (105,106). It is a class I CYP, consisting as a three-component system. The naturally not self-sufficient monooxygenase-domain generates a catalytically active enzyme through complexing with a ferredoxin reductase and a ferredoxin (107). It is assumed that the transfer from electrons in three-component systems might cause a slowing down of the catalytic activity, compared to self-sufficient CYPs (108). Rather unusual for CYPs is the preferred use of NADH as reducing equivalent (104). Oluwafemi et al. showed that the expression of CYP153A6 can be influenced in a purposeful way by altering different conditions: The enzyme concentration can be increased significantly by changing induction conditions as temperature, the amount of inducer IPTG and by the addition of iron-containing compounds as $FeCl_3*6H_2O$ and δ-ALA (δ-aminolevulinic acid) (109). The CYP153A6 operon can be very well expressed in *E. coli* and with such recombinant E. coli cells for the first time several g/L of octane were hydroxylated at the terminal position by a P450 enzyme (99). Frequently used homologs of CYP153A6 amongst many others are CYP153A7 and A13 and these enzymes were engineered for higher enzyme activity, altered regioselectivity and also fused with reductase domains to render it self-sufficient (50)

1.4.6. CYP154E1

The thermophilic microorganism *Thermofibida fusca* is of versatile interest for technological processes. It is a major plant cell wall degrader and of great use for biotechnological applications. The soil bacterium produces several extracellular enzymes e.g. cellulases and xylanases and is able to remediate agricultural and urban wastes due to its ability to degrade

cellulose and lignocellulose. Because of its high G-C content of 67.5%, it is predestined to endure high temperatures and pH-ranges from 4 to 10. *T. fusca* has a circular 3.642.249 bp (3.6 Mbp) chromosome that encodes for 3.117 proteins (110). The single chromosome includes ten open reading frames encoding for CYPs. These CYPs demonstrate enhanced temperature stability in contrast to enzymes from mesophilic hosts. Thermostability is a sought ability of CYPs and for their use on industrial scale. So far, only a few naturally thermostable CYPs have been reported in literature (111). One of them is CYP154E1 from *T. fusca*. The prokaryotic, soluble monooxygenase is thermostable (T_{50} at 63°C) and capable for hydroxylations of aromatic molecules, fatty acids and acyclic terpenoids. It is a catalyst for the synthesis of precursor molecules for agrochemicals, pharmaceuticals and natural products (64). Since the physiological electron transfer partners have not been identified yet, heterologous, well-known corresponding redox partner are used to accomplish the catalytic activity (112). A favourable redox partner system for the not self-sufficient enzyme consists of the NADH-dependent putidaredoxin reductase (PdR) and the putidaredoxin (Pdx) from *P. putida*. Using this system the regioselective hydroxylation of Grundmanns`s ketone, a building block in chemical synthesis of vitamin D_3 analogues, at position C-25 was performed for the first time (113). Vitamin D_3 and its biologically metabolites are involved and important for the treatment of diseases and metabolic disorders in the human organism (114). Also self-sufficient fusion proteins of CYP154 representatives have been made previously (54).

2. OBJECTIVES

The CYP superfamily is comprised of members with remarkable reactivity and substrate acceptance. CYPs are the most studied drug metabolizing enzymes and used in a vast range of biotechnological processes (86).

The aim of this thesis is the generation of novel eukaryotic and prokaryotic CYPs, well expressed in microbial hosts for whole-cell biocatalysis. The enzymes are able to catalyse reactions, which are difficult to achieve using chemical synthesis and can be used in the biosynthesis and metabolism of endogenous compounds like hormones, vitamins, fatty acids and defensive compounds, the detoxification of xenobiotics like polycyclic aromatic hydrocarbons (PAHs) or pesticides, the conversion of alkanes, APIs, aromatic compounds and more.

In the first part of this thesis, I want to generate end express novel eukaryotic and prokaryotic CYPs. I generate a variety of novel CYP505X mutants from *A. fumigatus* by the substitution of several aa residues located in the CYP505X monooxygenase sequence and express them in the hosts *E. coli* and *P. pastoris*. The selection of the affected target residues based on performed literature search and sequence as well as structural alignment using CYP102A1 from *B. megaterium* as a template. I choose fungal enzyme CYP505A1 from *F. oxysporum* for expression in *P. pastoris* due to its characteristic being a eukaryotic self-sufficient monooxygenase with the ability for ω-1 to ω-3 sub-terminal hydroxylation of saturated and unsaturated fatty acids. I aim to generate artificial fusion constructs with CYP153A6 from *Mycobacterium sp.* strain HXN1500 as well as CYP154E1 from *T. fusca TM51* through alteration of redox partners and creation of self-sufficient enzymes. Therefore, I fuse the monooxygenase from *Mycobacterium sp.* as well as from *T. fusca* to known electron transport systems as well as newer components as the reductase domain from CYP505X from *A. fumigatus* and PFOR from *R. ruber*.

In the second part of this thesis, I want to assess the protein level and the catalytic activity of the newly generated CYPs by using diverse model substrates and spectrophotometric enzyme assays.

3. MATERIAL AND METHODS

3.1. Media, buffer, reagents and chemicals

3.1.1. Cultivation media

BMD 1%: 50 mL/L 10x Dextrose, 200 mL/L 10x PPB, 100 mL/L 10x YNB, 2 mL/L 500x Biotin

BMD 1% + His (V=50mL): 2.5 mL 10x Dextrose, 10 mL 10x PPB, 5 mL 10x YNB, 0.1 mL 500x Biotin, 14.28 mL Histidine

BMM2: 10 mL/L MeOH, 200 mL/L 10x PPB, 100 mL/L 10x YNB, 2 mL/L 500x Biotin

BMM10: 50 mL/L MeOH, 200 mL/L 10x PPB, 100 mL/L 10x YNB, 2 mL/L 500x Biotin

SOC-media: 20 g/L tryptone, 0.58 g/L NaCl, 5 g/L yeast extract, 2 g/L $MgCl_2$, 0.16 g/L KCl, 2.46 g/L $MgSO_4$, 3.46 g/L Dextrose

LB liquid media: 5 g/L yeast extract, 10 g/L tryptone, 5 g/L NaCl

LB agar plates: 5 g/L yeast extract, 10 g/L tryptone, 5 g/L NaCl, 15 g/L bacto agar

TB liquid media: 24 g/L YeastExtract, 12 g/L casein, 4 mL 10% glycerol, 12.5 g/L K_2HPO_4, 2.3 g/L KH_2PO_4, pH 7.2 [K_2HPO_4 and KH_2PO_4 have to be sterilized(filter) separately to the other ingredients due to a complete dissolution of the ions]. Alternatively 50.8 g premixed TB media from Carl Roth, containing 24 g/L yeast extract and 12 g/L tryptone, were dissolved in 1 L H_2O. After adding of 4 mL 10% glycerol the media was sterilized

YPD liquid media: 10 g/L bacto yeast extract, 20 g/L bacto peptone, 100 mL/L 10x Dextrose

YPD agar plates: 10 g/L bacto yeast extract, 20 g/L bacto peptone, 15 g/L agar-agar, 100 mL/L 10x Dextrose

3.1.2. Stock solutions, buffers and reagents

3.1.2.1. Stock solutions

10x YNB: 134 g/L yeast nitrogen base

10x Dextrose: 220 g/L α-D-glucose monohydrate (D)

500x Biotin: 10 mg Biotin dissolved in 50 mL ddH_2O and filter sterilized (ø 0.2 µm).

Histidine: 7 mg Histidine dissolved in 50 mL ddH_2O and filter sterilized (ø 0.2 µm).

BEDS (pH 8.3): 10 mM bicine-NaOH, 3%(v/v) ethylene glycol, 5%(v/v) DMSO. The solution was filter sterilized (ø 0.2 µm).

1 M DTT: 1.54 g DTT dissolved in 10 mL ddH_2O and filter sterilized (ø 0.2 µm).

1 mM DTT: 1 mL/L 1 M DTT diluted with ddH_2O.

70% Ethanol: 70% (v/v) ethanol

60% Glycerol: 600 g/L glycerol

30% Glycerol: 300 g/L glycerol

10% Glycerol: 100 g/L glycerol

Trace Element-solution: 0.5 g/L $MgCl_2$, 30 g/L $FeCl_2*6H_2O$, 1 g/L $ZnCl_2*4H_2O$, 0.2 g/L $CoCl_2*6H_2O$, 1 g/L $NaMoO_4*2H_2O$, 0.5 g/L $CaCl_2*2H_2O$, 1 g/L $CuCl_2$, 0.5 g/L H_3BO_3, 100 mL/L HCl conc(37%), dissolved in ddH_2O and filter sterilized (ø 0.2 µm).

1 M K_2HPO_4: 174.18 g/mol K_2HPO_4 dissolved in ddH_2O.

1 M KH_2PO_4: 136.09 g/mol KH_2PO_4 dissolved in ddH_2O.

1 M NaOH: 40 g/L NaOH dissolved in ddH_2O.

3.1.2.2. Buffers

10x PPB (1 M K_2PO_4 buffer, pH 6.0): 30 g/L K_2HPO_4, 118 g/L KH_2PO_4, the pH was adjusted with concentrated KOH.

1 M PPB (pH 7.4): 802.0 mL/L 1 M K_2HPO_4, 198.0 mL/L 1 M KH_2PO_4

120 mM PPB (pH 7.4): 120 mL 1 M PPB (pH 7.4) diluted with 880 mL ddH_2O.

0.1 M PPB (pH 8.0): 94.0 mL 1 M K_2HPO_4 and 6.0 mL 1 M KH_2PO_4 diluted 1:10 with ddH_2O.

0.1 M PPB (pH 7.4): 100 mL 1 M PPB (pH 7.4) diluted with 900 mL ddH_2O.

0.1 M PPB (pH 7.4) with 20% Glycerol: 66.6 mL/100 mL 120 mM PPB (ph 7.4) mixed with 33,3 mL 60% Glycerol.

0.05 M PPB (pH 7.4): 100 mL 0.1 M PPB (pH 7.4) diluted with 100 mL ddH_2O.

1x MOPS: 50 nM MOPS (3-(N-morpholino)propanesulfonic acid), 50 mM Tris Base, 0.1% SDS, 1 mM EDTA, pH 7.7

50 mM MOPS: 10.5 mg/mL MOPS dissolved in ddH_2O.

50x TAE buffer: 242 g/L TRIS base, 100 mL 0.5 M EDTA, 57.1 mL acetic acid (conc.)

1x TAE buffer: 20 mL/L 50x TAE buffer

1 M HEPES (pH 7.4): 238.30 g/L HEPES, pH was adjusted with sodium hydroxide pellets.

P. pastoris lysis buffer (pH 8.0): 2% Triton X-100; 1% SDS; 100 mM NaCl; 10 mM TRIS-HCl, pH 8; 1 mM EDTA

E. coli lysis buffer: 0.5 µg/mL Lysozyme (551 U/mg), 0.1 µg/mL DNase I (650U/mg), 10 mM $MgCl_2$ dissolved in 0.1 M PPB (ph 8.0).

pNCA assay buffer: 50 mM Tris/HCl, 50 mM PPB (pH 7.4), 0.25 M KCl [1:1:1]

Lysis/Resuspension buffer: 50 mM MOPS, 10% Glycerol, 1 mM DTT, 0,1 mM EDTA, pH 7,4

3.1.2.3. Assay-Reagents

1 M IPTG: 238.3 mg/mL Isopropyl-β-D-thiogalactopyranosid dissolved in ddH_2O and filter sterilized (ø 0.2 µm).

100 mM IPTG: 23.83 mg/mL Isopropyl-β-D-thiogalactopyranosid dissolved in ddH_2O and filter sterilized (ø 0.2 µm).

20 mM IPTG: 4.77 mg/mL Isopropyl-β-D-thiogalactopyranosid dissolved in ddH_2O and filter sterilized (ø 0.2 µm).

1 M 5-aminolevulinic acid: 167.6 mg/mL 5-aminolevulinic acid dissolved in ddH_2O and filter sterilized (ø 0.2 µm).

0.5 M 5-aminolevulinic acid: 83.8 mg/mL 5-aminolevulinic acid dissolved in ddH_2O and filter sterilized (ø 0.2 µm).

1 M Thiamine hydrochloride: 337.3 mg/mL Thiamine hydrochloride dissolved in ddH_2O and filter sterilized (ø 0.2 µm).

0.05 M Thiamine hydrochloride: 16.86 mg/mL Thiamine hydrochloride dissolved in ddH_2O and filter sterilized (ø 0.2 µm).

80 mM KCN: 5.2 mg/mL KCN dissolved in ddH_2O.

1 mM 7-Benzyloxyreosrufin: 10 mg 7-Benzyloxyresorufin dissolved in 33 mL DMSO.

20 µM 7-Benzyloxyresorufin: 1 mM 7-Benzyloxyreosrufin diluted with 0.1 M PPB (pH 7.4).

1 mM MAMC: 6.16 mg MAMC (7-methoxy-4-(aminomethyl)Coumarin) dissolved in 30 mL DMSO.

NADPH regeneration media: 0.2 mM NADPH, 0.3 mM α-D-glucose monohydrate, 0.4 U/mL Glucose-6-phosphate dehydrogenase (G6PD) dissolved in 0.1 M PPB (pH 7.4).

25 mM Lauric acid (sodium dodecanoate): 5.56 mg/mL Sodium laurate dissolved in ddH_2O.

25 mM Myristic acid (sodium myristate): 5.71 mg/mL Myristic acid dissolved in DMSO.

25 mM n-Octane: 2.86 mg/mL octane dissolved in DMSO.

1 mM NADPH: 0.83 mg/mL NADPH dissolved in 0.1 M PPB (pH 8.0).

0.8 mM NADPH: 0.67 mg/mL NADPH dissolved in 0.1 M PPB (pH 8.0).

2 mM BCCE (7-Benzoxy-3-Carboxy-Coumarin Ethyl ester): 0.65 mg/mL BCCE dissolved in DMSO.

15 mM pNCA (p-nitrophenoxycarboxylate): 5.1 mg/mL pNCA dissolved in DMSO.

3.6 mM Polymyxin B sulfate: 5.0 mg/mL Polymyxin B sulfate dissolved in ddH_2O.

Catalase: 46 mg/mL dissolved in ddH_2O.

dNTP mix: 2 mM dATP, 2 mM dTTP, 2 mM dCTP, 2 mM dGTP

3.1.3. Chemicals

Acetic acid (100%)	Carl Roth GmbH, Karlsruhe, Germany
α-D-Glucose-monohydrate (D)	Carl Roth GmbH, Karlsruhe, Germany
Agar-Agar Kobe I	Carl Roth GmbH, Karlsruhe, Germany
Agarose Bioezym	Biozym Biotech Trading GmbH, Vienna, Austria
Ampicillin	Sigma-Aldrich GmbH, Vienna, Austria
Aqua bidest. „Fresenius“	Fresenius Kabi Austria GmbH, Graz, Austria
BactoTM peptone	Becton, Dickinson and Company, Sparks, USA
BactoTM yeast extract	Becton, Dickinson and Company, Sparks, USA
BCCE	Provided by Prof. Dr. Ulrich Schwaneberg, RWTH Aachen University, Germany
Benzonase® Nuclease	Merck Millipore, Darmstadt, Germany
Bicine	Carl Roth GmbH, Karlsruhe, Germany
BugBuster® 10X Protein Extract Reagent	Merck Millipore, Darmstadt, Germany
$CaCl_2*2H_2O$	Carl Roth GmbH, Karlsruhe, Germany
CO_2 (Carbon monoxide)	Linde Gas GmbH, Stadl-Paura, Austria
$CoCl_2*6H_2O$	Carl Roth GmbH, Karlsruhe, Germany
Coomassie brilliant blue staining solution	Bio-Rad Laboratories GesmbH, Vienna, Austria
$CuCl_2$	Carl Roth GmbH, Karlsruhe, Germany
D-Biotin (B)	Carl Roth GmbH, Karlsruhe, Germany
Difco™ yeast nitrogen base w/o AS	Becton, Dickinson and Company, Sparks, USA
DMSO (Dimethyl sulfoxide)	Sigma-Aldrich GmbH, Vienna, Austria
dATP (Deoxyadenosine triphosphate)	Thermo Scientific GmbH, Vienna, Austria
dCTP(Deoxycytidine triphosphate)	Thermo Scientific GmbH, Vienna, Austria

dGTP (Deoxyguanosine triphosphate)	Thermo Scientific GmbH, Vienna, Austria
dTTP (Deoxythymidine triphosphate)	Thermo Scientific GmbH, Vienna, Austria
dNAse I (RNase-free)	Thermo Scientific GmbH, Vienna, Austria
DTT (1,4-Dithiothreitol)	Carl Roth GmbH, Karlsruhe, Germany
EDTA (Ethylenediaminetetraacetic acid)	Carl Roth GmbH, Karlsruhe, Germany
Ethanol absolute	ChemLab NV, Zedelgem, Belgian
Ethidium bromide	Carl Roth GmbH, Karlsruhe, Germany
Ethylene glycol	Carl Roth GmbH, Karlsruhe, Germany
$FeCl_2*6H_2O$	Carl Roth GmbH, Karlsruhe, Germany
Glucose-6-phosphate dehydrogenase	Sigma-Aldrich GmbH, Vienna, Austria
Glycerine (G)	Carl Roth GmbH, Karlsruhe, Germany
HCl (Hydrochloric acid)	Carl Roth GmbH, Karlsruhe, Germany
H_3BO_3	Carl Roth GmbH, Karlsruhe, Germany
HEPES	Carl Roth GmbH, Karlsruhe, Germany
IPTG (Isopropyl-β-D-thiogalactopyranosid)	Carl Roth GmbH, Karlsruhe, Germany
Kanamycin	Carl Roth GmbH, Karlsruhe, Germany
KCl (Potassium chloride)	Carl Roth GmbH, Karlsruhe, Germany
KCN (Potassium cyanide)	Sigma-Aldrich GmbH, Vienna, Austria
KH_2PO_4 (Potassium dihydrogen phosphate)	Carl Roth GmbH, Karlsruhe, Germany
K_2HPO_4(di-Potassium hydrogen phosphate)	Carl Roth GmbH, Karlsruhe, Germany
KOH (Potassium hydroxide)	Carl Roth GmbH, Karlsruhe, Germany
Lauric acid (Sodium dodecanoate)	Sigma-Aldrich GmbH, Vienna, Austria
LB-media (Lysogeny-media)	Carl Roth GmbH, Karlsruhe, Germany

L-Histidine	Sigma-Aldrich GmbH, Vienna, Austria
LDS Sample buffer 4x	Thermo Scientific GmbH, Vienna, Austria
Liquid nitrogen	Air Liquide Austria GmbH, Graz, Austria
Lysozyme (form chicken egg white)	Sigma-Aldrich GmbH, Vienna, Austria
MAMC	BD Biosciences – Discovery Labware, USA
Methanol (≥ 99.8%)	Carl Roth GmbH, Karlsruhe, Germany
$MgCl_2$ (liquid)	Thermo Scientific GmbH, Vienna, Austria
$MgCl_2$ (solid)	Carl Roth GmbH, Karlsruhe, Germany
MOPS	Carl Roth GmbH, Karlsruhe, Germany
Myristic acid (Sodium myristate)	Sigma-Aldrich GmbH, Vienna, Austria
NaCl (Sodium chloride)	Carl Roth GmbH, Karlsruhe, Germany
NADPH	Carl Roth GmbH, Karlsruhe, Germany
$NaMoO_4*2H_2O$	Carl Roth GmbH, Karlsruhe, Germany
NaOAc (Sodium acetate)	Carl Roth GmbH, Karlsruhe, Germany
NaOH (Sodium hydroxide)	Carl Roth GmbH, Karlsruhe, Germany
Nitrogen (N2, liquid)	Linde Gas GmbH, Stadl-Paura, Austria
n-Octane	Sigma-Aldrich GmbH, Vienna, Austria
$Na_2S_2O_4$ (Sodium dithionite)	Sigma-Aldrich GmbH, Vienna, Austria
Palmitic acid (Sodium palmitate)	Carl Roth GmbH, Karlsruhe, Germany
Phenol/chloroform/isoamyl alcohol	Carl Roth GmbH, Karlsruhe, Germany
pNCA (p-nitrophenoxycarboxylate)	Provided by Prof. Dr. Ulrich Schwaneberg, RWTH Aachen University, Germany
Polymyxin B sulfate salt	Sigma-Aldrich GmbH, Vienna, Austria
Sample Reducing Agent 10x	Thermo Scientific GmbH, Vienna, Austria

SDS (Sodium dodecyl sulphate)	Carl Roth GmbH, Karlsruhe, Germany
TB-media (Terrific Broth-media)	Carl Roth GmbH, Karlsruhe, Germany
Thiamine hydrochloride	Sigma-Aldrich GmbH, Vienna, Austria
TRIS	Carl Roth GmbH, Karlsruhe, Germany
Triton X-100	Carl Roth GmbH, Karlsruhe, Germany
Tryptone/peptone	Carl Roth GmbH, Karlsruhe, Germany
Zeocin™	InvivoGen-Eubio, Vienna, Austria
$ZnCl_2$*$4H_2O$	Carl Roth GmbH, Karlsruhe, Germany
5-aminolevulinic acid	Sigma-Aldrich GmbH, Vienna, Austria
6x Mass Ruler DNA Loading Dye	Thermo Scientific GmbH, Vienna, Austria
7-Benzyloxyresorufin	Sigma-Aldrich GmbH, Vienna, Austria

3.1.4. Antibiotics

Ampicillin stock (100 mg/mL):	100 µg/mL for *E. coli*
Kanamycin stock (100 mg/mL):	100 µg/mL for *E. coli*
Zeocin™ stock (100 mg/mL):	100 µg/mL used for *P. pastoris*
	25 µg/mL for *E. coli*

3.1.5. Kits

CloneJET PCR Cloning Kit	Thermo Scientific GmbH, Vienna, Austria
GeneJET Plasmid Miniprep Kit	Thermo Scientific GmbH, Vienna, Austria
GoTaq® qPCR Master Mix	Promega Madison, WI, USA
Pierce™ BCA Protein Assay Kit	Thermo Scientific GmbH, Vienna, Austria
Pierce™ Coomassie (Bradford) Protein Kit	Thermo Scientific GmbH, Vienna, Austria

Pierce™ SDS-PAGE Sample Prep Kit	Thermo Scientific GmbH, Vienna, Austria
Wizard® SV Gel/PCR Clean-Up System	Promega GmbH, Mannheim, Germany

3.2. Devices, instruments and software

The laboratory equipment, all technical devices, software programs and webtools used in this thesis.

3.2.1. Centrifuges and associated materials

Eppendorf Centrifuge 5415 R	Eppendorf AG, Hamburg, Germany
Eppendorf Centrifuge 5415 D	Eppendorf AG, Hamburg, Germany
Eppendorf Centrifuge 5810 R	Eppendorf AG, Hamburg, Germany
Avanti™ centrifuge J-20 XP,	Beckman Coulter™, Inc., Vienna Austria
JA-10 Rotor, Fixed angle,	Beckman Coulter™, Inc., Vienna Austria
JA-25.50 Rotor, Fixed angle,	Beckman Coulter™, Inc., Vienna Austria
VialTweeter Ultrasonic Homogenizer,	Hielscher Ultrasonics GmbH, Teltow, Germany
Nalgene® Labware 30 mL Centrifuge Bottles,	Thermo Scientific GmbH, Vienna, Austria
Nalgene® Labware 500 mL Centrifuge Bottles,	Thermo Scientific GmbH, Vienna, Austria

3.2.2. Shakers and incubators

Binder drying oven	Binder GmbH, Tuttlingen, Germany
Eppendorf Thermomixer comfort (1.5 mL)	Eppendorf AG, Hamburg, Germany
Infors HT Multitron Std. incubator shaker (25 mm)	Infors AG, Bottmingen, Switzerland
Infors HT Orbitron shaker	Infors AG, Bottmingen, Switzerland
Infors HT RS306 rotary shaker (50 mm)	Infors AG, Bottmingen, Switzerland

Titramax 1000 (1,5 mm)	Heidolph Instr., Schwabach, Germany

3.2.3. PCR Cycler

GeneAmp® PCR System 2720 Thermal Cycler	Applied Biosystems, FosterCity, CA, USA

3.2.4. Photometers, platereaders and associated materials

DU 800 Spectrophotometer	Beckman Coulter, Inc., Fullton, CA, USA
Eppendorf BioPhotometer plus	Eppendorf AG, Hamburg, Germany
NanoDrop 2000c Spectrophotometer	Peqlab Biotech GmbH, Polling, Austria
Semi-micro cuvette 10x4x45 mm, Polystyrene	Sarstedt AG & Co., Nümbrecht, Germany
Spectramax Plus 384	Molecular Devices, München, Germany
SynergyMx monochrome Multi-Mode Plate Reader	Biotek Inc., Winooski, United States

3.2.5. Gel electrophoresis, devices and associated materials

3.2.5.1. Agarose gel electrophoresis

Basic (power supply)	Bio-Rad Laboratories, Vienna, Austria
BioImaging Systems Gel HR Camera 6100 Series	UVP®, Cambridge, UK Power Pac™
Biozym LE Agarose/Biozym	Biotech Trading GmbH, Vienna, Austria
Digital printer UP-D897	Sony, Vienna, Austria
GelDoc-It™ Imaging Systems	UVP®, Cambridge, UK
GeneRuler™ 1kb DNA-Ladder	Thermo Scientific GmbH, Vienna, Austria
PowerEase® 500 Power Supply	InvitrogenTM, Lofer, Austria

Sub-cell GT electrophoresis system	Bio-Rad Laboratories, Vienna, Austria
Transilluminator Chroma 43	Vetter GmbH, Germany
Transilluminator Benchtop 2UV	UVP®, Cambridge, UK
6x DNA Loading Dye	Thermo Scientific GmbH, Vienna, Austria

3.2.5.2. SDS-PAGE

Novex® Sharp Prestained Protein Standard	Thermo Scientific GmbH, Vienna, Austria
NuPage® 4-12% Bis-Tris Gel, 1.0 mm x 10 well	Thermo Scientific GmbH, Vienna, Austria
NuPage® 4-12% Bis-Tris Gel, 1.0 mm x 15 well	Thermo Scientific GmbH, Vienna, Austria
NuPage® MOPS SDS Running Buffer (20x)	Thermo Scientific GmbH, Vienna, Austria
NuPage® LDS Sample Buffer (4x)	Thermo Scientific GmbH, Vienna, Austria
PageRuler™ Prestained Protein Standard	Thermo Scientific GmbH, Vienna, Austria
Power Ease 500	Thermo Scientific GmbH, Vienna, Austria
XCell SureLock™	Thermo Scientific GmbH, Vienna, Austria

3.2.5.3. Electroporation materials

Electroporation cuvettes 2 mm	Bridge Bioscience™, Rochester, NY, USA
Gene Pulser™	Bio-Rad Laboratories, Vienna, Austria
Capacitance Extender 1652087	Bio-Rad Laboratories, Vienna, Austria
Pulse Controller P/N 1652098	Bio-Rad Laboratories, Vienna, Austria

3.2.6. Reaction tubes

Microcentrifuge tubes, 1.5 mL with lid	Greiner Bio GmbH, Frickenhausen, Germany
Microcentrifuge tubes, 2.0 mL with lid	Greiner Bio GmbH, Frickenhausen, Germany
PP-Tube, sterile, 15 mL	Greiner Bio GmbH, Frickenhausen, Germany
PP-Tube, sterile, +/- support skirt, 50 mL	Greiner Bio GmbH, Frickenhausen, Germany

3.2.7. Pipettes and pipette tips

Acura® manual 855 multichannel micropipette, 5-50 µl
Socrex Isba SA, Ecublens,Swiss

Biohit Proline® multichannel electronic pipettor, 8 channels, 5-100 µL
Biohit Oyj, Helsinki, Finnland

Biohit Proline® multichannel electronic pipettor, 8 channels, 50-1200 µL
Biohit Oyj, Helsinki, Finnland

Biohit Tips 300 µL Single Tray
Biohit Oyj, Helsinki, Finnland

Biohit Tips 1200 µL Bulk
Biohit Oyj, Helsinki, Finnland

Eppendorf Research® Series 2100 Adjustable Volume, Single Channel Pipette, 0.1-2.5 µL
Eppendorf AG, Hamburg, Germany

Eppendorf Research® Series 2100 Adjustable Volume, Single Channel Pipette, 0.5 -10 µL
Eppendorf AG, Hamburg, Germany

Eppendorf Research® Series 2100 Adjustable Volume, Single Channel Pipette, 2 - 20 µL
Eppendorf AG, Hamburg, Germany

Eppendorf Research® Series 2100 Adjustable Volume, Single Channel Pipette, 20 - 200 µL
Eppendorf AG, Hamburg, Germany

Eppendorf Research® Series 2100 Adjustable Volume, Single Channel Pipette, 100 - 1000 µL
Eppendorf AG, Hamburg, Germany

Pipette tips, micro P10	Greiner Bio-One GmbH, Frickenhausen, Germany
Pipette tips 200	Greiner Bio-One GmbH, Frickenhausen, Germany
Pipette tips 1000	Greiner Bio-One GmbH, Frickenhausen, Germany

3.2.8. Microtiterplates

Bel-Art 96-well Deep Well Plates	Bel-Art Products, Wayne, NJ, United States
Cover for Deep Well Plate	Bel-Art Products, Wayne, NJ, United States
Microplate 96-well, flat bottom, PS	Greiner Bio-One GmbH, Frickenhausen, Germany
MicroAmp® Optical 96-well Plate	Applied Biosystems, Foster City, CA, USA
MicroAmp® Optical Adhesive Covers	Applied Biosystems, Foster City, CA, USA

Nunc™ MicroWell™ 96-well Optical-Bottom Plates with Polymer Base
Thermo Fisher Scientific Inc., Rochester, NY, United States

3.2.9. Other devices and materials

arium® basic ultrapure water system	Sartorius Stedim Biotech GmbH,
Certoclav LVEL 12L	CertoClav GmbH, Traun, Austria
Hamilton® Polyplast lab pH electrode	Sigma-Aldrich GmbH, Vienna, Austria
inoLab® pH720 pH meter	WTW, Weilheim, Germany
Masterflex® L/S™ tubing pump	Cole-Parmer, Barrington, IL, USA
MR 2002 Magnetic Stirrer	Heidolph Instruments, Schwabach, Germany
MR 3000 Magnetic Stirrer	Heidolph Instruments, Schwabach, German
MT PG12001-S DeltaRange Balance	Mettler Toledo Inc., Greifensee, Switzerland
NanoDrop 2000c spectrophotometer	Peqlab Biotechnologie GmbH, Polling, Austria
Sartorius Analytical BL 120S scale	Sartorius Biotech GmbH, Göttingen, Germany
Vortex-Genie 2	Scientific Industries Inc., Bohemia, NY, USA
Rotilabo® syringe filters, CME, sterile, Ø 33 mm, 0.22 µm pore size	Carl Roth GmbH + Co. KG, Karlsruhe, Germany

3.2.10. Software and Webtools

3.2.10.1. Software

Gene Designer 1.1.4.1	DNA2.0 Inc., Menlo Park, CA, USA
CLC Main Workbench 6	QIAGEN N.V., Spoorstraat, Netherlands
7500 System SDS Software	Applied Biosystems, Foster City, USA
Nanodrop 2000	Thermo Scientific
Mendeley Desktop	Mendeley Inc., New York, NY, USA
SnapGene Viewer	GSL Biotech LLC, Chicago, IL, USA
VisionWorks™ LS Analysis Software	UVP®, Cambridge, UK

3.2.10.2. Webtools

ChemicalAbstractService	http://www.cas.org/products/scifinder
DNA sequence converter	http://www.bioinformatics.org/sms/rev_comp.html
DNA2.0	https://www.dna20.com/
EMBOSS 6.3.1: freak	http://mobyle.pasteur.fr/cgi-bin/portal.py#forms::freak
EMBOSS Needle	http://www.ebi.ac.uk/Tools/psa/emboss_needle/
Expasy Compute pI/Mw tool	http://expasy.org/tools/pi_tool.html (02. 03. 2011)
Expasy Translate Tool	http://web.expasy.org/translate/
Integrated DNA Technologies	http://eu.idtdna.com
NCBI PubMed	http://www.ncbi.nlm.nih.gov/pubmed
NCBI BLAST	http://blast.ncbi.nlm.nih.gov/Blast.cgi
OligoAnalyzer 3.1	http://eu.idtdna.com/calc/analyzer
RCSB ProteinDataBase	http://www.rcsb.org/pdb/home/home.do
RNA secondary structure prediction	http://www.genebee.msu.su/services/rna2_reduced.html
PyMOL	http://www.pymol.orf
Phyre2	http://www.sbg.bio.ic.ac.uk/phyre2/html/page.cgi
Swissmodel	http://www.swissmodel.expasy.org/
UniProtKB	http://www.uniprot.org/

3.3. Enzymes

The enzymes used in this thesis were handled according to the manufacturer's recommendations. Unit definitions refer to the respective definition of the producer.

3.3.1. Restriction enzymes

FastDigest *Bam*HI	10 U/µL (5'G^GATCCT3')	Thermo Scientific GmbH, Vienna, Austria

FastDigest *Eco*RI	10 U/µL (5'G^AATTC3')	Thermo Scientific GmbH, Vienna, Austria
FastDigest *Hind*III	10 U/µL (5'A^AGCTT3')	Thermo Scientific GmbH, Vienna, Austria
FastDigest *Not*I	10 U/µL (5'GC^GGCCGC3')	Thermo Scientific GmbH, Vienna, Austria
FastDigest *Sma*I	10 U/µL (5'CCC^GGG3')	Thermo Scientific GmbH, Vienna, Austria
FastDigest *Smi* (*Swa*I)	10 U/µL (5'ATTT^AAAT3')	Thermo Scientific GmbH, Vienna, Austria
FastDigest *Xba*I (*Cfr*9I)	10 U/µL (5'T^CTAGA3')	Thermo Scientific GmbH, Vienna, Austria
FastDigest *Xma*I	10 U/µL (5'C^CCGGG3')	Thermo Scientific GmbH, Vienna, Austria

3.3.2. Other enzymes

Catalase (from Bovine Liver)		Sigma-Aldrich GmbH, Vienna, Austria
FastAP Thermosen Alkaline Phosphatase	1 U/µL	Thermo Scientific GmbH, Vienna, Austria
Taq DNA Polymerase	5 U/µL	Promega GmbH, Mannheim, Germany
GoTaq® Polymerase	5 U/µL	Promega GmbH, Mannheim, Germany
Phusion High Fidelity DNA Polymerase	2 U/mL	Thermo Scientific GmbH, Vienna, Austria
T4 DNA Ligase	5 U/µL	Thermo Scientific GmbH, Vienna, Austria

3.4. Strains and plasmids

3.4.1. *P. pastoris* and *E. coli* strains

All *E. coli* and *P. pastoris* strains used in this thesis are deposited in the culture collection of the institute of molecular biotechnology (IMBT) in Graz, Austria. The used BG strains are designated as BSYBG.

***Escherichia coli* K12 Top 10F'** (IMBT strain collection number: CC1482)

Genotype: *F´(proAB, lacIq, lacZΔM15, Tn10(tet-r)), mcrA, Δ(mrr-hsdRMS mcrBC),Φ80ΔlacZΔM15, ΔlacX74, deoR, recA1, araD139(ara, leu), 7697, galU, galK, λ-, rpsL(streptomycin-r), endA1, nupG;*

***Escherichia coli* BL21 (DE3)** (IMBT strain collection number: CC1481)

Genotype: *F-, ompT, hsdDB(r-b, m-b), dcm, galλ(DE3) = T7 RNA polymerase gene carrying a λ prophage; DE3=lysogen of lDE3, carries a chromosomal copy of the T7 RNA polymerase gene under control of the lacUV5 promoter,*

***Escherichia coli* K12 DH5α-T1** (IMBT strain collection number: CC4689)

Genotype: *F- φ80lacZM15 Δ(lacZYA-argF) U169 recA1 endA1 hsdR17 (rk-, mk+) phoA supE44 thi-1 gyrA96 relA1 phoA tonA*

***Pichia pastoris* BG10** (obtained from BioGrammatics, Inc., Carlsbad California; stored in IMBT strain collection as BSYBG10 with the number: CC7287)

Genotype: *killer plasmid free*

***Pichia pastoris* BG11 (MutS)** (obtained from BioGrammatics, Inc., Carlsbad California; stored in IMBT strain collection as BSYBG11 with the number: CC7288)

Genotype: *killer plasmid free, aox1, AOX1::FLDTT*

***Pichia pastoris* CBS7435 Wt** (IMBT strain collection number: CC3444)

Genotype: *Wild-type*

***Pichia pastoris* CBS7435 MutS** (IMBT strain collection number: CC3445 (65))

Genotype: *aox1, AOX1::FRT*

3.4.2. Control strains from the Institute of Molecular Biotechnology (IMBT) culture collection

The activity of CYPs, which were generated during this thesis, was compared to control strains. The control strains were withdrawn from the culture collection of the IMBT and the culture collection of Thomas Vogl, which is located in the IMBT.

CYP102A1 (BM3) - *Escherichia coli* K12 DH5α-T1 (IMBT strain collection number: CC5098)

Vector: pBM3BamSacEco

Gene designation: CYP450 BM-3 (*Bacillus megaterium*), obtained from Caltech, FH Arnold lab

CYP2D6 - *Pichia pastoris* CBS7435 Wt (Reference to the dissertation of Dr.Thomas Vogl; Strain number: TV318)

Vector: pPpT4_S

Gene designation: pPpT4mutZeoMlyI-intArg4-bidi-HsCYP2D6-HsCPRmutBmrI-pDAS1,2nat-rev

3.4.3. Used vectors during the thesis

pPpB1_S (IMBT collection number: 6075)

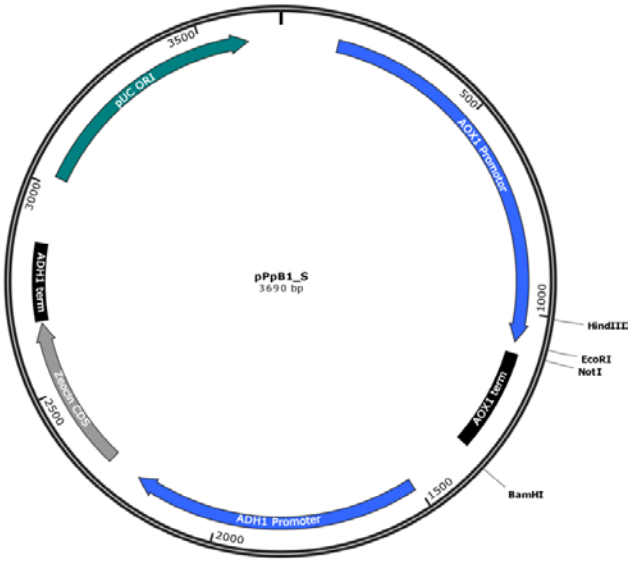

Figure 11: pPpB1_S: *AOX1* promotor, *AOX1* term: *AOX1* transcription terminator, *ADH1* promotor: alcohol dehydrogenase 1 promotor, Zeocin CDS: Zeocin^{TM} resistance gene, *ADH1* term: alcohol dehydrogenase 1 transcription terminator, pUC ORI: pUC origin of replication

pPpT4_S (IMBT collection number: 6070)

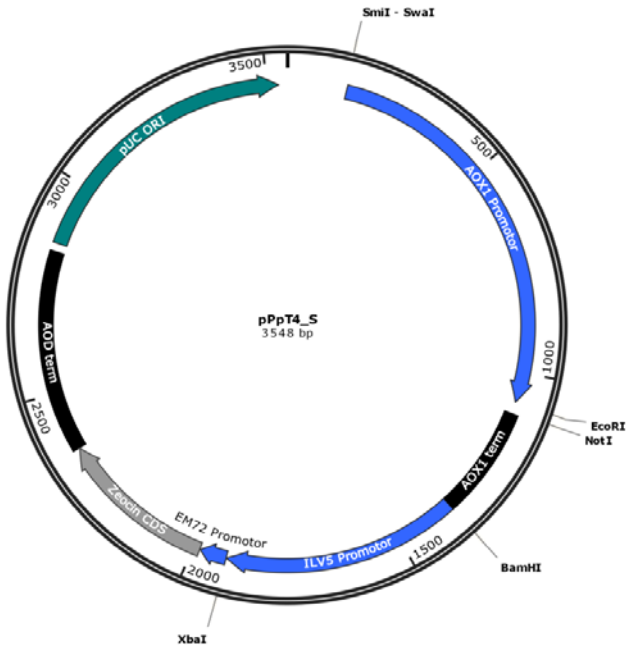

Figure 12: pPpT4_S: *AOX1* promotor, *AOX1* term: *AOX1* transcription terminator, *ILV5* promotor: eukaryotic promotor, *EM72* promotor: synthetic prokaryotic promotor, Zeocin CDS: Zeocin^{TM} resistance gene, *AOD* term: *AOD* transcription terminator, pUC ORI: pUC origin of replication

pMS470Δ8 (IMBT collection number: 993)

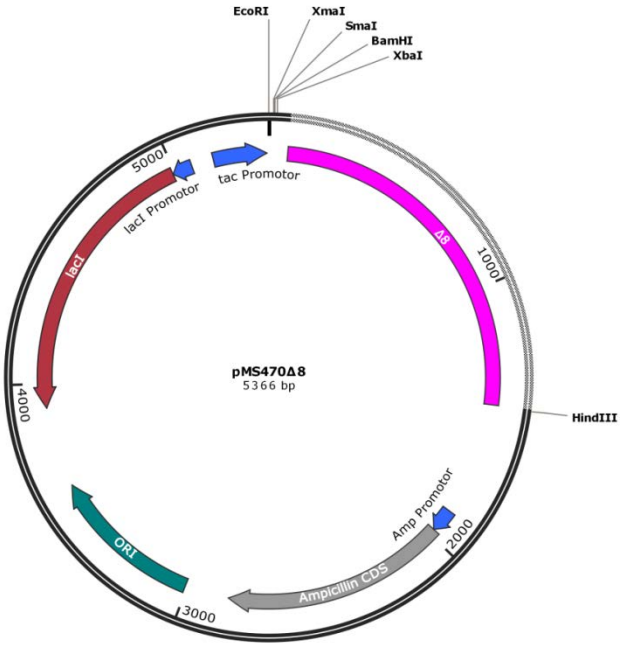

Figure 13: pMS470Δ8: Δ8: stuffer fragment, Amp promotor: Ampicillin promotor, Ampicillin CDS: Ampicillin resistance cassette, ORI: origin of replication, *lacI*: lac repressor gene, *lacI* promotor: *lac*-promotor (*lac*-operon), *tac* promotor

pD441-SR [CYP153A6-M1] (ordered from DNA2.0, Gene ID: 196392)

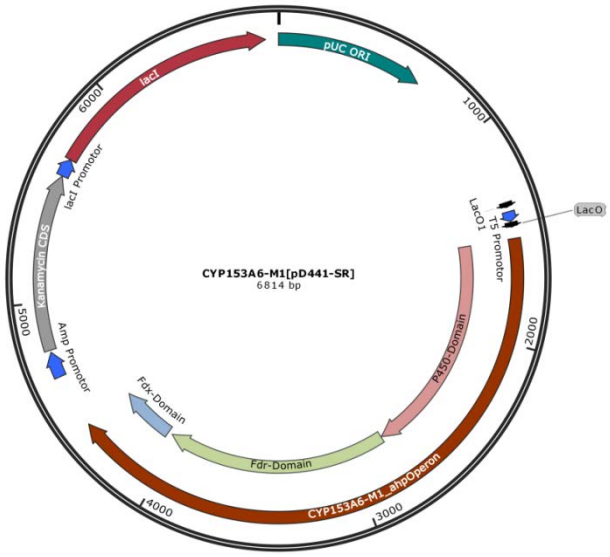

Figure 14: CYP153A6-M1 in the vector pD441-SR: pUC ORI: pUC origin of replication, *LacO1*/*lacO*: regulatory genes of the lac operon, *T5* promotor, CYP153A6-M1_ahpOperon, P450-domain: monooxygenase (1260bp), *FdR*-domain: *ferredoxin reductase* (1272bp), *Fdx*-domain: *ferredoxin* (318bp), Amp promotor: Ampicillin promotor, Kanamycin CDS: Kanamycin resistance cassette, *lacI* promotor: *lac*-promotor (*lac*-operon), *lacI*: *lac*-repressor (regulatory gene)

3.5. Protocols and methods

3.5.1. Transformation and preparation protocols

3.5.1.1. Preparation of *Escherichia coli* BL21 and DH5α-T1 competent cells

Single colonies of the *E. coli* strains BL21 and DH5α-T1 were inoculated into 1 L baffled-flasks filled with 300 mL LB liquid media and grown overnight at 37°C and 200 rpm. The next day, the optical density of the precultures at 600 nm was determined and 4 mL of each preculture were used to inoculate 400 mL LB-media filled in baffled-flasks, and the main culture was grown for 2-3 hours to an A_{600} of 0.7-0.8. The main cultures were then filled in chilled, sterile centrifuge bottles and incubated for 30 minutes on ice. Cooling the cells on ice during the whole procedure is important for the transformation efficiency of the competent cells. The cultures were then centrifuged at 2000 x g for 15 minutes at 4°C. The supernatant was discarded and the cell pellets were resuspended in 500 mL chilled (0-4°C), sterile water. This step was repeated twice. After the third centrifugation step at 2000 x g for 15 minutes at 4°C, the water was decanted and the cells were resuspended in 50 mL sterile, cooled 10% glycerol (0-4°C). A last centrifugation step at 4000 x g for 15 minutes at 4°C was done, the supernatant was decanted and the pellets were resuspended in 3 mL 10% glycerol. 80 µL of the various cell suspensions were aliquoted in sterile 1.5 mL tubes, shock frozen in a liquid N_2-bath and stored at -80°C.

3.5.1.2. Transformation of *E. coli* BL21, DH5α-T1 and TOP10 competent cells

E. coli Top10F` electrocompetent cells were prepared according to Seidman et al. (107). Approximately 2 µL of circular DNA (from an assembly cloning, a ligation reaction or a plasmid preparation) and 40 µL of competent cells were mixed, transferred into a precooled electroporation cuvette and incubated for approximately five minutes on ice. Afterwards the transformation was performed and the cells were pulsed with 2.5 kV, 200 Ω and 25 µF using the Bio-Rad Gene Pulse System. 1 mL SOC-media was added and the cells were regenerated at 37°C and 600 rpm for 45 minutes. After that regeneration step the cell suspension was plated out on LB agar plates supplemented with antibiotics and incubated at 37°C overnight.

3.5.1.3. Preparation and transformation of electrocompetent *Pichia pastoris* BSYBG10, BSYBG11, CBS7435 Wt and CBS7435 MutS

The preparation and transformation of *P. pastoris* strains CBS7435 Wt, CBS7435 MutS, BSYBG10 and BSYBG11 was done as described by Lin-Cereghino et al. (108). The *P. pastoris* strains were grown overnight in 30 mL YPD liquid media at 28°C and 100 rpm. The next day, the precultures were normalized to a starting OD_{600} of 0.15-0.2 in a volume of 50 mL and were grown to an OD_{600} of 0.8-1.0 for 4-5 hours. The cultures were then centrifuged at 500 x g and 4°C for 5 minutes. The supernatants were decanted and a 9 mL ice-cold BEDS solution, supplemented with 1 mL DTT, was used to resuspend the pellets. Then, the suspensions were shaken for 5 minutes with the hands to become warm to the touch. Again a centrifugation step was performed with the same setting as be described before, the supernatants were discarded and the pellets were resuspended in 1 mL BEDS. After that the cells were directly used for a transformation.

The amount of DNA added to the competent cells depends on the size of the fragment and the copy number. Approximately 3-4 µg of linearized DNA and 80 µL of the competent cells were mixed in an electroporation cuvette and incubated for 5 minutes on ice. The transformation was carried out with a Bio-rad Gene Pulse System using 2.0 kV, 200 Ω and 25 µF. 500 µL 1 M sorbitol and 500 µL YPD were added for resuspension and then the cells were incubated for 2 hours at 90 rpm and 28°C to regenerate. Then the transformants were plated out on YPD agar plates supplemented with the antibiotics and incubated for two days at 28°C.

3.5.2. DNA isolation from *E. coli* (Plasmid minilysate preparation)

The isolation of vector DNA was performed with the GeneJET Plasmid Miniprep Kit. Cells material was streaked out on an LB agar plates supplemented with antibiotics, and incubated overnight at 37°C. Then cell material was abraded from the plate with a toothpick and handled according to the manufacturer's recommendation with the following deviations: After washing the column with the washing solution, a drying step at 37°C was performed for 10 minutes to increase the plasmid yield. Plasmid elution was done with 35 µL ddH_2O. The plasmid DNA was either directly used or stored at -20°C.

3.5.3. DNA purification

DNA purification was performed after DNA restriction, PCR reactions or preparative agarose gel electrophoresis through the Wizard® SV Gel and PCR Clean-Up System.

The elution step was performed with 35 µL ddH_2O.

3.5.4. Restriction endonuclease reactions

The used restriction enzymes were obtained either from Fisher Scientific or NEB (New EngIand Biolabs). As in the manufacturer's guideline, 1 µL enzyme was used to digest 1 µg of DNA. Digest reactions performed with Fisher Scientific FastDigest enzymes were incubated at 37°C for 1 hour. Digest reactions performed with common Fisher Scientific and NEB enzymes were incubated overnight and enzyme inactivation was done according to the manufacturer's guidelines. In Table 1, a typical reaction mixture is shown.

Table 1: Reaction mixture for a restriction endonuclease reaction

10x reaction buffer	10 µL
DNA	x µL
Restriction enzyme	1 µL
ddH_2O	up to 20 µL

3.5.5. Ligation reactions and assembly cloning

Ligation reactions were performed with a T4 DNA ligase according to the manufacturer's guideline. 50 ng of vector backbone DNA and insert DNA equivalent to a molar ratio of 1:3 were used. The reaction was incubated at room temperature for 10-20 minutes. Afterwards the ligase was heat inactivated at 65°C for ten minutes or at 70°C for five minutes. 2-4 µL of the ligase reaction mixture were used for further transformation. In Table 2, a general ligation mixture is shown.

Table 2: Reaction mixture for a ligation reaction

2x reaction buffer	10 µL
Digestion fragment / PCR product	x µL
pJET1.2 blunt cloning vector or linearized vector DNA(50 ng/µL)	1µL
T4 DNA ligase	1 µL
ddH2O	up to 20 µL

For assembly cloning, performed according to Gibson et al. (109), 50 ng of vector DNA, insert DNA in an equimolar ratio and ddH_2O to a total volume of 5 µL were mixed and added to 15 µL of an assembly master mix. The reaction mixture was incubated at 50°C for one hour.

2-4 µL of the reaction mixture were used for the *E. coli* transformation. The whole procedure was performed on ice. It was possible to assemble up to five fragments.

3.5.6. pJET1.2/blunt vector cloning

To clone DNA fragments, gBlocks and PCR products into the pJET 1.2/blunt cloning vector, the CloneJET PCR Cloning Kit was used according to the manufacturer's guideline. The ligation mix was incubated for 15 minutes at room temperature. 2-4 µL of the mix together with 40 µl of electrocompetent *E. coli* cells were used for the transformations. In Table 3, a pJET cloning mixture is shown.

Table 3: Reaction mixture for pJET1.2/blunt vector cloning

2x reaction buffer	10 µL
DNA fragment, gBlock or PCR product	1 µL
pJET 1.2/blunt cloning vector	1 µL
T4 DNA ligase	1 µL
ddH2O	up to 20 µL

3.5.7. Preparation of *E. coli* and *P. pastoris* glycerol stocks

Overnight cultures (ONCs) of the *E. coli* and *P. pastoris* strains were grown in 50 mL tubes at 100 rpm and 37°C or 30°C, respectively. 500 µL of the cultures were pipetted in cryogenic tubes with 500 µL of 40% glycerol to obtain a final concentration of 20%. Through this method, the strains can be stored over a long time period at -80°C.

3.5.8. PCR procedures

The polymerase chain reaction (PCR) was used to amplify DNA fragments.

3.5.8.1. Standard PCR

Standard PCR reactions were accomplished with a Phusion High Fidelity DNA polymerase. 25-50 ng of vector DNA were used together with 0.5 µM of each fw- and rev-primer and dNTPs to a final concentration of 2 mM. The other reaction components were added according to the manufacturer's guideline. Instead of HF buffer also a GC buffer can be used, if the fragment has a high GC-content. A standard reaction mixture is listed in Table 4.

Table 4: A standard reaction mixture for PCR

5x Phusion HF or GC buffer	10 µL
2mM dNTP	5 µL
Forward primer (0.5µM)	2.5 µL
Reverse primer(0.5µM)	2.5 µL
Template DNA	x µL
Phusion DNA polymerase (2 U/ µL)	0.5 µL
ddH_2O	up to 50 µL

The PCR reaction conditions were chosen depended on the length of the PCR product, the melting temperature of the primers and the requirements of the polymerase. The operation capacity of the Phusion DNA polymerase is stated to be 1 kb per 10 - 30 seconds elongation time. If the PCR products were larger than 3 kb an elongation time of one minute per kbp was used. The annealing temperature of the PCR was chosen 2°C below the melting temperature of the primers. If no or only a low amount of the PCR fragment was obtained, the annealing temperature was altered between 58°C, 62°C and 70°C to increase the PCR yield. In Table 5, a standard PCR time profile is depicted.

Table 5: A standard PCR time profile used for the Phusion polymerase (purchased from Thermo Scientific)

Initial denaturation	98°C – 30 sec	
Denaturation	98°C – 10 sec	25 – 35 cycles
Annealing	58°C – 20 sec	
Elongation	72°C – 10-30 sec/kb	
Final elongation	72°C – 5 min	
Holding	4°C - ∞	

3.5.8.2. ColonyPCR (cPCR)

ColonyPCR was used to screen *E. coli* single colonies for the presence of an inserted DNA fragment. For this type of PCR, the GoTaq DNA polymerase (Promega) was used. Single colonies from transformation plates were picked with a pipette tip and mixed with a prepared reaction mix (depicted in Table 6). The initial denaturation temperature time was set to five minutes to break up the cell walls (Table 7). The obtained PCR product was separated in a 1% control agarose gel to get information about a correct uptake and size of the DNA fragment. In case a correct band for the insert was obtained, the *E. coli* single colony was streaked out for plasmid isolation (Miniprep) and for further proceedings.

Table 6: cPCR reaction mixture

5 x green GoTaq flexi buffer	10 µl
25mM $MgCl_2$	5 µL
2mM dNTP	5 µL
Forward primer (0.5µM)	2.5 µL
Reverse primer(0.5µM)	2.5 µL
Template DNA	0 µL
GoTag flexi DNA polymerase	0.8 µL
ddH_2O	up to 50 µL

Table 7: cPCR time profile

Initial denaturation	95°C – 5 min	
Denaturation	95°C – 15 sec	25 cycles
Annealing	58°C – 20 sec	
Elongation	72°C – 1 min/kb	
Final elongation	72°C – 5 min	
Holding	4°C - ∞	

3.5.8.3. Overlap extension-PCR (oe-PCR)

Overlap extension PCR (oe-PCR) was used to fuse linear fragments like gBlocks or PCR products. It is a 2-step process (Table 8, Table 9). In the 1st PCR step, no external primers were used to generate an oe-PCR template fragment, since the overlapping regions of the templates act as primers themselves. In the 2nd step, primers were added to amplify the DNA template fragment. The oe-PCR was performed with a Phusion High Fidelity DNA polymerase. In the 1st step 10 ng of the largest fragment and the other fragments in an equimolar ratio were used in a total volume of 25 µL. In the 2nd step buffer, dNTPs, polymerase and 0.5µM fw – and rev-primer were added.

Table 8: oe-PCR reaction mixture

Components	**1st step**	**2nd step**
5x Phusion HF or GC buffer	5 µL	5 µL
2mM dNTP	2.5 µL	2.5 µL
Forward primer (0.5µM)	-	2.5 µL
Reverse primer(0.5µM)	-	2.5 µL
Template fragment 1	x µL	-
Template fragment 2	x µL	-
Phusion DNA polymerase (2 U/ µL)	0.3 µL	0.3 µL
ddH_2O	up to 25 µL	up to 25 µL

Table 9: oe-PCR time profile

Conditions	1st step		2nd step	
Initial denaturation	98°C – 30 sec		98°C – 30 sec	
Denaturation	98°C – 10 sec	25 cycles	98°C – 10 sec	20 cycles
Annealing	60°C – 20 sec		60°C – 20 sec	
Elongation	72°C – 10-30 sec/kb		72°C – 10-30 sec/kb	
Final elongation	72°C – 5-10 min		72°C – 5-10 min	
Holding	4°C - ∞		4°C - ∞	

3.5.9. Micro-scale cultivation in 96-deep well plates (DWP) of *E. coli* expressing CYPs under the control of P_{T5} or P_{tac}

In order to screen randomly chosen *E. coli* clones expressing CYP variants, a micro-scale cultivation was performed in 96-deep well plates (DWP). *E. coli* single colony cells were picked and transferred to a DWP plate filled with 350 µl/well LB-media (preculture). The plate was incubated for 24 hours at 250 rpm (with a shaker-orbit of 5 cm) and 80% humidity. After one day a new DWP was filled with 400 µL/well TB-media mixed with the additives, 10 µM IPTG as inducing agent for expression, 0.5 mM 5-aminolevulinic acid as a precursor in heme biosynthesis, 250 µL/L of a trace element-solution and antibiotics. Cell material was transferred from the preculture-DWP to the main culture by using a stamp and cultivated at 250 rpm (shaker-orbit = 5 cm) and 26°C between 20 - 32 hours, depending on the assay that was made afterwards. Upon cultivation, the DWP was centrifuged at 3000 x g and 4°C for 15 minutes, the supernatant was discarded carefully and the pelleted cells were either used directly for measurements or stored at -20°C. An inoculation scheme of a DWP is shown in Figure 15.

	1	2	3	4	5	6	7	8	9	10	11	12
A	X	X	X	X	X	X	X	X	X	X	X	X
B	X	X	X	X	X	X	X	X	X	X	X	X
C	X	X	X	X	X	X	X	X	X	X	X	X
D	X	X	X	X	X	X	X	X	X	X	X	X
E	X	X	X	X	X	X	X	X	X	X	X	X
F	X	X	X	X	X	X	X	X	X	X	X	X
G	X	X	X	X	X	X	X	X	X	X	X	X
H	PC	PC	PC	NC	NC	NC	NC	NC	NC	ST	ST	ST

Figure 15: Scheme of a DWP for *E. coli* cultivation. X: Randomly chosen single clone that express a CYP variant, PC: Positive control - a strain (from the IMBT strain collection) that expresses a CYP enzyme, NV: Negative control – a strain that do not express CYPs, ST: Sterile control - the wells were filled only with media as a sterile control.

3.5.10. Micro-scale cultivation in 96-deep well plates (DWP) of *P. pastoris* expressing CYPs under the control of P_{AOX1}

To screen random *P. pastoris* clones for the expression of CYPs, micro-scale DWP cultivations were performed similar as described in the protocol by Weis et al. (110). Single colonies were transferred to DWP filled with 250 µL BMD1% per well and cultivated for 60 hours at 320 rpm (shaker-orbit = 5 cm) and 28°C. Subsequently 250 µL BMM2% were added to the wells for the induction of recombinant gene expression. After 12, 24 and 36 hours of induction, 50 µL BMM10 were added to the wells. 48 hours after the start of the induction, the cells were either centrifuged at 500 rpm and 21°C for 5 minutes and used for a CYP activity assay or stored at 4°C overnight.

3.5.11. Measurement of the optical density at 600 nm

For measuring the cell growth of the chosen *E. coli* or *P. pastoris* clones, the OD_{600} was determined. Therefore 10 µL of the cell suspension from the DWP was mixed with 190 µL ddH_2O in a clear flat bottom microtiterplate (MTP). The optical density was measured with the SynergyMx plate reader at 600 nm.

3.5.12. Small-scale cultivation of *E. coli*-mutants in 2 L-shake flasks

Upon testing the generated CYP variants in the two *E. coli* strains BL21 and DH5α-T1 with different activity-assays, the best two clones were chosen for scale-up cultivation. A single

colony of each of the variants was at first inoculated in 10 mL TB-media containing antibiotics (Ampicillin or Kanamycin) in a 50 mL tube and incubated at 37°C and 100 rpm overnight. The main cultures were cultivated in 450 mL TB-media supplemented antibiotics and 250 µL/L of a trace element-solution in 2 L-round bottom flasks. Cell suspension from the ONCs was added to reach a starting OD of approximately 0.012 and the cultures were incubated at 30°C and 100 rpm. After 10 hours of cultivation, 0.5 mM 5-aminolevulinic acid and 1 M IPTG were added to start the expression of the heterologous enzymes for 24 hours at 30°C and 100 rpm.

3.5.13. Cell disruption of *E. coli* mutants

After cultivating *E. coli* mutants in 2 L-round bottom flasks for 24 hours, cell disruption via sonification was performed to get the cell lysates with the soluble CYPs. First, the cultivation media was transferred into a 500 mL centrifuge bottle. A centrifugation step for 15 minutes at 5000 rpm and 4°C was done. The pellet was resuspended with 25 mL of a Lysis/Resuspension buffer in a 30 mL centrifuge bottle. An ultrasonic homogenizer (duty cycle =70-80, output control =7-8) was used for cell disruption. These settings have a major effect on the homogeneity of the disrupted cell solution. The total cell lysate extract was filled in a 30 mL centrifuge bottle and a 2nd centrifugation step was performed at 20 000 rpm and 4°C for 1 hour. Afterwards the cell lysates were aliquoted and stored at -20°C for further examinations.

3.5.14. Protein quantitation

To calculate the amount of protein that has been produced in soluble form during either DWP or 2 L-shake flask cultivation, two different types of protein assays were applied. These assays were used to quantify the total protein amount in the solution and not only the CYP content.

3.5.14.1. BCA-Assay

To quantify the total protein content after the *E. coli* micro-scale DWP cultivation, the cells were lysed with BugBuster® 10X Protein Extract Reagent and the Pierce™ BCA Protein Assay Kit and the manufacturer's microplate procedure protocol were applied by using the cell-free lysate as samples. To generate a calibration curve, BSA solutions with

concentrations of 62.5, 125, 250, 500, 750, 1000, 1500 and 2000 µg/mL were used. Undiluted and 1:10 with ddH_2O diluted samples were used. After incubation time of one hour at 37°C the absorption at 562 nm was determined.

3.5.14.2. Bradford-Assay

The Bradford-assay was used to measure the total protein content after *E. coli* 2 L-shake flask cultivation and subsequent cell disruption. The assay was carried out by using the manufacturer's guideline of the Pierce™ Coomassie (Bradford) Protein Kit (Thermo Scientific GmbH, Vienna, Austria). BSA solutions in the range from 62.5 to 2000 µg/mL were used for calibration and 10 µL of the cell lysates (chapter 3.5.13.) were mixed with 490 µL of ddH_2O (1:50 dilution). 3 µL of the diluted samples and the standards were mixed with 200 µL Bradford-reagent and the total protein concentration was measured at 595 nm.

3.5.15. Agarose gel electrophoresis

For the separation of DNA fragments with various sizes, an agarose gel electrophoresis was performed. A 1% agarose gel was made through mixing 2.5 g of agarose with 250 mL 1x TAE buffer. After heating and dissolving the solution in a microwave, approximately 2 µL ethidium bromide were added. The DNA samples were mixed with 6x Loading Dye and loaded into the slots. 10 µL of a GeneRuler™ 1kb DNA-Ladder was used as standard. A preparative gel ran for 80 - 90 minutes at 90 V and a control gel for 50 minutes at 120 V. Subsequently, the gels were analysed with a GelDoc-It™ Imaging Systems.

3.5.16. SDS-PAGE and Coomassie staining

Proteins/enzymes from the cell lysates (chapter 3.5.13.) were separated according to their conformation, charge and length by SDS-PAGE. The protein-content from the cell lysates was determined by a Bradford assay. 10 µg total proteins mixed with 5 µL of LDS sample buffer (4x) in a final volume of 20 µL was incubated at 75°C for 10 minutes. 10 µl of the samples and 3-5 µL of the protein ladder, either Novex® Sharp Prestained Protein ladder or PageRuler™ Prestained Protein ladder NuPage® were loaded on 4-12% Bis-Tris Gels. 1x MOPS buffer was used as running buffer. After loading, the separation process was carried out for 50 minutes at 200 V and 120 mA.

Staining of the gels was done with a Coomassie staining solution for 30 minutes. The staining solution was added to the gel in small container, which was then put in a microwave for approximately ten seconds. Destaining was performed by receptively rinsing the gel with SDS destaining solution for 20 minutes and performing short heating steps. After staining and destaining, the gel was rinsed with ddH2O.

3.6. Codon optimization

The DNA sequences of the monooxygenase domain from *Mycobacterium sp.* strain HXN1500 and the PFOR-reductase from *Rhodococcus ruber* were codon optimized for the expression in either *P. pastoris* or *E. coli*. The DNA-/amino acid-sequences were retrieved from NCBI and EMBOSS and optimized with the GeneDesigner software from DNA2.0. The Pichia_high methanol and the E. coli_CII codon usage tables were used for codon optimization. The most common restriction sites and sequence-motifs like cryptic splicing motifs, A/T and G/C pentameric sequences and RNA destabilizing sequences were removed. The Mobyle Portal-freak software was used to analyse the GC-content, which was set to prevent local minima below 40 % and local maxima above 70 %. The GeneBee-software was used to identify secondary structures with a free energy higher than -20kcal/mol that have an effect on ribosome processivity. The sequences were ordered as double stranded DNA fragments (gBlocks, monooxygenase domain: B15064, B15064; PFOR domain: B15068).

3.7. Screening Assays

In order to find out, whether the newly generated CYP variants were produced by the host-organism in a biologically and catalytically active conformation, different assays were performed: A CO-based assay for conformation studies, four different activity-assays, where the conversion of coumarin derivatives were observed and a cofactor-depletion assay to test the activity of the generated CYP450-mutants.

3.7.1. Carbon monoxide (CO)-difference spectra-assay

Screening for the presence of CYPs in *E. coli* or *P. pastoris*, relies on the ability of the heme-complex inside the enzyme to interact with CO. If there is an elapse of interaction between the Fe^{2+}-ion in the centre of the heme and a carbon monoxide-molecule, a change in the spectrum can be observed. The assay was performed according to the method described by Gudiminchi et al. (111) with *E. coli* and *P. pastoris* whole cells and *E. coli* cell lysates. Upon micro-scale

cultivation, the cells were pelleted (chapter 3.5.9./ 10.), resuspended in 220 µL 0.1 M PPB (pH 7.4) and vortexed to make the suspension homogenous. 140 µL of the whole-cell suspensions or 180 µl of the cell lysates were transferred into a clear flat bottom MTP. 20 µL of 80 mM KCN and a pipette tip-peak full of $Na_2S_2O_4$ (Sodium dithionite) were added. First a reference spectrum was recorded between 400 – 500 nm with 1 nm interval with a SynergyMx plate reader. The MTP was mixed for 10 seconds before recording. Afterwards, the MTP was exposed to a CO stream for 3 minutes in an airtight container placed inside a laboratory fume hood and then the spectrum was recorded again. The absorbance difference between A450 – A490 was used to quantify the CYP content by applying the following formula (8).

$$\text{CYP450 concentration [µM]} = \frac{(A450 - A490) * 1000 * 0.596}{91}$$

1000 = Multiplication factor

0.596 = thickness of the 96-well plate [cm]

91 = extinction coefficient $[\frac{mM}{cm}]$

3.7.2. NADPH depletion-assay

The NADPH depletion assay is a spectrophotometric assay to characterize the catalytic activity of monooxygenases. The depletion of the cofactor NADPH is measured during the conversion of a reporter substrate. This decrease can be monitored in a direct or indirect way. In this thesis, the depletion of NADPH was measured directly, based on guidelines from Glieder and Meinhold (112). The *E. coli* strains were cultivated and pelleted as described in chapter 3.5.9.. The cells were resuspended in the DWP with 750 µL/well *E. coli* lysis buffer and incubated for 1 hour at 37°C and 100 rpm to initiate cell lysis. For resuspension, an optical adhesive well plate-cover was put onto the DWP and then the plate was vortexed until the pellets were resolved. During lysis, 25 mM lauric acid as substrate and 0.8 mM NADPH as cofactor were prepared. After cell lysis, 200 µL of the lysates were pipetted into an optical MTP, sealed with an adhesive cover, put into a MTP and centrifuged for 20 minutes at 1700 x g. Measurements were performed in a clear flat bottom MTP with undiluted, 1:10, 1:100 and 1:1000 diluted samples (0.1 M PPB, pH 8.0). First, 100 µL 0.1 M PPB (pH 8.0) and 50 µL of the lysate/dilution were added to the MTP. 8 µL of lauric acid were added to a final concentration of 8 mM. The reaction was started by addition of 50 µL NADPH and the

decrease in absorbance at 340 nm was recorded for 3 minutes. The substrate and the cofactor were added to the samples directly before starting the measurement. As a reference a MTP containing buffer, lysate, NAPH, but no substrate was prepared and measured.

3.7.3. 7-benzyloxyresorufin-assay

7-benzyloxyresorufin, a derivative of the group of 7-alkoxyresorufins, was used as a testing reagent to implement a fluorescent based screening assay for CYP variants. In Figure 16, a reaction scheme is shown (113). *E. coli* cells were cultivated as described in chapter 3.5.9., pelleted and resuspended in 80 µL 0.1 M PPB (pH 7.4). 30 µL thereof were pipetted into a black flat bottom MTP. 150 µL of the 20 µM 7-benzyloxyresorufin-solution (dissolved in 0.1 M PPB (pH 7.4)) were added. The reaction was started by the addition of 20 µL of an NADPH regeneration media and formation of the fluorescent product was monitored over 15 minutes at 24°C on a SynergyMx plate reader (λ_{ex} = 530 nm, λ_{em} = 580 nm).

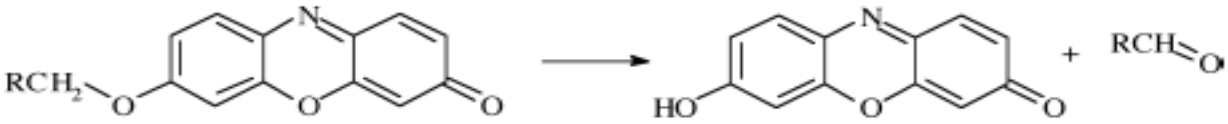

Figure 16: Alkoxyresorufin O-dealkylation reaction scheme; Benzyloxyresorufin: R = C_6H_5

3.7.4. 7-benzoxy-3-carboxycoumarin ethyl ester (BCCE)-assay

The fluorogenic substrate 7-benzoxy-3-carboxycoumarin ethyl ester (BCCE) was provided by Prof. Ulrich Schwaneberg and his research group at the RWTH Aachen University (Figure 17). The assay was accomplished according to Ruff et al. (114). *E. coli* cells were cultivated as described in chapter 3.5.9., pelleted and resuspended in 0.05 M PPB (pH 7.4). 50 µl of the cell suspension were transferred into a black flat bottom MTP. 2 µL of a 2 mM BCCE-solution were added and the plate was incubated for 5 minutes at 700 rpm. Afterwards the fluorescent signal was recorded every 20 seconds for 20 minutes (λ_{ex} = 400 nm, λ_{em} = 440 nm) on a SynergyMx plate reader.

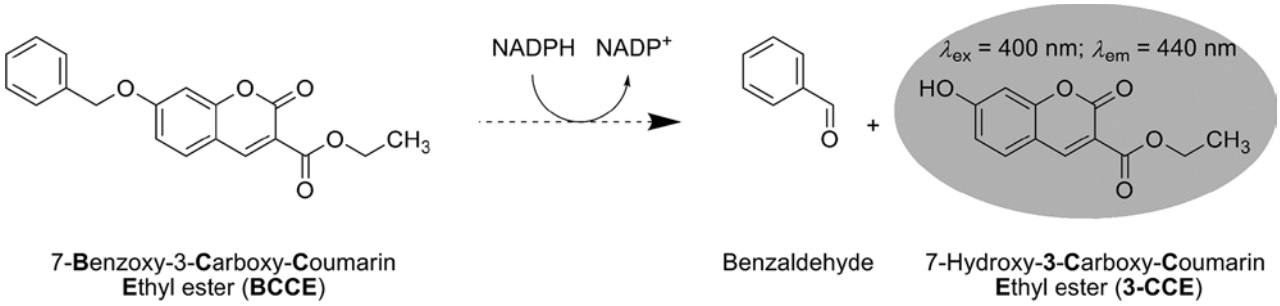

Figure 17: Scheme of a CYP-catalyzed 7-benzoxy-3-carboxycoumarin ethyl ester (BCCE) conversion [9]

3.7.5. 12-p-nitrophenoxycarboxylate (12-pNCA)-assay

12-p-nitrophenoxycarboxylic acid (12-pNCA) is converted through ω-hydroxylation of CYPs to its detectable, yellow product p-nitrophenolate (Figure 18). The substrate pNCA was provided by Prof. Ulrich Schwaneberg and his research group at the RWTH Aachen University and the spectrophotometric assay was performed with minor deviations according to Schwaneberg et al. (115). The assay was carried out in the same DWP that was used for cultivation and gene expression. 250 µL 0.1 M PPB (pH 8.0) were used for resuspension of the cell pellets. 5 µL of 3.6 mM Polymyxin B sulfate were added and the plate was incubated for 20 minutes at room temperature and 1000 rpm on a Titramax 1000. After addition of 5 µL 15 mM pNCA and 5 µL catalase the plate was incubated again for 5 minutes and 1000 rpm. The pNCA hardly dissolves in DMSO. Therefore it is recommended to put the pNCA-solution on a thermomixer to dissolve the substrate through heating and tossing. The reaction was started through addition of 50 µL 1 mM NADPH and the conversion was carried out for 1 hour at room temperature and 1000 rpm. The conversion was stopped by addition of 200 µL 1 M NaOH and the plate was centrifuged for 20 minutes and 4000 rpm at room temperature. 200 µL of the supernatant were transferred into a clear flat bottom MTP and the absorbance was measured at 405 nm with a SynergyMx plate reader.

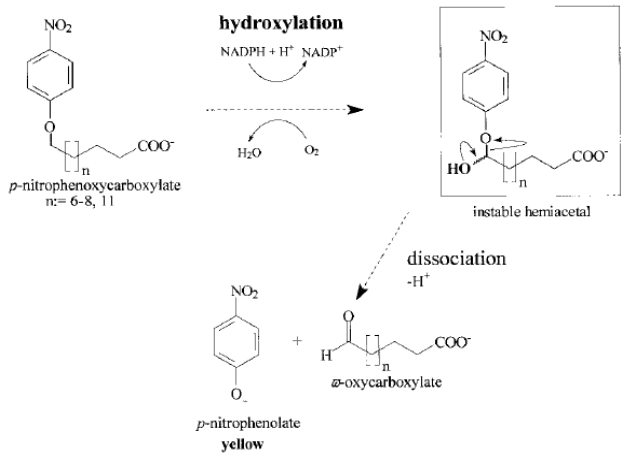

Figure 18: Scheme of a CYP-catalyzed p-nitrophenoxycarboxylic acid (pNCA) conversion (115)

3.7.6. 7-methoxy-4-(aminomethyl)-coumarin (MAMC)-assay

MAMC is an artificial designed molecule, selective for eukaryotic, e.g. the human CYP450 CYP2D6. The substrate specificity can be tested by conversion to a reaction product 7-hydroxy-4-(aminomethyl)coumarin (HAMC) (Figure 19) (116). *P. pastoris* cells were cultivated according to Weis (chapter 3.5.10.), the pelleted cells were resuspended in 200 µL 0.1 M PPB (pH 7.4) and centrifuged at 500 rpm and 21°C for 5 minutes. After repeating the resuspension step, 95 µL of the cell solution were transferred to a black flat bottom MTP. 5 µL of 1 mM MAMC were added and the conversion was observed with a SynergyMx plate reader (λ_{ex} = 405 nm, λ_{em} = 480 nm) for 90 minutes.

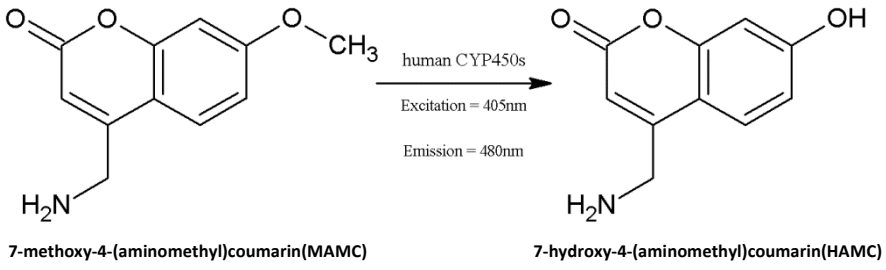

Figure 19: Conversion of MAMC to the fluorescent metabolite HAMC

3.8. CYP variants used in this thesis

In scope of this thesis, I generated a variety of P450 enzymes and tested these new mutants for their catalytic activity towards fluorogenic substrates. All synthetic DNA fragments (gBlocks and primers), generated and used during this master thesis were ordered from IDT (purchased by bisy) and are listed in the Appendix.

3.8.1. Construction of CYP505X plasmid variants

3.8.1.1. Expression in *E. coli*

The wild-type enzyme CYP505X (Accession Nr.: EAL92660) from *A. fumigatus* was codon optimized for expression in *E. coli* (denoted as M1/Wt). Based on sequence alignment among the P450 domains of P505X and CYP102A1 from *B. megaterium* and previously published aa substitutions in the sequence of BM3, mutants were generated in silico (Table 10).

Table 10: Well characterized aa substitutions in CYP102A1 with specification of the references for the respective mutations compared to the performed aa substitutions in CYP505X. *No aa substitution needed due to the presence of the planned aa at the specific spot in the sequence of CYP505X.

Designation	AA substitution in CYP102A1 from *B. megaterium*		AA substitution in CYP505X from *A. fumigatus*
		Effect on the catalytic properties	
M1/Wt	Wild-type	Preferred substrates are alcohols, fatty amides, medium- to long-chain fatty acids and unsaturated fatty acids (72,76).	Wild-type
M2	A74G, L188Q	Hydroxylation of large PAHs at high rates (>min^{-1}) (84).	G77G*, A192Q
M3	A238V, A264V, L437F	Conversion of limonene to perillyl alcohol with a selectivity of 97% (117).	I242V, A268V, L451F
M4	F87V, A328L	Conversion of geranylacetone to allylic alcohols with an efficiency of 80% (118).	F90V, A332L
M5	F87A	Hydroxylation of testosterone at positions 2β and 15β. Broaden regiospecificity and shift in hydroxylation of fatty acids away from the terminal position (115,119–123)	F90A
M6	A82N, F87A	100% regioselective hydroxylation of progesterone at position 2β (121).	V85N, F90A
M7	F87A, A330W	Increased regioselective conversion of testosterone and progesterone (121).	F90A, L334W
M8	R47I, T49I, Y51I, F87A	Testosterone hydroxylation with 94% selectivity for position 2β (121).	W50I, R52I, F54I, F90A
M9	R47Y, T49F, V78L, A82M, F87A	Testosterone hydroxylation with efficiency of 85% (15β-selectivity of 96%) (121).	W50Y, R52F, I81L, V85M, F90A
M10	R47Y, T49F, V78I, A82M, F87A	Testosterone hydroxylation with efficiency of 91% (15β-selectivity of 94%) (121).	W50Y, R52F, I81I*, V85M, F90A
M11	R47L, E64G, F81I, A82W, F87V, E143G, L188Q, Y198C, E267V, H285Y, G415S	Positive effect on substrate entrance and product exit. Activity towards dextromethorphan, clozapine, diclofenac and acetaminophen (76,124,125).	W50L, E67G, G84I, V85W, F90V, D147G, A192Q, T203C, E271V, N289Y, A428S

This served as a starting point for the design of gBlocks containing the different aa substitutions (B14001 – B14013). The CYP505X-mutants (denoted as M1/Wt-M11) were cloned in the vector pMS470Δ8 (chapter 3.4.3.). The vector was cut with *Eco*RI and *Hind*III and the 1274 bp stuffer fragment Δ8 was removed. First the gBlock E3-CYP505 (B14001), with overhangs to the promotor and the terminator was cloned to the linearized vector backbone to obtain pMS470E3. The gBlock E3_CYP505 (B14001) harbours the major part of the reductase domain of CYP505X which is the same in all of the generated constructs. pMS470E3 was cut with *Eco*RI for linearization and 2 gBlocks respectively, which include the monooxygenase domain of CYP505X with the specific mutation and a part of the reductase domain, were cloned in the vector backbone by assembly cloning to obtain the CYP variants [M1/Wt (B14003, B14002), M2 (B14002, B14004), M3 (B14005, B14006), M4 (B14007, B14002), M6(B14008, B14002), M7 (B14009, B14002), M8 (B140010, B14002), M9 (B140011, B14002), M11 (B140012, B140013)] (Figure 20). As an example, variant CYP505X-M1/Wt is shown in Figure 21. The CYP variants M5 and M10 were made by introducing a single point mutation in the CYP sequences of the mutants M6 and M9. Therefore, primers were ordered [(M5: B14023, B14024), (M10:B14021, B14022)]. The plasmids CYP505X-M6 and CYP505X-M9 were used to amplify the fragments of CYP505X-M5 and CYP505X-M10, respectively. In one PCR, M6/M9 was used with primer B14020 and primers B14024/B14022. In another PCR, M6/M9 was used with primer B14018 and primers B14023/B14021. The generated PCR fragments were fused with the linearized pMS470 through assembly cloning to get M5 and M10 (Figure 22).

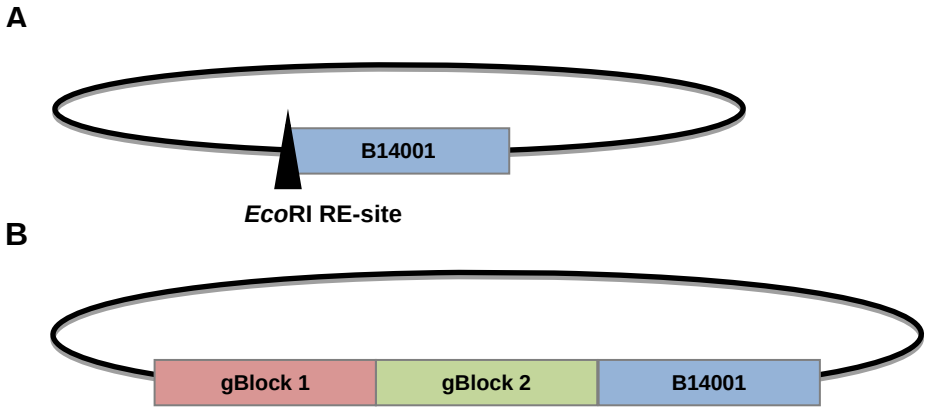

Figure 20: Scheme of the procedure for generating the CYP505X mutants M1/Wt-M4, M6-M9 and M11. **A:** After cloning the gBlock E3-CYP505 (B14001) to the linearized vector pMS470, pMS470E3 was cut with EcoRI for linearization. **B:** 2 gBlocks for each construct, which include the monooxygenase domain of CYP505X with the specific mutation, were cloned in the linearized vector backbone by assembly cloning. [M1/Wt (B14003, B14002), M2 (B14002, B14004), M3 (B14005, B14006), M4 (B14007, B14002), M6 (B14008, B14002), M7 (B14009, B14002), M8 (B140010, B14002), M9 (B140011, B14002), M11 (B140012, B140013)]

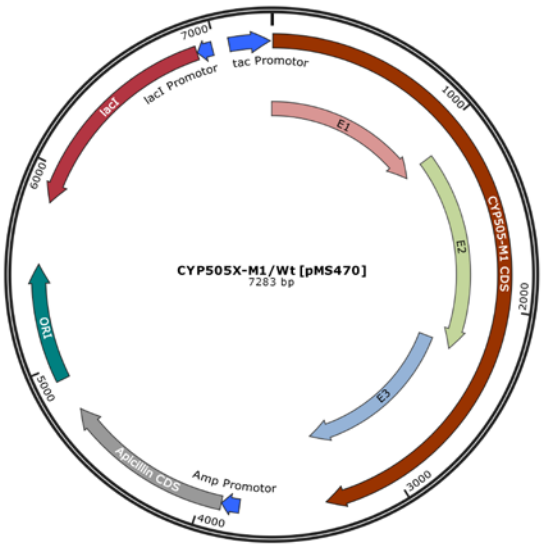

Figure 21: CYP505X-M1/Wt in vector pMS470Δ8: CYP505X-M1/Wt CDS: CYP505X-Mutant 1 coding DNA sequence, E1 – E3: building blocks (E1 = 1131 bp, E2 = 1197 bp, E3 = 1222 bp), Amp promotor: Ampicillin promotor, Ampicillin CDS: Ampicillin resistance cassette, ORI: Origin of replication, *lacI*: *lac* repressor gene, *lacI* promotor: *lac*-promotor (*lac*-operon), *tac* promotor

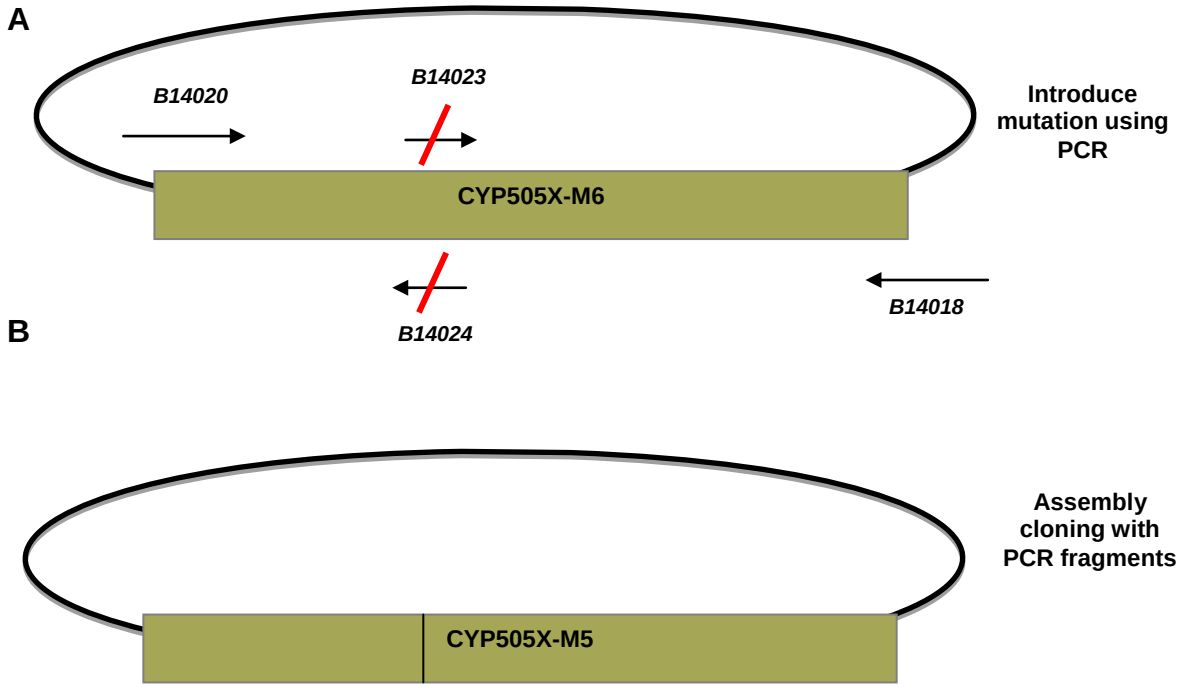

Figure 22: Formation of the mutants M5 and M10 shown here with M5. A: CYP505X-M6 was used to run two PCRs to generate 2 fragments. One time, M6 was used with primer B14020 and B14024. In the second, M6 was used with B14018 and B14023. **B:** The generated PCR fragments were fused with linearized pMS470 by assembly cloning.

3.8.1.2. Expression in *P. pastoris*

The wild-type enzyme CYP505X (Accession Nr.: EAL92660) from *A. fumigatus* was codon optimized for expression in *P. pastoris* and ordered from DNA2.0 (purchased by bisy) cloned in the vector pPpT4_S (Appendix S 1). To express the gene of interest also the vector pPpB1_S, CYP505X-M12 was digested with *Eco*RI, *Not*I and *Xba*I to obtain the CYP505X-M12 insert fragment. pPpB1_S was digested with *Eco*RI and *Not*I and the linearized vector and the gene of interest were ligated to generate CYP505X-M13.

3.8.2. Construction of CYP505A1 (Cytochrome P450foxy) plasmid variants

The fungal enzyme CYP505A1 (known as CYP450foxy; Accession Nr.: BAA82526) from *F. oxysporum* was codon optimized for expression in *P. pastoris* and ordered from DNA2.0 (purchased by bisy) cloned in vector pPpT4_S, labelled as CYP505A1-M1 (Appendix S 2). For expression in vector pPpB1_S, CYP505A1-M1 was digested with *Eco*RI, *Not*I and *Xba*I to remove the CYP505A1 insert fragment. pPpB1_S was digested with *Eco*RI and *Not*I and the linearized vector and the gene of interest were ligated (CYP505A1-M2).

3.8.3. Construction of CYP153A6 plasmid variants

CYP153A6-M1, containing the complete operon from *Mycobacterium sp.* strain HXN1500 (P450 monooxygenase, Ferredoxin reductase [FdR], Ferredoxin [Fdx]) (99), was ordered from DNA2.0 (purchased by bisy) in the vector pD441-SR for expression in *E. coli* (Figure 14) employing a T5 promoter. A fusion variant, consisting of the monooxygenase domain from the CYP153A6 operon and the reductase domain of CYP505X (CYP153A6-M2, Figure 23) was generated. A PCR, using the plasmid CYP153A6-M1 as template and the primers B15053 and B15054, was made to amplify the monooxygenase domain of *Mycobacterium sp.* HXN1500 and another PCR with the plasmid CYP505X-M2 and primers B15055 and B15056 was made to amplify the CYP505X-reductase domain. The vector pMS470Δ8 was cut with *Eco*RI and *Hind*III to remove the stuffer fragment Δ8. The PCR fragments were added to the vector backbone by assembly cloning. Another fusion variant, CYP153A6-M3 (Figure 24) was generated for expression in *P. pastoris*. Therefore, the *Mycobacterium sp.* HXN1500 monooxygenase domain was codon optimized and ordered on two gBlocks B15064 and B15131. A PCR was done with plasmid CYP505X-M12 and primers B15057 and B15058 to amplify the CYP505X-reductase domain. The vector pPpT4_S was cut with

*Eco*RI and *Not*I. The gBlocks and the PCR-fragment were cloned into vector backbone with assembly cloning. To use the vector pD441-SR as a negative control, the plasmid CYP153A6-M1 was digested with *Xba*I and *Xma*I to get rid of the complete operon of *Mycobacterium sp.* HXN1500 and subsequent a ligation with T4-ligase was performed overnight. The religated vector was transformed in host *E. coli* TOP10 as described in chapter 3.5.1.2..

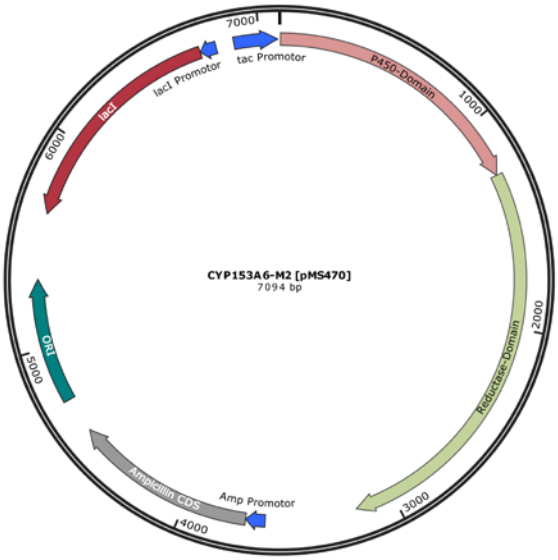

Figure 23: CYP13A6-M2 in vector pMS470Δ8: The plasmid contains the monooxygenase from *Mycobacterium sp.* HXN1500 (1260 bp) directly fused to the reductase domain from CYP505X-M2 from *A.fumigatus* (1914 bp), Amp promotor: Ampicillin promotor, Ampicillin CDS: Ampicillin resistance cassette, ORI: Origin of replication, *lacI*: *lac* repressor gene, *lacI* promotor: *lac*-promotor (*lac*-operon), *tac* promotor

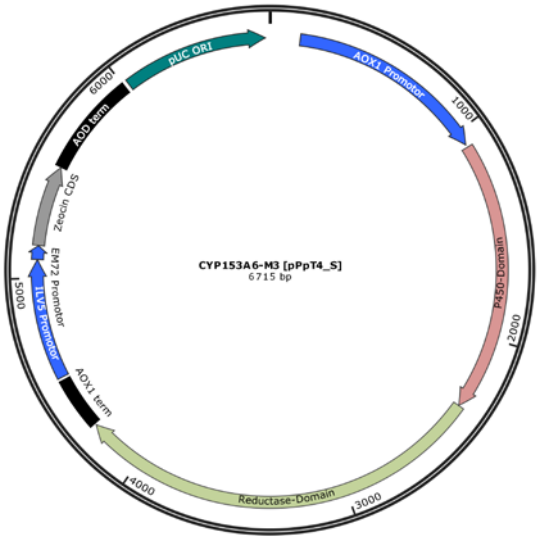

Figure 24: CYP153A6-M3 in vector pPpT4_S: The plasmid contains the monooxygenase from *Mycobacterium sp.* HXN1500 (1260 bp) directly fused to the reductase domain from CYP505X-M12 from *A.fumigatus* (1914 bp), *AOX1* term: *AOX1* transcription terminator, *ILV5* promotor: eukaryotic promotor, *EM72* promotor: synthetic prokaryotic promotor, Zeocin CDS: Zeocin^{TM} resistance gene, *AOD* term: *AOD* transcription terminator, pUC ORI: pUC origin of replication, *AOX1* promotor

3.8.4. Construction of CYP154E1 plasmid variants

CYP154E1-M1 consists of the vector pMS470Δ8, harbouring the monooxygenase from *Thermobifida fusca TM51* (Accession Nr.: EOR69921.1) coexpressed with redoxpartners putidaredoxin reductase (PdR) and putidaredoxin (Pdx) from *Pseudomonas putida* (polycistronic operon) (105). Therefore, the monooxygenase sequence was codon optimized for expression in *E. coli*. After in silico-generation of the three-component system via CLC workbench, three gBlocks (B15065, B15066, and B15067) and two Primers (B15075, B15077) were designed and gBlocks were fused via oePCR. The vector pMS470Δ8 was cut with *Eco*RI and *Hind*III and the oePCR-product was cloned into the vector backbone using assembly cloning (Figure 25). For CYP154E1-M2, the monooxygenase from *T. fusca TM51* was amplified from CYP154E1-M1 by PCR with primers B15060 and B15061. The PFOR-reductase from *R. ruber* (NCBI: AY957485.1) was codon optimized for expression in *E. coli* and ordered as gBlock B15068. Vector pMS470Δ8 was cut with *Eco*RI and *Hind*III and fused with the PCR-product and the gBlock by assembly cloning (Figure 26). For CYP154E1-M3, the monooxygenase from *T. fusca TM51* was amplified from CYP154E1-M1 by PCR with primers B15060 and B15062. A PCR with CYP505X-M2 and primers B15055 and B15056 was made to amplify the CYP505X-reductase domain. The vector pMS470Δ8 was cut with *Eco*RI and *Hind*III. The PCR fragments were cloned into the vector backbone pMS470 using assembly cloning (Figure 27).

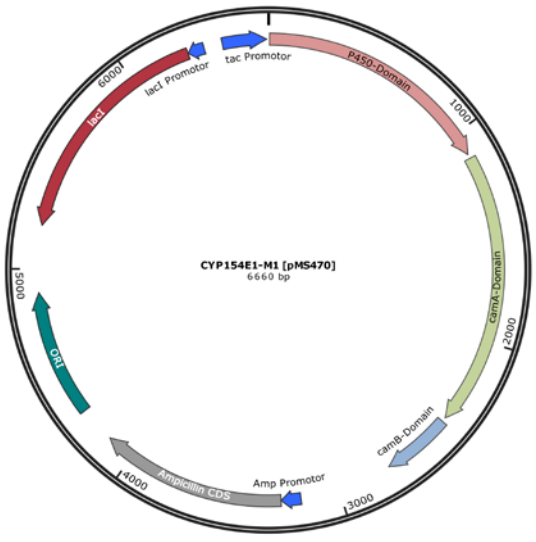

Figure 25: CYP154E1-M1 in vector pMS470Δ8: The plasmid contains the monooxygenase from *T. fusca* (1101 bp) coexpressed with the putidaredoxin reductase (camA, 1272 bp) and the putidaredoxin(camB, 324 bp) from *P. putida*, Amp promotor: Ampicillin promotor, Ampicillin CDS: Ampicillin resistance cassette, ORI: Origin of replication, *lacI*: *lac* repressor gene, *lacI* Promotor: *lac*-promotor (*lac*-operon), *tac* promotor

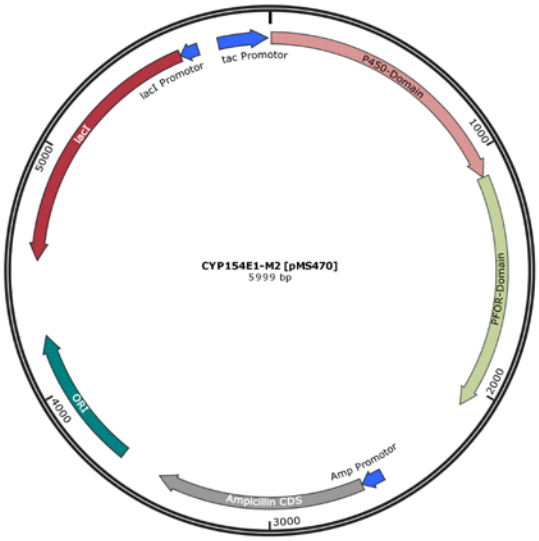

Figure 26: CYP154E1-M2 in vector pMS470Δ8: The plasmid contains the monooxygenase from *T. fusca* (1101 bp) directly fused to the PFOR-reductase from *R.ruber* (978bp), Amp Promotor: Ampicillin promotor, Ampicillin CDS: Ampicillin resistance cassette, ORI: Origin of replication, *lacI*: *lac* repressor gene, *lacI* Promotor: *lac*-promotor (*lac*-operon), *tac* promotor

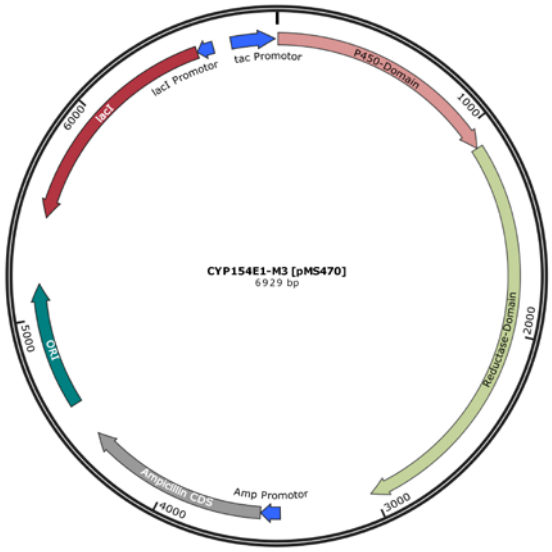

Figure 27: CYP154E1-M3 in pMS470Δ8: The plasmid contains the monooxygenase from *T. fusca* (1101 bp) directly fused to the reductase domain from CYP505X-M2 from *A.fumigatus* (1908 bp), Amp promotor: Ampicillin promotor, Ampicillin CDS: Ampicillin resistance cassette, ORI: Origin of replication, *lacI*: *lac* repressor gene, *lacI* Promotor: *lac*-promotor (*lac*-operon), *tac* promotor

3.9. *E. coli* and *P. pastoris* strains

All strains that were generated during this thesis are listed in Table 11. All strains were stored as 20% glycerol stocks in my internal strain collection at the Institute of Molecular Biotechnology (IMBT). Interesting strains were transferred to the strain collection of the institute (IMBT).

Table 11: *E. coli* and *P. pastoris* strains generated during the master thesis.

Term	Host strain	Resistance Marker	Internal Strain Collection [#]	IMBT Strain Collection [#]
Cytochrome P450s				
CYP505X-M1/Wt [pMS470]	TOP 10 F`	Amp	20	7831
CYP505X-M2 [pMS470]	TOP 10 F`	Amp	21	7832
CYP505X-M3 [pMS470]	TOP 10 F`	Amp	22	7833
CYP505X-M4 [pMS470]	TOP 10 F`	Amp	23	7834
CYP505X-M5 [pMS470]	TOP 10 F`	Amp	24	7835
CYP505X-M6 [pMS470]	TOP 10 F`	Amp	25	7836
CYP505X-M7 [pMS470]	TOP 10 F`	Amp	26	7837
CYP505X-M8 [pMS470]	TOP 10 F`	Amp	27	7838
CYP505X-M9 [pMS470]	TOP 10 F`	Amp	28	7839
CYP505X-M10 [pMS470]	TOP 10 F`	Amp	29	7840
CYP505X-M11 [pMS470]	TOP 10 F`	Amp	30	7841
CYP505X-M12 [pPpT4_S]	TOP 10 F`	Zeo	31	7842
CYP505X-M13 [pPpB1_S]	TOP 10 F`	Zeo	32	7843
CYP505A1-M1 [pPpT4_S]	TOP 10 F`	Zeo	33	7844
CYP505A1-M2 [pPpB1_S]	TOP 10 F`	Zeo	34	7845
CYP153A6-M1 [pD441_SR]	TOP 10 F`	Kan	35	7846
CYP153A6-M2 [pMS470]	TOP 10 F`	Amp	47	7847
CYP153A6-M3 [pPpT4_S]	TOP 10 F`	Zeo	51	7848
CYP154E1-M1 [pMS470]	TOP 10 F`	Amp	48	7849
CYP154E1-M2 [pMS470]	TOP 10 F`	Amp	49	7850
CYP154E1-M3 [pPpT4_S]	TOP 10 F`	Amp	50	7851
Generated Cytochrome P450 mutants in *E. coli*				
CYP505X-M1/Wt_ BSYEJE1.1 [pMS470]	BL21 (DE3)	Amp	55	7852
CYP505X-M1/Wt _ BSYEJE1.2 [pMS470]	BL21 (DE3)	Amp	56	-
CYP505X-M1/Wt _ BSYEJE1.3 [pMS470]	BL21 (DE3)	Amp	57	-
CYP505X-M1/Wt _ BSYEJE2.1 [pMS470]	DH5α-T1	Amp	58	7853
CYP505X-M2_ BSYEJE4.1 [pMS470]	DH5α-T1	Amp	59	7854
CYP505X-M2_ BSYEJE4.2 [pMS470]	DH5α-T1	Amp	60	-
CYP505X-M2_ BSYEJE4.3 [pMS470]	DH5α-T1	Amp	61	-
CYP505X-M3_ BSYEJE5.1 [pMS470]	BL21 (DE3)	Amp	62	-
CYP505X-M3_ BSYEJE5.2 [pMS470]	BL21 (DE3)	Amp	63	-
CYP505X-M4_ BSYEJE7.1 [pMS470]	BL21 (DE3)	Amp	64	-
CYP505X-M4_ BSYEJE7.2 [pMS470]	BL21 (DE3)	Amp	65	-
CYP505X-M5_ BSYEJE9.1 [pMS470]	BL21 (DE3)	Amp	66	-
CYP505X-M5_ BSYEJE9.2 [pMS470]	BL21 (DE3)	Amp	67	-
CYP505X-M5_ BSYEJE10.1 [pMS470]	DH5α-T1	Amp	68	7855
CYP505X-M6_ BSYEJE11.1 [pMS470]	BL21 (DE3)	Amp	69	7856

CYP505X-M6_ BSYEJE12.1 [pMS470]	DH5α-T1	Amp	70	-
CYP505X-M6_ BSYEJE12.2 [pMS470]	DH5α-T1	Amp	71	-
CYP505X-M7_ BSYEJE13.1 [pMS470]	BL21 (DE3)	Amp	72	-
CYP505X-M7_ BSYEJE13.2 [pMS470]	BL21 (DE3)	Amp	73	-
CYP505X-M8_ BSYEJE15.1 [pMS470]	BL21 (DE3)	Amp	74	7857
CYP505X-M8_ BSYEJE15.2 [pMS470]	BL21 (DE3)	Amp	75	-
CYP505X-M8_ BSYEJE15.3 [pMS470]	BL21 (DE3)	Amp	76	-
CYP505X-M9_ BSYEJE18.1 [pMS470]	DH5α-T1	Amp	77	7858
CYP505X-M9_ BSYEJE18.2 [pMS470]	DH5α-T1	Amp	78	-
CYP505X-M9_ BSYEJE18.3 [pMS470]	DH5α-T1	Amp	79	-
CYP505X-M10_ BSYEJE19.1 [pMS470]	BL21 (DE3)	Amp	80	7859
CYP505X-M10_ BSYEJE19.2 [pMS470]	BL21 (DE3)	Amp	81	-
CYP505X-M10_ BSYEJE19.3 [pMS470]	BL21 (DE3)	Amp	82	-
CYP505X-M10_ BSYEJE20.1 [pMS470]	DH5α-T1	Amp	83	7860
CYP505X-M11_ BSYEJE21.1 [pMS470]	BL21 (DE3)	Amp	84	-
CYP505X-M11_ BSYEJE22.1 [pMS470]	DH5α-T1	Amp	85	-
CYP153A6-M1_ BSYEJE23.1 [pD441_SR]	BL21 (DE3)	Kan	86	7861
CYP153A6-M1_ BSYEJE23.2 [pD441_SR]	BL21 (DE3)	Kan	87	-
CYP153A6-M1_ BSYEJE24.1 [pD441_SR]	DH5α-T1	Kan	88	7862
CYP153A6-M1_ BSYEJE24.2 [pD441_SR]	DH5α-T1	Kan	89	-
CYP153A6-M2_ BSYEJE25.1 [pMS470]	BL21 (DE3)	Amp	90	-
CYP153A6-M2_ BSYEJE25.2 [pMS470]	BL21 (DE3)	Amp	91	-
CYP154E1-M1_ BSYEJE27.1 [pMS470]	BL21 (DE3)	Amp	92	-
CYP154E1-M1_ BSYEJE28.1 [pMS470]	DH5α-T1	Amp	93	-
CYP154E1-M2_ BSYEJE29.1 [pMS470]	BL21 (DE3)	Amp	94	-
CYP154E1-M2_ BSYEJE30.1 [pMS470]	DH5α-T1	Amp	95	-
CYP154E1-M3_ BSYEJE31.1 [pMS470]	BL21 (DE3)	Amp	96	-
CYP154E1-M3_ BSYEJE31.2 [pMS470]	BL21 (DE3)	Amp	97	-
Generated Cytochrome P450 mutants in *P. pastoris*				
CYP505X-M12_ BSYPJE1.1 [pPpT4_S]	CBS7435 Wt	Zeo	98	7863
CYP505X-M12_ BSYPJE1.2 [pPpT4_S]	CBS7435 Wt	Zeo	99	-
CYP505X-M12_ BSYPJE2.1 [pPpT4_S]	CBS7435 MutS	Zeo	100	-
CYP505X-M13_ BSYPJE5.1 [pPpB1_S]	CBS7435 Wt	Zeo	101	7864
CYP505X-M13_ BSYPJE5.2 [pPpB1_S]	CBS7435 Wt	Zeo	102	-
CYP505X-M13_ BSYPJE7.1 [pPpB1_S]	BSYBG10	Zeo	103	-
CYP505A1-M1_ BSYPJE9.1 [pPpT4_S]	CBS7435 Wt	Zeo	104	7865
CYP505A1-M1_ BSYPJE10.1 [pPpT4_S]	CBS7435 MutS	Zeo	105	-
CYP505A1-M1_ BSYPJE11.1 [pPpT4_S]	BSYBG10	Zeo	106	7866
CYP505A1-M1_ BSYPJE12.1 [pPpT4_S]	BSYBG11	Zeo	107	-
CYP505A1-M2_ BSYPJE14.1 [pPpB1_S]	CBS7435 MutS	Zeo	108	-
CYP505A1-M2_ BSYPJE15.1 [pPpB1_S]	BSYBG10	Zeo	109	7867
CYP505A1-M2_ BSYPJE15.2 [pPpB1_S]	BSYBG10	Zeo	110	-

4. RESULTS AND DISCUSSION

4.1. Characterization of *P. pastoris* strains from BioGrammatics (BG)

Novel *P. pastoris* strains, which were used for CYP expression, had been obtained from BG and deposited in Graz as BSYBG strains. The BSYBG strains were characterized regarding their growth behaviour by cultivating them using three different types of media (BMD1% containing 1% dextrose, BMD1% supplemented with histidine and BMM containing 1% methanol as carbon source. The *P. pastoris* strains CBS 7435 Wt and mutS strains were used as references.

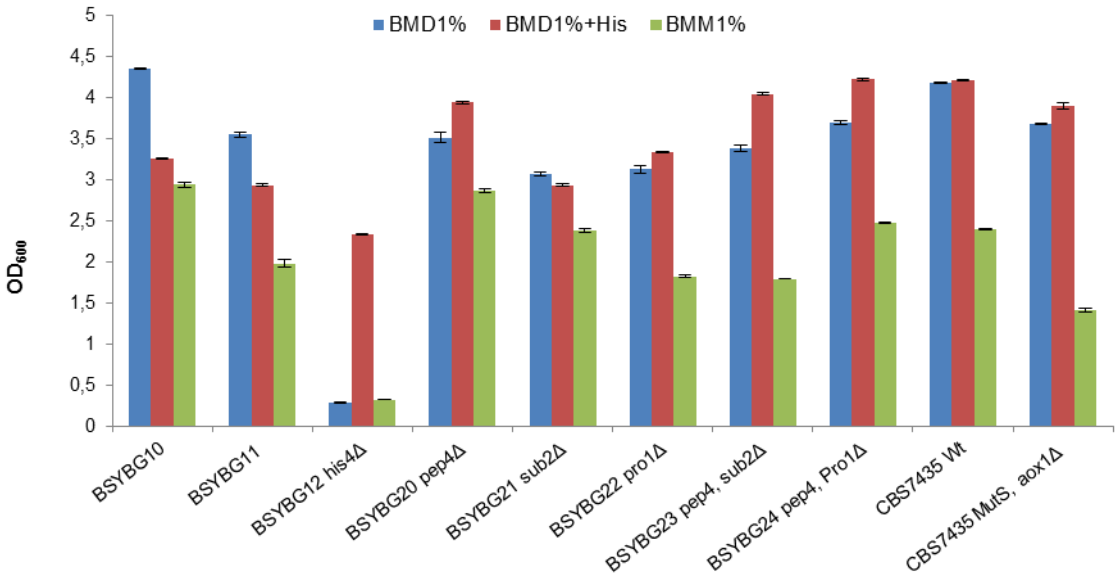

Figure 28: OD_{600} of different *P. pastoris* strains. The strains were cultivated for 48 hours at 30°C and 100 rpm in different cultivation media (BMD1%, BMD1%+His, BMM1%).

Over a time period of 48 hours the *P. pastoris* strains were grown in a 96-DWP in 250 µL minimal media for a rough characterization of their phenotype. Then the optical density at 600 nm was measured. The growth behaviour of the BSYBG strains is displayed in Figure 28. BSYBG12 his4Δ, which lacks the histidinol dehydrogenase and requires histidine as an essential aa for development, showed reduced growth in BMD1% and BMM1% media, but reached an up to 8-fold higher OD_{600} in histidine supplemented media. The variant BSYBG11, where the *AOX1* gene had been knocked out, showed slower growth on BMM1% media, which contains methanol as C-source, compared to the wildtype stain BSYBG10. The same was observed for CBS 7435 MutS, where the *AOX1* gene had been knocked out, and CBS 7435 Wt, respectively. Reduced growth of the BSYBG strains in BMD1%+His media compared to BMD1% was observed. Supplementation of media with histidine should not

affect cell growth in a disadvantageous way. A possible reason might be that the experiment was performed in a DWP. The characterization experiment should be repeated in shake flasks. For CYP expression and activity tests in this thesis, BSYBG10, BSYBG11, CBS7435 Wt and CBS7435 MutS were used.

4.2. Implementation of the cultivation conditions for micro-scale cultivation of *E. coli*

The cultivation conditions have a substantial influence on the outcome of micro-scale cultivation in DWPs, when expressing CYPs in *E. coli*. In the course of the thesis the cultivation parameters for CYP expression in *E. coli* were improved. First the preculture was incubated overnight at 37°C and 300 rpm. For the main culture, about 8.8 µL of the preculture were inoculated in 191.7 µL TB-media (200 µL/well) to an approximate starting OD_{600} of 0.2. After the main culture reached an OD_{600} of 0.8, induction was done with IPTG (final concentration: 1 mM) and the cultivation took place overnight at 250 rpm and 30°C. A IPTG concentration of 2 mM in the cultivation media might have a negative effect on CYP production since it was observed that higher concentrations of IPTG (1 mM) can cause cytotoxic effects (126). In order to increase CYP production, various parameters were changed and thereby the amount of biologically active enzyme was increased. The highest CYP levels were obtained when the preculture was incubated for 24 hours at 250 rpm, 28°C and 80% humidity. For the main culture, 400 µL/well TB-media were used and mixed with 5-aminolevulinic acid and a trace element-solution. The induction was carried out with 10 µM IPTG. Furthermore, the cell material from the preculture was transferred to the main culture using a metallic stamp and the cultivation was accomplished at 250 rpm and 26°C between 20 - 32 hours (depending on the assay, which was performed afterwards). The positive effect of using the altered cultivation conditions is shown in Figure 29, which depicts a CO-difference spectra-assay with CYP505X-M3. In panel A the CO spectra-assay was performed with *E. coli* whole cells cultivated by using the initial settings. As a control, sterile cultivation media was measured. Here no disturbing interactions between the media and components of the assay such as sodium dithionite or KCN were observed. There are expression peaks at 420 nm as well as 450 nm with CYP505X-M3. However, there was no distinct peak at 450 nm with the CYP-sample. No active CYP505X-M3 was produced with *E. coli* BL21 cells and only 30 nM of enzyme was generated with *E. coli* DH5α-T1 cells. Both samples as well as the negative controls showed a noticeable peak at 420 nm. The 420 nm peak indicates an inactive CYP conformation due to an ineffective expression, misfolding or a conformational change in the structure leading to a loss of the necessary Fe-Thiolate linkage in the heme, responsible

for the peak at 450 nm. 600 nM active CYPs were produced by the positive control expressing CYP102A1 from *B. megaterium*. I observed that altering the cultivation conditions influenced the production of CYP102A1 and CYP505X in different host strains (Figure 29, panel A and B). Using the altered cultivation protocol (result of CYP505X-M3 is seen in panel B), generally less inactive enzyme was produced compared to the initial routine. The change of the cultivation parameters merely had a positive effect on BL21 cells indicated by expression of 135 nM biologically active CYP505X-M3, while the yield of active expressed enzyme by DH5α-T1 cells decreased to 16 nM. The quantity of the positive control CYP102A1, expressed in DH5α-T1 cells, also decreased from 600 nM to 230 nM (Figure 32). The cultivation parameters had a major influence on the CYP production; they need to be adjusted to every host strain and CYP. For the thesis, the amended cultivation routine was used.

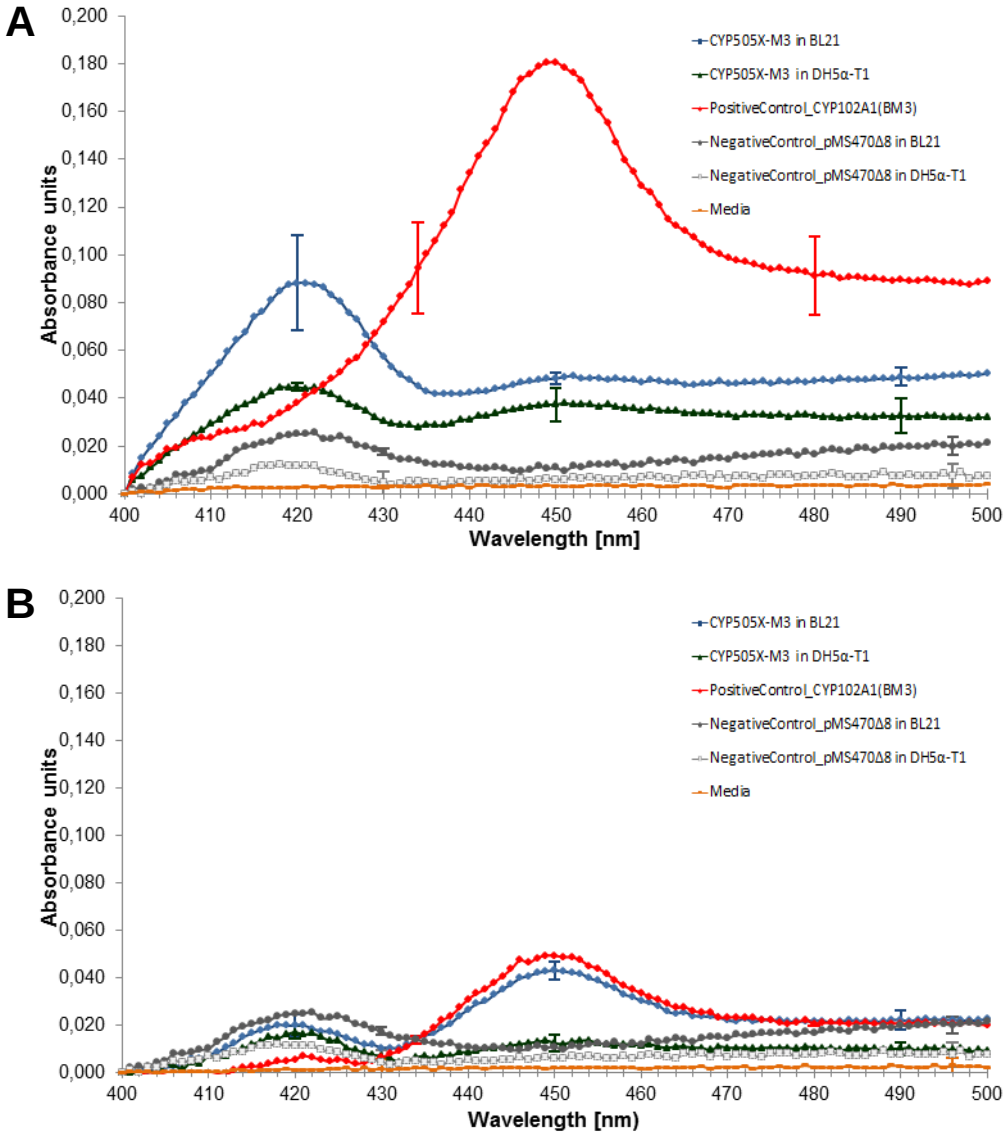

Figure 29: CO spectrum of CYP505X-M3 expressed in *E. coli* BL21 or DH5α-T1 using various cultivation conditions. Biological tetraplicates (BL21) and triplicates (DH5α-T1) are shown. As a positive control CYP102A1 (BM3) was expressed in *E. coli* DH5α-T1. As a negative control *E. coli* BL21 / DH5α-T1 were transformed with the empty vector pMS470Δ8, which does not contain a CYP gene. The data points were normalized to 0. **A**: The preculture was incubated overnight at 37°C and 300 rpm. The main culture was started with an OD of 0.2 in 200 µL/well TB-media. 100 µg/L ampicillin was added as selection marker. Induction was done with 2 mM IPTG. Cultivation of the main culture took place overnight at 250 rpm and 30°C. **B:** The influence of altered cultivation parameters on CYP production: The preculture was incubated for 24 hours at 250 rpm and 80% humidity. For the main culture, 400 µL/well TB-media were used and mixed with 0.5 mM 5-aminolevulinic acid, 250 µL/L of a trace-element solution and ampicillin as selection marker. Induction was conducted with 10 µM IPTG. The cell material from the preculture was transferred to the main culture by stamping and the cultivation was accomplished at 250 rpm and 26°C for 24 hours.

4.3. Heterologous expression of CYPs

In the course of this thesis, a variety of prokaryotic and eukaryotic CYPs (chapter 3.8.) was expressed in the host systems *E.coli* and *P. pastoris* and the applicability of the strains as

whole-cell biocatalysts was tested. An overview is shown in Table 11 (chapter 3.9). Various screening assays were used to determine the catalytic activity of the newly generated CYPs.

During the cultivation of the CYP505X mutants (M1/Wt – M11), a blueish phenotype could be observed with *E. coli* DH5α-T1 clones expressing CYP505X-M9 (Figure 30). The aa tryptophan is converted by the endogenous enzyme tryptophanase to indole, a metabolite of tryptophan. Further, indole is oxidized by the heterologous CYP505X to the insoluble pigment indigo. The production of indigo indicates the expression of functional CYPs (CYP505X-M9). Moreover it suggests that this mutant is capable to accept larger substrates and to degrade a wide range of aromatic compounds and xenobiotics (127).

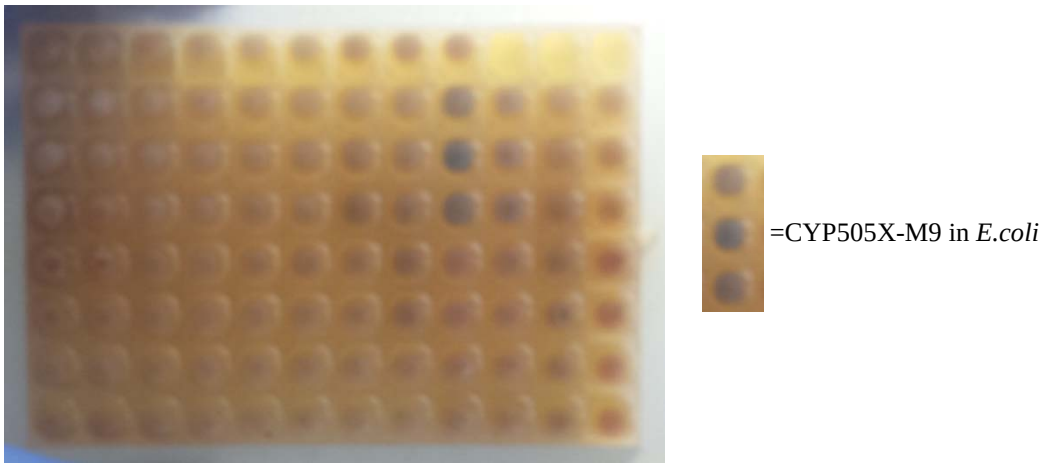

Figure 30: Formation of the pigment indigo due to the metabolization of the aa tryptophan.

4.3.1. Expression of CYP505X in *E. coli*

4.3.1.1. Carbon monoxide (CO)-difference spectra-assay

The CO-difference spectra-assay was performed to analyse the enzymes levels and to provide information about its biological conformation and activity.

By comparing the CO difference spectra of various *E. coli* strains expressing CYP505X variants, more biologically active enzyme was produced in *E. coli* BL21 compared to *E. coli* DH5α-T1 (Figure 31). Comparing the wild-type to the mutant variants resulted in an increase in the amount of actively expressed CYP505X through selective mutagenesis.

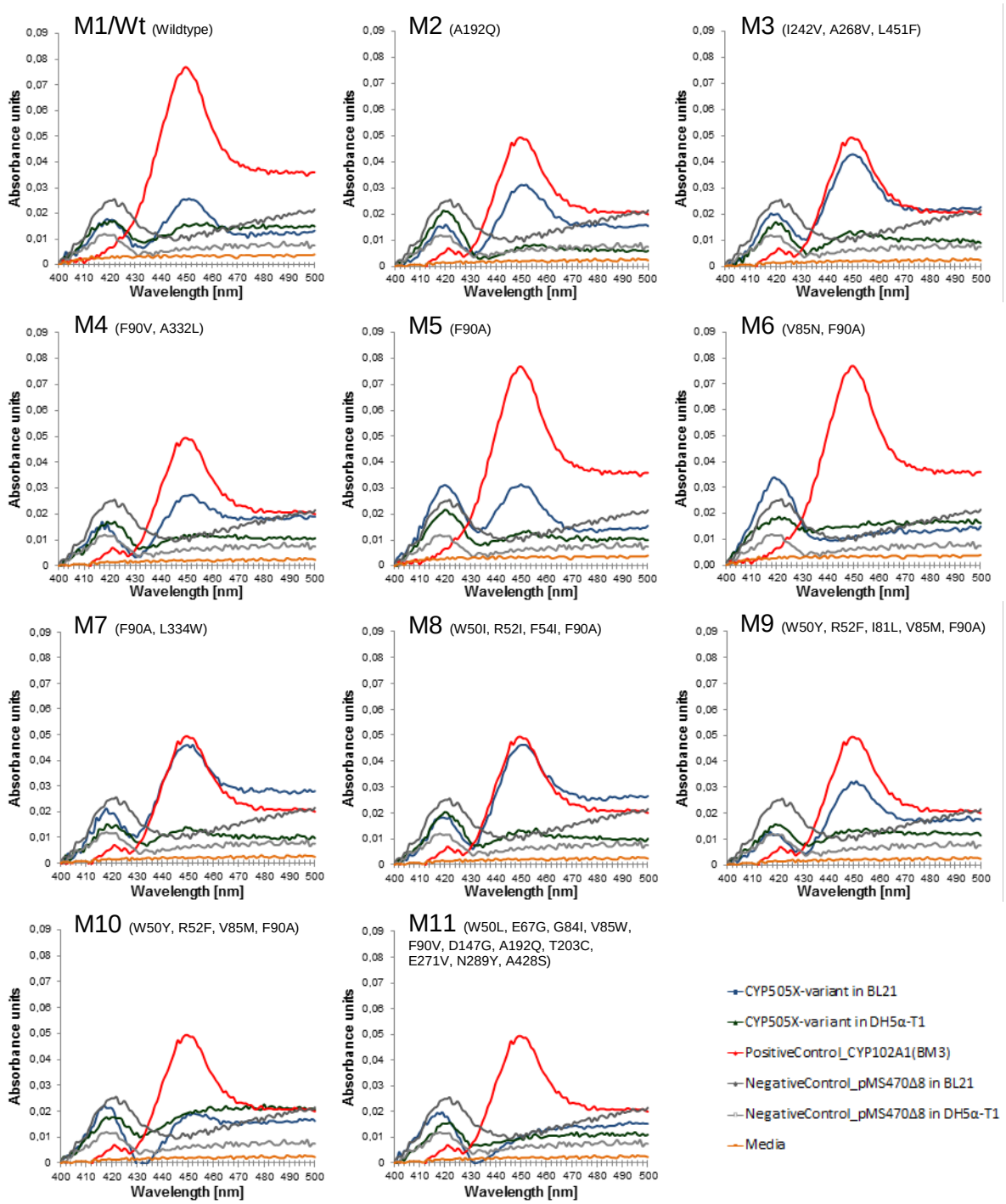

Figure 31: CO spectra of CYP505X M1/Wt-M11 expressed in *E. coli* BL21 or DH5α-T1. Biological tetraplicates (BL21) and triplicates (DH5α-T1) are shown. As a positive control CYP102A1 (BM3) was expressed in *E. coli* DH5α-T1. As negative controls *E. coli* BL21 and DH5α-T1 were transformed with the empty vector pMS470Δ8, which does not contain a CYP gene. Data points are normalized to 0.

The aa substitution at position 192 from alanine to glutamine in M2 resulted in an increase of active CYP505X to 106.4 nM in contrast to the wild-type enzyme (83.5 nM). An explanation therefore could be that glutamine forms the most common rotameric conformation (20.8%) and thereby a spatial approximation is formed from the glutamine-residue to alanine at position 77 resulting in a better folding and a higher stability of the enzyme. The highest

amount of actively expressed enzyme (136.0 nM) was obtained with mutant M3. However, also the control enzyme CYP102A1 showed different expression yields in the individual experiments. The three substitutions at position 242, 268 and 451 do not occur in the direct vicinity to each other; however the positions 268 and 451 are very close to the heme domain on the catalytic side, which may cause folding advantages and an improved incorporation of heme in the active site. Phenylalanine at position 451 might led to an increase in stability through the interaction with the isoleucine at position 81. For M6, the exchange of aa valine to asparagine in the centre of the monooxygenase at position 85 had a negative effect on correct protein folding of CYP505X. Asparagine, a bigger, more hydrophilic aa than valine, might be responsible for ineffective folding. CYP505X-M9, where valine at position 85 was exchanged to methionine, was actively produced (90.1 nM). Since methionine is also a hydrophobic aa it seems that the right hydropathy in the core is important for correct folding. M8 produced 134.3 nM of enzyme. Beside the substitution at position 90 from phenylalanine to alanine there are additional exchanges from tryptophan at position 50, arginine at position 52 and phenylalanine at position 54 to the unpolar isoleucine. Changes in close proximity might enhance protein production and correct folding (85). M11 showed no active CYP505X expression. On the one hand there might be too many interfering mutations in the aa sequence to constrain the peptide backbone in a biologically active conformation. On the other hand, M11 incorporates tryptophan instead of valine at position 85. Although they are both hydrophobic, tryptophan is a bulky aa with an aromatic indole ring system, which might influence correct folding. Comparing M4 with M5, the substitution from alanine to leucine at position 332 had no enhancing influence on the protein production. By collating the enzyme concentrations of both, it appears that this replacement caused an adverse effect, resulting in 57.0 nM biologically active M4 compared with 115.0 nM of biologically active M5. There appears to be also a difference whether valine or alanine were incorporated at position 90 instead of phenylalanine. Generally, it seems that small and hydrophobic aa apparently have a positive effect on expression when incorporated at this position. The exchange from leucine to tryptophan at position 334 in M7 (124.4 nM) did not affect the expression in a strong way compared to M5. M10 was expressed in low levels and reached with 19.7 nM of biologically active enzyme the lowest CYP concentration produced in *E. coli* BL21.

Besides the influence on the level of post-translational folding of proteins, the introduced mutations could affect the behaviour on transcriptional level as well. Lower yields of active expressed CYP could be a consequence caused by the exchange of nucleotides at transcriptionally important positions such as regions within the promotor sequence and a

resulting formation of more unstable mRNA. The arise of unstable mRNA in *E. coli* could lead to an attenuated protein synthesis. Also a complete stop in the translation process is possible through mRNA degradation, initiated by an endonucleolytic attack mediated by the enzyme Rnase E with subsequent degradation by various types of exonucleases as PNPase, Rnase II or the oligoribonuclease (128). The substitution of nucleotides within the gene of interest could ensure that sulfur bonds, required for stability and shape, cannot get formed and thus lead to a dysfunctional protein as well as that premature stop signals are formed in the sequence leading to a subsequent abort of the translation and a truncated ineffective protein (129). Through existing research work and literature search as well as the selective alteration of the initial nucleotide sequence only within the CYP-coding sequence, these sources of error can be excluded for this thesis.

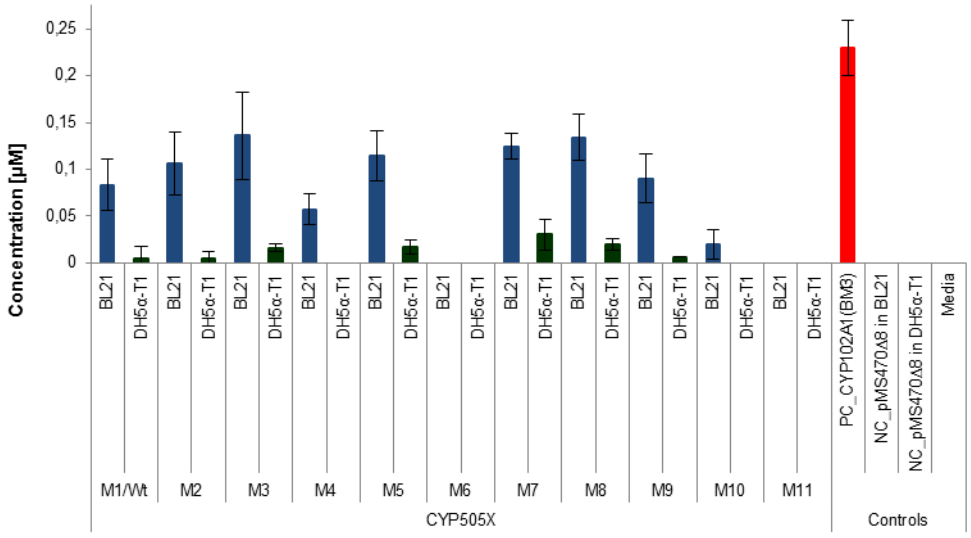

Figure 32: CYP concentration [in µM] of CYP505X mutant variants expressed in *E. coli* BL21 or DH5α-T1. As a positive control CYP102A1 (BM3) was expressed in *E. coli* DH5α-T1. As negative controls *E. coli* BL21 and DH5α-T1 were transformed with the empty vector pMS470Δ8, which does not contain a CYP gene. The formula used for calculation is pictured in chapter 3.7.1.. Concentrations are averages of triplicates (BL21) and tetraplicates (DH5α-T1).

Higher enzyme yields were obtained with the expression host *E. coli* BL21 compared to *E. coli* DH5α-T1 and I recommend to use this strain for expression of CYP505X in combination with the cultivation protocol developed during the thesis. The enzyme concentration of the different *E. coli* BL21 strains ranged from 19.7 nM to 136.0 nM and from 4.4 nM to 30.5 nM when expression was performed in *E. coli* DH5α-T1. 230 nM of the positive control CYP102A1 were produced in E. coli DH5α-T1. Based on the results of this assay, the variants M6 and M11 expressed in *E. coli* BL21 and DH5α-T1 as well as M4 expressed in *E. coli* DH5α-T1 were not produced in a biologically active conformation (Figure 32)

4.3.1.2. NADPH depletion-assay

The NADPH depletion-assay was performed to characterize the catalytic activity in lysates of the generated CYP variants and to detect the possible ability of substrate conversion. This was done by directly monitoring the depletion of cofactor NADPH at 340 nm, which is proportional to product formation (Figure 33).

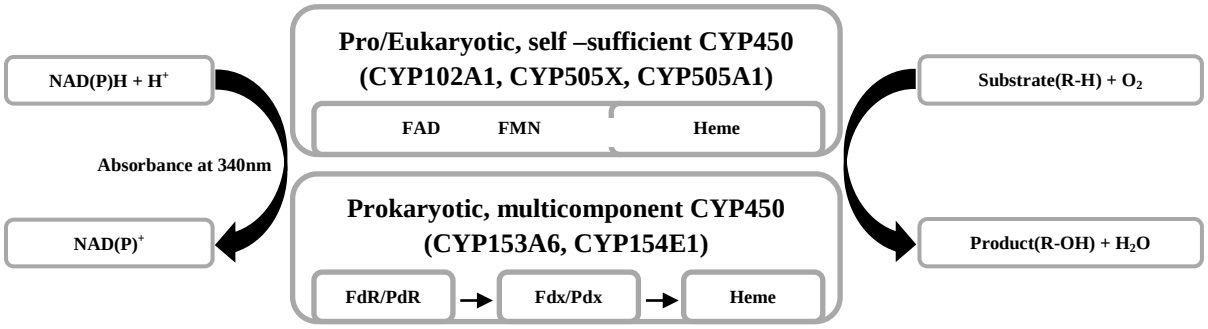

Figure 33: Electron transfer pathway in different CYP450s. NAD(P)H = β-Nicotinamide adenine dinucleotide phosphate-reduced, $NADP^+$ = β-Nicotinamide adenine dinucleotide phosphate, FAD = Flavin adenine dinucleotide, FMN = Flavin mononucleotide, FdR = Ferredoxin reductase, PdR = Putidaredoxin reductase, Fdx = Ferredoxin, Pdx = Putidaredoxin

The natural substrates of *B. megaterium* CYP102A1 are fatty acids (96). Lauric acid was used as substrate and electron acceptor, because the CYP505X wild-type enzyme from *A. fumigatus* was used to convert lauric acid in a previous study (48). NADPH depletion at 340 nm is shown in Figure 34.

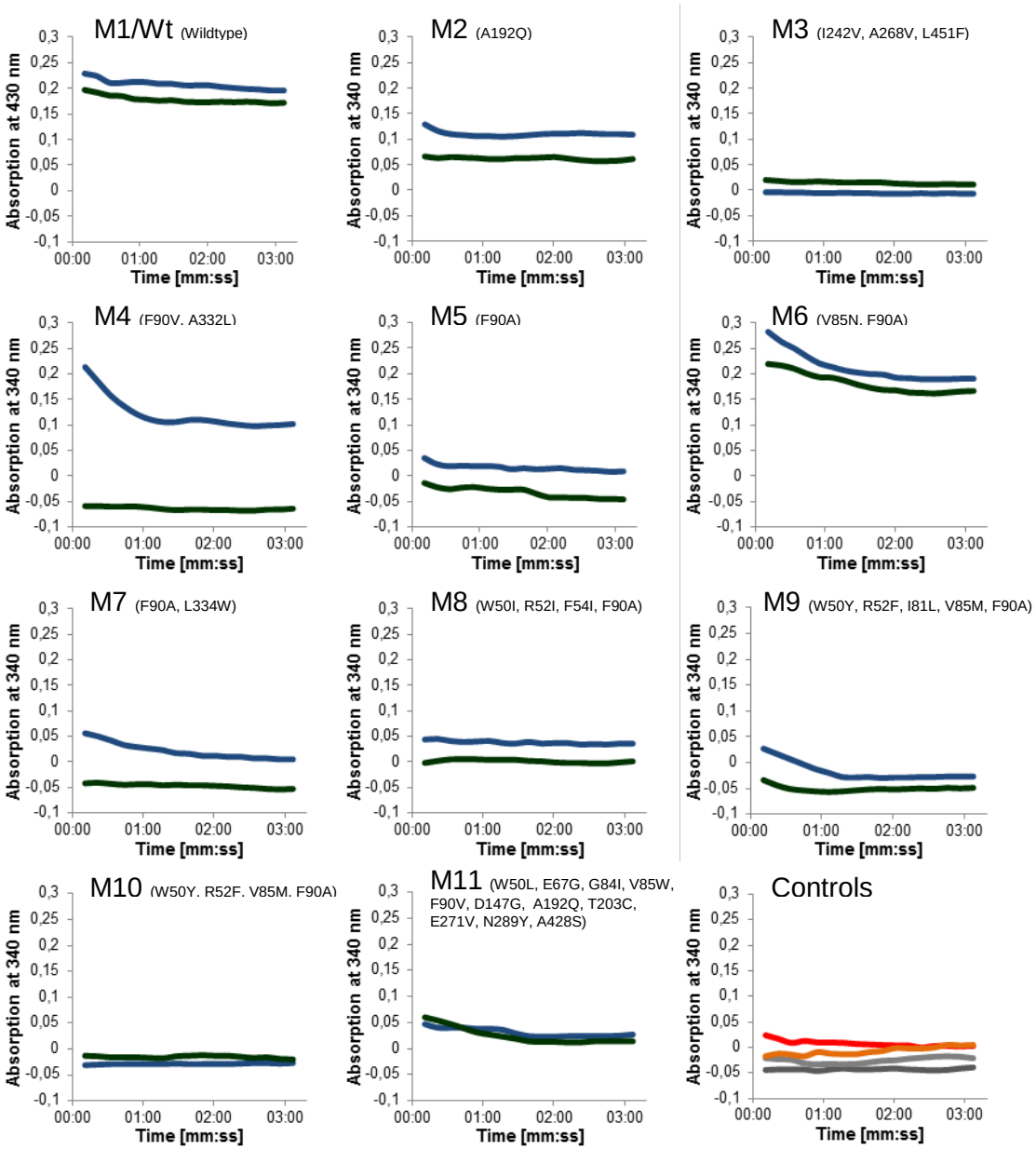

Figure 34: NADPH depletion at 340 nm measured for three minutes using CYP505X mutant variants expressed in *E. coli* BL21 (blue line) or DH5α-T1 (green line). 1:100 dilutions of the samples were used for the measurements. As a positive control CYP102A1 (BM3) was expressed in *E. coli* DH5α-T1 (red line). As negative controls *E. coli* BL21 (dark grey line) and DH5α-T1 (light grey line) were transformed with the empty vector pMS470Δ8, which does not contain a CYP gene. TB–media was used as sterile control (yellow line).

It remains unclear, if one of these CYP505X variants converted the substrate lauric acid at higher rates compared to the wild-type. NADPH was oxidized in most of the samples. However, NADPH oxidation might be caused by uncoupled effects. e.g. oxidation of the cofactor, where the reducing equivalents of the cofactor become uncoupled to substrate oxidation (112). In the course of such uncoupled reactions, oxygen is reduced by the supplied electrons from the cofactor and released as hydrogen peroxides, superoxides or water. The consequence, apart from the inactivation of the enzyme due to formation of active oxygen

species, is the low efficiency of the catalytic cycle and the identification of false positives in screening processes (112,121,130). Another possibility for a low NADPH depletion can be a low affinity of an enzyme to the substrate. In Table 12, the initial NADPH consumption rates in dependence of the NADPH depletion and the levels of biologically active CYP are shown.

Table 12: Catalytic properties of CYP505X variants M1/Wt-M11 expressed in *E. coli* BL21 or DH5α-T1. NADPH depletion was measured at 340 nm over three minutes as µmol NADPH / min. Expression of native enzyme was determined by CO-difference spectra-assay as nM CYP. NADPH consumption rates were measured as nmol NADPH / min / nmol protein. As a positive control CYP102A1 (BM3) was expressed in *E. coli* DH5α-T1. As negative controls *E. coli* BL21 and DH5α-T1 were transformed with the empty vector pMS470Δ8, which does not contain a CYP gene.

Construct		NADPH depletion [µmol / min]		Native CYP [nM]		Rate of NADPH consumption [min^{-1}]	
		BL21	DH5α-T1	BL21	DH5α-T1	BL21	DH5α-T1
CYP505X	M1/Wt	10.4	18.0	83.5	4.4	124.6	4090.9
	M2	31.1	0.0	106.4	4.4	292.3	0
	M3	0.0	27.3	136.0	16.4	0	1664.6
	M4	58.3	14.2	57.3	0.0	1017.5	0
	M5	18.5	48.0	114.6	17.5	161.4	2742.9
	M6	42.5	15.3	0.0	0.0	0	0
	M7	12.5	0.0	124.4	30.6	100.5	0
	M8	9.3	13.1	134.3	19.6	69.2	668.4
	M9	3.8	9.3	90.1	6.5	42.2	1430.8
	M10	7.6	0.0	19.6	0.0	387.8	0
	M11	4.9	31.1	0.0	0.0	0	0
Controls	NC_pMS470α8	0.0	0.0	0.0	0.0	0	0
	PC_CYP102A1 (BM3)	8.7		229.2		38.0	

The NADPH consumption rate varies among the different *E. coli* strains. A potential reason might be an ineffective cell lysis and separation process of the lysate throughout the preparation of the assay. There is no direct correlation between the amount of active expressed CYP and the quantity of oxidized NADPH. Referring to the obtained NADPH depletion results, the mutants M2 – M6 and M11 demonstrated a higher consumption of NADPH as the wild-type. Considering the obtained results from the CO-difference spectra-assay and the fact that no active enzyme was produced, it can be assumed that the values of M6 and M11 were generated due to uncoupled cofactor oxidation. The highest consumption of NADPH was obtained with M4, expressed in *E. coli* BL21 (58.3 µmol / min). By taking in the calculation the enzyme quantity used for the assay, M4 reached a consumption rate of 1017.5 nmol NADPH / min / nmol actively expressed enzyme. The highest NADPH consumption rate was obtained for the wild-type enzyme M1/Wt expressed in *E. coli* DH5α-T1 with 4090.9 nmol / min / nmol protein. CYP102A1 had with 38.0 nmol / min / nmol protein a low turnover of NADPH. In general, *E. coli* DH5α-T1 expressed enzyme variants exhibited higher NADPH consumption rates compared to the same variants expressed with

BL21. However, I recommend to revaluate the outcome of this assay with an analytical chromatographic method like high performance liquid chromatography (HPLC) or gas chromatography (GC) to determine the product formation of the individual mutants. Since also the very good substrate lauric acid with the well expressed control protein CYP102A1 did not give significant and reliable data indicating strong enzyme activity there seemed to be a systematic mistake in all assays such as for example the application of wrong dilution factors. An endpoint determination for NADPH absorption at 340nm could help to identify such mistakes.

4.3.1.3. 7-benzyloxyresorufin-assay

Several types of alkoxyresorufins are commonly used for whole-cell fluorescent screening assays. CYP102A1 from *B. megaterium* and engineered mutants are known to convert different types of alkoxyresorufins (113,124). The generated CYP variants were tested for their ability to convert 7-benzyloxyresorufin to the fluorescent product resorufin. When measuring the kinetic of 7-benzyloxyresorufin only a signal noise and scattering of the data points was detected (Appendix S 3). For this reason the presence of produced resorufin was determined using emission spectrum analysis.

In Figure 35, the spectra of CYP505X M1/Wt-M11 are shown. The yellow fluorescence of resorufin can be detected at 580 nm. At 580 nm, a peak was only obtained with the positive control CYP102A1. The generated mutants of CYP505X did not exhibit O-dealkylation of 7-benzyloxyresorufin to the product resorufin since the peaks at 580 nm were the same level as the negative controls. There is also an unexpected peak displayed at 620 nm both with the negative controls as well as the generated mutants and the positive control. No peak was detected at 620 nm with the sterile control. Since the appearance of 7-benzyloxyreorufin is in an orange colour (either as a powder or in a dissolved state) and orange points at its wavelength range of 585 nm – 650 nm a maximum at 620 nm, this could be an indication for the presence of the substrate. A lower peak at 620 nm indicates less substrate available. Comparing the mutants, the DH5α-T1 constructs did not change their behaviour in a strong way, related to the course of the spectra. In contrast to that, the spectra of the BL21 constructs changed from mutant to mutant. It is seen that the negative control in strain DH5α-T1 has the similar spectral characteristic as the mutant variants in DH5α-T1. That is not the case with the negative control and the mutant variants in BL21. On the one hand, this can be because of a strain-mediated cause such as different efficiencies in the uptake of the substrate and a background-conversion of 7-benzyloxyreorufin by different host cells. Consequently, the

mutants in BL21 can accommodate substrate in a different way, although better as the negative control but worse than the mutants in DH5α-T1. On the other hand, the lower peak can imply the lower presence of substrate because of a conversion. And if it doesn't result in the conversion to the product Resorufin, a different regioselective conversion of 7-benzyloxyreorufin might cause the decrease of the peaks at 620 nm. A more precise statement can be made by following HPLC. I propose to optimize and repeat this assay. Alternatively the measurement of a commercial sample of the product resorufin could have helped to identify the potential problem with this assay.

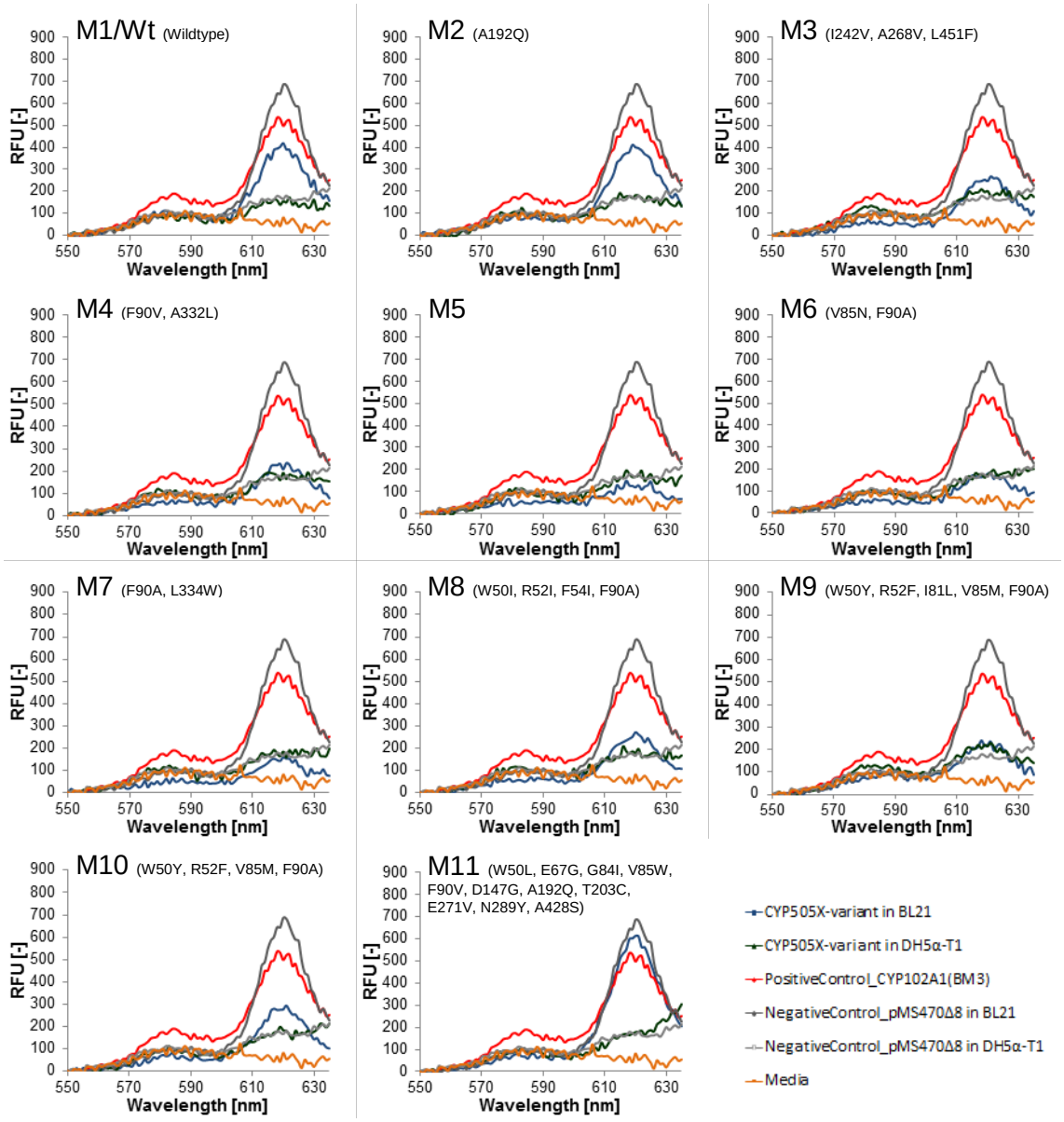

Figure 35: Determination of resorufin fluorescence spectra (λex = 530 nm, λem = 580 nm) with CYP505X M1/Wt-M11 expressed in *E. coli* BL21 or DH5α-T1. Biological tetraplicates (BL21) and triplicates (DH5α-T1) are shown. As a positive control CYP102A1 (BM3) was expressed in *E. coli* DH5α-T1. As negative controls *E. coli* BL21 and DH5α-T1 were transformed with the empty vector pMS470Δ8, which does not contain a CYP gene.

4.3.1.4. 7-benzoxy-3-carboxycoumarin ethyl ester (BCCE)-assay

Ruff et al. demonstrated an O-dealkylation of the substrate 7-benzoxy-3-carboxycoumarin ethyl ester (BCCE), where the ethyl ester is cleaved to the corresponding carboxylic acid by CYP102A1 variants from *B. megaterium* (114). The carboxylic acid displays a specific fluorescence and can be recorded (λex = 400 nm, λem = 440 nm). The newly constructed CYP variants were tested on their ability to convert BCCE. Positive control CYP102A1 from *B. megaterium* as well as the negative controls *E. coli* BL21 and DH5α-T1 cells, harbouring the pMS470 vector without the CYP450 genes of interest, revealed a low noise-to-signal ratio and low fluorescence could be detected. Both *E. coli* BL21 and *E. coli* DH5α-T1 cells can exploit the substrate.

The wild-type CYP505X as well as some mutants (M2, M5, M7, M8, M9 and M10) were able to convert the substrate whereby the wild-type and M2 exhibited only low turnovers (Figure 36). Nearly all aa mutations of the single variants (except I242, N289 and A428) are located in the surrounding of the active site. The mutation A192Q of M2 changed the hydrophobicity of the active site. The shift from a hydrophobic to a polar aa might facilitate the incorporation of the substrate. The mutation at position F87 in CYP102 (BM3) turned out as an attractive industrial tool with enhanced substrate specificity (131). The homologous position F90 from CYP505 seems also to be a key residue for substrate recognition. This aa is in the direct environment of the heme domain in the catalytic core and might influence the access behaviour for compounds. The mutants M5, which contain the exchange at position 90 from phenylalanine to alanine, also converted the substrate. Phenylalanine and alanine are hydrophobic, but the more bulky phenylalanine might impede access to the active site.

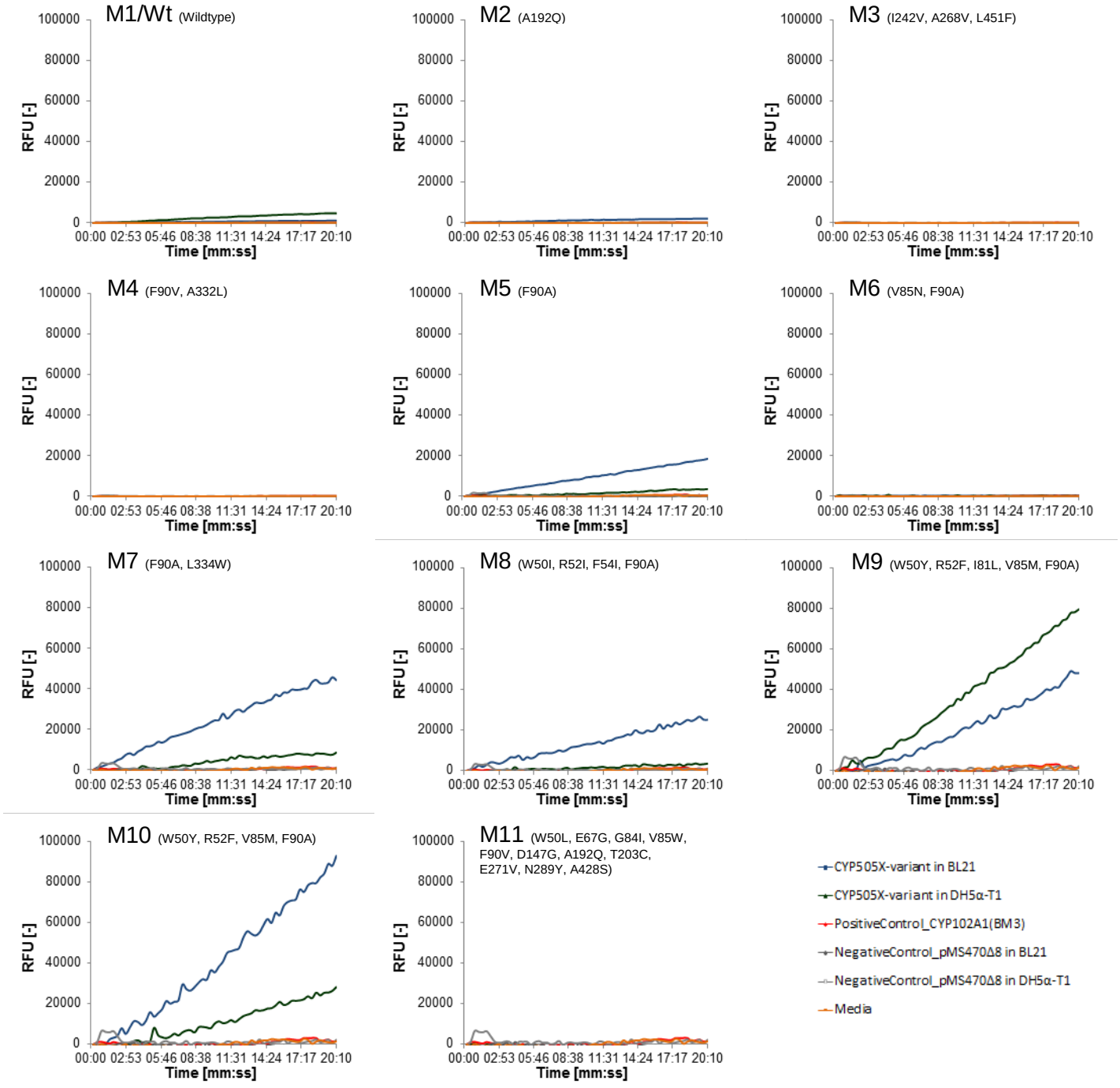

Figure 36: Conversion over time of BCCE by CYP505X M1/Wt-M11 expressed in *E. coli* BL21 or DH5α-T1. Biological tetraplicates (BL21) and triplicates (DH5α-T1) are shown. As a positive control CYP102A1 (BM3) was expressed in *E. coli* DH5α-T1. As negative controls *E. coli* BL21 and DH5α-T1 were transformed with the empty vector pMS470Δ8, which does not contain a CYP gene. Data points are normalized to 0.

M4 as well as M6 have one additional mutation compared to M5, namely alanine to leucine at position 332 (M4) and valine to asparagine at position 85 (M6) and they did not convert the model-substrate. In M4, F90 and A332 are both located ahead of the axial plane. The change of only F90A as in M5 allows some conversion of BCCE. However, exchange from phenylalanine to valine at position 90 together with the mutation A332L could have hindered

the substrate to get in contact with the catalytic core. In M6, the change to the bigger, hydrophilic aa asparagine at position 85 could have had an effect on correct folding. The lack of substrate conversion might most probably be caused by the lack of active enzyme. In M7, the additional mutation to F90A through the exchange of leucine to tryptophan at position 334 seems to be an advantage for BCCE-conversion. There was a 2.6-fold higher production of the carboxylic acid compared to M5 (Figure 37). With M8, the additional exchanges of tryptophan at position 50, arginine at position 52 and phenylalanine at position 54 to the unpolar isoleucine led to an increased product formation compared to M5. The change from the basic arginine to the hydrophobic isoleucine results in an omission of the bigger guanidinium group of arginine. All three exchanges caused a conformational change in the monooxygenase structure. The mutations could have facilitated the substrate`s access to the active centre. M9 and M10 showed the highest conversion rates of all mutants. It seems that the exchange of isoleucine to leucine at position 81 in M9 has no additional benefit for converting this substrate. By comparing M9 with M10 even a negative effect can be observed. Further the exchanges W50Y and R52F alter polarity and might have a positive impact on substrate recognition. There cannot be said whether incorporation of methionine at position 85 has a positive effect. The efficacy of this mutation could be covered by W50Y and R52F. Another reason for the inability of some of the generated mutants to convert the substrate could be that the enzyme structure changed through aa substitutions and subsequently the affinity was lowered.

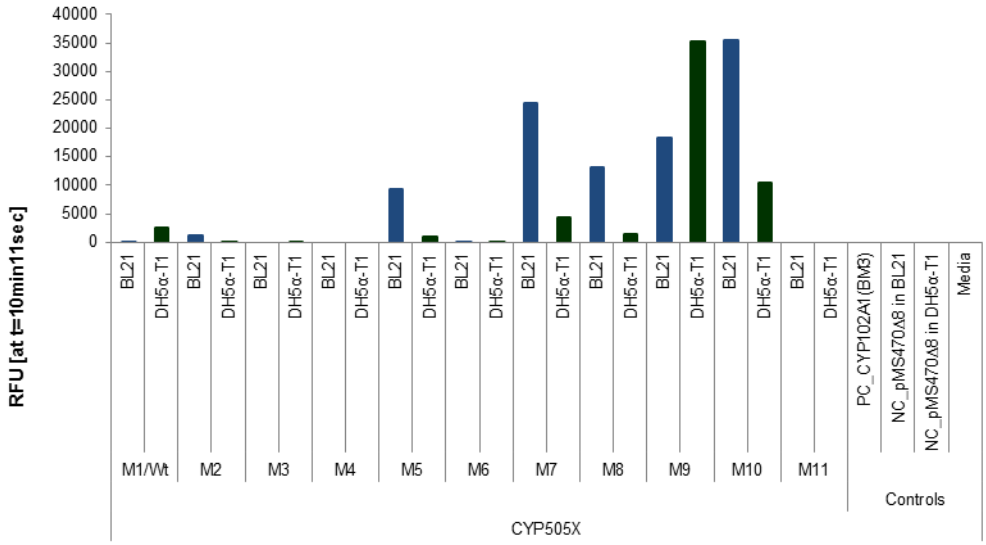

Figure 37: BCCE conversion by the individual CYP505X mutants after 10 minutes and 11 seconds. As a control CYP102A1 (BM3) was expressed in *E. coli* DH5α-T1. As negative controls *E. coli* BL21 and DH5α-T1 were transformed with the empty vector pMS470Δ8, which does not contain a CYP gene.

4.3.1.5. 12-p-nitrophenoxycarboxylate (12-pNCA)-assay

The pNCA-assay can be performed in a short time and substrate formation can be detected even with the naked eye. The assay was used to screen variants of CYP102A1 from *B. megaterium* generated by directed evolution (122). Furthermore it was demonstrated that mutant CYP102A1 (F87A) showed a higher conversion of 12-pNCA compared to the wild-type enzyme (115). The eukaryotic CYP505X from *A. fumigatus* and the two prokaryotic enzymes CYP153A6 and CYP154E1 from M*ycobacterium sp.* HXN1500 and *T. fusca TM51* were tested for the conversion of pNCA.

As illustrated in Figure 38, the CYP505X wild-type enzyme and CYP505X-M2 (A192Q) from CYP505X were able to convert the 12-pNCA to a greater extend compared to CYP102A1 (BM3).

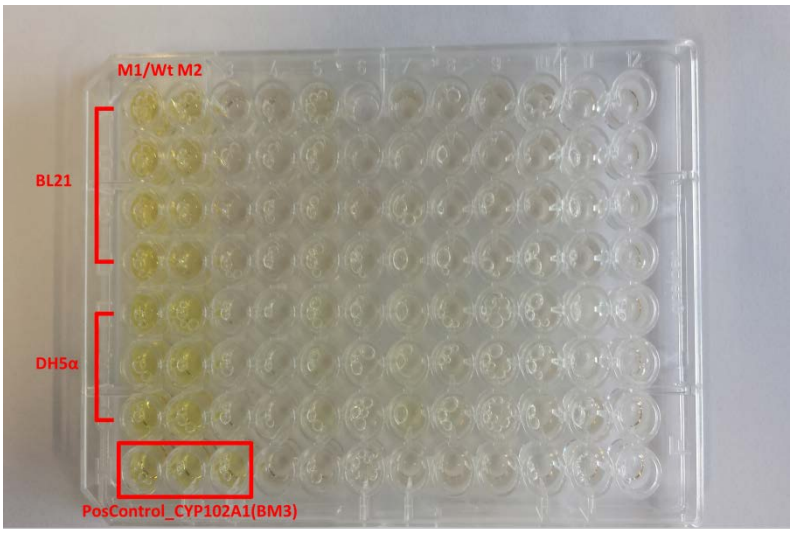

Figure 38: 12-pNCA-assay with CYP505X M1/Wt-M11 expressed in *E. coli* BL21 or DH5α-T1. Biological tetraplicates (BL21) and triplicates (DH5α-T1) are shown. As negative controls *E. coli* BL21 (96-MTP well H4-H6) and *E. coli* DH5α-T1 (96-MTP well H7-H9) bearing the empty vector pMS470Δ8 were used. TB-media was used as a sterile control (96-MTP well H10-H12).

M1/Wt expressed in BL21 showed an approximately 2.0-fold higher formation of p-nitrophenolate than the positive control (Figure 39). None of the mutations had a beneficial effect on pNCA conversion. Using M2 a slightly reduced (BL21) or similar (DH5a-T1) product formation was observed compared to the wildtype enzyme M1/Wt. Most probably the mutation A192Q impedes the access of the substrate to the catalytic centre. However the mutant was still able to produce p-nitrophenolate at 1.75-fold higher rates compared to the positive control CYP121A1 (BM3). Most of the other variants converted the substrate at lower levels compared to CYP121A1 (BM3).

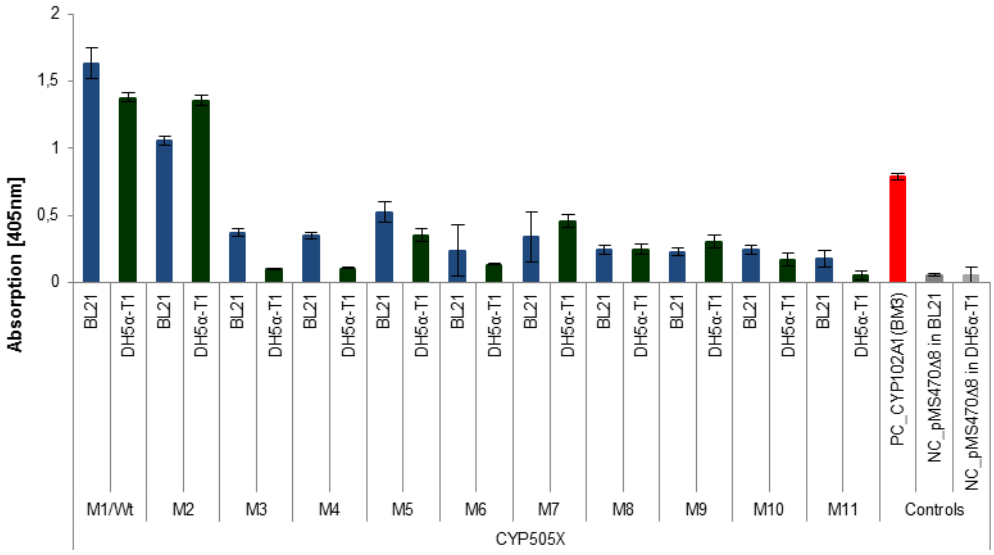

Figure 39: p-Nitrophenolate formation at 405 nm by CYP505X M1-M11 expressed in *E. coli* BL21 and DH5α-T1. As a positive control CYP102A1 (BM3) was expressed in *E. coli* DH5α-T1. As negative controls *E. coli* BL21 and DH5α-T1 were transformed with the empty vector pMS470Δ8, which does not contain a CYP gene.

4.3.2. Expression of CYP505X in *P. pastoris*

4.3.2.1. Carbon monoxide (CO)-difference spectra-assay

The CO-difference spectra-assay was performed with generated *P. pastoris* mutants to determine the concentration of the enzyme and to get information about their biological conformation and activity.

The *P. pastoris* codon optimized wild-type enzyme CYP505X was cloned in the expression vectors pPpT4_S and pPpB1_S to generate CYP505X-M12 and M13, respectively. The *P. pastoris* host strains BSYBG10, BSYBG11, CBS7435 Wt and CBS7435 MutS were transformed with the plasmids. In Figure 40, the CO spectra of CYP505X-M12, expressed in the four different *P. pastoris* strains, is shown. No peak at 450 nm was obtained for the positive control expressing the human CYP2D6. That is an unexpected result, since the CO-difference spectra-assay was used to quantify CYP2D6 by Gudiminchi et al. (111). The negative controls (*P. pastoris* Wt strains) did not produce active CYP, indicated by the peak at 420 nm. When using yeast whole cells for CO-difference spectrum, a 420 nm peak results from the expression of native cytochrome oxidases (132).

Different CYP505X levels were obtained using the *P. pastoris* host strains. BSYBG10 generated approximately 97 nM of active enzyme and its derivative BSYBG11 was able to produce 159 nM. Both CBS7435 Wt and MutS could produce higher amounts of active enzyme (137 nM and 186 nM, respectively). Both MutS strains produced more correctly folded protein. The MutS strains use the weaker Aox2 for methanol utilization resulting in a slow growth and a longer time period, where methanol is available for induction of the protein expression. In addition to weaker methanol utilization the cells have a reduced metabolism and less oxidative stress, which also has an influence on expression (59). The CO spectra showed that the enzyme CYP505X from *A. fumigatus* was catalytically active expressed in the heterologous host *P. pastoris*.

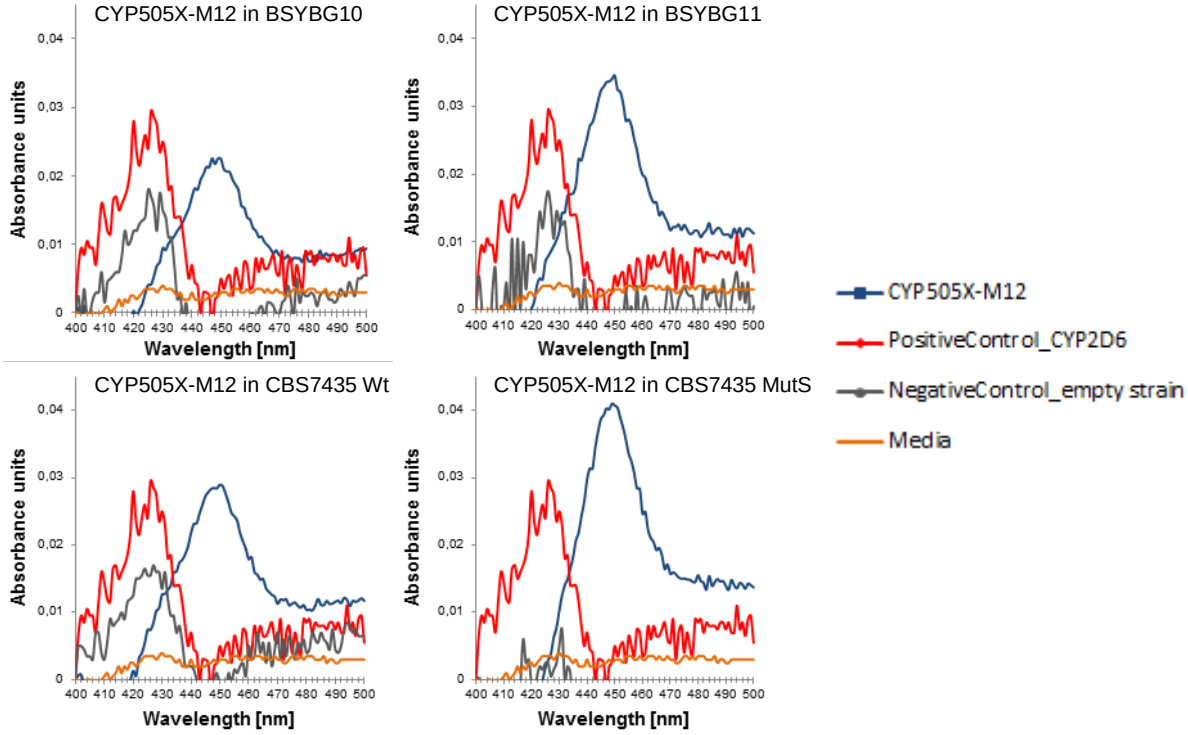

Figure 40: CO spectra of CYP505X-M12 (in vector pPpT4_S) expressed in the *P. pastoris* strains BSYBG10, BSYBG11, CBS7435 Wt and CBS7435 MutS. Data points are averages of 15 clones and normalized to 0. As a positive control human CYP2D6 was expressed in *P. pastoris* CBS7435 Wt. The *P. pastoris* strains BSYBG10, BSYBG11, CBS7435 Wt and CBS7435 MutS were used as negative controls.

Altering the expression vector from pPpT4_S to pPpB1_S had an influence in expression of native CYP. The CYP505X levels of the four *P. pastoris* strains were lower, when pPpB1_S was used as expression vector compared to the vector pPpT4_S (Figure 40 / Figure 41). Using the pPpB1_S vector, BSYBG10 and BSYBG11 produced 76 nM and 42 nM CYP and CBS7435 Wt and its derivative CBS7435 MutS generated 110 nM and 52 nM, respectively.

Approximately 2-fold higher active CYP levels were obtained with the Wt strains compared to the MutS strains, when the pPpB1_S plasmid was used (Figure 42).

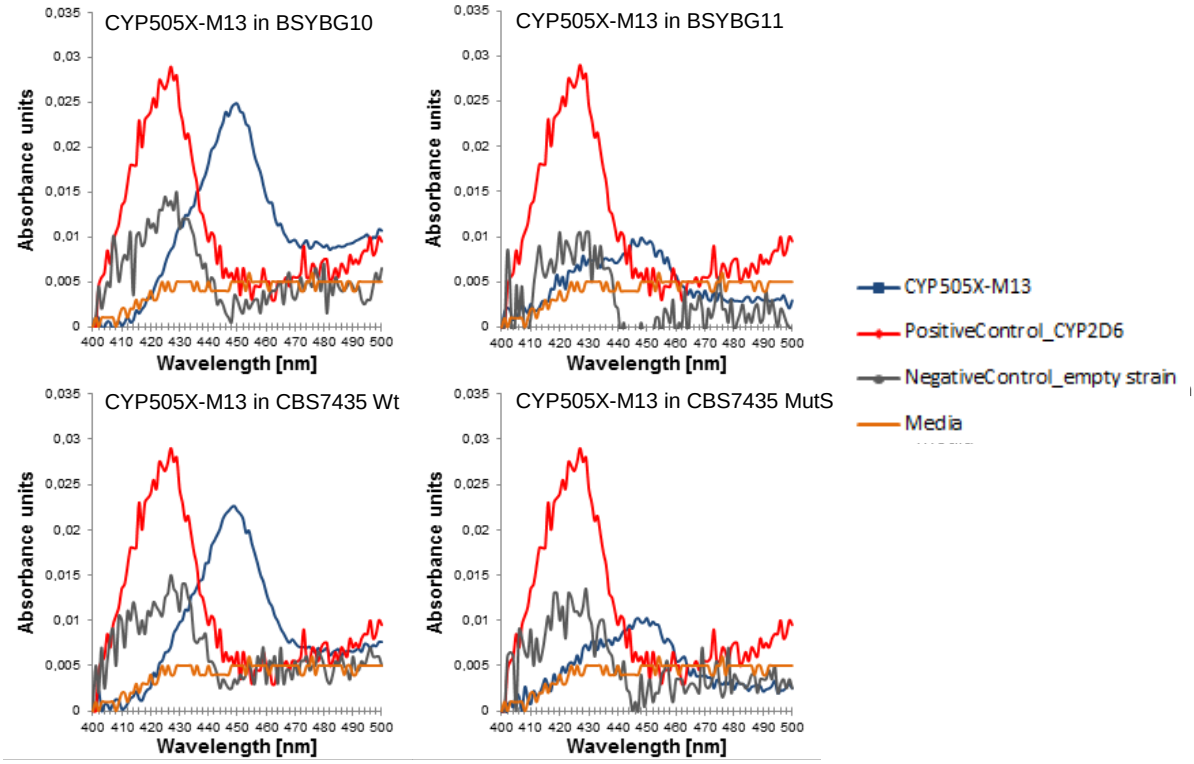

Figure 41: CO spectra of CYP505X-M13 (in vector pPpB1_S) expressed in the *P. pastoris* strains BSYBG10, BSYBG11, CBS7435 Wt and CBS7435 MutS. Data points are averages of 15 clones and normalized to 0. As a positive control human CYP2D6 was expressed in *P. pastoris* CBS7435 Wt. The *P. pastoris* strains BSYBG10, BSYBG11, CBS7435 Wt and CBS7435 MutS were used as negative controls.

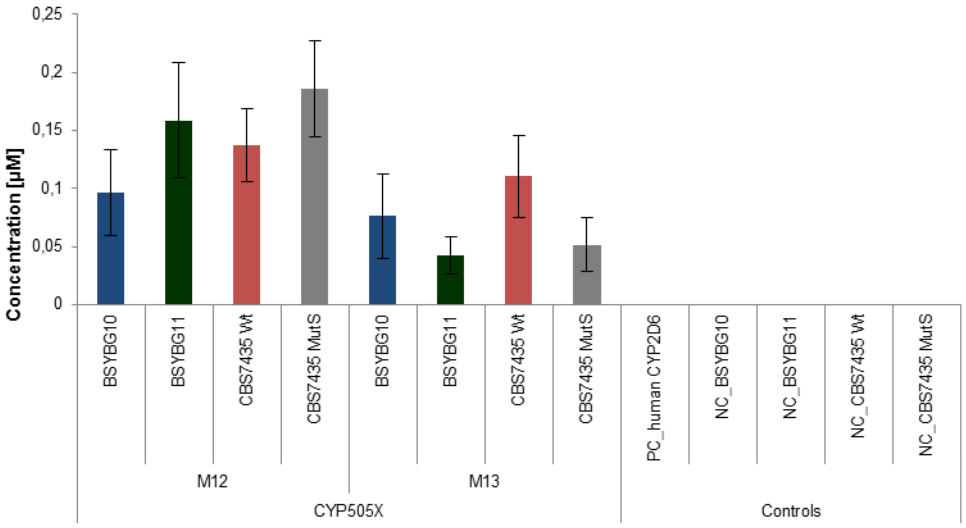

Figure 42: CYP concentration [in µM] of CYP505X-M12 and M13 expressed in the *P. pastoris* strains BSYBG10, BSYBG11, CBS7435 Wt and CBS7435 MutS. As a positive control human CYP2D6 was expressed in *P. pastoris* CBS7435 Wt. As negative controls the *P. pastoris* strains BSYBG10, BSYBG11, CBS7435 Wt and CBS7435 MutS (without an integrated expression cassette) were used. Formula used for calculation is shown in chapter 3.7.1.. Concentrations are averages of 15-fold replicates.

4.3.2.2. 7-methoxy-4-(aminomethyl)-coumarin (MAMC)-assay

A whole-cell activity assay was performed with CYP505X constructs using MAMC as substrate. The O-demethylation of MAMC to its product HAMC (7-methoxy-4-(aminomethyl)-coumarin was recorded using the excitation wavelength 405 nm and the emission wavelength 480 nm. The *P. pastoris* strains BSYBG10 and CBS7435 Wt were used as negative controls. The human CYP2D6 was used as a positive control, because of its ability to convert this substrate (111).

As pictured in Figure 43, M12 and M13 were not able to convert MAMC in contrast to the human CYP2D6. This result was not surprising at all because of the knowledge about the synthetic substrate MAMC and its selectivity for CYP2D6 (116).

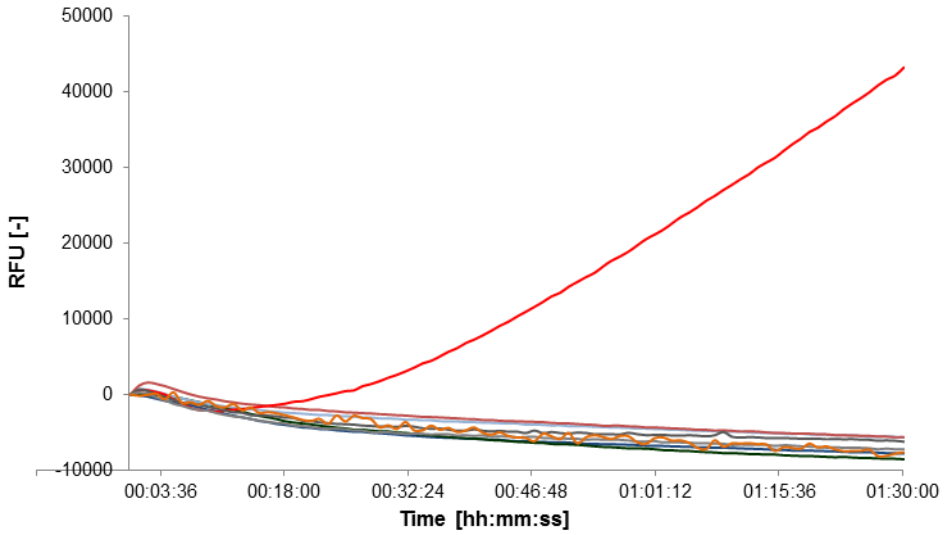

Figure 43: Conversion over time of MAMC by CYP505X-M12 (CYP505X in vector pPpT4_S) / -M13 (CYP505X in vector pPpB1_S) in *P. pastoris* BSYBG10 (---- / ----) or CBS7435 Wt (---- / ----). Data points are averages of 42 clones and normalized to 0. As positive control the human CYP2D6 expressed in *P. pastoris* CBS7435 Wt (----) was used. Negative controls were BSYBG10 (----) and CBS7435 Wt (----) (without an integrated CYP expression plasmid). Minimal media was used as sterile control (----).

4.3.3. Expression of CYP505A1 in *P. pastoris*

4.3.3.1. Carbon monoxide (CO)-difference spectra-assay

The soluble eukaryotic CYP505A1 from the fungus *F. oxysporum* was codon optimized for the expression in *P. pastoris*. CYP505A1-M1 and M2 were cloned in the expression vectors pPpT4_S and pPpB1_S. The four *P. pastoris* host strains BSYBG10, BSYBG11, CBS7435 Wt and CBS7435 MutS were transformed with the CYP expression vectors.

Using the pPpT4_S expression vector only low amounts of approximately 82 nM and 60 nM CYP505A1 were produced with BSYBG11 and CBS7435 MutS. The Wt strains did not produce active CYP505A1 (Figure 44 / Figure 46).

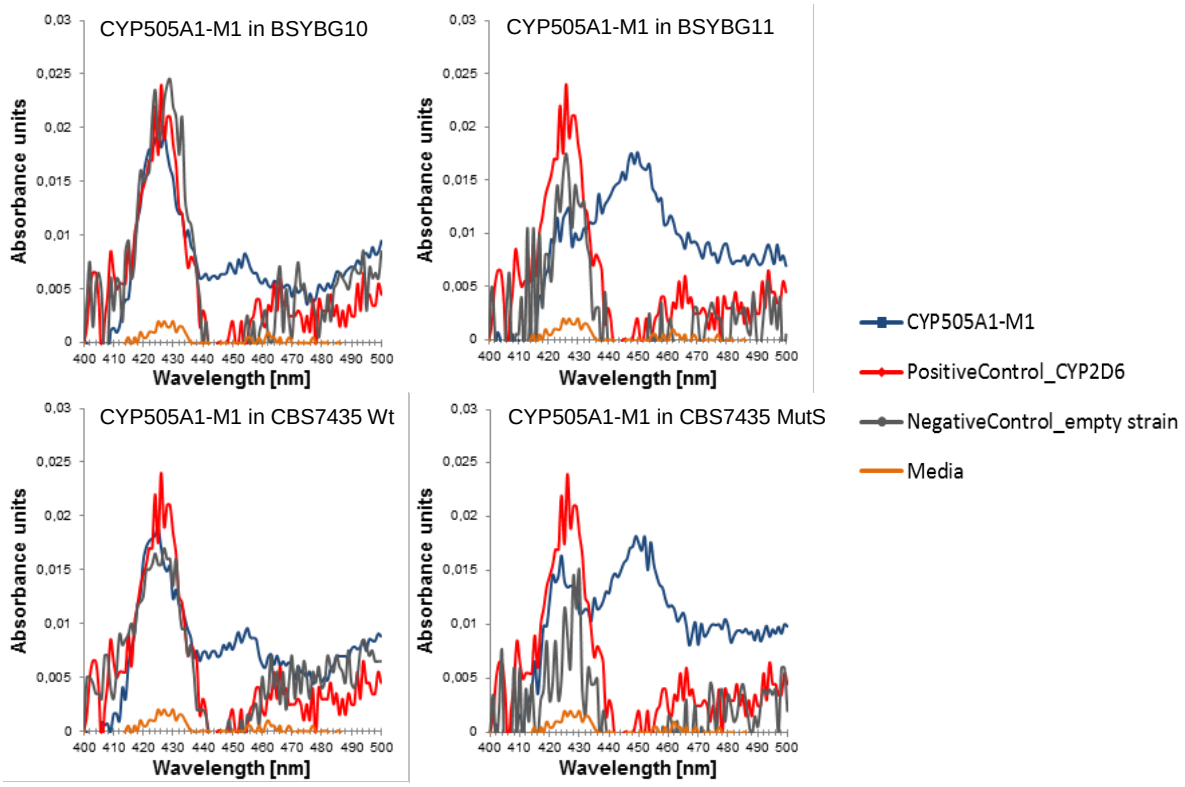

Figure 44: CO spectra of CYP505A1-M1 (in vector pPpT4_S) expressed in the *P. pastoris* strains BSYBG10, BSYBG11, CBS7435 Wt and CBS7435 MutS. Data points are averages of 15 clones and normalized to 0. As a positive control human CYP2D6 was expressed in *P. pastoris* CBS7435 Wt. The *P. pastoris* strains BSYBG10, BSYBG11, CBS7435 Wt and CBS7435 MutS were used as negative controls.

Using the pPpB1_S expression vector, the CYP levels were similar compared to the strains harbouring the pPpT4_S plasmid. 31 nM and 24 nM CYP were obtained with the *P. pastoris* Wt strains BSYBG10 and CBS7435. The enzyme production using BSYBG11 and CBS7435 MutS was a little higher compared to M1 resulting in 74 nM and 51 nM CYP (Figure 45 / Figure 46).

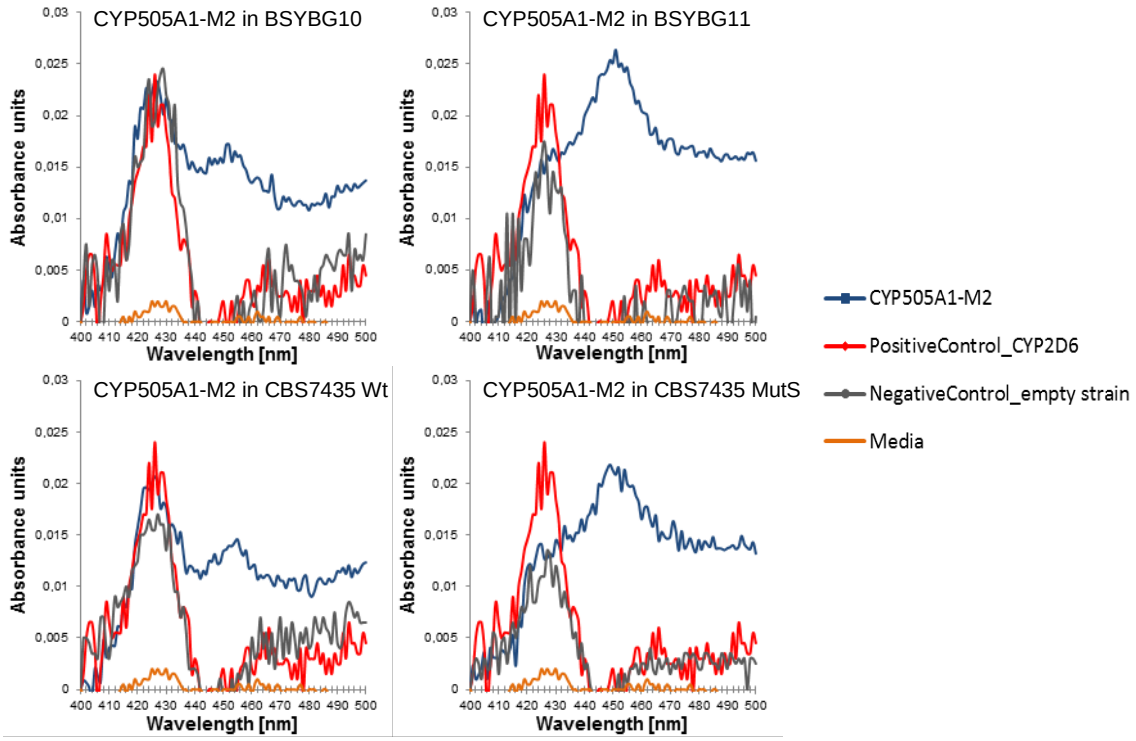

Figure 45: CO spectra of CYP505A1-M2 (in vector pPpB1_S) expressed in the *P. pastoris* strains BSYBG10, BSYBG11, CBS7435 Wt and CBS7435 MutS. Data points are averages of 15 clones and normalized to 0. As a positive control human CYP2D6 was expressed in *P. pastoris* CBS7435 Wt. The *P. pastoris* strains BSYBG10, BSYBG11, CBS7435 Wt and CBS7435 MutS were used as negative controls.

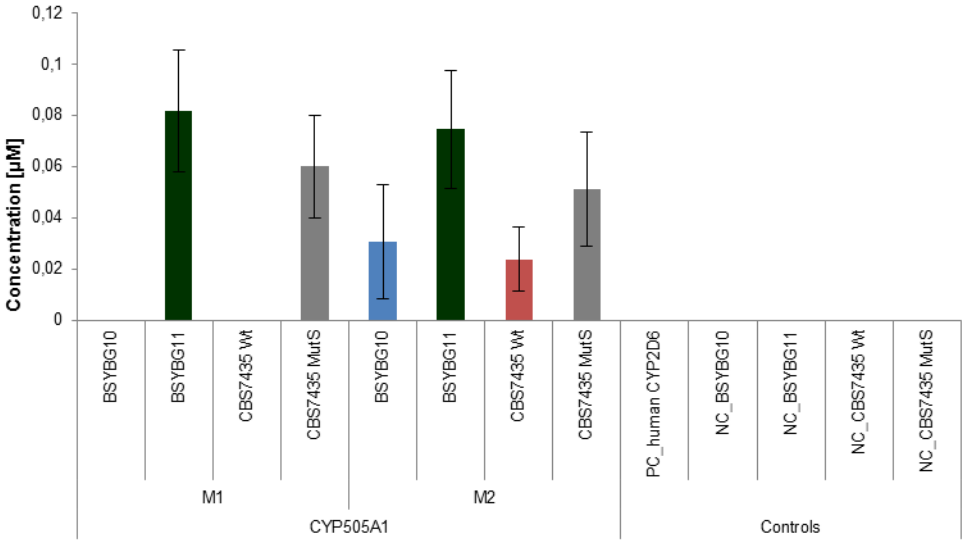

Figure 46: CYP450 concentration [in µM] of CYP505A1-M1 and M2 expressed in the *P. pastoris* strains BSYBG10, BSYBG11, CBS7435 Wt and CBS7435 MutS. As a positive control human CYP2D6 was expressed in *P. pastoris* CBS7435 Wt. The *P. pastoris* strains BSYBG10, BSYBG11, CBS7435 Wt and CBS7435 MutS were used as negative controls. Formula used for calculation is shown in chapter 3.7.1. The concentrations are averages of 15-fold replicates.

4.3.3.2. 7-methoxy-4-(aminomethyl)-coumarin (MAMC)-assay

CYP505A1, integrated into BSYBG10 and CBS7435 Wt, was not active on MAMC and did not form HAMC by O-demethylation. The human CYP2D6 was able to convert the synthetic substrate (Figure 47).

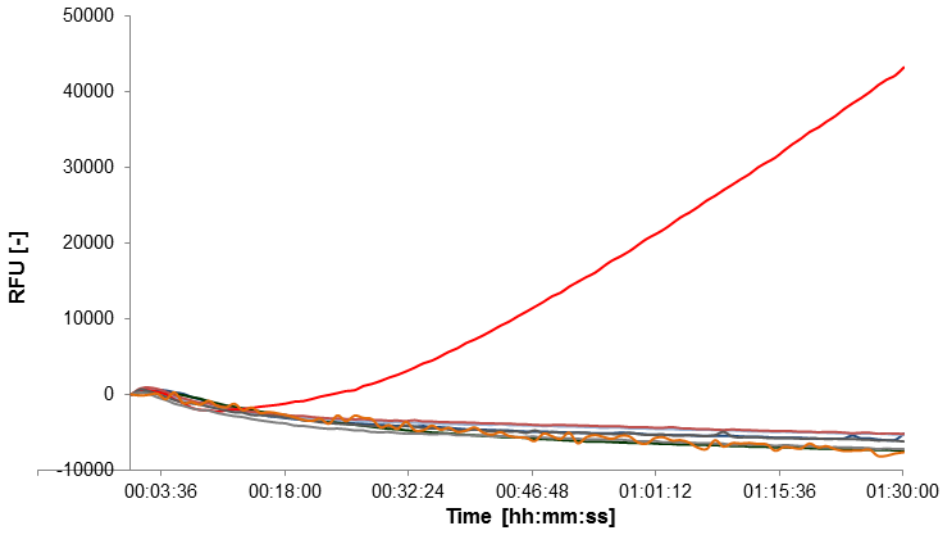

Figure 47: Conversion over time of MAMC by CYP505A1-M1 (CYP505A1 in vector pPpT4_S) / -M2 (CYP505A1 in vector pPpB1_S) expressed in *P. pastoris* BSYBG10 (---- / ----) or CBS7435 Wt (---- / ----). Data points are averages of 42 clones and normalized to 0. As positive control the human CYP2D6 expressed in P. pastoris CBS7435 Wt (----) was used. Negative controls were BSYBG10 (----) and CBS7435 Wt (----) (without an integrated CYP expression plasmid). Minimal media was used as sterile control (----).

4.3.4. Expression of CYP153A6 in *E. coli*

4.3.4.1. Carbon monoxide (CO)-difference spectra-assay

With the generated mutant CYP153A6-M1 it has been even observed that the expression behaviour changed due to an alteration in the cultivation protocol (chapter 4.2.). The CO spectra of CYP153A6-M1, expressing the whole operon of *Mycobacterium sp*. including the monooxygenase, the ferredoxin reductase (FdR) and the ferredoxin (Fdx), is shown in Figure 48. In panel A, a recorded CO spectrum of CYP153A6-M1 after cultivation with the initial cultivation conditions is depicted. 62 nM and 111 nM CYP were produced with *E. coli* BL21 and *E. coli* DH5α-T1 cells, respectively. 596 nM of the positive control CYP102A1 were obtained. Altering the cultivation parameters led to an increase in protein yield when using *E.coli* BL21 cells as host organism, depicted in panel B. Using *E. coli* BL21 cells, a 2.7-fold higher amount (170 nM) of correctly folded CYP153A6-M1 was obtained. *E. coli* DH5α-T1 cells produced with 46 nM only approximately 1.6-fold less protein and the enzyme concentration of the positive control was approximately 340 nM, the 1.75-fold less compared to the initial cultivation (Figure 48, Panel A). As in chapter 4.2, it can be seen the different behaviour of the two expression strains at different cultivation conditions. By comparing the hosts, it became evident that *E. coli* DH5α-T1 reacts negatively to the change in the cultivation conditions such as the extension of the cultivation time. This is indicated with CYP505X, CYP153A6 and the used positive control CYP102A1, all expressed in *E. coli* DH5α-T1 at a lower level as with the initial conditions. In contrast, when using the altered cultivation protocol, more biologically active enzyme was obtained with *E. coli* BL21 cells as host organism. Beneath more active enzyme, also a lot of CYP was detected in a biologically inactive form. It can be concluded that the choice of the expression host affect the yield of biologically active expressed CYP. In case of use of *E. coli* BL21 cells as CYP expression host to accomplish high transformation efficiencies and high-level expression, I recommend the use of the altered protocol for cultivation. If you want to use *E. coli* DH5α-T1 as CYP expression host due to its superior transformation efficiency, enhanced insert stability and plasmid yield, I recommend to use the initial cultivation protocol (57,58).

For CYP153A6, I suggest the optimization of the cultivation routine to avoid misfolding and increase the yield of catalytically active enzyme. The altered cultivation routine was used for the production of the generated constructs CYP153A6-M1 and M2.

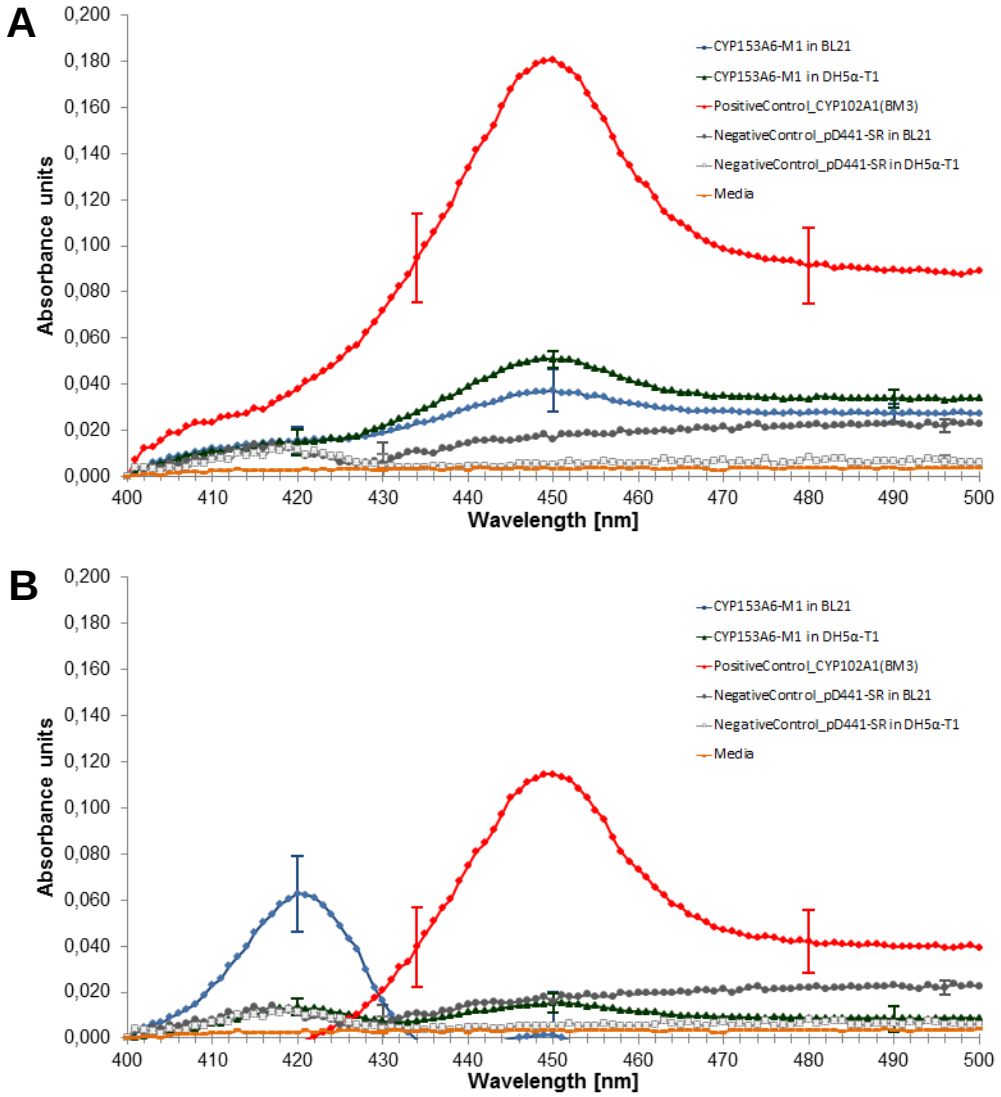

Figure 48: CO spectrum of CYP153A6-M1 expressed in *E. coli* BL21 or DH5α-T1 using various cultivation conditions. M1 contains the complete operon from *Mycobacterium sp.* strain HXN1500 (P450 monooxygenase, Ferredoxin reductase [FdR], Ferredoxin [Fdx]). Data points are averages of 24 clones (BL21) / 18 clones (DH5α-T1) and are normalized to 0. As a positive control CYP102A1 (BM3) was expressed in *E. coli* DH5α-T1. As a negative control *E. coli* BL21 / DH5α-T1 strains bearing the empty vector pD441-SR were used. The data points were normalized to 0. **A**: The preculture was incubated overnight at 37°C and 300 rpm. The main culture was started with an OD of 0.2 in 200 µL/well TB-media. Ampicillin was added as selection marker. Induction was done with 2 mM IPTG. Cultivation of the main culture took place overnight at 250 rpm and 30°C. **B:** The optimized cultivation parameters: The preculture was incubated for 24 hours at 250 rpm and 80% humidity. For the main culture, 400 µL/well TB-media were used and mixed with 0.5 mM 5-aminolevulinic acid, 250 µL/L of a trace-element solution and ampicillin as selection marker. Induction was conducted with 10 µM IPTG. The cell material from the preculture was transferred to the main culture by stamping and cultivation was accomplished at 250 rpm and 26°C for 24 hours.

By fusing the CYP505X-reductase domain from *A. fumigatus* to the monooxygenase from *Mycobacterium sp.* to generate CYP153A6-M2, the yield of biologically active enzyme increased (Figure 49). BL21 cells expressed a 2.7-fold higher amount of CYP153A6-M2 (450 nM) compared to CYP153A6-M1 (170 nM). However it also has to be mentioned that a

different promoter was used for M2 compared to the operon in M1. DH5α-T1 cells and the positive control CYP102A1 yielded 30 nM and 340 nM CYP, respectively (Figure 50). The yield of CYP153A6-M2 in DH5α-T1 was around 0.65-fold less than with CYP153A6-M1 in DH5α-T1.

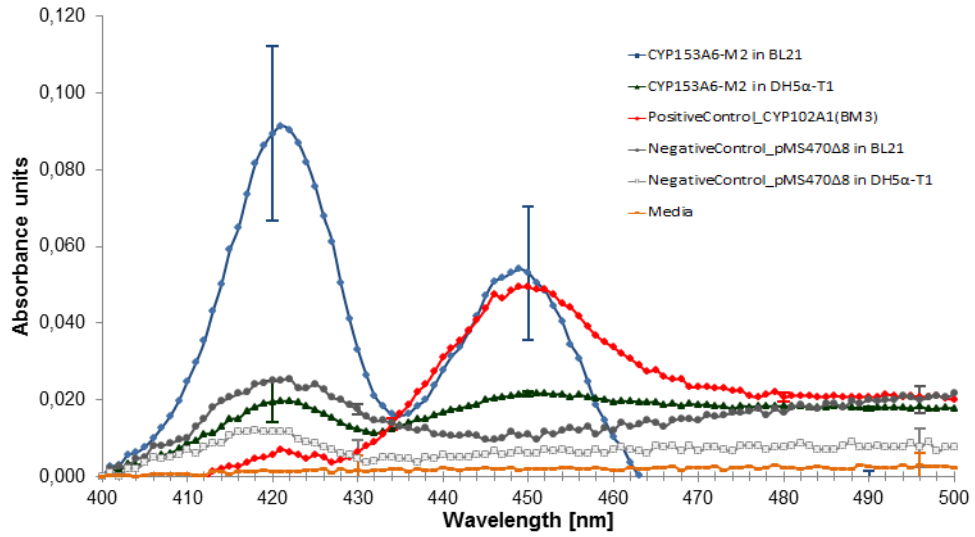

Figure 49: CO spectrum of CYP153A6-M2 expressed in *E. coli* BL21 or DH5α-T1. M2 is a fusion construct consisting of the monooxygenase domain from the CYP153A6-M1 operon and the reductase domain of CYP505X. Data points are averages of 24 clones (BL21) / 18 clones (DH5α-T1) and are normalized to 0. As a positive control CYP102A1 (BM3) was expressed in *E. coli* DH5α-T1. As negative controls *E. coli* BL21 and DH5α-T1 were transformed with the empty vector pMS470Δ8, which does not contain a CYP gene. Data points are normalized to 0.

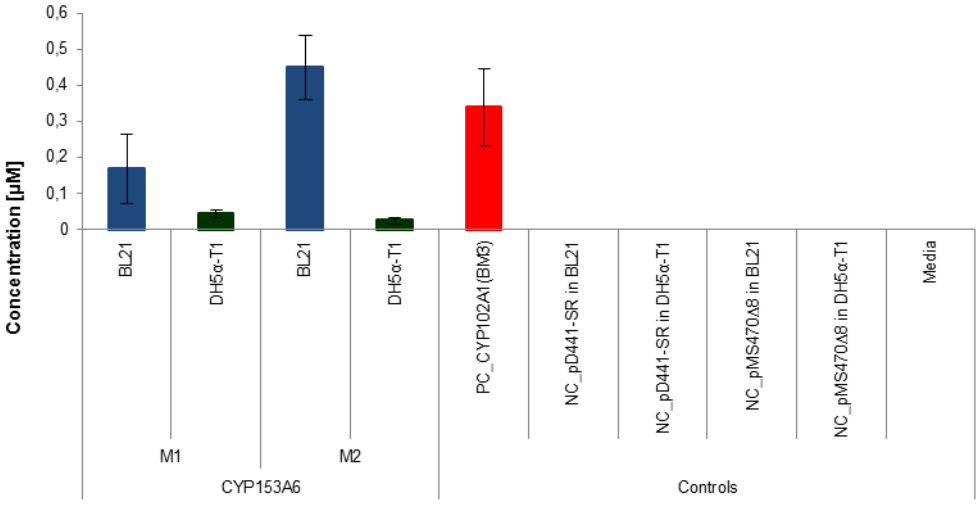

Figure 50: CYP concentration [in µM] of CYP153A6-M1 and M2 in *E. coli* BL21 or DH5α-T1. M1 contains the complete operon from *Mycobacterium sp.* strain HXN1500 (P450 monooxygenase, Ferredoxin reductase [FdR], Ferredoxin [Fdx]). M2 is a fusion construct consisting of the monooxygenase domain from the CYP153A6-M1 operon and the reductase domain of CYP505X. As a positive control CYP102A1 (BM3) was expressed in *E. coli* DH5α-T1. As a negative control *E. coli* BL21 and DH5α-T1 were transformed with the vectors pD441-SR (M1) and pMS470Δ8 (M2). 24-fold (BL21) and 18-fold (DH5α-T1) replicates are shown.

4.3.4.2. NADPH depletion-assay

CYP153A6 was used to convert C12-fatty acids (50). Despite the fact that NADH is the preferred cofactor for electron transfer in the CYP153A6 operon system, NADPH can also be used for activity screening (96). There is a decrease of the cofactor NADPH, pictured in Figure 51.

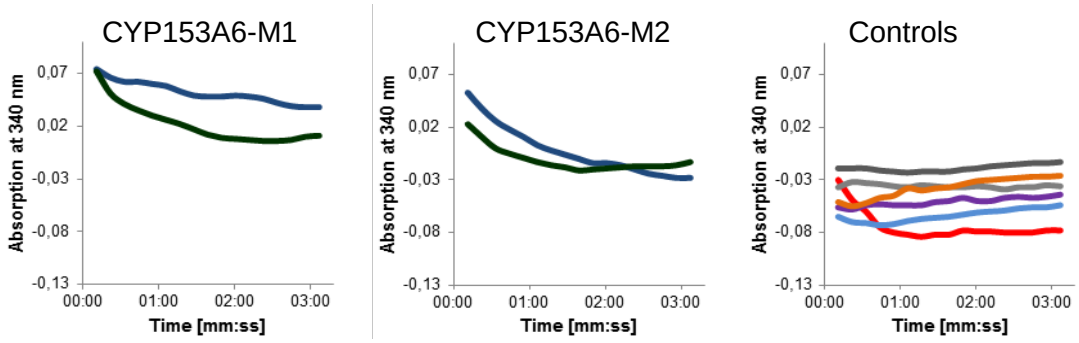

Figure 51: NADPH depletion at 340 nm measured for three minutes using CYP153A6-M1 and M2 expressed in *E. coli* BL21 (blue line) or DH5α-T1 (green line). 1:10 dilutions were used for the measurements. Controls: As a positive control CYP102A1 (BM3) was expressed in *E. coli* DH5α-T1 (red line). As negative controls *E. coli* BL21 and DH5α-T1 were transformed with the empty vectors pD441-SR (BL21 dark grey line, DH5α-T1 light grey line) and pMS470Δ8 (BL21 blue line, DH5α-T1 purple line). TB–media was used as sterile control (yellow line).

The catalytic properties of the CYP153A6 mutants are shown in Table 13. M1 and M2 consumed the cofactor NADPH. The highest NADPH depletion was obtained with M1in *E. coli* DH5α-T1 resulting in a consumption of 51.3 µmol / min and a NADPH consumption rate of 1117.7 nmol NADPH / min / nmol actively produced enzyme. The positive control CYP102A1 reached a NADPH consumption rate of 72.1 nmol NADPH / min / nmol active produced enzyme. However, it remains unclear if the oxidation of NADPH is coupled to product formation.

Table 13: Catalytic properties of CYP153A6-M1 and M2 expressed in *E. coli* BL21 or DH5α-T1. NADPH depletion was measured at 340 nm over three minutes as µmol NADPH / min. Expression of native enzyme was determined by CO-difference spectra-assay as nM CYP. NADPH consumption rates were measured as nmol NADPH / min / nmol protein. As a positive control CYP102A1 (BM3) was expressed in *E. coli* DH5α-T1. As negative controls *E. coli* BL21 and DH5α-T1 were transformed with the empty vectors pD441-SR and pMS470Δ8, which does not contain a CYP gene.

Construct		NADPH depletion [µmol / min]		Native CYP [nM]		Rate of NADPH consumption [min^{-1}]	
		BL21	DH5α-T1	BL21	DH5α-T1	BL21	DH5α-T1
CYP153A6	M1	42.0	51.3	168.7	45.9	249.0	1117.7
	M2	17.5	45.8	449.0	25.5	39.0	1796.1
Controls	NC_pD441-SR	0.0	0.0	0.0	0.0	0.0	0.0
	NC_pMS470Δ8	0.0	0.0	0.0	0.0	0.0	0.0
	PC_CYP102A1 (BM3)	24.5		340.0		72.1	

4.3.4.3. 7-benzyloxyresorufin-assay

The results of this assay for the constructs CYP153A6-M1 and M2 are shown in Figure 52.

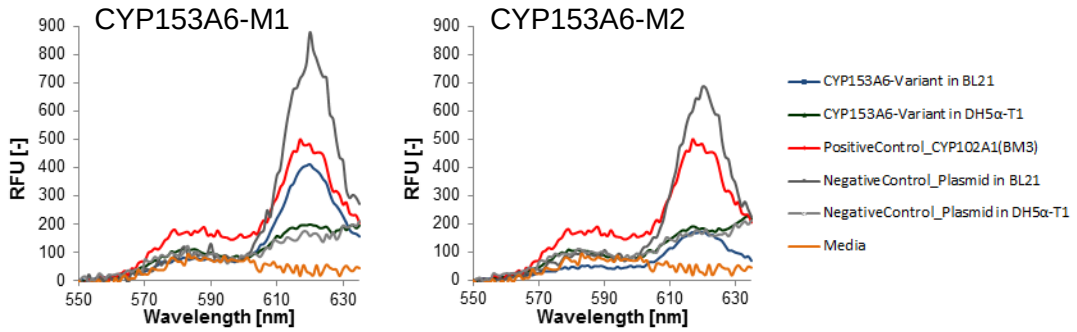

Figure 52: Determination of the resorufin fluorescence spectra (λex = 530 nm, λem = 580 nm) with CYP153A6-M1 and M2 expressed in *E. coli* BL21 or DH5α-T1. Data points are averages of 24 clones (BL21) / 18 clones (DH5α-T1) and normalized to 0. As a positive control CYP102A1 (BM3) was expressed in *E. coli* DH5α-T1. As negative controls *E. coli* BL21 and DH5α-T1 were transformed with the empty vectors pD441-SR (M1) or pMS470Δ8 (M2), which does not contain a CYP gene.

The outcome of this assay with the mutants M1 and M2 of CYP153A6 is comparable to the obtained outcome with the CYP505X mutants. Only the positive control CYP102A1 exhibited a peak at 580 nm and a conversion from 7-benzyloxyresorufin to resorufin. The positive control as well as the tested mutants and the negative controls in BL21 and DH5α-T1 displayed a peak at 620 nm, although no remarkable change in the behaviour of the mutants and the negative controls in DH5α-T1 is seen, whether with M1 or M2. But the course of the peak at 620 nm is changing with the BL21 mutants as well as the negative controls. The weaker peak at 620 nm of M2 could imply a higher ability of a new regioselective conversion.

4.3.4.4. 7-benzoxy-3-carboxycoumarin ethyl ester (BCCE)-assay

The mutants M1 and M2 of CYP153A6 showed no conversion of BCCE (Figure 53).

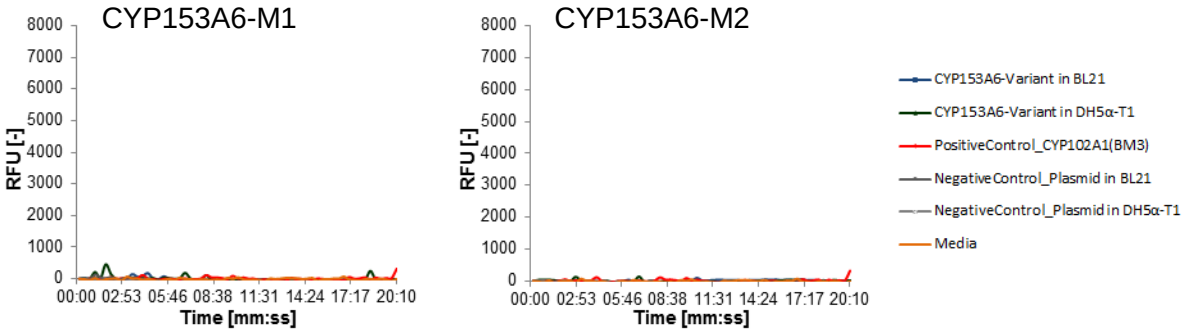

Figure 53: Conversion over time of BCCE by CYP153A6-M1 and M2 expressed in *E. coli* BL21 or DH5α-T1. Data points are averages of 24 clones (BL21) / 18 clones (DH5α-T1) and normalized to 0. As a positive control CYP102A1 (BM3) was expressed in *E. coli* DH5α-T1. As negative controls *E. coli* BL21 and DH5α-T1 were transformed with the empty vectors pD441-SR (M1) or pMS470Δ8 (M2), which does not contain a CYP gene.

4.3.4.5. 12-p-nitrophenoxycarboxylate (12-pNCA)-assay

12-pNCA was not converted by any of the generated CYP153A6 variants (Figure 54). The detected absorption rates of CYP153A6 M1 and M2, whether expressed with BL21 or DH5α-T1, originated in contaminations of the MTP wells by cell debris which had been carried along during the transfer of the supernatant from the DWP to the MTP.

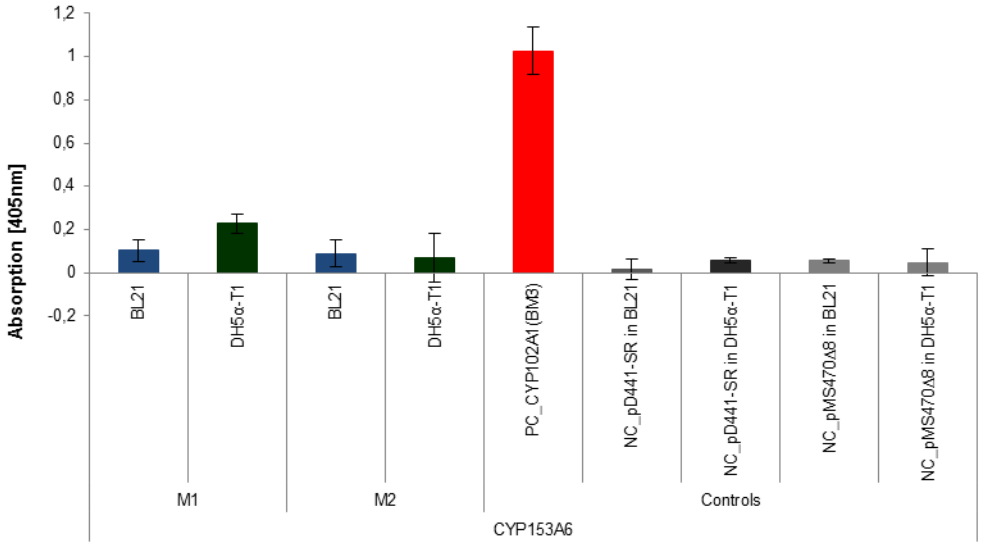

Figure 54: p-Nitrophenolate formation at 405 nm by CYP153A6-M1 and M2 expressed in *E. coli* BL21 or DH5α-T1. As a positive control CYP102A1 (BM3) was expressed in *E. coli* DH5α-T1. As negative controls *E. coli* BL21 and DH5α-T1 were transformed with the empty vectors pD441-SR (M1) or pMS470Δ8 (M2), which does not contain a CYP gene.

4.3.5. Expression of CYP154E1 in *E. coli*

4.3.5.1. Carbon monoxide (CO)-difference spectra-assay

No active CYP was obtained with the *E. coli* strains BL21 and DH5a-T1 expressing the generated CYP154E1 variants. The positive control produced 226 nM CYP102A1 (Figure 55).

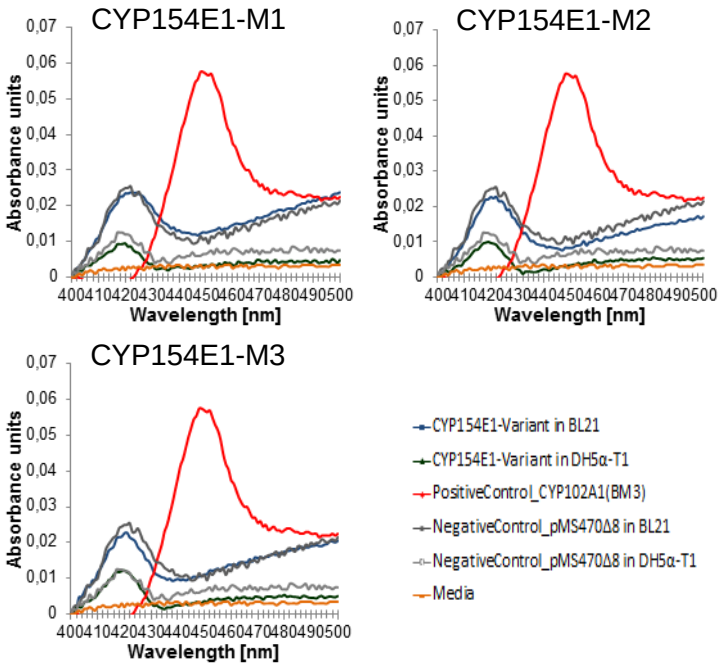

Figure 55: CO spectra of CYP154E1 M1-M3 expressed in *E. coli* BL21 or DH5α-T1. M1 harbours the monooxygenase domain from *T. fusca TM51* coexpressed with the putidaredoxin reductase (PdR) and the putidaredoxin (Pdx) from *P. putida*. M2 is a fusion construct made of the monooxygenase domain from *T. fusca TM51* fused with the PFOR-reductase from *R. ruber*. M3 is a fusion construct made of the monooxygenase domain from *T. fusca TM51* fused to the reductase domain from CYP505X. Data points are averages of 16 clones (BL21) / 12 clones (DH5α-T1) and normalized to 0. As a positive control CYP102A1 (BM3) was expressed in *E. coli* DH5α-T1. As negative controls *E. coli* BL21 and DH5α-T1 were transformed with the empty vector pMS470Δ8, which does not contain a CYP gene.

Neither CYP154E1-M1, co-expressing the CYP of *T. fusca* together with the electron transport partners putidaredoxin reductase (PdR) and putidaredoxin (Pdx) (M1) nor the fusion proteins with PFOR (M2) or the reductase domain from CYP505X (M3) yielded a peak at 450 nm. However, a peak at 420 nm was obtained with all three mutants either expressed in *E. coli* BL21 or DH5α-T1. A shift in the enzyme structure due to an incorrect folding might have led to a protonation of the heme binding cysteine. The significant thiolate group gets refracted and a thiol group emerges. By omission of this enzyme-affecting conjunction, a conformation change and a loss of the bioactive property occur, detectable with the peak at 420 nm.

4.3.5.2. NADPH depletion-assay

Saturated fatty acids can be used for determination of the enzymatic activity of CYP154E1 (104). M1 and M2 as well as the positive control CYP102A1 showed a depletion of NADPH (Figure 56).

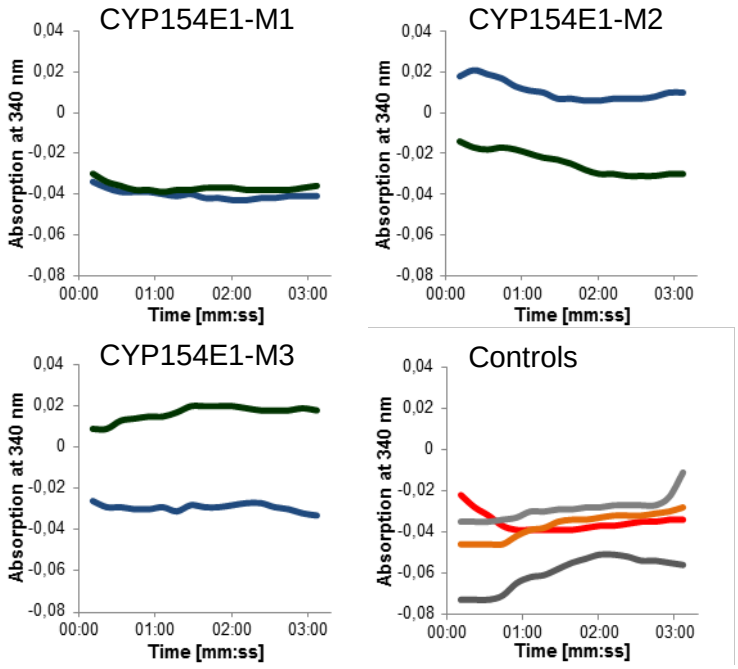

Figure 56: NADPH depletion at 340 nm measured for three minutes of CYP154E1 M1-M3 expressed in *E. coli* BL21 (blue line) or DH5α-T1 (green line). 1:10 dilutions were used for the measurements. Controls: As a positive control CYP102A1 (BM3) was expressed in *E. coli* DH5α-T1 (red line). As negative controls *E. coli* BL21 (dark grey line) and DH5α-T1 (light grey line) were transformed with the empty vector pMS470Δ8, which does not contain a CYP gene. TB–media was used as sterile control (yellow line).

Since for the entire generated CYP154E1 enzyme mutants no biologically active expressed form was detected with the CO-difference spectra-assay, it can be presumed that the recorded data resulting from background activity. The results from the NADPH depletion assay are summarized in Table 14.

Table 14: Catalytic properties of CYP154E1 M1-M3 expressed in *E. coli* BL21 or DH5α-T1. NADPH depletion was measured at 340 nm over three minutes as µmol NADPH / min. Expression of native enzyme was determined by CO-difference spectra-assay as nM CYP. NADPH consumption rates were measured as nmol NADPH / min / nmol protein. As a positive control CYP102A1 (BM3) was expressed in *E. coli* DH5α-T1. As negative controls *E. coli* BL21 and DH5α-T1 were transformed with the empty vector pMS470Δ8, which does not contain a CYP gene.

Construct		NADPH depletion [µmol / min]		Native CYP [nM]		Rate of NADPH consumption [min^{-1}]	
		BL21	DH5α-T1	BL21	DH5α-T1	BL21	DH5α-T1
CYP154E1	M1	24.5	14.7	0.0	0.0	0.0	0.0
	M2	19.6	8.7	0.0	0.0	0.0	0.0
	M3	0.0	0.0	0.0	0.0	0.0	0.0
Controls	NC_pMS470Δ8	0.0	0.0	0.0	0.0	0.0	0.0
	PC_CYP102A1(BM3)	32.2		225.9		142.5	

4.3.5.3. 7-benzyloxyresorufin-assay

The results of this assay with the CYP154E1 mutant variants are different to the obtained results with the CYP505X and CYP153A6 mutants (Figure 57). Compared with the other CYP450 variants, there is only a peak at 580 nm. The positive control as well as the generated mutants, the negative controls and the sterile control showed the same output, concluding that no conversion of 7-benzyloxyresorufin took place.

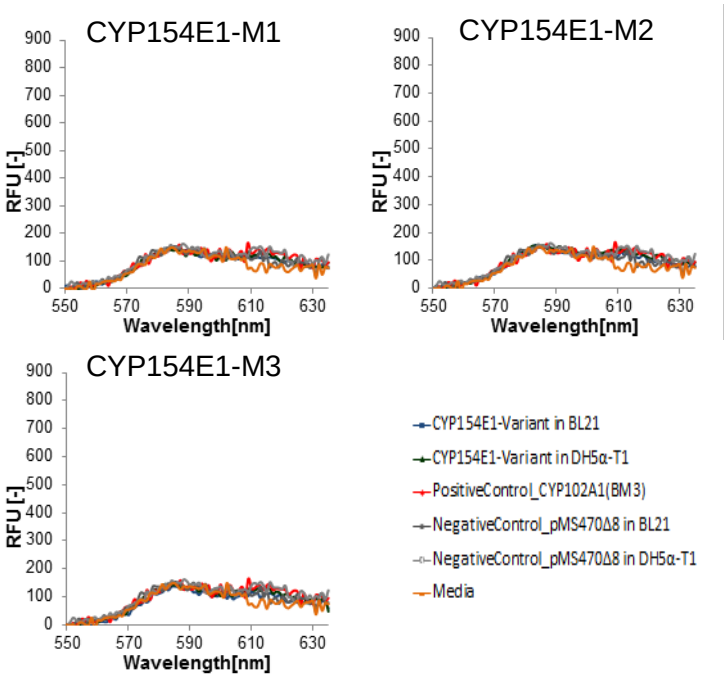

Figure 57: Determination of Resorufin fluorescence spectra (λex = 530 nm, λem = 580 nm) with CYP154E1 M1-M3 expressed in *E. coli* BL21 or DH5α-T1. Data points are averages of 16 clones (BL21) / 12 clones (DH5α-T1) and normalized to 0. As a positive control CYP102A1 (BM3) was expressed in *E.coli* DH5α-T1. As a negative control the empty vector pMS470Δ8, which does not contain a CYP gene, was transformed in *E.coli* BL21 / DH5α-T1.

4.3.5.4. 7-benzoxy-3-carboxycoumarin ethyl ester (BCCE)-assay

As pictured in Figure 58, CYP154E1 M1-M3 did not convert BCCE.

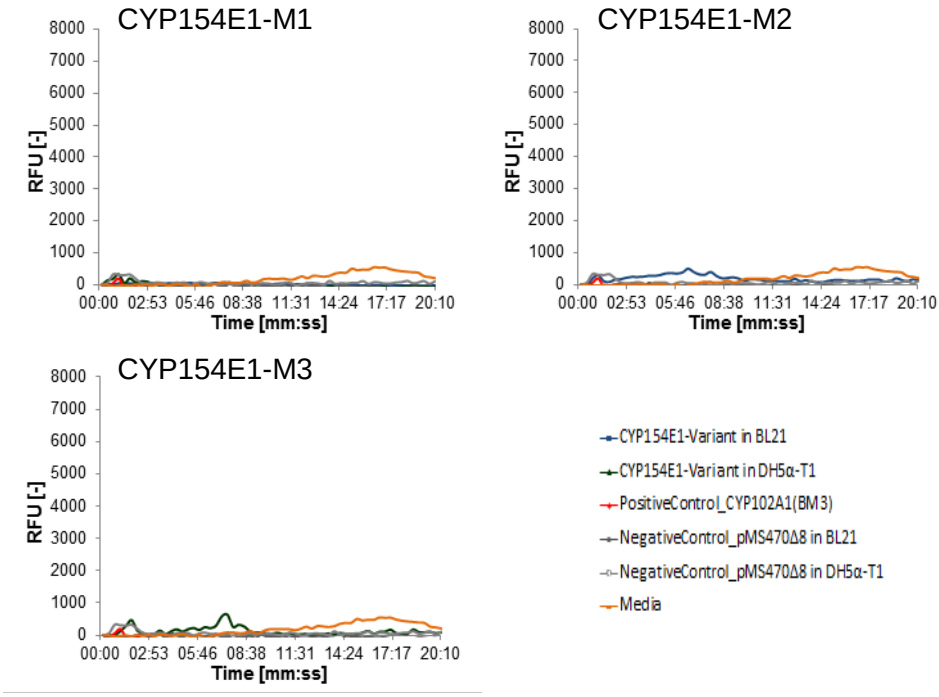

Figure 58: Conversion over time of BCCE by CYP154E1 M1-M3 expressed in *E. coli* BL21 or DH5α-T1. Data points are averages of 16 clones (BL21) / 12 clones (DH5α-T1) and normalized to 0. As a positive control CYP102A1 (BM3) was expressed in *E. coli* DH5α-T1. As a negative control the empty vector pMS470Δ8, which does not contain a CYP gene, was transformed in *E. coli* BL21 / DH5α-T1.

4.3.4.5. 12-p-nitrophenoxycarboxylate (12-pNCA)-assay

In contrast to the mutants M1/Wt and M2 of CYP505X, no conversion of 12-pNCA was obtained with the generated constructs of CYP154E1. A positive conversion was reached by CYP102A1. The measurement values of the mutants M1, M2 and M3 were formed through contamination with components of the lysed cells. These contaminations could be prevented by using a higher concentrated NaOH for cell lysis. Further it has shown that after stopping the conversion through addition of NaOH, a longer resting time (up to one hour) of the DWP has reduced the probability to carry contaminations to the MTP.

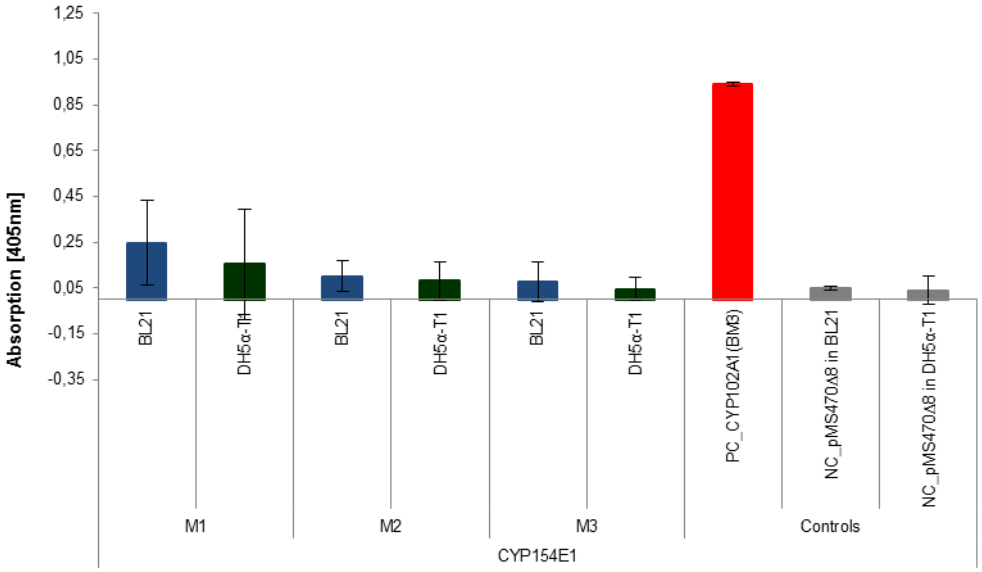

Figure 59: p-Nitrophenolate formation at 405 nm by CYP154E1 M1-M3 in *E. coli* BL21 or DH5α-T1. As a positive control CYP102A1 (BM3) was expressed in *E. coli* DH5α-T1. As a negative control the empty vector pMS470Δ8, which does not contain a CYP gene, was transformed in *E. coli* BL21 / DH5α-T1.

4.4. Upscaling and its impact on enzyme behaviour

The best *E. coli* BL21 or DH5α-T1 clones of the generated CYP variants CYP505X, CYP153A6 and CYP154E1 were chosen based on the obtained results of the performed assays when testing the different enzyme mutants in whole cells. For CYP505X, the selection of the further used mutants was based on the results of the CO-difference spectra-assay, the BCCE-assay and the pNCA-assay. For CYP153A6 and CYP154E1, the obtained output of the CO-difference spectra-assay was used for the selection of qualified mutants. The chosen *E. coli* clones were used for small scale cultivation (chapter 3.5.12.) in 2 L-shake flasks (clones are listed in Table 11, "Generated Cytochrome P450 mutants in *E. coli*"). To obtain the soluble, non-membrane bound CYP variants in a cell-free lysate, cell disruption via sonification was performed (chapter 3.5.13.). In Figure 60, samples of cell-free lysates are shown. The colour of the solution changed depending on whether BL21 or DH5α-T1 cells were used for enzyme production. By comparing the cell-free lysates to the obtained results from the CO-difference spectra-assay (Figure 62, Figure 64), a correlation between the colour intensity and the amount of active produced CYP in the cell lysate can be observed. More reddish cell free lysates (e.g. CYP153A6-M1 23.2) also contain more active produced CYP (up to 1 µM). The cell free lysates from the CYP505X-M6 and M11 clones were more transparent, for both also no CYP production was determined with the CO difference spectra-assay.

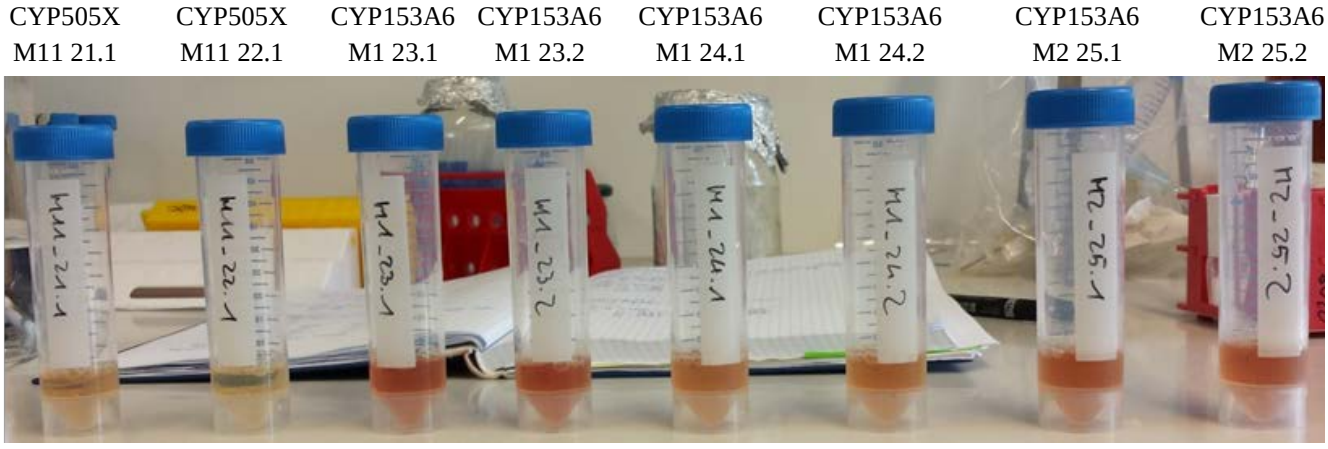

Figure 60: Cell-free lysates from CYP expressing strains (CYP505X-M11, CYP153A6-M1 and CYP153A6-M2) after small-scale cultivation and cell disruption. Odd numbers (e.g. 21.1) are from *E. coli* BL21 cells. Even numbers (e.g. 22.1) are from *E. coli* DH5α-T1 cells.

With the cell-free lysates, a CO-difference spectra-assay was done to determine the amount of biologically active expressed CYP.

4.4.1. Carbon monoxide (CO)-difference spectra-assay

The CYP yields of the respective mutants were higher compared to the cultivations in DWPs. The upscaling to a larger cultivation volume led to hardly any formation of biologically inactive CYP. In Figure 61 and Figure 63, the spectra of CYP505X-M3 and CYP153A6-M1 are shown.

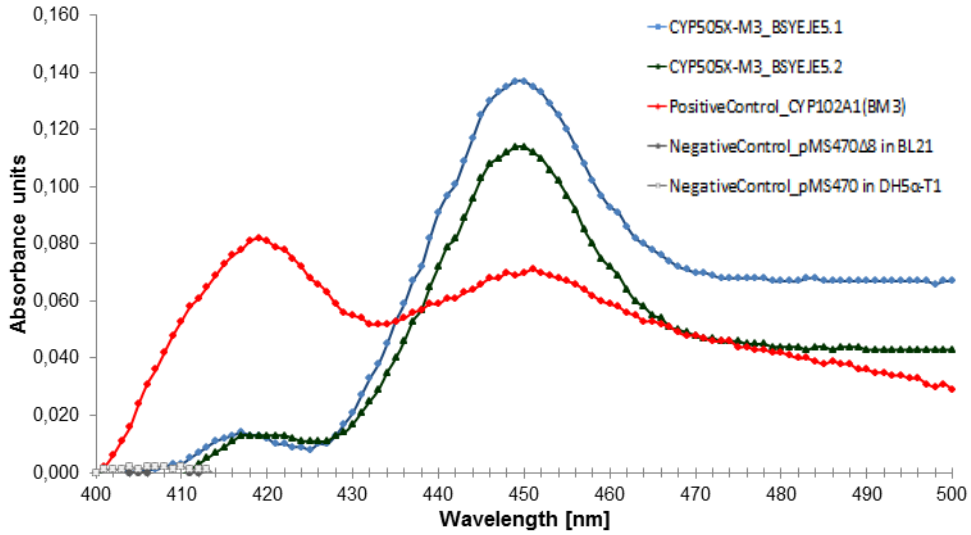

Figure 61: CO spectrum with cell-free lysates of CYP505X-M3 mutants. As a positive control CYP102A1 (BM3) was expressed in *E. coli* DH5α-T1. As negative controls *E. coli* BL21 and DH5α-T1 were transformed with the empty vector pMS470Δ8 / pMS470, which does not contain a CYP gene. Data points are normalized to 0. Odd numbers (e.g. 5.1, 5.2) are from *E. coli* BL21 cells. Even numbers are from *E. coli* DH5α-T1 cells.

In Figure 61, only a small peak at 420 nm was obtained for the two different CYP505X-M3 clones. In comparison to Figure 29, the peak at 420 nm decreased and a relative increase of the 450 nm peak was observed. For the positive control CYP102A1, the larger cultivation volume did not increase the relative amount of active CYP. The concentration of active enzyme decreased to 222 nM (Figure 62) while the proportion of inactive expressed enzyme increased compared to the cultivation in DWPs. No peaks at 420 nm and 450 nm were obtained with cell-free lysates of the control strains, which did not express a CYP, proving that the hosts *E. coli* BL21 and DH5α-T1 cells don't express any CYP. That is an interesting fact, because when performing the CO-difference spectra-assay with whole cells after micro-scale cultivation, a peak at 420 nm was obtained for the control strains. An explanation for that significant peak at 420 nm in whole-cell samples is the expression of the endogenous *E. coli* cytochrome oxidase with its absorption maxima at 416 nm (133). However it remains unclear why there is only a peak at 420 nm with the whole-cell samples but not with the cell-free lysates.

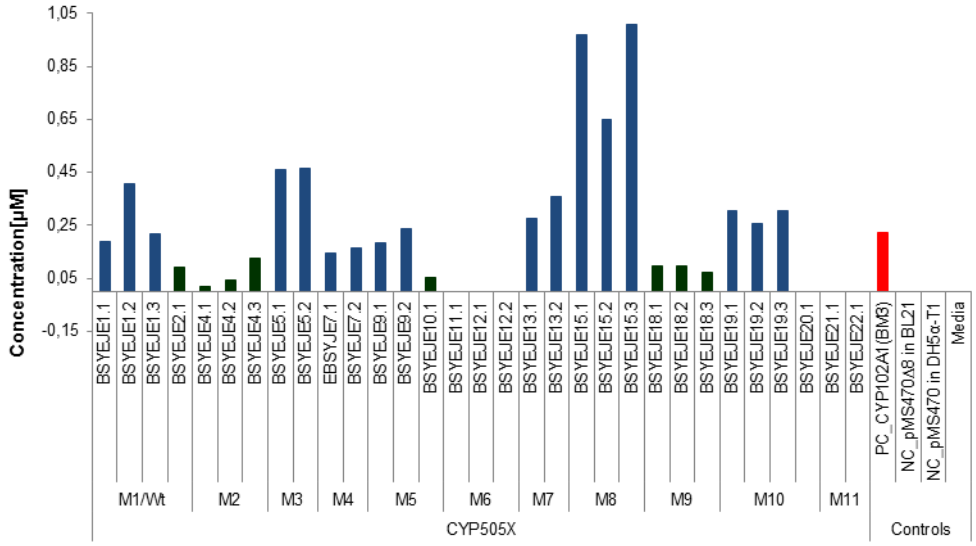

Figure 62: CYP concentrations [in µM] of best CYP505X mutant variants in *E. coli* BL21 or DH5α-T1. As a positive control CYP102A1 (BM3) was expressed in *E. coli* DH5α-T1. As negative controls *E. coli* BL21 and DH5α-T1 were transformed with the empty vector pMS470Δ8, which does not contain a CYP gene. Formula used for calculation is pictured in chapter 3.7.1. Odd numbers (e.g. 1.1) are from *E. coli* BL21 cells. Even numbers (e.g. 2.1) are from *E. coli* DH5α-T1 cells.

For most of the mutants the results from the DWP cultivation were transferable to shake flask scale. No signal was detected at 450 nm for M6 and M11, neither when cultivating in DWPs nor shake flasks and no matter if BL21 or DH5α-T1 were used as expression host. The strongest production of active wild-type CYP505X was obtained with M1/Wt-BSYEJE1.2 resulting in 405 nM. The small scale cultivation of CYP505X-M3 yielded with 460 nM on the average a 3.4-fold higher protein production of biologically active enzyme as when performing the CO-difference spectra-assay with whole cells. The highest quantity of actively produced CYP505X was obtained with mutant M8-BSYEJE15.3, resulting in 1010 nM and a 7.5-fold higher output compared to the output of the whole-cell measurements.

Similar results were obtained for the CYP153A6 mutants. The amount of the positive control CYP102A1 decreased to 180 nM, whereas the yield of the generated CYP mutants increased. The positive control was expressed to a great extend in a biologically inactive conformation on the contrary to the engineered enzymes, where the quantity of ineffective expressed protein declined. Especially the mutant M1 showed, in comparison to all the other mutants, a significant increase in CYP expression resulting in a 6-fold increase, compared to the outcome of M1 in whole cells (Figure 50), and a yield of 1041 nM biologically active CYP (Figure 63 / Figure 64). It couldn't get purified a higher amount of enzyme from the selected variants of mutant M2. By testing the generated whole-cell mutant with the CO-difference spectra-assay, the outcome of M2 was with 450 nM the highest amount of all expressed CYPs

After small scale cultivation the amount of active produced enzyme was approximately 1.2-fold higher (544 nM).

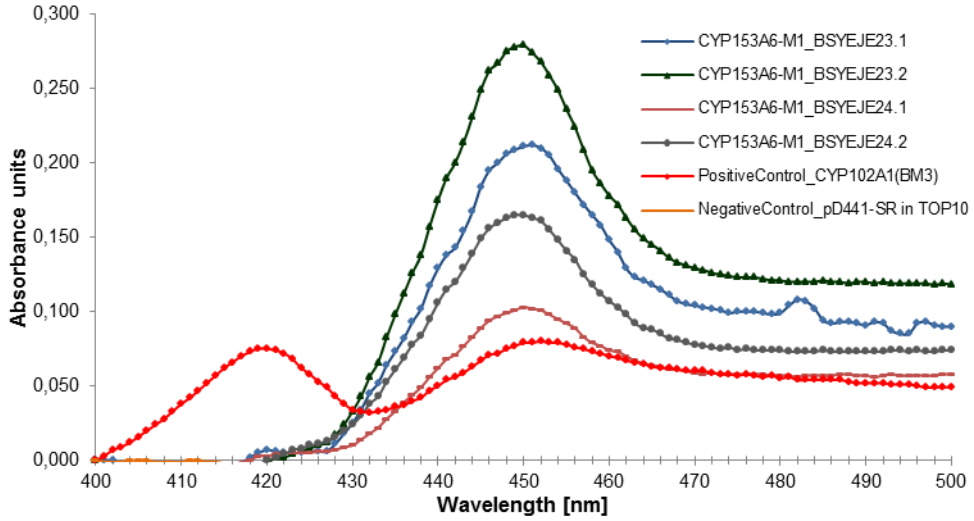

Figure 63: CO spectrum with cell-free lysates of chosen CYP153A6-M1 mutants. As a positive control CYP102A1 (BM3) was expressed in *E. coli* DH5α-T1. As a negative control *E. coli* TOP10 was transformed with the empty vector pD441-SR. Data points are normalized to 0. Odd numbers (e.g. 23.1) are from *E. coli* BL21 cells. Even numbers (e.g. 24.1) are from *E. coli* DH5α-T1 cells.

The measurement values of the negative control displayed a static course with no peak at any wavelength proving that *E. coli* Top10 cells are not able to generate heme-containing CYPs by themselves.

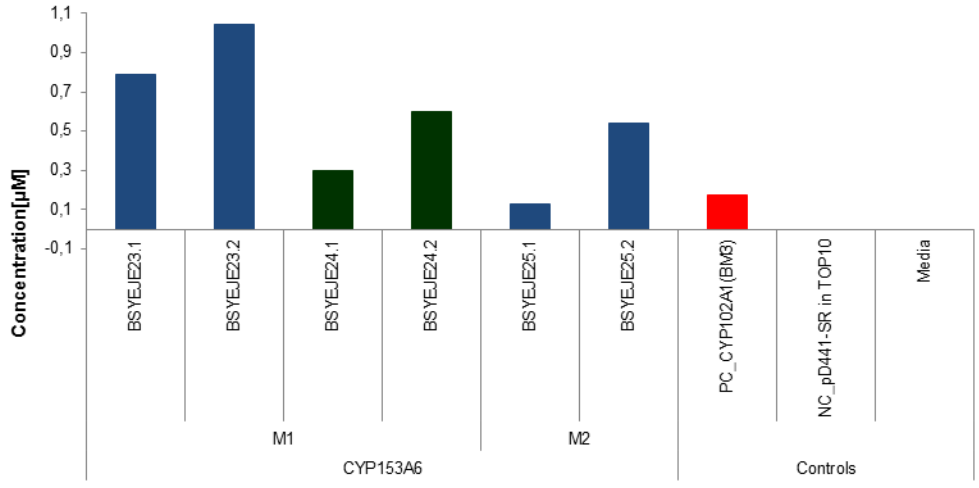

Figure 64: CYP enzyme concentration [in µM] of best CYP153A6 mutant variants in *E. coli* BL21 or DH5α-T1. As a positive control CYP102A1 (BM3) was expressed in *E. coli* DH5α-T1. As a negative control *E. coli* TOP10 was transformed with the empty vector pD441-SR. Formula used for calculation is pictured in chapter 3.7.1. Odd numbers (e.g. 23.1) are from *E. coli* BL21 cells. Even numbers (e.g. 24.1) are from *E. coli* DH5α-T1 cells.

The CO spectra of the chosen clones of the prokaryotic CYP154E1 constructs expressed in *E. coli* BL21 or DH5α-T1 showed a low amount of biologically active expressed enzyme. That is an unexpected result since these engineered constructs did not provide any informative output by testing them as whole-cell biocatalysts by various assays in this thesis. On the basis of the diagram in Figure 65, it can be assumed that every of the three generated constructs is expressed in a biologically active conformation. With whole cells none of the CYP154E1 constructs was expressed in an active form. It may be necessary to disrupt the cells to obtain the generated mutants in an active state.

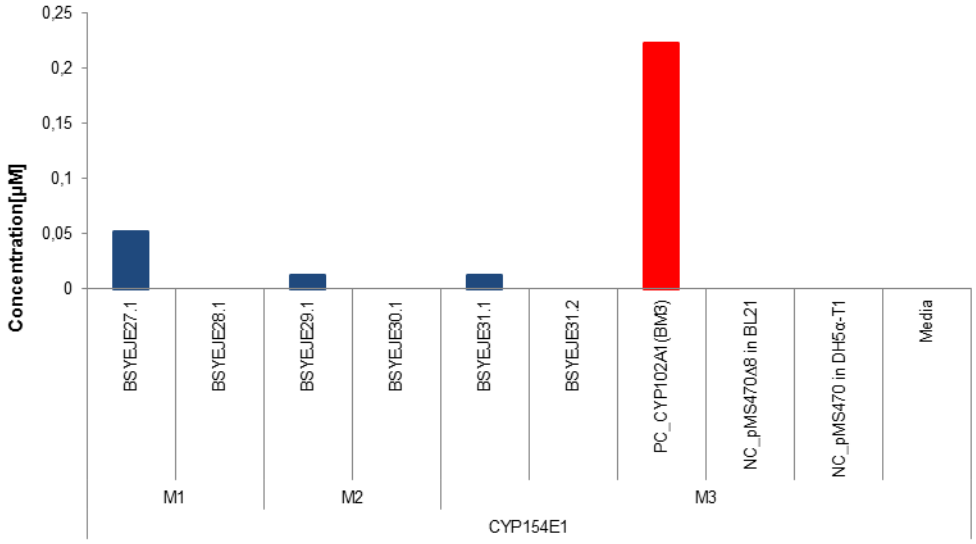

Figure 65: CYP450-Enzyme concentration [in µM] of best CYP154E1 mutant variants in *E. coli* BL21 or DH5α-T1. As a positive control CYP102A1 (BM3) was expressed in *E. coli* DH5α-T1. As negative controls *E. coli* BL21 and DH5α-T1 were transformed with the empty vector pMS470Δ8, which does not contain a CYP gene. Formula used for calculation is pictured in chapter 3.7.1. Odd numbers (e.g. 27.1) are from *E. coli* BL21 cells. Even numbers (e.g. 28.1) are from *E. coli* DH5α-T1 cells.

4.4.2. SDS-PAGE using CYP variants

In order to survey the total protein content from the purified cell lysate, a Bradford-assay was done (chapter 3.5.14.2.). In Table 15, the total protein contents of the cell-free lysates and the relative CYP amounts are shown.

Table 15: List of generated CYP450 clones. The total protein content [in mg/mL], the relative CYP450 amount [in mg/mL] and its quantity on total protein [in %] are summarized.

CYP450-variant	Mutant	Clone [Host]	Total protein content [mg/mL]	CYP450 amount [mg/mL]	Quota (in %)
CYP505X	M1/Wt	BSYEJE1.1 [BL21]	6,55	0,024	0,36
CYP505X	M1/Wt	BSYEJE1.2 [BL21]	3,39	0,051	1,49
CYP505X	M1/Wt	BSYEJE1.3 [BL21]	8,42	0,027	0,32
CYP505X	M1/Wt	BSYEJE2.1 [DH5α-T1]	15,78	0,011	0,07
CYP505X	M2	BSYEJE4.1 [DH5α-T1]	5,49	0,002	0,04
CYP505X	M2	BSYEJE4.2 [DH5α-T1]	7,85	0,006	0,07
CYP505X	M2	BSYEJE4.3 [DH5α-T1]	2,48	0,015	0,63
CYP505X	M3	BSYEJE5.1 [BL21]	12,84	0,057	0,44
CYP505X	M3	BSYEJE5.2 [BL21]	9,72	0,058	0,60
CYP505X	M4	BSYEJE7.1 [BL21]	6,02	0,018	0,30
CYP505X	M4	BSYEJE7.2 [BL21]	11,17	0,020	0,18
CYP505X	M5	BSYEJE9.1 [BL21]	6,86	0,023	0,33
CYP505X	M5	BSYEJE9.2 [BL21]	10,60	0,029	0,28
CYP505X	M5	BSYEJE10.1 [DH5α-T1]	10,82	0,007	0,06
CYP505X	M6	BSYEJE11.1 [BL21]	12,84	-	-
CYP505X	M6	BSYEJE12.1 [DH5α-T1]	6,21	-	-
CYP505X	M6	BSYEJE12.2 [DH5α-T1]	10,67	-	-
CYP505X	M7	BSYEJE13.1 [BL21]	10,82	0,034	0,32
CYP505X	M7	BSYEJE13.2 [BL21]	9,03	0,045	0,50
CYP505X	M8	BSYEJE15.1 [BL21]	11,36	0,121	1,06
CYP505X	M8	BSYEJE15.2 [BL21]	9,80	0,081	0,82
CYP505X	M8	BSYEJE15.3 [BL21]	11,89	0,126	1,06
CYP505X	M9	BSYEJE18.1 [DH5α-T1]	13,68	0,012	0,09
CYP505X	M9	BSYEJE18.2 [DH5α-T1]	13,53	0,012	0,09
CYP505X	M9	BSYEJE18.3 [DH5α-T1]	11,85	0,009	0,08
CYP505X	M10	BSYEJE19.1 [BL21]	12,77	0,038	0,30
CYP505X	M10	BSYEJE19.2 [BL21]	13,07	0,032	0,24
CYP505X	M10	BSYEJE19.3 [BL21]	13,49	0,038	0,28
CYP505X	M10	BSYEJE20.1 [DH5α-T1]	13,76	-	-
CYP505X	M11	BSYEJE21.1 [BL21]	14,56	-	-
CYP505X	M11	BSYEJE22.1 [BL21]	13,00	-	-
CYP153A6	M1	BSYEJE23.1 [BL21]	11,09	0,037	0,33
CYP153A6	M1	BSYEJE23.2 [BL21]	9,76	0,049	0,50
CYP153A6	M1	BSYEJE24.1 [DH5α-T1]	13,23	0,014	0,11
CYP153A6	M1	BSYEJE24.2 [DH5α-T1]	11,05	0,028	0,25
CYP153A6	M2	BSYEJE25.1 [BL21]	14,03	0,015	0,11
CYP153A6	M2	BSYEJE25.2 [BL21]	12,77	0,064	0,50
CYP154E1	M1	BSYEJE27.1 [BL21]	11,70	0,002	0,02
CYP154E1	M1	BSYEJE28.1 [DH5α-T1]	12,78	-	-
CYP154E1	M2	BSYEJE29.1 [BL21]	12,86	0,001	0,01
CYP154E1	M2	BSYEJE30.1 [DH5α-T1]	14,90	-	-
CYP154E1	M3	BSYEJE31.1 [BL21]	11,45	0,001	0,01
CYP154E1	M3	BSYEJE31.2 [BL21]	9,89	-	-
PC_CYP102A1 (BM3) in DH5α-T1	-	-	1,68	0,021	1,23
NC1_pMS470Δ8 in BL21	-	-	17,56	-	-
NC2_pMS470 in DH5α-T1	-	-	12,13	-	-
NC3_pD441-SR in TOP10	-	-	12,47	-	-

The relative CYP amount was calculated using the detected enzyme concentration from the CO-difference spectra-assay and the molecular weight of the enzyme (in Da). From every

construct the two best clones were selected and 10 µg of the total lysate protein content were used with a SDS-PAGE (chapter 3.5.16.) to separate the proteins with respect to their molecular mass and demonstrate the presence of the prokaryotic and eukaryotic CYPs that were generated during this thesis.

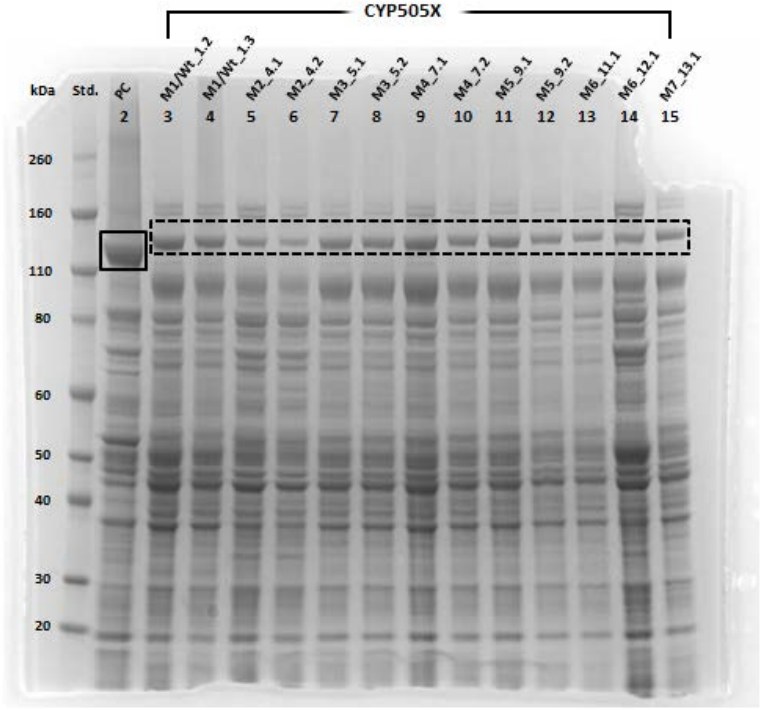

Figure 66: SDS-PAGE_Gel 1 - cell-free lysates of CYP expressing strains. PC is the positive control CYP102A1 (BM3) expressed in *E. coli* DH5α-T1. M1/Wt_1.2 – M7_13.1 are the CYP505X variants. Odd numbers (e.g. 1.2) are expressed in *E. coli* BL21 cells. Even numbers (e.g. 4.1) are expressed in *E. coli* DH5α-T1 cells. Used standard is Novex® Sharp Prestained Protein Standard. 10µg of total lysate protein was loaded onto a 1.0 mm x 15 well 4-12% Bis-Tris Gel (NuPage®).

On gel 1 (Figure 66), the lysates of CYP505X M1/Wt – M7 as well as the positive control CYP102A1 were shown. Because of the fact that the used lysates contain the total expressed protein, a variety of bands is shown. Using the negative controls from Figure 68 as comparative samples, this quantity of unspecific bands can be seen as background proteins of the host strains. However, the proteins of interest stand out from the other unspecific bands because of the fact that those were expressed due to selective induction resulting in a selectively increased yield and a darker band. CYP102A1 has 3174 bp and a molecular weight of 116.439 kDa leading to a straight, thicker black with the right size (lane 2, black square). In each of the CYP505X samples, a band between 110 kDa and 160 kDa was obtained. The fusion enzyme CYP505X from *A. fumigatus* has a molecular weight of 124.320 kDa (3360 bp). On gel 1 as well as on gel 2, the bands from the SDS PAGE (black dashed square) correlate with the calculated molecular weight.

The cell-free lysates of CYP505X M7 – M11 and the lysates from CYP153A6-M1 and M2 were loaded on gel 2 (Figure 67). Different bands were obtained for the mutants M1 and M2 of CYP153A6. Since M1 is a three component-system (operon) consisting of the P450 domain, a ferredoxin reductase (FdR) and a ferredoxin (Fdx) there are several bands. The P450 domain has 1260 bp and a molecular weight of 46.62 kDa. The FdR domain has 47.064 kDa and a length of 1272 bp and the Fdx domain has 318 bp with 11.766 kDa.

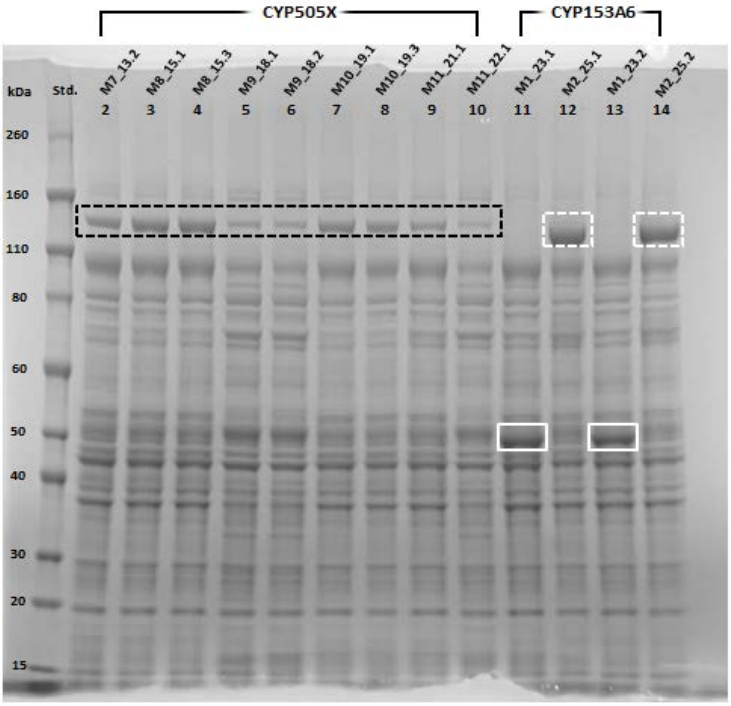

Figure 67: SDS-PAGE_Gel 2 - cell-free lysates of CYP expressing strains. M7_13.2 – M11_22.1 are CYP505X variants. M1_23.1 – M2_25.2 are CYP153A6 variants (M1_23.1/.2 is the operon, M2_25.1/.2 is the fusion). Odd numbers (e.g. 13.2) are expressed in *E. coli* BL21 cells. Even numbers (e.g. 18.1) are expressed in *E. coli* DH5α-T1 cells. Used standard is Novex® Sharp Prestained Protein Standard. 10µg of total lysate protein was loaded onto a 1.0 mm x 15 well 4-12% Bis-Tris Gel (NuPage®).

In lane 11 and 13, there can be seen a stronger band on the height between 40 kDa and 50 kDa (white squares). This indicates the presence of either the P450 domain or the FdR domain. Since these two proteins are very similar in size, they cannot be separated. For a better separation of these proteins, a more close-meshed gel (a higher gel percentage of the electrophoresis gel) and another buffer system would be needed. M2 is a fusion protein made by the P450 domain of CYP153A6 and the reductase domain from CYP505X. This fusion results in a protein with 3174 bp and a molecular weight of 117.438 kDa (gel 2, lane 12 and 14, white dashed squares).

On gel 3, the proteins from the cell-free lysates of the positive control, three negative controls, the lysates of CYP154E1 M1 - M3 and the lysates of CYP153A6 M1 and M2 are shown (Figure 68). In lane 2, the CYP102A1 is faintly visible a bit above the 115 kDa mark. Also the other characteristic band for that sample at approximately 53 kDa is depicted. The negative controls NC1, NC2 and NC3 can be used to gain information on the background proteins. NC1, seen in lane 3, was constructed by cloning the vector pMS470Δ8 in *E. coli* BL21. This vector contains a stuffer-fragment Δ8 with a length of 1274 bp, detectable at a height of 48 kDa (134). The lysates of the CYP154E1 constructs contain no heterologous proteins bands. For CYP154E1-M1, there should be bands at a height of 40.848 kDa (P450 domain, 1104 bp), 47.064 kDa (PdR domain, 1272 bp) and 11.988 kDa for the Pdx domain with 324 bp. For the fusion constructs M2 and M3, bands at 76.923 kDa (2079 bp) and 111.333 kDa (3009 bp).

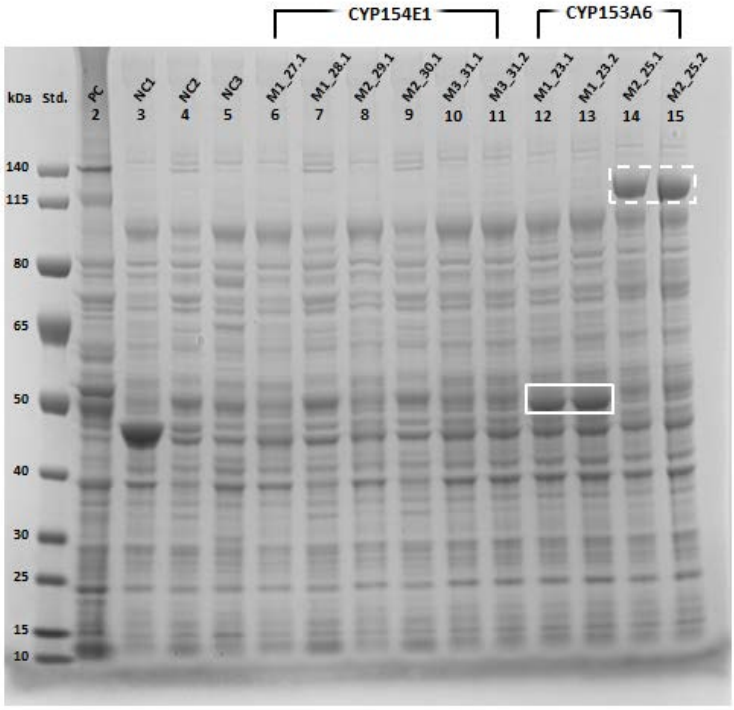

Figure 68: SDS-PAGE_Gel 3 - cell-free lysates of CYP expressing strains. PC is the positive control CYP102A1 (BM3) expressed in *E. coli* DH5α-T1. NC1 is the empty vector pMS470Δ8 in *E. coli* BL21. NC2 is the empty vector pMS470 in *E. coli* DH5α-T1. NC3 is the empty vector pD441-SR in *E. coli* TOP10. M1_27.1 – M3_31.2 are the CYP154E1 variants. M1_23.1 – M2_25.2 are the CYP153A6 variants (M1_23.1/.2 is the operon, M2_25.1/.2 is the fusion). Odd numbers (e.g. 27.1) are expressed in *E. coli* BL21 cells. Even numbers (e.g. 28.1) are expressed in *E. coli* DH5α-T1 cells. Used standard is PageRuler™ Prestained Protein Standard. 10µg of total lysate protein was loaded onto a 1.0 mm x 15 well 4-12% Bis-Tris Gel (NuPage®).

In lane 12 – 15 the lysates from CYP153A6-M1 and M2 were loaded. The gel presents the same results as displayed on gel 2 in Figure 67. For CYP153A6-M1, there is a band at 50 kDa

indicating the P450 domain and the FdR domain (white squares). The fusion protein CYP153A6-M2 is shown as a band approximately at 115 kDa (white dashed squares).

5. CONCLUSION AND OUTLOOK

The aim of this thesis was to generate a variety of novel eukaryotic and prokaryotic cytochrome P450 variants, expressed in microbial cells for whole cell biocatalysis. Various assays were implemented to determine the successful expression in the two host organisms, *E. coli* and *P. pastoris*, and the ability to convert selected model substrates. During the course of the Master thesis I focused on four different types of CYP450s: The eukaryotic enzymes CYP505X from *A. fumigatus* and CYP505A1 from *F. oxysporum* as well as the prokaryotic representatives CYP153A6 from *Mycobacterium sp.* and CYP154E1 from *T. fusca*. Moreover artificial CYPs were generated by exchanging specific aa residues in the natural CYP sequence or the fusion of single protein domains.

The lack of P450 genes and of homologous CYP expression can be an advantage, when *E. coli* is used as host for heterologous expression of CYPs.

This master thesis has shown that different *E. coli* strains, BL21 and DH5α-T1, prefer different cultivation conditions. If *E. coli* BL21 is used as expression strain, the modified cultivation protocol, which was drafted during the master thesis, should be used. If E. coli DH5α-T1 is the preferred host system, the initial cultivation protocoll for cultivation of *E. coli* should be used.

CO difference spectra, which were used to quantify CYP levels by exploiting the interaction between the CYP-centred heme complex and CO, showed that the quantity of biologically active enzyme can be enhanced by the substitution of single aa or the exchange of entire domains. The enzyme levels of CYP505X increased, e.g. by mutating isoleucine to valine at position 242, alanine to valine at position 268 and leucine to phenylalanine at position 451 to generate CYP505X-M3. CYP505X-M3 was able to produce a 1.6-fold higher amount of catalytically active enzyme compared to the wild-type CYP505X-M1/Wt. Some important positions in the structure of the CYP505X were identified. Phenylalanine at position 90 is an important residue in the catalytic centre for the catalytic activity of CYP505X and the correct folding. The same applies for the positions 50, 52, 54, 268 and 451. Altering the aa at this positions had a tremendous influence for the conversion of the model substrates. Thus exchanging these aa residues might have a positive effect on the conversion of pharmaceutical intermediates and APIs as well.

By generating a CYP153A6 fusion variant, it was possible to demonstrate that altering the electron-transferring domain can lead to a higher concentration of catalytically active

expressed enzyme. In this case the expression rate increased 2.6-fold in contrast to the wild-type construct. When expressing CYP154E1 no functional enzyme was produced. Similarly no M11 variant of CYP505X could be expressed so far

When measuring the enzyme activity through direct observation of NADPH cofactor depletion, it was found that this assay is a more difficult one with many possible sources of error. NADPH is a limiting factor. Through fast processing of NADPH, either by substrate conversion or by any uncoupled effects like cofactor oxidation, oxidation of any components of the tested cell lysates or the solvent (112), the assay has to be performed in an accurate, but quick manner. A good operational handling and the right equipment are indispensable for usable results. The use of dilutions of the generated cell lysates for the assay is recommended as NADPH is converted more slowly with less cell substance. Due to the possibility of uncoupled cofactor oxidation, this assay does not provide information on substrate specificity. Thus further coupling with analytical methods such as HPLC and GC is a perquisite.

Three different fluorogenic substrates were used to detect the catalytic activity of the CYPs. When using 7-benzyloxyresorufin as a testing substrate, no conversion of the substrate was observed by the generated mutants of CYP505X, CYP153A6 and CYP154E. However, with CYP505X and CYP153A6 a peak at 620 nm was detected for which no explanation is present. The whole emission spectrum looks different from what was expected. Positive controls including the product of the dealkylation reaction (resorufin) should be tested. The use of BCCE as substrate showed that some positions in the aa sequence of CYP505X were directly involved in the substrate conversion. The exchange at position 90 from phenylalanine to alanine has a major influence in substrate recognition. Through its position in the catalytic centre phenylalanine 90 could have a key function in the conversion of bulky substrates. Altering the position 90 and position 334, which are located in close spatial proximity, can lead to a further improvement for the conversion of interesting substrates. The clamp-like arrangement might directly influence substrate binding. Additionally, altering the positions 50, 52 and 54 improved substrate conversion. Mutant M9 and M10, which contain mutations at these positions, yielded the highest conversion rates. Through altering the aa residues, larger substrates might access the active centre more easily. Only the wild-type enzyme and the mutant M2 of CYP505X were able to convert 12-pNCA. Mutations in the wild-type sequence reduced the activity towards 12-pNCA.

Different *P. pastoris* strains were used for the expression of CYP505X and CYP505A1. Both enzymes can be expressed in an active conformation at low concentrations. Higher CYP

levels were produced by *P. pastoris* MutS strains. The *AOX1* deletion resulted in a slower growth under inductive conditions and higher production levels of the recombinant protein. No disturbing cell-mediated production of CYPs is significant which would complicate the evaluation. Further, the CYP expression level in *P. pastoris* is highly dependent in which integration locus in the genome the linearized expression cassette is integrated. Additional, the choice of the plasmid to use should be kept in mind to select the vector in appropriate manner between single and multi-copy for the respective experimental setup.

None of the CYPs, expressed in *P. pastoris*, were capable to convert MAMC, an artificially designed substrate for the mammalian enzyme CYP2D6.

To test the expression behaviour of the individual constructs in larger volumes, I selected the two best clones of each CYP variant and performed cultivations in 2 L-shake flasks. By changing the cultivation setup to a larger scale, the amount of inactively produced enzyme was reduced. Upscale experiments indicated that the host strains *E. coli* BL21 and DH5α-T1 do not produce any homologous CYP and that more native enzyme was possible to generate, however not in a much greater extent. Performing an SDS-PAGE confirmed the expression of the various CYPs. Distinct bands on the SDS-PAGE gels indicated that also artificial variants can be produced in the various hosts.

All of the generated enzyme variants have the potential to be an interesting alternative for biotechnological applications in the field of biosynthesis and the metabolism of a variety of compounds. Especially CYP505X from *A. fumigatus* and CYP153A6 from *Mycobacterium sp.* can be produced at high levels and might be improved for industrial processes.

Outlook

To enhance the performance and increase the possibility to get an even better enzyme, additional experiments might be performed: Some positions in the aa sequence of the monooxygenase domain of CYP505X from *A. fumigatus* e.g. position 50, 52 or 90 were identified to be involved in substrate recognition. It would be purposeful to test different aa exchanges at these positons e.g. by generating an Omnichange library (135) and to screen for an improved catalytic activity.

Additionally to the mutated positions in the CYP505X sequence, aa exchanges at position I259 and I414 might confer interesting properties to the enzyme. Mutations in these positions in the sequence of CYP102A1 from *B. megaterium* (R255, I401) increased the catalytic activity towards alkanes. (114,136).

Novel fusion variants might be generated, which contain the reductase domain of CYP102A1 from *B. megaterium* and the CYP505X or the CYP153A6 monooxygenase domain. These variants might exhibit altered catalytic properties compared to the CYPs generated during the Master's thesis.

NADH should be used for depletion assays employing CYP153 variants. In general the depletion assays need improvement in order to rely on the generated data. However, beside the spectrophotometric NADPH depletion-assay to determine the catalytic activity of CYP mutants, it might be used an assay including hexylmethylether (HME), a chromogenic octane mimic, and the uncoloured reagent Purpald for detection of a possible terminal hydroxylation capability. A terminal (ω) hydroxylation of the surrogate substrate hexylmethylether releases formaldehyde which further reacts with the Purpald to produce a dark purple product. Hydroxylation at the ω-2 carbon forms hexanal and a pink colour after reaction with Purpald. The formed compounds and thereby hydroxylation can be quantified at 550 nm (137,138).

Several strategies might be performed to further increase CYP production: The cultivation setup might be optimized for every individual CYP with respect to the temperature and the cultivation time. The protoporphyrin hemin might be used as an additive to increase the production of the heme containing enzymes (139). Higher CYP levels might also be reached by the use of autoinduction medium. This permits higher cell densities and a more flexible induction moment. Substrate transfer into the cells and subsequently substrate conversion might be enhanced by extra coexpression of an outer membrane protein like AlkL (50). Additionally the coexpression of a chaperon-system (e. g. GroEL/ES system) might increase the biologically active CYP concentration in the soluble fraction (48). Cell disruption by using a french press or an affinity tag purification can provide other possibilities that may result in higher CYP concentrations.

Finally, the generated mutants have to be tested with a broad range of different substrates or surrogate compounds to get an insight into the catalytic potential of these enzymes.

After optimization of cultivation conditions and thorough testing of the various generated CYP mutants using miscellaneous substrates, the long-term goal is the application as whole-cell biocatalysts with diverse substrate specificities and the capability to enable non-activated substrates and modify pharmaceutical ingredients. The use of whole-cell systems as carrier for CYP catalyzed reactions has the advantages that the cellular setting increases the enzyme stability and provides the needed co-factor NADPH (105,140). With the goal on focus to use

whole-cell catalysis in eco-friendly mild reaction conditions and processes with an improved environmental sustainability and economically effective production processes, a proper transport, preservation and storage stability of the enzyme systems is decisive. Lyophilization would be a possibility to keep the biocatalysts stable and active over a longer time period. With this method, the viability of the whole-cell catalysts remains at room temperature and transport is possible without dry ice. The possibility to lyophilize microorganism in MTPs is an additional advantage for storage because thereby, entire MTP-libraries can be created in a small space and by that, space and accumulating costs can be reduced.

6. BIBLIOGRAPHY

1. Estabrook RW. A passion for P450s (rememberances of the early history of research on cytochrome P450). Drug Metab Dispos. 2003;31(12):1461–73

2. Mueller GC, Miller JA. The metabolism of 4-dimethylaminoazobenzene by rat liver homogenates. J Biol Chem. 1948;176:535-544

3. Ryan KJ. Biological Aromatization of Steroids Kenneth. J Biol Chem. 1959;234:268-272

4. Klingenberg M. Pigments of rat liver microsomes. Arch Biochem Biophys. 1958;75(2):376–86

5. Society C. The Stoichiometry of C_{21} Hydroxylation of Steroids by Adrenocortical Microsomes. J Biol Chem. 1963;238(4):2–5

6. Omura T, Sato R. A New Cytochrome in Liver Microsomes. J Biol Chem. 1962;237:1375–6

7. Estabrook RW, Cooper DY, Rosenthal O. The light reversible carbon monoxide inhibition of the steroid C_{21}-hydroxylase system of the adrenal cortex. Biochem Z. 1963;338:741–55

8. Omura T, Sato R. The Carbon Monoxide-biding pigment of Liver Microsomes. J Biol Chem. 1964;239(7):2370–8

9. Cooper DY, Levin S, Narasimhulu S, Rosenthal O. Photochemical Action Spectrum of the Terminal Oxidase of Mixed Function Oxidase Systems. Science. 1965;147(3656):400–2

10. Hedegaard J, Gunsalus IC. Mixed function oxidation. IV. An induced methylene hydroxylase in camphor oxidation. J Biol Chem. 1965;240(10):4038–43

11. Katagiri M, Ganguli BN, Gunsalus IC. A soluble cytochrome P-450 functional in methylene hydroxylation. J Biol Chem. 1968;243(12):3543–6

12. Poulos TL. Heme enzyme structure and function. Chem Rev. 2014;114(7):3919–62

13. Nelson DR, Koymans L, Kamataki T, Stegeman JJ, Feyereisen R, Waxman DJ. P450 superfamily: update on new sequences, gene mapping, accession numbers and nomenclature. Pharmacogenetics. 1996;6(1):1–42

14. Harford-Cross CF, Carmichael AB, Allan FK, England PA, Rouch DA, Wong L-L. Protein engineering of cytochrome P450cam (CYP101) for the oxidation of polycyclic aromatic hydrocarbons. Protein Eng. 2000;13(2):121–8

15. Omura T. Recollection of the early years of the research on cytochrome P450. Proc Jpn Acad Ser B Phys Biol Sci. 2011;87(10):617–40

16. Nebert DW, Adesnik M, Coon MJ, Estabrook RW, Gonzalez FJ, Guengerich FP. The P450 gene superfamily: recommended nomenclature. DNA. 1987;6(1):1–11

17. Nebert DW, Wikvall K, Miller WL. Human cytochromes P450 in health and disease. Phil Trans R Soc. 2013;368: 383

18. Zanger UM, Schwab M. Cytochrome P450 enzymes in drug metabolism: Regulation of gene expression, enzyme activities, and impact of genetic variation. Pharmacol Ther. 2013;138(1):103–41

19. Pikuleva IA, Waterman MR. Cytochromes P450: Roles in diseases. J Biol Chem. 2013;288(24):17091–8

20. White PC, Speiser PW. Congenital adrenal hyperplasia due to 21-hydroxylase deficiency. Endocr Rev. 2000;21(3):245–91

21. White PC, Werkmeister J, New MI, Dupont B. Steroid 21-hydroxylase deficiency and the major histocompatibility complex. Hum Immunol. 1986;15(4):404–15

22. Wiley-Blackwell. Cytochrome P450. Br J Pharmacol. 2009;158(1):215–7

23. Guengerich FP. New trends in cytochrome P450 research at the half-century mark. J Biol Chem. 2013;288(24):17063–4

24. Doddapaneni H, Chakraborty R, Yadav JS. Genome-wide structural and evolutionary analysis of the P450 monooxygenase genes (P450ome) in the white rot fungus Phanerochaete chrysosporium: evidence for gene duplications and extensive gene clustering. BMC Genomics. 2005;6:92-98

25. Wijnen P, Op den Buijsch R, Drent M, Kuijpers P, Kuipers P, Neef C. Review article: The prevalence and clinical relevance of cytochrome P450 polymorphisms. Aliment Pharmacol Ther2007;26(2):211–9

26. Perera R, Sono M, Sigman J, Pfister TD, Lu Y, Dawson JH. Neutral thiol as a proximal ligand to ferrous heme iron: implications for heme proteins that lose cysteine thiolate ligation on reduction. Proc Natl Acad Sci U S A. 2003;100(7):3641–6

27. Nelson DR. Cytochrome P450 Nomenclature. Met Mol Biol. 1998;107:15–24

28. Graham SE, Peterson JA. How similar are P450s and what can their differences teach us. Arch Biochem Biophys. 1999;369(1):24–9

29. Nelson DR. Cytochrome P450: Structure, Mechanism, and Biochemistry. J Am Chem Soc. 2005;127(34):12147–8

30. Bernhardt R. Cytochromes P450 as versatile biocatalysts. J Biotechnol. 2006;124(1):128–45

31. Baj-rossi C, Micheli G, Carrara S. P450-Based Nano-Bio-Sensors for Personalized Medicine. Biosensors – Emerging materials and applications. 2005;447–81

32. Lamb DC, Waterman MR. Unusual properties of the cytochrome P450 superfamily. Philos Trans R Soc Lond B Biol Sci. 2013;368(1612):20-39

33. Brooks GT. Book review: Cytochrome P450: Structure, mechanism and biochemistry. Pestic Sci. 1998;52(4):409-21

34. Angelica MD, Fong Y. Heme Enzyme Structure and Function. Chem Rev. 2014;114(7): 3919–3962

35. Sirim D, Widmann M, Wagner F, Pleiss J. Prediction and analysis of the modular structure of cytochrome P450 monooxygenases. BMC Struct Biol. 2010;10(1):34-51

36. Hasemann CA, Kurumbail RG, Boddupalli SS, Peterson JA, Deisenhofer J. Structure and function of cytochromes P450: a comparative analysis of three crystal structures. Structure. 1995;3(1):41–62

37. Rupasinghe S, Schuler MA, Kagawa N, Yuan H, Lei L, Zhao B. The cytochrome P450 gene family CYP157 does not contain EXXR in the K-helix reducing the absolute conserved P450 residues to a single cysteine. FEBS Lett. 2006;580(27):6338–42

38. Pochapsky TC, Kazanis S, Dang M. Conformational Plasticity and Structure/Function relationships in CYP450. Antiox&Red Sig. 2010;13(8):3-96

39. Poulos TL, Finzel BC, Howard AJ. High-resolution crystal structure of cytochrome P450cam. J Mol Biol. 1987;195(3):687–700

40. Degennaro M, Hurd TR, Siekhaus DE, Biteau B, Jasper H, Lehmann R. Solution structural ensembles of substrate-free cytochrome P450cam$_{a,b}$. Biochem. 2013;20(2):233–43

41. Williams P, Cosme J, Sridhar V, Johnson EF, McRee DE. Mammalian microsomal cytochrome P450 monooxygenase: structural adaptations for membrane binding and functional diversity. Mol Cell. 2000;5(1):121–31

42 Berka K, Paloncýová M, Anzenbacher P, Otyepka M. Behavior of human cytochromes P450 on lipid membranes. J Phys Chem B. 2013;117(39):11556–64

43. Kitazume T, Takaya N, Nakayama N, Shoun H. Fusarium oxysporum fatty-acid subterminal hydroxylase (CYP505) is a membrane-bound eukaryotic counterpart of Bacillus megaterium cytochrome P450BM3. J Biol Chem. 2000;275(50):39734–40

44. Dong MS, Yamazaki H, Guo Z GF. Recombinant human cytochrome P450 1A2 and an N-terminal-truncated form: construction, purification, aggregation properties, and interactions with flavodoxin, ferredoxin, and NADPH-cytochrome P450 reductase. Arch Biochem Biophys. 1996;327(1):11–9

45. Omura T, Sanders E, Estabrook RW, Cooper DY, Rosenthal O. Isolation from adrenal cortex of a nonheme iron protein and a flavoprotein functional as a reduced triphosphopyridine nucleotide-cytochrome P-450 reductase. Arch Biochem Biophys. 1966;117(3):660–73

46. Hannemann F, Bichet A, Ewen KM, Bernhardt R. Cytochrome P450 systems--biological variations of electron transport chains. Biochim Biophys Acta. 2007;1770(3):330–44

47. Guengerich FP, Munro AW. Unusual cytochrome P450 enzymes and reactions. J Biol Chem. 2013;288(24):17065–73

48. Wen LP, Fulco AJ. Cloning of the gene encoding a catalytically self-sufficient cytochrome P-450 fatty acid monooxygenase induced by barbiturates in Bacillus megaterium and its functional expression and regulation in heterologous (Escherichia coli) and homologous (Bacillus megaterium) Hosts. J Biol Chem. 1987;262(14):6676–82

49. Gustafsson MCU, Roitel O, Marshall KR, Noble MA, Chapman SK, Pessegueiro A. Expression , Purification , and Characterization of Bacillus subtilis Cytochromes P450 CYP102A2 and CYP102A3 : Flavocytochrome Homologues of P450 BM3 from Bacillus megaterium. Biochemistry. 2004;43:5474–87

50. Weis R, Winkler M, Schittmayer M, Kambourakis S, Vink M, David Rozzell J. A diversified library of bacterial and fungal bifunctional cytochrome P450 enzymes for drug metabolite synthesis. Adv Synth Catal. 2009;351(13):2140–6

51. Mot R De, Parret AHA. A novel class of self-sufficient cytochrome P450 monooxygenases in prokaryotes. Curr Trends Microbiol. 2002;10(11):502–8

52. Roberts G, Grogan G, Greter A, Flitsch SL, Turner NJ. Identification of a New Class of Cytochrome P450 from a Rhodococcus sp. J Bacteriol. 2002 Jul 15;184(14):3898–908

53. Bakkes PJ, Biemann S, Bokel A, Eickholt M, Girhard M, Urlacher VB. Design and improvement of artificial redox modules by molecular fusion of flavodoxin and flavodoxin reductase from Escherichia coli. Sci Rep. 2015;5(7):121-58

54 Makino T, Katsuyama Y, Otomatsu T, Misawa N, Ohnishi Y. Regio- and stereospecific hydroxylation of various steroids at the 16 position of the D ring by the Streptomyces griseus cytochrome P450 CYP154C3. Appl Environ Microbiol. 2014;80(4):1371–9

55. Scheps D, Honda Malca S, Richter SM, Marisch K, Nestl BM, Hauer B. Synthesis of ω-hydroxy dodecanoic acid based on an engineered CYP153A fusion construct. Microb Biotechnol. 2013;6(6):694–707

56. Roberts GA, Celik A, Hunter DJB, Ost TWB, White JH, Chapman SK. A self-sufficient cytochrome p450 with a primary structural organization that includes a flavin domain and a [2Fe-2S] redox center. J Biol Chem. 2003;278(49):48914–20

57. Kulig JK, Spandolf C, Hyde R, Ruzzini AC, Eltis LD, Grönberg G, Hayes MA GG. A P450 fusion library of heme domains from Rhodococcus jostii RHA1 and its evaluation for the biotransformation of drug molecules. Bioorg Med Chem. 2015;23(17):5603–9

58. Agematu H, Matsumoto N, Fujii Y, Kabumoto H, Doi S, Machida K. Hydroxylation of testosterone by bacterial cytochromes P450 using the Escherichia coli expression system. Biosci Biotechnol Biochem. 2006;70(1):307–11

59. Reed JR, Eyer M, Backes WL. Functional interactions between cytochromes P450 1A2 and 2B4 require both enzymes to reside in the same phospholipid vesicle: Evidence for physical complex formation. J Biol Chem. 2010;285(12):8942–52

60. Guengerich FP, Isin EM. Mechanisms of cytochrome P450 reactions. Acta Chim Slov. 2008;55(1):7–19

61. Blount ZD. The unexhausted potential of *E. coli*. elife. 2015;4:1–12

62. Cabrita LD, Dai W, Bottomley SP. A family of E. coli expression vectors for laboratory scale and high throughput soluble protein production. BMC Biotechnol. 2006;6(Lic):12-17

63. Khow O, Suntrarachun S. Strategies for production of active eukaryotic proteins in bacterial expression system. Asian Pac J Trop Biomed. 2012;2(2):159–62

64. Bogazkaya AM, Bühler CJ Von, Kriening S. Supporting Information for Selective allylic hydroxylation of acyclic terpenoids by CYP154E1 from Thermobifida fusca. Beilstein J Org Chem. 2014;10:1347–1353

65. Cregg JM, Madden KR, Barringer KJ, Thill GP, Stillman CA. Functional characterization of the two alcohol oxidase genes from the yeast Pichia pastoris. Mol Cell Biol. 1989;9(3):1316–23

66. Kurtzman CP. Biotechnological strains of Komagataella (Pichia) pastoris are Komagataella phaffii as determined from multigene sequence analysis. J Ind Microbiol Biotechnol. 2009;36(11):1435–8

67. Näätsaari L, Krainer FW, Schubert M, Glieder A, Thallinger GG. Peroxidase gene discovery from the horseradish transcriptome. BMC Genomics. 2014;15(1):227

68. Küberl A, Schneider J, Thallinger GG, Anderl I, Wibberg D, Hajek T. High-quality genome sequence of Pichia pastoris CBS7435. J Biotechnol. 2011;154(4):312–20

69. Lin-Cereghino J, Cereghino JL, Cregg JM. Heterologous protein expression in the methylotrophic yeast Pichia pastoris. FEMS Microbiol Rev. 2000;24(1):45–66

70. Rußmayer H, Buchetics M, Gruber C, Valli M, Grillitsch K, Modarres G. Systems-level organization of yeast methylotrophic lifestyle. BMC Biol. 2015;13(1):80

71. Näätsaari L, Mistlberger B, Ruth C, Hajek T, Hartner FS, Glieder A. Deletion of the Pichia pastoris KU70 Homologue Facilitates Platform Strain Generation for Gene Expression and Synthetic Biology. PLoS One. 2012;7(6):e39720

72. Cregg JM, Vedvick TS, Raschke WC. Recent advances in the expression of foreign genes in Pichia pastoris. Biotechnology. 1993;11(8):905–10

73. Sturmberger L, Chappell T, Geier M, Krainer F, Day KJ, Vide U, Trstenjak S, Schiefer A, Richardson T, Soriaga L, Darnhofer B, Birner-Gruenberger R, Glick BS, Tolstorukov I, Cregg J, Madden K GA. Refined Pichia pastoris reference genome sequence. J Biotechnol. 2016;S0168-1656(16):30203–6

74. Somers JM, Bevan EA. The inheritance of the killer character in yeast. Genet Res. 1969;13(1):71–83

75. Toh EA, Wickner RB. A mutant killer plasmid whose replication depends on a chromosomal “superkiller” mutation. Genetics. 1979;91(4):673–82

76. Woolford CA, Daniels LB, Park FJ, Jones EW, Van Arsdell JN, Innis MA. The PEP4 gene encodes an aspartyl protease implicated in the posttranslational regulation of Saccharomyces cerevisiae vacuolar hydrolases. Mol Cell Biol. 1986;6(7):2500–10

77. Stahl ML, Ferrari E. Replacement of the Bacillus subtilis subtilisin structural gene with an In vitro-derived deletion mutation. J Bacteriol. 1984;158(2):411–8

78. Li W, Brandriss MC. Proline biosynthesis in Saccharomyces cerevisiae: molecular analysis of the PRO1 gene, which encodes gamma-glutamyl kinase. J Bacteriol. 1992;174(12):4148–56

79. Fulco J, Miura Y. (ω-2) Hydroxylation of Fatty Acids by a Soluble System from Bacillus megaterium. J Biol Chem. 1974;249(6):1880–8

80. Fulco AJ. P450BM-3 and other inducible bacterial P450 cytochromes: biochemistry and regulation. Annu Rev Pharmacol Toxicol. 1991;31:177–203

81. Govindaraj S, Poulos TL. Probing the structure of the linker connecting the reductase and heme domains of cytochrome P450BM-3 using site-directed mutagenesis. Protein Sci. 1996;5(7):1389–93

82. Porter TD. An unusual yet strongly conserved flavoprotein reductase in bacteria and mammals. Trends Biochem Sci. 1991;16(4):154–8

83. Whitehouse CJC, Bell SG, Wong L-L. P450(BM3) (CYP102A1): connecting the dots. Chem Soc Rev. 2012;41(3):1218–60

84. Kitazume T, Tanaka A, Takaya N, Nakamura A, Matsuyama S, Suzuki T. Kinetic analysis of hydroxylation of saturated fatty acids by recombinant P450foxy produced by an Escherichia coli expression system. Eur J Biochem. 2002;269(8):2075–82

85. Nakayama N, Takemae A, Shoun H. Cytochrome P450foxy, a catalytically self-sufficient fatty acid hydroxylase of the fungus Fusarium oxysporum. J Biochem. 1996;119(3):435–40

86. Jung ST, Launchil R, Arnold FH. Cytochrome P450: taming a wild type enzyme. Curr Opin Biotechnol. 2011;22(6):809–817

87. Lewis JC, Bastian S, Bennett CS, Fu Y, Mitsuda Y, Chen MM, Greenberg WA, Wong CH, Arnold FH. Chemoenzymatic elaboration of monosaccharides using engineered cytochrome P450BM3 demethylases. Proc Natl Acad Sci USA. 2009;106(39):16550-16555

88. Dietrich JA, Yoshikuni Y, Fisher KJ, Woolard FX, Ockey D, McPhee DJ. A novel semi-biosynthetic route for artemisinin production using engineered substrate-promiscuous P450(BM3). ACS Chem Biol. 2009;4(4):261–7

89. Lewis JC, Mantovani SM, Fu Y, Snow CD, Komor RS, Wong C-H. Combinatorial Alanine Substitution Enables Rapid Optimization of Cytochrome P450BM3 for Selective Hydroxylation of Large Substrates. ChemBioChem. 2010;11(18):2502–5

90. Braun A, Halwachs B, Geier M, Weinhandl K, Guggemos M, Marienhagen J. MuteinDB: The mutein database linking substrates, products and enzymatic reactions directly with genetic variants of enzymes. Database. 2012;2012:1–9

91. Graham-Lorence S, Truan G, Peterson JA, Falck JR, Wei S, Helvig C. An active site substitution, F87V,converts cytochrome P450 BM-3 into a regio- and stereoselective (14S,15R)-arachidonic acid epoxygenase. J Biol Chem. 1997;272(2):1127–35

92. Li Q, Ogawa J, Schmid RD, Ogawa JUN. Engineering Cytochrome P450 BM-3 for Oxidation of Polycyclic Aromatic Hydrocarbons Engineering Cytochrome P450 BM-3 for Oxidation of Polycyclic Aromatic Hydrocarbons. Society. 2001;67(12):1–6

93. Carmichael AB, Wong LL. Protein engineering of Bacillus megaterium CYP102. The oxidation of polycyclic aromatic hydrocarbons. Eur J Biochem. 2001;268(10):3117–25

94. Nierman W, Pain A, Anderson M, Wortman J, Kim H, Arroyo J. Genomic sequence of the pathogenic and allergenic filamentous fungus Aspergillus fumigatus. Nature. 2005;438(7071):1151–6

95. Galagan JE, Calvo SE, Cuomo C, Ma L, Wortman JR, Batzoglou S. Sequencing of Aspergillus nidulans and comparative analysis with A . fumigatus and A . oryzae. Nature. 2005;438(12):1105–15

96. Nazmul Hussain Nazir KHM, Ichinose H, Wariishi H. Molecular characterization and isolation of cytochrome P450 genes from the filamentous fungus Aspergillus oryzae. Arch Microbiol. 2010;192(5):395–408

97. Deng J, Carbone I, Dean RA. The evolutionary history of cytochrome P450 genes in four filamentous Ascomycetes. BMC Evol Biol. 2007;7:30

98. Gordon TR, Martyn RD. The evolutionary biology of Fusarium oxysporum. Annu Rev Phytopathol. 1997;35(1):111–28

99. Sutherland JB, Pometto III AL, Crawford DL. Lignocellulose degradation by Fusarium species. Can J Bot. 1983;61(4):1194–8

100. Floudas D, Binder M, Riley R, Barry K, Blanchette RA, Henrissat B. The Paleozoic origin of enzymatic lignin decomposition reconstructed from 31 fungal genomes. Science. 2012;336(6089):1715–9

101. Durairaj P, Malla S, Nadarajan SP, Lee P-G, Jung E, Park HH. Fungal cytochrome P450 monooxygenases of Fusarium oxysporum for the synthesis of ω-hydroxy fatty acids in engineered Saccharomyces cerevisiae. Microb Cell Fact. 2015;14(1):45

102. Smith I. *Mycobacterium tuberculosis* pathogenesis and molecular determinants of virulence. Clin Microbiol Rev. 2003;16(3):463–96

103. Funhoff EG. Hydroxylation and epoxidation reactions catalyzed by CYP153 enzymes. Enzyme Microb Technol. 2007;40(4):806–12

104. Funhoff EG, Bauer U, García-Rubio I, Witholt B, van Beilen JB. CYP153A6, a soluble P450 oxygenase catalyzing terminal-alkane hydroxylation. J Bacteriol. 2006;188(14):5220–7

105. Belanger JT. Perillyl Alcohol: Applications in Oncology. Altern Med Rev. 1998;3(6):448–57

106. Cornelissen S, Julsing MK, Volmer J, Riechert O, Schmid A, Bühler B. Whole-cell-based CYP153A6-catalyzed (S)-limonene hydroxylation efficiency depends on host background and profits from monoterpene uptake via AlkL. Biotechnol Bioeng. 2013;110(5):1282–92

107. Gudiminchi RK, Randall C, Opperman DJ, Olaofe O a, Harrison STL, Albertyn J. Whole-cell hydroxylation of n-octane by Escherichia coli strains expressing the CYP153A6 operon. Appl Microbiol Biotechnol. 2012;96(6):1507–16

108. Pennec A, Jacobs CL, Opperman DJ, Smit MS. Revisiting Cytochrome P450-Mediated Oxyfunctionalization of Linear and Cyclic Alkanes. Adv Synth Catal. 2015;357(1):118–30

109. Olaofe OA, Fenner CJ, Gudiminchi RK, Smit MS, Harrison STL. The influence of microbial physiology on biocatalyst activity and efficiency in the terminal hydroxylation of n-octane using Escherichia coli expressing the alkane hydroxylase, CYP153A6. Microb Cell Fact. 2013;12(1):8

110. Lykidis A, Mavromatis K, Ivanova N, Anderson I, Land M, DiBartolo G. Genome sequence and analysis of the soil cellulolytic actinomycete Thermobifida fusca YX. J Bacteriol. 2007;189(6):2477–86

111. Schallmey A, den Besten G, Teune IGP, Kembaren RF, Janssen DB. Characterization of cytochrome P450 monooxygenase CYP154H1 from the thermophilic soil bacterium Thermobifida fusca. Appl Microbiol Biotechnol. 2011;89(5):1475–85

112. von Bühler C, Le-Huu P, Urlacher VB. Cluster screening: an effective approach for probing the substrate space of uncharacterized cytochrome P450s. ChemBioChem. 2013;14(16):2189–98

113. Hernández-Martín A, von Bühler CJ, Tieves F, Fernández S, Ferrero M, Urlacher VB. Whole-cell biotransformation with recombinant cytochrome P450 for the selective oxidation of Grundmann's ketone. Bioorg Med Chem. 2014;22(20):5586–92

114. Jones G, Strugnell SA, DeLuca HF. Current understanding of the molecular actions of vitamin D. Physiol Rev. 1998;78(4):1193–231

115. Seidman CE, Struhl K, Sheen J, Jessen T. Introduction of plasmid DNA into cells. Curr Protoc Mol Biol. 2001;1:1-12

116. Lin-Cereghino J, Wong WW, Xiong S, Giang W, Luong LT, Vu J. Condensed protocol for competent cell preparation and transformation of the methylotrophic yeast Pichia pastoris. Biotechniques. 2005;38(1):44, 46, 48

117. Gibson DG, Young L, Chuang R-Y, Venter JC, Hutchison CA, Smith HO. Enzymatic assembly of DNA molecules up to several hundred kilobases. Nat Methods. 2009;6(5):343–5

118. Weis R, Luiten R, Skranc W, Schwab H, Wubbolts M, Glieder A. Reliable high-throughput screening with Pichia pastoris by limiting yeast cell death phenomena. FEMS Yeast Res. 2004;5(2):179–89

119. Gudiminchi RK, Geier M, Glieder A, Camattari A. Screening for cytochrome P450 expression in Pichia pastoris whole cells by P450-carbon monoxide complex determination. Biotechnol J. 2013;8(1):146–52

120. Glieder A, Meinhold P. High-throughput Screens Based on NAD (P) H Depletion. Directed Enzyme Evolution: Screening and Selection Methods. 2003;230:157-170

121. Lussenburg BM, Babel LC, Vermeulen NPE, Commandeur JNM. Evaluation of alkoxyresorufins as fluorescent substrates for cytochrome P450 BM3 and site-directed mutants. Anal Biochem. 2005;341(1):148–55

122. Ruff AJ, Dennig A, Wirtz G, Blanusa M, Schwaneberg U. Flow Cytometer-Based High-Throughput Screening System for Accelerated Directed Evolution of P450 Monooxygenases. ACS Catal. 2012;2(12):2724–8

123. Schwaneberg U, Schmidt-Dannert C, Schmitt J, Schmid RD. A continuous spectrophotometric assay for P450 BM-3, a fatty acid hydroxylating enzyme, and its mutant F87A. Anal Biochem. 1999;269(2):359–66

124. Onderwater RCA, Venhorst J, Commandeur JNM, Vermeulen NPE. Design, Synthesis, and Characterization of 7-Methoxy-4-(aminomethyl)coumarin as a Novel and Selective Cytochrome P450 2D6 Substrate Suitable for High-Throughput Screening. Chem Res Toxicol. 1999;12:555-559

125. Seifert A, Antonovici M, Hauer B, Pleiss J. An efficient route to selective bio-oxidation catalysts: an iterative approach comprising modeling, diversification, and screening, based on CYP102A1. ChemBioChem. 2011;12(9):1346–51

126. Seifert A, Vomund S, Grohmann K, Kriening S, Urlacher VB, Laschat S. Rational design of a minimal and highly enriched CYP102A1 mutant library with improved regio-, stereo- and chemoselectivity. ChemBioChem. 2009;10(5):853–61

127. Bogazkaya AM, von Bühler CJ, Kriening S, Busch A, Seifert A, Pleiss J. Selective allylic hydroxylation of acyclic terpenoids by CYP154E1 from Thermobifida fusca YX. Beilstein J Org Chem. 2014;10:1347–53

128. Cirino PC, Arnold FH. Regioselectivity and Activity of Cytochrome P450 BM-3 and Mutant F87A in Reactions Driven by Hydrogen Peroxide. Adv Synth Catal. 2002;344(9):932–7

129. Kille S, Zilly FE, Acevedo JP, Reetz MT. Regio- and stereoselectivity of P450-catalysed hydroxylation of steroids controlled by laboratory evolution. Nat Chem. 2011;3(9):738–43

130. Wong TS, Arnold FH, Schwaneberg U. Laboratory Evolution of Cytochrome P450 BM-3 Monooxygenase for Organic Cosolvents. Biotechnol Bioeng. 2004;85(3):351–8

131. Carmichael AB, Wong LL. Protein engineering of Bacillus megaterium CYP102: The oxidation of polycyclic aromatic hydrocarbons. Eur J Biochem. 2001;268(10):3117–25

132. van Vugt-Lussenburg BM, Stjernschantz E, Lastdrager J, Oostenbrink C, Vermeulen NPE, Commandeur JNM. Identification of critical residues in novel drug metabolizing mutants of cytochrome P450 BM3 using random mutagenesis. J Med Chem. 2007;50(3):455–61

133. Damsten MC, van Vugt-Lussenburg BM, Zeldenthuis T, de Vlieger JSB, Commandeur JNM, Vermeulen NPE. Application of drug metabolising mutants of cytochrome P450 BM3 (CYP102A1) as biocatalysts for the generation of reactive metabolites. Chem Biol Interact. 2008;171(1):96–107

134. Glieder A, Meinhold P. High-throughput Screens Based on NAD (P) H Depletion. Directed Enzyme Evolution: Screening and Selection Methods. 2003;230:157-170

135. Hart S, Koch KR, Woods DR. Identification of indigo-related pigments produced by Escherichia coli containing a cloned Rhodococcus gene. J Gen Microbiol. 1992;138(1):211–6

136. Jain C. Degradation of mRNA in Escherichia coli. IUBMB Life. 2002;54:315–21

137. Deutscher MP. Degradation of RNA in bacteria: Comparison of mRNA and stable RNA. Nucleic Acids Res. 2006;34(2):659–66

138. Gillam EMJ. Engineering cytochrome p450 enzymes. Chem Res Toxicol. 2008;21(1):220–31

139. Appel D, Lutz-Wahl S, Fischer P, Schwaneberg U, Schmid RD. A P450 BM-3 mutant hydroxylates alkanes, cycloalkanes, arenes and heteroarenes. J Biotechnol. 2001;88(2):167–71

140. Andersen MD, Møller BL. Use of methylotropic yeast Pichia pastoris for expression of cytochromes P450. Methods Enzymol. 2002;357:333–42

140. Pritchard MP, McLaughlin L, Friedberg T. Establishment of functional human cytochrome P450 monooxygenase systems in Escherichia coli. Methods Mol Biol. 2006;320:19–29

142. Napora-Wijata K, Strohmeier G, Sonavane MN, Avi M, Robins K, Winkler M. Enantiocomplementary Yarrowia lipolytica Oxidoreductases: Alcohol Dehydrogenase 2 and Short Chain Dehydrogenase/Reductase. Biomolecules. 2013;3(3):449–60

143. Dennig A, Shivange AV., Marienhagen J, Schwaneberg U. Omnichange: The sequence independent method for simultaneous site-saturation of five codons. PLOS ONE. 2011;6(10): e26222

144. Glieder A, Farinas ET, Arnold FH. Laboratory evolution of a soluble , self-sufficient , highly active alkane hydroxylase. Nat Biotechnol. 2002;20(11):1135–9

145. Meinhold P, Peters MW, Hartwick A, Hernandez AR, Arnold FH. Engineering cytochrome P450 BM3 for terminal alkane hydroxylation. Adv Synth Catal. 2006;348(6):763–72

146. Pennec A, Jacobs CL, Opperman DJ. Revisiting Cytochrome P450-Mediated Oxyfunctionalization of Linear and Cyclic Alkanes. Adv Synth Catal. 2015;357(1):118-130

147. Varnado CL, Goodwin DC. System for the expression of recombinant hemoproteins in Escherichia coli. Protein Expr Purif. 2004;35(1):76–83

148. Braun A, Geier M, Bühler B, Schmid A, Mauersberger S, Glieder A. Steroid biotransformations in biphasic systems with Yarrowia lipolytica expressing human liver cytochrome P450 genes. Microb Cell Fact. 2012;11:106

7. ABBREVIATIONS

aa	amino acid
ADH1	alcohol dehydrogenase 1
AdR	adrenodoxin reductase
Adx	adrenodoxin
Amp	Ampicillin
AOX1	alcohol oxidase 1
AOX2	alcohol oxidase 2
API	Active Pharmaceutical Ingredient
BCCE	7-benzoxy-3-carboxycoumarin ethyl ester
BG	BioGrammatics
BMD	buffered minimal glucose medium
BMG	buffered minimal glycerol medium
BMM	buffered minimal methanol medium
bp	base pair
Cat1	catalase 1
CO	carbon monoxide
CPR	cofactor-cytochrome P450 reductase
CYP450	Cytochrome Pigment 450
Cys	cysteine
Da	Dalton
DNA	Deoxyribonucleic acid
dNTP	deoxynucleoside triphosphate
DTT	Dithiothreitol
DWP	deep well plate
EC	Enzyme Commission
FAD	flavinadenininucleotide

FdR	ferredoxin reductase
Fdx	ferredoxin
FMN	flavinmononucleotide
GOI	gene of interest
HAMC	7-hydroxy-4-(aminomethyl)-coumarin
HME	Hexylmethylether
IPGT	Isopropyl-β-D-thiogalactopyranosid
Kan	Kanamycin
kDa	Kilodalton
LB	Lysogeny Broth
MAMC	7-methoxy-4-(aminomethyl)-coumarin
Mbp	Megabasepair
MTP	microtiter plate
MUT	methanol utilization pathway
NADH	β-Nicotinamide adenine dinucleotide-reduced
NADPH	β-Nicotinamide adenine dinucleotide phosphate-reduced
nm	nanometer
OD	optical density
oe-PCR	overlap extension-Polymerase Chain Reaction
ONC	Overnight Culture
ORI	Origin of replication
PAH	Polycyclic aromatic hydrocarbon
PCR	Polymerase Chain Reaction
PdR	putidaredoxin reductase
Pdx	putidaredoxin
PFOR	phthalate family oxygenase reductase
PFOS	phthalate family oxygenase system
pNCA	p-nitrophenoxycarboxylate

rcf	relative centrifugal force
rpm	revolutions per minute
SDS-PAGE	Sodium Dodecyl Sulfate Polyacrylamide Gel Electrophorese
SOC	Super Optimal broth with Catabolite repression
TB	Terrific Broth
Wt	wild-type
YPD	Yeast extract Peptone Dextrose medium
Zeo	Zeocin

8. LIST OF FIGURES

9. LIST OF TABLES

10. APPENDIX

gBlocks and primers

All gBlocks and primers used during this master thesis were ordered from IDT (purchased by bisy).

gBlocks

CYP505X: (gBlocks for the generation of CYP505X M1-M4, M6-M9, M11)

*Eco*RI restriction site Altered base triplets for the generation of CYP505X-mutants

B14001 E3-CYP505 gBlocks® Gene Fragments 1001-1250 bp (Length = 1169 bp)

GATAACAATTTCACACAGGAAACAGAATTCGACGCGATGCTGACTATTCGTAAACCGTCCCAGGCGCCGAAAGGTTCCACTT
CTATCCCACTGGACACGCCGATCTCTGCATTCGAACTGCTGTCTACCTACGTTGAGCTGTCTCAGCCAGCGTCTAAACGTGATC
TGACTGCTCTGGCGGATGCGGCTATTACTGACGCTGATGCTCAAGCGGAACTGCGCTATCTGGCGTCCAGCCCTACGCGCTTC
ACGGAAGAAATCGTTAAAAAGCGTATGTCTCCTCTGGACCTGCTGATCCGCTACCCTTCCATCAAGCTGCCGGTCGGTGATTT
CCTGGCCATGCTGCCTCCTATGCGCGTTCGCCAGTATTCTATCTCTTCCAGCCCGCTGGCAGATCCGTCTGAGTGCAGCATTAC
CTTCTCCGTACTGAACGCTCCAGCACTGGCTGCTGCATCTCTGCCACCGGCAGAACGTGCTGAAGCTGAACAGTACATGGGCG
TGGCTTCTACTTATCTGAGCGAGCTGAAGCCAGGTGAACGTGCGCACATCGCTGTTCGTCCGTCCCACTCTGGTTTCAAACCG
CCGATGGACCTGAAAGCCCCGATGATTATGGCCTGCGCTGGTTCTGGCCTGGCGCCTTTTCGTGGTTTCATTATGGATCGTGCT
GAGAAGATTCGTGGTCGCCGCAGCAGCGTTGGTGCGGACGGCCAACTGCCGGAGGTGGAACAGCCGGCGAAAGCAATCCTG
TATGTGGGCTGTCGTACCAAAGGCAAAGATGATATTCACGCGACGGAACTGGCTGAATGGGCCCAGCTGGGTGCTGTGGACG
TACGTTGGGCCTACAGCCGTCCGGAAGACGGCTCTAAAGGTCGTCATGTTCAGGATCTGATGCTGGAAGATCGTGAGGAACT
GGTTTCCCTGTTCGATCAGGGTGCACGCATCTACGTTTGCGGCAGCACTGGCGTAGGCAACGGTGTTCGTCAGGCGTGCAAAG
ACATCTACCTGGAACGCCGTCGCCAGCTGCGTCAGGCTGCACGTGAACGTGGTGAAGAGGTGCCGGCGGAAGAAGACGAAG
ATGCTGCTGCTGAACAATTCCTGGATAACCTGCGTACTAAAGAACGTTATGCCACCGATGTTTTCACTTGAGGATCCTCTAGA
AATAATTTTG

B14002 E2-CYP505 gBlocks® Gene Fragments 1001-1250 bp (Length = 1198 bp)

TGAACAAAGACGAACCTATCGTAATCATTCTGGATAAACTGCACCGTGACCCGCAGGTTTATGGTCCGGACGCTGAAGAGTT
CAAACCGGAACGTATGCTGGACGAGAACTTTGAGAAACTGCCGAAGAACGCATGGAAACCGTTCGGCAACGGTATGCGCGC
GTGTATCGGTCGTCCTTTTGCGTGGCAGGAAGCGCTGCTGGTTGTAGCAATCCTGCTGCAAAACTTCAACTTCCAAATGGACG
ACCCGTCTTACAACCTGCACATCAAACAGACCCTGACTATCAAACCGAAAGATTTCCACATGCGTGCTACTCTGCGTCATGGT
CTGGACGCGACCAAGCTGGGCATCGCCCTGTCTGGTTCTGCTGACCGTGCTCCGCCGGAATCCTCTGGCGCAGCGTCCCGTGT
TCGCAAACAAGCAACTCCACCAGCAGGCCAGCTGAAACCGATGCATATCTTCTTTGGTTCCAACACCGGTACGTGCGAAACG
TTTGCACGTCGCCTGGCAGACGATGCGGTTGGTTATGGTTTCGCAGCTGATGTCCAGTCTCTGGATTCTGCGATGCAGAACGT
ACCGAAAGATGAACCTGTGGTTTTCATCACCGCGAGCTATGAAGGTCAACCACCAGATAACGCCGCACACTTCTTCGAATGG
CTGTCCGCCCTGAAGGAGAACGAACTGGAAGGTGTAAACTACGCAGTTTTTGGTTGTGGTCACCACGACTGGCAGGCAACCT
TCCACCGTATTCCAAAAGCTGTTAACCAGCTGGTAGCGGAACACGGTGGTAACCGTCTGTGCGACCTGGGTCTGGCAGACGCT
GCCAATTCCGATATGTTTACCGATTTTGACAGCTGGGGTGAATCCACTTTCTGGCCAGCGATTACTTCCAAATTTGGCGGTGGC
AAATCCGATGAACCAAAACCTAGCTCTAGCCTGCAAGTGGAAGTCTCTACCGGTATGCGTGCTTCTACCCTGGGCCTGCAACT
GCAAGAAGGCCTGGTTATTGATAACCAGCTGCTGTCTGCTCCGGACGTTCCGGCGAAACGTATGATCCGCTTCAAACTGCCGA
GCGATATGTCTTATCGTTGTGGTGATTACCTGGCTGTACTGCCTGTGAACCCGACGTCTGTTGTCCGTCGTGCGATCCGCCGTT
TCGACCTGCCGTGGGACGCGATGCTGACTATTCGTAAAC

B14003 E1-CYP505 gBlocks® Gene Fragments 1001-1250 bp (Length = 1132 bp)

GATAACAATTTCACACAGGAAACAGAATTCATGTCTGAAAGCAAAACCGTTCCGATTCCGGGTCCACGTGGTGTGCCGCTGCT
GGGTAACATCTACGACATTGAACAGGAAGTACCGCTGCGTAGCATCAACCTGATGGCCGATCAATATGGTCCGATCTACCGT
CTGACGACCTTCGGCTGGAGCCGTGTCTTTGTTTCCACTCACGAGCTGGTAGACGAAGTATGTGACGAAGAGCGCTTTACTAA
AGTTGTTACCGCTGGCCTGAATCAGATTCGTAACGGTGTCCACGACGGCCTGTTCACTGCGAATTTTCCGGGCGAAGAAAACT
GGGCGATTGCACATCGTGTTCTGGTGCCAGCTTTCGGCCCACTGTCCATTCGTGGTATGTTCGATGAGATGTACGACATCGCC
ACTCAGCTGGTGATGAAATGGGCACGTCATGGCCCGACCGTCCCGATCATGGTGACTGACGATTTCACCCGTCTGACCCTGGA
TACCATCGCGCTGTGCGCGATGGGCACTCGCTTTAACTCCTTCTACCATGAAGAAATGCACCCGTTTGTGGAAGCGATGGTGG
GCCTGCTGCAAGGCTCTGGTGATCGTGCGCGTCGTCCGGCACTGCTGAACAACCTGCCGACTTCCGAGAACTCCAAATACTGG
GACGACATCGCATTCCTGCGTAACCTGGCACAGGAACTGGTTGAAGCACGTCGTAAAAACCCGGAAGACAAGAAAGACCTGC
TGAACGCACTGATCCTGGGTCGCGATCCGAAAACTGGCAAAGGTCTGACGGACGAATCTATTATCGACAACATGATTACCTTT
CTGATCGCGGGCCACGAAACCACCTCTGGCCTGCTGTCCTTTCTGTTCTACTATCTGCTGAAAACTCCAAACGCTTACAAAAA
GGCGCAGGAAGAGGTAGACAGCGTTGTTGGCCGCCGTAAAATTACGGTTGAAGATATGTCCCGCCTGCCGTATCTGAACGCA
GTTATGCGCGAAACCCTGCGTCTGCGTTCTACTGCTCCTCTGATTGCTGTTCACGCGCACCCGGAAAAGAACAAAGAAGATCC
AGTAACCCTGGGTGGCGGCAAGTATGTGCTGAACAAAGACGAACCTATCGTAATC

B14004 M2-E1.0-CYP505 gBlocks® Gene Fragments 1001-1250 bp (Length = 1132 bp)

GATAACAATTTCACACAGGAAACAGAATTCATGTCTGAAAGCAAAACCGTTCCGATTCCGGGTCCACGTGGTGTGCCGCTGCT
GGGTAACATCTACGACATTGAACAGGAAGTACCGCTGCGTAGCATCAACCTGATGGCCGATCAATATGGTCCGATCTACCGT
CTGACGACCTTCGGCTGGAGCCGTGTCTTTGTTTCCACTCACGAGCTGGTAGACGAAGTATGTGACGAAGAGCGCTTTACTAA
AGTTGTTACCGCTGGCCTGAATCAGATTCGTAACGGTGTCCACGACGGCCTGTTCACTGCGAATTTTCCGGGCGAAGAAAACT
GGGCGATTGCACATCGTGTTCTGGTGCCAGCTTTCGGCCCACTGTCCATTCGTGGTATGTTCGATGAGATGTACGACATCGCC
ACTCAGCTGGTGATGAAATGGGCACGTCATGGCCCGACCGTCCCGATCATGGTGACTGACGATTTCACCCGTCTGACCCTGGA
TACCATCGCGCTGTGCGCGATGGGCACTCGCTTTAACTCCTTCTACCATGAAGAAATGCACCCGTTTGTGGAAGCGATGGTGG
GCCTGCTGCAAGGCTCTGGTGATCGTCAGCGTCGTCCGGCACTGCTGAACAACCTGCCGACTTCCGAGAACTCCAAATACTGG
GACGACATCGCATTCCTGCGTAACCTGGCACAGGAACTGGTTGAAGCACGTCGTAAAAACCCGGAAGACAAGAAAGACCTGC
TGAACGCACTGATCCTGGGTCGCGATCCGAAAACTGGCAAAGGTCTGACGGACGAATCTATTATCGACAACATGATTACCTTT
CTGATCGCGGGCCACGAAACCACCTCTGGCCTGCTGTCCTTTCTGTTCTACTATCTGCTGAAAACTCCAAACGCTTACAAAAA
GGCGCAGGAAGAGGTAGACAGCGTTGTTGGCCGCCGTAAAATTACGGTTGAAGATATGTCCCGCCTGCCGTATCTGAACGCA
GTTATGCGCGAAACCCTGCGTCTGCGTTCTACTGCTCCTCTGATTGCTGTTCACGCGCACCCGGAAAAGAACAAAGAAGATCC
AGTAACCCTGGGTGGCGGCAAGTATGTGCTGAACAAAGACGAACCTATCGTAATC

B14005 M3-E1.1-CYP505 gBlocks® Gene Fragments 1001-1250 bp (Length = 1132 bp)

GATAACAATTTCACACAGGAAACAGAATTCATGTCTGAAAGCAAAACCGTTCCGATTCCGGGTCCACGTGGTGTGCCGCTGCT
GGGTAACATCTACGACATTGAACAGGAAGTACCGCTGCGTAGCATCAACCTGATGGCCGATCAATATGGTCCGATCTACCGT
CTGACGACCTTCGGCTGGAGCCGTGTCTTTGTTTCCACTCACGAGCTGGTAGACGAAGTATGTGACGAAGAGCGCTTTACTAA
AGTTGTTACCGCTGGCCTGAATCAGATTCGTAACGGTGTCCACGACGGCCTGTTCACTGCGAATTTTCCGGGCGAAGAAAACT
GGGCGATTGCACATCGTGTTCTGGTGCCAGCTTTCGGCCCACTGTCCATTCGTGGTATGTTCGATGAGATGTACGACATCGCC
ACTCAGCTGGTGATGAAATGGGCACGTCATGGCCCGACCGTCCCGATCATGGTGACTGACGATTTCACCCGTCTGACCCTGGA
TACCATCGCGCTGTGCGCGATGGGCACTCGCTTTAACTCCTTCTACCATGAAGAAATGCACCCGTTTGTGGAAGCGATGGTGG
GCCTGCTGCAAGGCTCTGGTGATCGTGCGCGTCGTCCGGCACTGCTGAACAACCTGCCGACTTCCGAGAACTCCAAATACTGG
GACGACATCGCATTCCTGCGTAACCTGGCACAGGAACTGGTTGAAGCACGTCGTAAAAACCCGGAAGACAAGAAAGACCTGC
TGAACGCACTGGTCCTGGGTCGCGATCCGAAAACTGGCAAAGGTCTGACGGACGAATCTATTATCGACAACATGATTACCTTT
CTGATCGTGGGCCACGAAACCACCTCTGGCCTGCTGTCCTTTCTGTTCTACTATCTGCTGAAAACTCCAAACGCTTACAAAAA
GGCGCAGGAAGAGGTAGACAGCGTTGTTGGCCGCCGTAAAATTACGGTTGAAGATATGTCCCGCCTGCCGTATCTGAACGCA
GTTATGCGCGAAACCCTGCGTCTGCGTTCTACTGCTCCTCTGATTGCTGTTCACGCGCACCCGGAAAAGAACAAAGAAGATCC
AGTAACCCTGGGTGGCGGCAAGTATGTGCTGAACAAAGACGAACCTATCGTAATC

B14006 M3-E2.0-CYP505 gBlocks® Gene Fragments 1001-1250 bp (Length = 1198 bp)

TGAACAAAGACGAACCTATCGTAATCATTCTGGATAAACTGCACCGTGACCCGCAGGTTTATGGTCCGGACGCTGAAGAGTT
CAAACCGGAACGTATGCTGGACGAGAACTTTGAGAAACTGCCGAAGAACGCATGGAAACCGTTCGGCAACGGTATGCGCGC
GTGTATCGGTCGTCCTTTTGCGTGGCAGGAAGCGCTGCTGGTTGTAGCAATCCTGCTGCAAAACTTCAACTTCCAAATGGACG
ACCCGTCTTACAACCTGCACATCAAACAGACCTTCACTATCAAACCGAAAGATTTCCACATGCGTGCTACTCTGCGTCATGGT
CTGGACGCGACCAAGCTGGGCATCGCCCTGTCTGGTTCTGCTGACCGTGCTCCGCCGGAATCCTCTGGCGCAGCGTCCCGTGT
TCGCAAACAAGCAACTCCACCAGCAGGCCAGCTGAAACCGATGCATATCTTCTTTGGTTCCAACACCGGTACGTGCGAAACG
TTTGCACGTCGCCTGGCAGACGATGCGGTTGGTTATGGTTTCGCAGCTGATGTCCAGTCTCTGGATTCTGCGATGCAGAACGT
ACCGAAAGATGAACCTGTGGTTTTCATCACCGCGAGCTATGAAGGTCAACCACCAGATAACGCCGCACACTTCTTCGAATGG
CTGTCCGCCCTGAAGGAGAACGAACTGGAAGGTGTAAACTACGCAGTTTTTGGTTGTGGTCACCACGACTGGCAGGCAACCT
TCCACCGTATTCCAAAAGCTGTTAACCAGCTGGTAGCGGAACACGGTGGTAACCGTCTGTGCGACCTGGGTCTGGCAGACGCT
GCCAATTCCGATATGTTTACCGATTTTGACAGCTGGGGTGAATCCACTTTCTGGCCAGCGATTACTTCCAAATTTGGCGGTGGC
AAATCCGATGAACCAAAACCTAGCTCTAGCCTGCAAGTGGAAGTCTCTACCGGTATGCGTGCTTCTACCCTGGGCCTGCAACT
GCAAGAAGGCCTGGTTATTGATAACCAGCTGCTGTCTGCTCCGGACGTTCCGGCGAAACGTATGATCCGCTTCAAACTGCCGA
GCGATATGTCTTATCGTTGTGGTGATTACCTGGCTGTACTGCCTGTGAACCCGACGTCTGTTGTCCGTCGTGCGATCCGCCGTT
TCGACCTGCCGTGGGACGCGATGCTGACTATTCGTAAAC

B14007 M4-E1.2-CYP505 gBlocks® Gene Fragments 1001-1250 bp (Length = 1132 bp)

GATAACAATTTCACACAGGAAACAGAATTCATGTCTGAAAGCAAAACCGTTCCGATTCCGGGTCCACGTGGTGTGCCGCTGCT
GGGTAACATCTACGACATTGAACAGGAAGTACCGCTGCGTAGCATCAACCTGATGGCCGATCAATATGGTCCGATCTACCGT
CTGACGACCTTCGGCTGGAGCCGTGTCTTTGTTTCCACTCACGAGCTGGTAGACGAAGTATGTGACGAAGAGCGCTTTACTAA
AGTTGTTACCGCTGGCCTGAATCAGATTCGTAACGGTGTCCACGACGGCCTGGTCACTGCGAATTTTCCGGGCGAAGAAAACT
GGGCGATTGCACATCGTGTTCTGGTGCCAGCTTTCGGCCCACTGTCCATTCGTGGTATGTTCGATGAGATGTACGACATCGCC
ACTCAGCTGGTGATGAAATGGGCACGTCATGGCCCGACCGTCCCGATCATGGTGACTGACGATTTCACCCGTCTGACCCTGGA
TACCATCGCGCTGTGCGCGATGGGCACTCGCTTTAACTCCTTCTACCATGAAGAAATGCACCCGTTTGTGGAAGCGATGGTGG
GCCTGCTGCAAGGCTCTGGTGATCGTGCGCGTCGTCCGGCACTGCTGAACAACCTGCCGACTTCCGAGAACTCCAAATACTGG
GACGACATCGCATTCCTGCGTAACCTGGCACAGGAACTGGTTGAAGCACGTCGTAAAAACCCGGAAGACAAGAAAGACCTGC
TGAACGCACTGATCCTGGGTCGCGATCCGAAAACTGGCAAAGGTCTGACGGACGAATCTATTATCGACAACATGATTACCTTT
CTGATCGCGGGCCACGAAACCACCTCTGGCCTGCTGTCCTTTCTGTTCTACTATCTGCTGAAAACTCCAAACGCTTACAAAAA
GGCGCAGGAAGAGGTAGACAGCGTTGTTGGCCGCCGTAAAATTACGGTTGAAGATATGTCCCGCCTGCCGTATCTGAACGCA
GTTATGCGCGAAACCCTGCGTCTGCGTTCTACTTTACCTCTGATTGCTGTTCACGCGCACCCGGAAAAGAACAAAGAAGATCC
AGTAACCCTGGGTGGCGGCAAGTATGTGCTGAACAAAGACGAACCTATCGTAATC

B14008 M6-E1.3-CYP505 gBlocks® Gene Fragments 1001-1250 bp (Length = 1132 bp)

GATAACAATTTCACACAGGAAACAGAATTCATGTCTGAAAGCAAAACCGTTCCGATTCCGGGTCCACGTGGTGTGCCGCTGCT
GGGTAACATCTACGACATTGAACAGGAAGTACCGCTGCGTAGCATCAACCTGATGGCCGATCAATATGGTCCGATCTACCGT
CTGACGACCTTCGGCTGGAGCCGTGTCTTTGTTTCCACTCACGAGCTGGTAGACGAAGTATGTGACGAAGAGCGCTTTACTAA
AGTTGTTACCGCTGGCCTGAATCAGATTCGTAACGGTAACCACGACGGCCTGGCCACTGCGAATTTTCCGGGCGAAGAAAAC
TGGGCGATTGCACATCGTGTTCTGGTGCCAGCTTTCGGCCCACTGTCCATTCGTGGTATGTTCGATGAGATGTACGACATCGCC
ACTCAGCTGGTGATGAAATGGGCACGTCATGGCCCGACCGTCCCGATCATGGTGACTGACGATTTCACCCGTCTGACCCTGGA
TACCATCGCGCTGTGCGCGATGGGCACTCGCTTTAACTCCTTCTACCATGAAGAAATGCACCCGTTTGTGGAAGCGATGGTGG
GCCTGCTGCAAGGCTCTGGTGATCGTGCGCGTCGTCCGGCACTGCTGAACAACCTGCCGACTTCCGAGAACTCCAAATACTGG
GACGACATCGCATTCCTGCGTAACCTGGCACAGGAACTGGTTGAAGCACGTCGTAAAAACCCGGAAGACAAGAAAGACCTGC
TGAACGCACTGATCCTGGGTCGCGATCCGAAAACTGGCAAAGGTCTGACGGACGAATCTATTATCGACAACATGATTACCTTT
CTGATCGCGGGCCACGAAACCACCTCTGGCCTGCTGTCCTTTCTGTTCTACTATCTGCTGAAAACTCCAAACGCTTACAAAAA
GGCGCAGGAAGAGGTAGACAGCGTTGTTGGCCGCCGTAAAATTACGGTTGAAGATATGTCCCGCCTGCCGTATCTGAACGCA
GTTATGCGCGAAACCCTGCGTCTGCGTTCTACTGCTCCTCTGATTGCTGTTCACGCGCACCCGGAAAAGAACAAAGAAGATCC
AGTAACCCTGGGTGGCGGCAAGTATGTGCTGAACAAAGACGAACCTATCGTAATC

B14009 M7-E1.4-CYP505 gBlocks® Gene Fragments 1001-1250 bp (Length = 1132 bp)

GATAACAATTTCACACAGGAAACAGAATTCATGTCTGAAAGCAAAACCGTTCCGATTCCGGGTCCACGTGGTGTGCCGCTGCT
GGGTAACATCTACGACATTGAACAGGAAGTACCGCTGCGTAGCATCAACCTGATGGCCGATCAATATGGTCCGATCTACCGT
CTGACGACCTTCGGCTGGAGCCGTGTCTTTGTTTCCACTCACGAGCTGGTAGACGAAGTATGTGACGAAGAGCGCTTTACTAA
AGTTGTTACCGCTGGCCTGAATCAGATTCGTAACGGTGTCCACGACGGCCTGGCCACTGCGAATTTTCCGGGCGAAGAAAACT
GGGCGATTGCACATCGTGTTCTGGTGCCAGCTTTCGGCCCACTGTCCATTCGTGGTATGTTCGATGAGATGTACGACATCGCC
ACTCAGCTGGTGATGAAATGGGCACGTCATGGCCCGACCGTCCCGATCATGGTGACTGACGATTTCACCCGTCTGACCCTGGA
TACCATCGCGCTGTGCGCGATGGGCACTCGCTTTAACTCCTTCTACCATGAAGAAATGCACCCGTTTGTGGAAGCGATGGTGG
GCCTGCTGCAAGGCTCTGGTGATCGTGCGCGTCGTCCGGCACTGCTGAACAACCTGCCGACTTCCGAGAACTCCAAATACTGG
GACGACATCGCATTCCTGCGTAACCTGGCACAGGAACTGGTTGAAGCACGTCGTAAAAACCCGGAAGACAAGAAAGACCTGC
TGAACGCACTGATCCTGGGTCGCGATCCGAAAACTGGCAAAGGTCTGACGGACGAATCTATTATCGACAACATGATTACCTTT
CTGATCGCGGGCCACGAAACCACCTCTGGCCTGCTGTCCTTTCTGTTCTACTATCTGCTGAAAACTCCAAACGCTTACAAAAA
GGCGCAGGAAGAGGTAGACAGCGTTGTTGGCCGCCGTAAAATTACGGTTGAAGATATGTCCCGCCTGCCGTATCTGAACGCA
GTTATGCGCGAAACCCTGCGTCTGCGTTCTACTGCTCCTTGGATTGCTGTTCACGCGCACCCGGAAAAGAACAAAGAAGATCC
AGTAACCCTGGGTGGCGGCAAGTATGTGCTGAACAAAGACGAACCTATCGTAATC

B140010 M8-E1.5-CYP505 gBlocks® Gene Fragments 1001-1250 bp (Length = 1132 bp)

GATAACAATTTCACACAGGAAACAGAATTCATGTCTGAAAGCAAAACCGTTCCGATTCCGGGTCCACGTGGTGTGCCGCTGCT
GGGTAACATCTACGACATTGAACAGGAAGTACCGCTGCGTAGCATCAACCTGATGGCCGATCAATATGGTCCGATCTACCGT
CTGACGACCTTCGGCATTAGCATCGTCATTGTTTCCACTCACGAGCTGGTAGACGAAGTATGTGACGAAGAGCGCTTTACTAA
AGTTGTTACCGCTGGCCTGAATCAGATTCGTAACGGTGTCCACGACGGCCTGGCCACTGCGAATTTTCCGGGCGAAGAAAACT
GGGCGATTGCACATCGTGTTCTGGTGCCAGCTTTCGGCCCACTGTCCATTCGTGGTATGTTCGATGAGATGTACGACATCGCC
ACTCAGCTGGTGATGAAATGGGCACGTCATGGCCCGACCGTCCCGATCATGGTGACTGACGATTTCACCCGTCTGACCCTGGA
TACCATCGCGCTGTGCGCGATGGGCACTCGCTTTAACTCCTTCTACCATGAAGAAATGCACCCGTTTGTGGAAGCGATGGTGG
GCCTGCTGCAAGGCTCTGGTGATCGTGCGCGTCGTCCGGCACTGCTGAACAACCTGCCGACTTCCGAGAACTCCAAATACTGG
GACGACATCGCATTCCTGCGTAACCTGGCACAGGAACTGGTTGAAGCACGTCGTAAAAACCCGGAAGACAAGAAAGACCTGC
TGAACGCACTGATCCTGGGTCGCGATCCGAAAACTGGCAAAGGTCTGACGGACGAATCTATTATCGACAACATGATTACCTTT
CTGATCGCGGGCCACGAAACCACCTCTGGCCTGCTGTCCTTTCTGTTCTACTATCTGCTGAAAACTCCAAACGCTTACAAAAA
GGCGCAGGAAGAGGTAGACAGCGTTGTTGGCCGCCGTAAAATTACGGTTGAAGATATGTCCCGCCTGCCGTATCTGAACGCA
GTTATGCGCGAAACCCTGCGTCTGCGTTCTACTGCTCCTCTGATTGCTGTTCACGCGCACCCGGAAAAGAACAAAGAAGATCC
AGTAACCCTGGGTGGCGGCAAGTATGTGCTGAACAAAGACGAACCTATCGTAATC

B140011 M9-E1.6-CYP505 gBlocks® Gene Fragments 1001-1250 bp (Length = 1132 bp)

GATAACAATTTCACACAGGAAACAGAATTCATGTCTGAAAGCAAAACCGTTCCGATTCCGGGTCCACGTGGTGTGCCGCTGCT
GGGTAACATCTACGACATTGAACAGGAAGTACCGCTGCGTAGCATCAACCTGATGGCCGATCAATATGGTCCGATCTACCGT
CTGACGACCTTCGGCTATAGCTTTGTCTTTGTTTCCACTCACGAGCTGGTAGACGAAGTATGTGACGAAGAGCGCTTTACTAA
AGTTGTTACCGCTGGCCTGAATCAGCTGCGTAACGGTATGCACGACGGCCTGGCCACTGCGAATTTTCCGGGCGAAGAAAAC
TGGGCGATTGCACATCGTGTTCTGGTGCCAGCTTTCGGCCCACTGTCCATTCGTGGTATGTTCGATGAGATGTACGACATCGCC
ACTCAGCTGGTGATGAAATGGGCACGTCATGGCCCGACCGTCCCGATCATGGTGACTGACGATTTCACCCGTCTGACCCTGGA
TACCATCGCGCTGTGCGCGATGGGCACTCGCTTTAACTCCTTCTACCATGAAGAAATGCACCCGTTTGTGGAAGCGATGGTGG
GCCTGCTGCAAGGCTCTGGTGATCGTGCGCGTCGTCCGGCACTGCTGAACAACCTGCCGACTTCCGAGAACTCCAAATACTGG
GACGACATCGCATTCCTGCGTAACCTGGCACAGGAACTGGTTGAAGCACGTCGTAAAAACCCGGAAGACAAGAAAGACCTGC
TGAACGCACTGATCCTGGGTCGCGATCCGAAAACTGGCAAAGGTCTGACGGACGAATCTATTATCGACAACATGATTACCTTT
CTGATCGCGGGCCACGAAACCACCTCTGGCCTGCTGTCCTTTCTGTTCTACTATCTGCTGAAAACTCCAAACGCTTACAAAAA
GGCGCAGGAAGAGGTAGACAGCGTTGTTGGCCGCCGTAAAATTACGGTTGAAGATATGTCCCGCCTGCCGTATCTGAACGCA
GTTATGCGCGAAACCCTGCGTCTGCGTTCTACTGCTCCTCTGATTGCTGTTCACGCGCACCCGGAAAAGAACAAAGAAGATCC
AGTAACCCTGGGTGGCGGCAAGTATGTGCTGAACAAAGACGAACCTATCGTAATC

B140012 M11-E1.7-CYP505 gBlocks® Gene Fragments 1001-1250 bp (Length = 1132 bp)

GATAACAATTTCACACAGGAAACAGAATTCATGTCTGAAAGCAAAACCGTTCCGATTCCGGGTCCACGTGGTGTGCCGCTGCT
GGGTAACATCTACGACATTGAACAGGAAGTACCGCTGCGTAGCATCAACCTGATGGCCGATCAATATGGTCCGATCTACCGT
CTGACGACCTTCGGCCTGAGCCGTGTCTTTGTTTCCACTCACGAGCTGGTAGACGAAGTATGTGACGGCGAGCGCTTTACTAA
AGTTGTTACCGCTGGCCTGAATCAGATTCGTAACATTTGGCACGACGGCCTGGTTACTGCGAATTTTCCGGGCGAAGAAAACT
GGGCGATTGCACATCGTGTTCTGGTGCCAGCTTTCGGCCCACTGTCCATTCGTGGTATGTTCGATGAGATGTACGACATCGCC
ACTCAGCTGGTGATGAAATGGGCACGTCATGGCCCGACCGTCCCGATCATGGTGACTGGTGATTTCACCCGTCTGACCCTGGA
TACCATCGCGCTGTGCGCGATGGGCACTCGCTTTAACTCCTTCTACCATGAAGAAATGCACCCGTTTGTGGAAGCGATGGTGG
GCCTGCTGCAAGGCTCTGGTGATCGTCAGCGTCGTCCGGCACTGCTGAACAACCTGCCGTGCTCCGAGAACTCCAAATACTGG
GACGACATCGCATTCCTGCGTAACCTGGCACAGGAACTGGTTGAAGCACGTCGTAAAAACCCGGAAGACAAGAAAGACCTGC
TGAACGCACTGATCCTGGGTCGCGATCCGAAAACTGGCAAAGGTCTGACGGACGAATCTATTATCGACAACATGATTACCTTT
CTGATCGCGGGCCACGTTACCACCTCTGGCCTGCTGTCCTTTCTGTTCTACTATCTGCTGAAAACTCCATATGCTTACAAAAAG
GCGCAGGAAGAGGTAGACAGCGTTGTTGGCCGCCGTAAAATTACGGTTGAAGATATGTCCCGCCTGCCGTATCTGAACGCAG
TTATGCGCGAAACCCTGCGTCTGCGTTCTACTGCTCCTCTGATTGCTGTTCACGCGCACCCGGAAAAGAACAAAGAAGATCCA
GTAACCCTGGGTGGCGGCAAGTATGTGCTGAACAAAGACGAACCTATCGTAATC

B140013 M11-E2.1-CYP505 gBlocks® Gene Fragments 1001-1250 bp (Length = 1198 bp)

TGAACAAAGACGAACCTATCGTAATCATTCTGGATAAACTGCACCGTGACCCGCAGGTTTATGGTCCGGACGCTGAAGAGTT
CAAACCGGAACGTATGCTGGACGAGAACTTTGAGAAACTGCCGAAGAACGCATGGAAACCGTTCGGCAACGGTATGCGCGC
GTGTATCGGTCGTCCTTTTGCGTGGCAGGAAGCGCTGCTGGTTGTATCTATCCTGCTGCAAAACTTCAACTTCCAAATGGACG
ACCCGTCTTACAACCTGCACATCAAACAGACCCTGACTATCAAACCGAAAGATTTCCACATGCGTGCTACTCTGCGTCATGGT
CTGGACGCGACCAAGCTGGGCATCGCCCTGTCTGGTTCTGCTGACCGTGCTCCGCCGGAATCCTCTGGCGCAGCGTCCCGTGT
TCGCAAACAAGCAACTCCACCAGCAGGCCAGCTGAAACCGATGCATATCTTCTTTGGTTCCAACACCGGTACGTGCGAAACG
TTTGCACGTCGCCTGGCAGACGATGCGGTTGGTTATGGTTTCGCAGCTGATGTCCAGTCTCTGGATTCTGCGATGCAGAACGT
ACCGAAAGATGAACCTGTGGTTTTCATCACCGCGAGCTATGAAGGTCAACCACCAGATAACGCCGCACACTTCTTCGAATGG
CTGTCCGCCCTGAAGGAGAACGAACTGGAAGGTGTAAACTACGCAGTTTTTGGTTGTGGTCACCACGACTGGCAGGCAACCT
TCCACCGTATTCCAAAAGCTGTTAACCAGCTGGTAGCGGAACACGGTGGTAACCGTCTGTGCGACCTGGGTCTGGCAGACGCT
GCCAATTCCGATATGTTTACCGATTTTGACAGCTGGGGTGAATCCACTTTCTGGCCAGCGATTACTTCCAAATTTGGCGGTGGC
AAATCCGATGAACCAAAACCTAGCTCTAGCCTGCAAGTGGAAGTCTCTACCGGTATGCGTGCTTCTACCCTGGGCCTGCAACT
GCAAGAAGGCCTGGTTATTGATAACCAGCTGCTGTCTGCTCCGGACGTTCCGGCGAAACGTATGATCCGCTTCAAACTGCCGA
GCGATATGTCTTATCGTTGTGGTGATTACCTGGCTGTACTGCCTGTGAACCCGACGTCTGTTGTCCGTCGTGCGATCCGCCGTT
TCGACCTGCCGTGGGACGCGATGCTGACTATTCGTAAAC

CYP153A6: (gBlocks for the generation of CYP153A6-M3 - *P. pastoris* cod. opt. P450)

N-terminal overhang to vector *Eco*RI restriction site Overhang for Gibson cloning

C-terminal overhang to CYP505X-reductase

B15131 CYP153A6-M3_ReMono_gBlock1 gBlocks® Gene Fragments 751-1000 bp (Length = 1000 bp)

CTTGAGAAGATCAAAAAACAACTAATTATTGAAAGAATTCCGAAACGATGACTGAGATGACTGTCGCCGCTTCTGATGCAAC
TAATGCCGCATACGGAATGGCTCTGGAGGATATTGACGTCTCTAACCCAGTCCTGTTTAGAGACAATACTTGGCACCCATACT
TTAAGAGATTAAGAGAGGAAGACCCTGTCCACTACTGTAAATCATCCATGTTCGGACCATACTGGTCTGTCACCAAGTACCGT
GACATTATGGCTGTGGAAACCAACCCTAAGGTTTTCTCTTCTGAAGCCAAATCAGGTGGTATTACTATCATGGATGATAACGC
AGCTGCTTCTCTGCCAATGTTCATTGCAATGGACCCACCTAAGCATGACGTGCAAAGAAAGACTGTTTCCCCTATTGTCGCTC
CTGAAAACTTAGCCACTATGGAATCTGTTATCAGACAAAGAACCGCTGACTTGCTTGACGGTTTACCTATCAACGAAGAGTTT
GACTGGGTTCATAGAGTTTCCATTGAATTGACCACTAAGATGCTGGCCACCCTGTTTGACTTCCCTTGGGACGACAGAGCTAA
GTTGACTAGATGGTCTGATGTTACCACTGCTTTGCCTGGTGGTGGAATCATCGACTCTGAGGAACAAAGAATGGCTGAGTTGA
TGGAATGTGCTACCTACTTCACTGAGTTGTGGAACCAGAGAGTTAACGCTGAACCAAAGAACGACCTTATCTCCATGATGGCT
CACTCTGAGTCAACTCGTCACATGGCACCTGAGGAGTACTTGGGAAACATCGTTTTGTTGATCGTGGGTGGTAACGATACTAC
CAGAAACTCCATGACCGGTGGTGTTCTTGCTTTGAATGAGTTTCCAGACGAGTACAGAAAGCTGTCAGCCAACCCAGCTTTGA
TTTCCTCTATGGTTTCTGAGATCATCCGTTGGCAGACTCCATTGTCCCACATGAGACGTACTGCATTGGAAGACATCGAGTTCG
GTGG

B15064 CYP153A6-M3_Mono_gBlock2 gBlocks® Gene Fragments 251-500 bp (Length = 347 bp)

GGAAGACATCGAGTTCGGTGGAAAGCACATTAGACAAGGTGATAAGGTTGTTATGTGGTATGTTTCAGGTAACCGTGATCCA
GAAGCAATTGACAACCCTGACACCTTCATCATTGATAGAGCCAAGCCTAGACAACACCTTTCTTTCGGTTTCGGTATTCACAG
ATGCGTCGGAAACAGACTTGCTGAATTGCAATTGAACATTTTGTGGGAGGAGATTTTGAAACGTTGGCCTGACCCACTTCAAA
TCCAAGTGCTTCAGGAACCTACCAGAGTCTTATCTCCATTCGTCAAGGGTTATGAATCCTTGCCAGTTAGAATCAACGCTGCT
CCGCCCGAATCTTCG

CYP154E1: **(gBlocks for the generation of CYP154E1-M1, *E. coli* cod. opt. PFOR for CYP154E1-M2)**

*Eco*RI restriction site Start/End of CYP154E1 *Hind*III Restriction site

B15065 CYP154E1-M1_gBlock1 gBlocks® Gene Fragments 751-1000 bp (Length = 992 bp)

GGATAACAATTTCACACAGGAAACAGAATTCATGGCGTTTCCTGGTAATCTGGAAGTTTGGGCTCTGACTCACGATGCCCCAC
TGCGTAACGCACTGGCGGACGAATCCGTCTTCGTTCGTGGTTGGCGCAACTGGCGTGCACTGATGGCGGGCGAAGTTGATCCT
ACCCACCCTGTAGCTAACATGCTGCGCGTTGAATCTATGCTGGCTCGTTCCGGCGCCGATCACAAGCGTATGCGTGGTCTGGT
TCAGGCCGCTTTTACTCGTCGTCGTGTTGAAGCACTGCGTCCTCGTATCGAAGAAATTACTAACGAACTGCTGGATCGTATGG
ATGAATCTGATGGCGTTGTAGACCTGAAAGCAGCATACAGCTTCCCGCTGCCGATTCGTGTTATCTCTGAACTGCTGGGCCTG
AACGAGGAGGATCACCTGACCCTGCAAACTCTGGTGACCCGTACCCTGAGCGGCACCGATCCAGAAGCGAACGCAGACGCAT
TCACCTTCGTGGCGAGCCTGATCGAAGCGAAACGTAAAAATCTGGACGACGGCCTGATTTCCGCGATGATTGAGGCCCGTGC
CGAAGACGGTGACCGTCTGAGCGAAACCGAACTGATTCATAACACTCTGCTGCTGATTATCGGTGGTTTCGAAACCACGATG
GGTATGATCTCTAACTCTGTTCAGCTGCTGCTGACTCACCCGGACCAGCTGCACCTGCTGCGTACGGGCCAGGCGAGCTGGGA
AAACGCCATCGAAGAATGCCTGCGTTTCGAGTCTGCCGTGGTCATGCTGCCGTTCCTGTATACTACGCGCGATGTTGAAATTG
ACGGTATCACTATTCCGGCTGGTGATGCCGTGCTGATCGGTTTCGGCCCAGCAAACCGTGACCCGCAGGCCTATGATGATCCG
GATCGTTTCGACATCACCCGTCCGCGTCCACGTCACCTGGCCTTTGGTCATGGTGCTCACCTGTGTCTGGGTGCAGCCCTG

B15066 CYP154E1-M1_gBlock2 gBlocks® Gene Fragments 751-1000 bp (Length = 987 bp)

TCTGGGTGCAGCCCTGGCTCGTCTGGAGCTGCTGATCGCTCTGCCGGCTCTGTTCGAACGTTTCCCGGACATCACCCTGGTTGG
TGAAGCTCCGCCGACTCCGACTGTGTTCATGAACCACCCACTGAGCCGTCCTGTGCTGCTGCGTCCGAAGCCGTAAGGATCTA
GGAGGATAAAGAAATGGTGAACGCAAACGACAACGTGGTCATCGTCGGTACCGGACTGGCTGGCGTTGAGGTCGCCTTCGGC
CTGCGCGCCAGCGGCTGGGAAGGCAATATCCGGTTGGTGGGGGATGCGACGGTAATTCCCCATCACCTACCACCGCTATCCA
AGGCTTACTTGGCCGGCAAAGCCACAGCGGAAAGCCTGTACCTGAGAACCCCAGATGCCTATGCAGCGCAGAACATCCAACT
ACTCGGAGGCACACAGGTAACGGCTATCAACCGCGACCGACAGCAAGTAATCCTATCGGATGGCCGGGCACTGGATTACGAC
CGGCTGGTATTGGCTACCGGAGGGCGTCCAAGACCCCTACCGGTGGCCAGTGGCGCAGTTGGAAAGGCGAACAACTTTCGAT
ACCTGCGCACACTCGAGGACGCCGAGTGCATTCGCCGGCAGCTGATTGCGGATAACCGTCTGGTGGTGATTGGTGGCGGCTA
CATTGGCCTTGAAGTGGCTGCCACCGCCATCAAGGCGAACATGCACGTCACCCTGCTTGATACGGCAGCCCGGGTTCTGGAGC
GGGTTACCGCCCCGCCGGTATCGGCCTTTTACGAGCACCTACACCGCGAAGCCGGCGTTGACATACGAACCGGCACGCAGGT
GTGCGGGTTCGAGATGTCGACCGACCAACAGAAGGTTACTGCCGTCCTCTGCGAGGACGGCACAAGGCTGCCAGCGGATCTG
GTAATCGCCGGGATTGGCCTGATACCAAACTGCGAGTTGGCCAGTGCGGCCGGCCTGCAGGTTGATAACGGCATCGTGAT

B15067 CYP154E1-M1_gBlock3 gBlocks® Gene Fragments 751-1000 bp (Length = 853 bp)

CAGGTTGATAACGGCATCGTGATCAACGAACACATGCAGACCTCTGATCCCTTGATCATGGCCGTCGGCGACTGTGCCCGATT
TCACAGTCAGCTCTATGACCGCTGGGTGCGTATCGAATCGGTGCCCAATGCCTTGGAGCAGGCACGAAAGATCGCCGCCATC
CTCTGTGGCAAGGTGCCACGCGATGAGGCGGCGCCCTGGTTCTGGTCCGATCAGTATGAGATCGGATTGAAGATGGTCGGAC
TGTCCGAAGGGTACGACCGGATCATTGTCCGCGGCTCTTTGGCGCAACCCGACTTCAGCGTTTTCTACCTGCAGGGAGACCGG
GTATTGGCGGTCGATACAGTGAACCGTCCAGTGGAGTTCAACCAGTCAAAACAAATAATCACGGATCGTTTGCCGGTTGAAC
CAAACCTACTCGGTGACGAAAGCGTGCCGTTAAAGGAAATCATCGCCGCCGCCAAAGCTGAACTGAGTAGTGCCTGAGGATC
TAGGAGGATAAAGAAATGTCTAAAGTAGTGTATGTGTCACATGATGGAACGCGTCGCGAACTGGATGTGGCGGATGGCGTCA
GCCTGATGCAGGCTGCAGTCTCCAATGGTATCTACGATATTGTCGGTGATTGTGGCGGCAGCGCCAGCTGTGCCACCTGCCAT
GTCTATGTGAACGAAGCGTTCACGGACAAGGTGCCCGCCGCCAACGAGCGGGAAATCGGCATGCTGGAGTGCGTCACGGCCG
AACTGAAGCCGAACAGCAGGCTCTGCTGCCAGATCATCATGACGCCCGAGCTGGATGGCATCGTGGTCGATGTTCCCGATAG
GCAATGGTAAAAGCTTGGCTGTTTTGGCG

B15068 CYP154E1-M2_PFOR_gBlock gBlocks® Gene Fragments 751-1000 bp (Length = 999 bp)

CAACATCCTGTAACTATTGGCGAACCATCCACTCGCTCCGTATCTCGCACTGTGACGGTGGAACGCCTGGATCGTATCGTTGA
CGATGTTCTGCGTGTAGTGCTGCGTGCACCTGCAGGCAATGCACTGCCTGCATGGACTCCTGGTGCGCACATCGACGTTGATC
TGGGTGCTCTGAGCCGTCAGTACTCTCTGTGTGGTGCACCGGATGCTCCGACTTATGAGATCGCAGTACTGCTGGACCCAGAA
TCCCGTGGCGGTTCTCGTTACGTGCACGAACAGCTGCGTGTTGGTGGTAGCCTGCGCATTCGTGGTCCACGTAACCACTTCGC
TCTGGACCCTGACGCAGAACACTACGTTTTCGTTGCAGGTGGCATCGGCATTACTCCAGTTCTGGCCATGGCTGACCACGCTC
GTGCTCGTGGCTGGTCTTATGAGCTGCACTATTGTGGTCGTAACCGTTCTGGTATGGCGTACCTGGAACGTGTTGCTGGTCATG
GCGATCGTGCTGCGCTGCACGTTAGCGCAGAGGGTACGCGTGTTGATCTGGCTGCACTGCTGGCAACTCCTGTTTCTGGCACT
CAAATCTACGCCTGTGGTCCAGGTCGTCTGCTGGCTGGTCTGGAGGATGCCTCTCGTCATTGGCCAGATGGTGCTCTGCATGTT
GAGCATTTCACCAGCTCCCTGACCGCTCTGGACCCAGATGTCGAACACGCGTTTGATCTGGACCTGCGTGACAGCGGTCTGAC
CGTCCGTGTCGAACCTACTCAGACCGTGCTGGACGCTCTGCGTGCCAACAACATTGACGTACCATCTGATTGCGAAGAAGGTC
TGTGCGGTTCCTGTGAAGTCACTGTGCTGGAAGGTGAAGTGGACCACCGTGACACCGTACTGACCAAAGCTGAACGTGCAGC
GAATCGTCAGATGATGACTTGCTGCAGCCGTGCATGTGGCGACCGTCTGACTCTGCGTCTGTAAAAGCTTGGCTGTTTTGGCG
G

Primers (for amplification, colony-PCR, overlap extension-PCR and sequencing)

P12408	PAOX800f	CTGTTCTAACCCCTACTTG
P12575	OriAmpF	GAGCGTCAGACCCCGTAGAAAAGATCAAAGGATCTTCTTG
P12882	KanMX6_rv	CTGATTGCCCGACATTATC
P14176	aox1fw_RTcr	GAAGCTGCCCTGTCTTAAACCTT
P14899	AOXseq_rv	TCCCAAACCCCTACCACAAG
B14014	ptac_seq_fw	CGACATCATAACGGTTCTGGCAAATATTC
B14015	pMS470d8_Rv	GTTTTATCAGACCGCTTCTGCG
B14016	E3_seq_rv	GCAGAGATCGGCGTGTCC
B14017	E3_seq_fw	GAACGTGGTGAAGAGGTGCC
B14018	E3-BamHI-d8-rv	TCTCATCCGCCAAAACAGCCGGATCCTCAAGTGAAAACATCGGTG
B14019	pTac-E3-EcoRI_fw	GATAACAATTTCACACAGGAAACAGAATTCGACGCGATGCTGACTATTC GTAAAC
B14020	ptac-E1-fw	GATAACAATTTCACACAGGAAACAGAATTCATGTCTGAAAGCAAAACCG TTC
B14021	M10-I81I-fw	CTGAATCAGATTCGTAACGGTATGC
B14022	M10-I81I-rv	CATACCGTTACGAATCTGATTCAGG
B14023	M5-V85V-fw	GTAACGGTGTCCACGACG
B14024	M5-V85V-rv	CGTCGTGGACACCGTTAC
B14031	pMS470-E3_1220_Rv	CTGCCGCCAGGCAAATTC
B14032	pMS470-E3_1260_Rv	GGCGTTTCACTTCTGAGTTCG
B14033	pMS470-E3_1510_Rv	CAGGATGGCCTTCTGCTTAATTTG
B15019	E2-seq_Fwd:	TGTACTGCCTGTGAACCC
B15020	E2-seq_Rev:	GCATCGGTTTCAGCTGGC
B15053	CYP153A6-M1_Mono_Fw	GATAACAATTTCACACAGGAAACAGAATTCATGACCGAAATGACGGTG GC
B15054	CYP153A6-M1_Mono_Rv	AGGATTCCGGCGGAGCGGCGTTGATGCGCACG
B15055	CYP505_Red_Fw	GCTCCGCCGGAATCCT
B15056	CYP505_Red_Rv	CGCCAAAACAGCCAAGCTTTCATTAAGTGAAAACATCGGTGGCATAACG
B15057	CYP505-M12_Red_Fw	GCTCCGCCCGAATCTTCG
B15058	CYP505-M12_Red_Rv	CCTCTTGAGCGGCCGCCTATCACGTAAACACATCAGTCGCATAAC

B15059	CYP153A6-M3_Mono_Fw	AAACAACTAATTATTGAAAGAATTCCGAAACGATGACTGAGATGACTGTCGCC
B15060	CYP154E1_Mono_Fw	GATAACAATTTCACACAGGAAACAGAATTCATGGCGTTTCCTGGTAATCTGG
B15061	CYP154E1-M2_Mono_Rv	GGTTCGCCAATAGTTACAGGATGTTGCGGCTTCGGACGCAG
B15062	CYP154E1-M3_Mono_Rv	AGG ATT CCG GCG GAG CCGG CTT CGG ACG CAG
B15073	CYP153A6-M3_g1Red_Rv	TAACTCGTGACGCGGCACCCGAAGATTCGGGCGGAGCAG
B15074	CYP154E1-M1_g1_Fw	GATAACAATTTCACACAGGAAACAGAATTCATGGCGTTTCCTGGTAATCTGGAA
B15075	CYP154E1-M1_g2_Rv	CAGAGGTCTGCATGTGTTCGTTGATCACGATGCCGTTATCAACCTG
B15076	CYP154E1-M1_g3_Rv	CTGTATCAGGCTGAAAATCTTCTCTCATCCGCCAAAACAGCCAAGCTTTTAC
B15077	CYP153A6-M3_g1_Rv	ACATAACAACCTTATCACCTTGTCTAATGTGCTTTCCACCGAACTCGATGTCTTCC
B15181	M3-Mono_Rv	CGTCTGGAAACTCATTCAAAGCAAGA
B15182	M3-Mono_Fwd	TCTTGCTTTGAATGAGTTTCCAGACG
B15183	M3-Red_Fwd	CACGATCAGAAAGCCTAGCCAG
B15184	M3-Red.2_Fwd	ATAACATTCTCCGTGCTGAACGC
B15185	M3-Red_Rv	CATCCTCTTTTTGACGATCTCCTCG

Genes

All genes used during this master thesis were ordered from DNA2.0 (purchased by bisy).

DNA sequence of CYP505X-M12

N-terminal overhang to vector *Eco*RI restriction site

C-terminal overhang to vector *Hind*III Restriction site

TATTGAAAGAATTCAAAATGTCAGAATCAAAAACTGTGCCAATTCCTGGACCTCGCGGCGTACCGCTTCTTGGAAACATCTAC
GACATCGAGCAGGAAGTTCCACTGAGGTCGATCAATCTCATGGCTGACCAGTATGGTCCCATCTACCGCCTCACTACCTTTGG
CTGGAGCCGAGTATTCGTTTCTACACACGAGCTGGTCGATGAAGTTTGCGACGAGGAGAGGTTCACCAAAGTGGTCACTGCC
GGGCTTAATCAGATTCGCAACGGTGTCCACGACGGCCTTTTCACGGCGAACTTTCCGGGCGAAGAGAACTGGGCCATCGCTC
ACCGAGTTCTGGTCCCTGCATTCGGCCCGTTGAGTATCAGGGGAATGTTTGACGAGATGTATGACATCGCTACCCAACTTGTG
ATGAAATGGGCCCGCCATGGCCCCACAGTACCCATCATGGTTACTGACGACTTTACCCGGCTCACCCTTGATACTATAGCGTT
ATGTGCAATGGGGACACGCTTCAACTCTTTCTACCATGAGGAGATGCACCCGTTTGTGGAGGCTATGGTTGGGTTACTCCAGG
GGTCGGGCGATCGTGCGAGGCGCCCCGCGCTCCTTAACAATTTGCCTACCTCCGAGAACTCTAAGTATTGGGACGACATCGCA
TTTCTAAGAAATCTGGCGCAGGAGCTCGTCGAGGCTAGGCGCAAGAATCCGGAGGATAAGAAGGATCTGCTCAACGCCCTCA
TTCTGGGGCGTGACCCAAAGACCGGAAAGGGTCTAACAGACGAGTCCATTATCGACAATATGATAACTTTCTTGATTGCCGGC
CATGAAACGACCAGCGGCCTGCTAAGCTTCTTGTTCTACTACTTACTTAAGACCCCTAACGCGTACAAGAAGGCGCAAGAGG
AAGTGGACTCGGTGGTCGGACGACGGAAAATCACAGTGGAGGACATGTCTCGGCTCCCGTACCTCAACGCAGTCATGCGCGA
GACTCTGAGGCTGAGGAGTACAGCCCCTCTGATCGCTGTCCATGCGCACCCAGAGAAGAACAAGGAGGATCCGGTCACGTTG
GGGGGTGGCAAATACGTGCTGAACAAGGACGAGCCCATCGTGATAATCTTGGACAAATTGCATCGGGATCCACAGGTCTACG
GCCCCGATGCCGAAGAGTTCAAGCCTGAGCGGATGCTGGATGAAAACTTTGAAAAGCTTCCAAAGAATGCCTGGAAGCCCTT
CGGGAATGGAATGAGGGCCTGTATTGGCCGTCCGTTCGCGTGGCAGGAGGCTCTGCTCGTTGTGGCCATTCTGTTGCAAAATT
TCAATTTCCAAATGGACGACCCGTCATACAACTTGCACATTAAGCAGACGCTAACCATCAAGCCTAAGGATTTTCACATGAGG
GCAACGTTGCGGCATGGCCTTGATGCCACAAAATTGGGCATCGCCCTCTCTGGAAGTGCAGATAGGGCTCCGCCCGAATCTTC
GGGTGCCGCGTCACGAGTTAGAAAGCAGGCCACCCCACCCGCTGGCCAGCTAAAGCCTATGCACATCTTCTTTGGCTCCAACA
CGGGGACGTGCGAAACGTTCGCTCGACGTTTAGCCGATGATGCCGTCGGCTACGGTTTCGCGGCGGACGTGCAGAGCCTGGA
CAGCGCGATGCAAAACGTGCCAAAAGACGAGCCGGTGGTGTTCATCACCGCGTCCTATGAGGGACAGCCACCCGATAACGCG
GCACACTTTTTCGAGTGGTTGTCTGCACTTAAGGAAAACGAATTGGAAGGGGTGAACTATGCGGTGTTCGGTTGTGGCCACCA
TGATTGGCAAGCCACCTTCCACCGCATTCCAAAAGCTGTCAATCAGCTCGTGGCAGAACATGGCGGCAATCGGCTCTGCGATC
TCGGACTGGCGGACGCTGCAAACAGCGACATGTTCACGGATTTCGACAGCTGGGGAGAGTCTACATTCTGGCCTGCCATCAC
ATCGAAGTTCGGCGGAGGCAAAAGCGACGAACCTAAGCCGAGCTCATCCCTCCAAGTGGAAGTTTCCACCGGGATGCGCGCT
TCGACCCTTGGACTGCAGCTGCAGGAAGGATTGGTGATCGACAATCAACTACTCTCCGCCCCTGATGTACCCGCTAAGCGGAT
GATCCGGTTTAAACTACCCTCCGACATGTCCTACCGCTGCGGGGACTACCTGGCGGTTCTCCCCGTCAACCCAACAAGCGTTG
TTCGCCGTGCCATTCGCCGGTTCGATCTCCCTTGGGATGCGATGCTCACGATCAGAAAGCCTAGCCAGGCGCCGAAGGGGTCT
ACCTCGATCCCCCTTGACACACCCATCTCCGCATTCGAGCTGCTGTCGACCTATGTCGAACTGTCACAACCGGCTTCCAAGAG
AGATCTCACTGCATTGGCGGATGCTGCTATAACTGACGCAGACGCCCAAGCGGAGCTACGATACCTTGCGTCAAGCCCAACC
AGGTTCACCGAGGAGATCGTCAAAAAGAGGATGTCTCCACTCGACCTCCTCATTCGTTACCCGAGCATAAAGTTGCCAGTTGG
CGATTTTCTGGCTATGCTGCCGCCGATGAGAGTGCGCCAGTACTCGATTTCGTCCAGCCCATTAGCTGATCCCTCTGAGTGCA
GTATAACATTCTCCGTGCTGAACGCGCCCGCACTGGCCGCCGCTAGTCTACCGCCGGCGGAAAGAGCCGAGGCTGAGCAATA
CATGGGTGTCGCTTCCACGTACCTTAGCGAGCTCAAGCCAGGGGAGCGGGCCCACATTGCTGTCCGCCCAAGTCATTCCGGCT
TTAAGCCACCCATGGACCTTAAGGCCCCGATGATTATGGCGTGCGCCGGCTCAGGACTCGCACCGTTTAGGGGCTTCATTATG
GACAGGGCGGAGAAAATACGGGGCAGACGATCCTCAGTAGGAGCGGACGGCCAGCTCCCTGAGGTTGAGCAGCCTGCCAAA
GCTATTCTTTACGTGGGCTGCAGAACAAAGGGGAAGGACGACATCCACGCTACTGAGCTGGCAGAGTGGGCCCAATTAGGTG
CAGTCGACGTCCGCTGGGCCTATAGCAGACCAGAGGATGGTAGCAAGGGCCGCCACGTGCAGGACCTCATGCTGGAGGACA
GGGAAGAACTGGTGTCACTGTTCGACCAGGGTGCAAGGATATACGTATGCGGCAGTACGGGTGTTGGGAATGGTGTCCGTCA
AGCCTGTAAAGACATCTATTTGGAGAGGAGGCGGCAGCTGCGCCAGGCCGCCAGGGAAAGGGGGGAAGAGGTCCCAGCCGA
GGAGGACGAGGACGCAGCAGCGGAGCAGTTTCTTGATAATCTTCGCACAAAGGAGCGTTATGCGACTGATGTGTTTACGTGA
TAGGCGGCCGCTCAAGAGGA

DNA sequence of CYP505A1-M1

N-terminal overhang to vector *Eco*RI restriction site

C-terminal overhang to vector *Hind*III Restriction site

TATTGAAAGAATTCAAAATGGCAGAGTCCGTACCGATTCCAGAACCACCAGGCTACCCCTTAATCGGCAATCTCGGAGAGTTT
ACCAGCAACCCTCTATCGGATCTCAACAGGCTGGCGGATACGTACGGCCCGATTTTTCGGCTTCGCCTGGGTGCCAAGGCTCC
GATCTTTGTTTCGTCCAACTCCCTCATTAACGAGGTCTGCGATGAAAAGAGGTTCAAAAAGACTCTCAAGTCGGTTCTTAGTC
AAGTTCGCGAGGGCGTACACGACGGCCTCTTTACGGCTTTCGAGGATGAGCCCAACTGGGGCAAAGCACATAGGATCCTGGT
CCCGGCGTTTGGGCCTCTGAGTATCCGGGGAATGTTCCCCGAGATGCACGATATTGCCACTCAGCTGTGCATGAAGTTCGCCC
GTCACGGCCCTAGGACCCCTATCGACACCTCGGACAACTTTACTCGGCTCGCACTCGACACCTTGGCTCTGTGCGCCATGGAC
TTCAGGTTTTACTCCTACTACAAGGAGGAGTTGCACCCCTTCATCGAGGCTATGGGCGATTTCCTCACCGAATCTGGCAACCG
GAATAGACGCCCTCCGTTTGCCCCGAACTTTCTGTATCGCGCTGCGAACGAAAAGTTCTACGGCGATATTGCCCTTATGAAGT
CTGTTGCGGACGAGGTCGTCGCAGCACGCAAAGCATCGCCGAGCGACCGCAAAGATCTACTAGCTGCCATGCTTAACGGCGT
GGACCCACAGACGGGGGAGAAGCTGAGCGATGAGAACATTACCAACCAGTTGATTACATTCCTGATTGCGGGCCACGAGACA
ACGTCTGGTACTCTCTCCTTCGCTATGTATCAACTGCTTAAGAACCCGGAGGCATATTCTAAAGTGCAGAAGGAGGTCGATGA
GGTCGTTGGAAGGGGTCCTGTGTTGGTGGAACATTTGACGAAGCTCCCATACATCTCGGCGGTTTTGAGAGAAACGCTTAGGC
TCAATTCTCCCATCACGGCGTTCGGCCTTGAAGCCATCGACGATACGTTCCTGGGCGGGAAGTACCTCGTCAAGAAGGGGGA
GATAGTTACTGCGCTGCTGAGCCGGGGCCACGTGGACCCAGTTGTCTATGGCAACGACGCGGATAAGTTCATACCCGAGCGG
ATGCTCGACGACGAGTTCGCACGCCTCAATAAGGAGTATCCAAATTGTTGGAAACCCTTTGGAAACGGGAAGAGGGCCTGCA
TTGGTCGTCCCTTCGCTTGGCAAGAATCACTGTTAGCGATGGTCGTGCTGTTCCAGAACTTTAACTTCACGATGACGGATCCG
AATTACGCACTAGAGATTAAGCAGACTCTCACCATAAAGCCTGACCACTTTTACATTAATGCTACGCTGAGACACGGCATGAC
CCCTACCGAGCTGGAACACGTGTTAGCGGGCAACGGTGCTACGTCATCGTCCACACATAACATTAAGGCGGCAGCGAACCTG
GACGCCAAGGCCGGCTCAGGAAAACCGATGGCCATCTTCTACGGGAGCAACTCCGGCACATGCGAAGCGCTTGCGAACCGTC
TTGCAAGCGACGCCCCCTCTCATGGTTTCTCCGCGACGACAGTTGGGCCGCTCGATCAAGCAAAGCAAAATCTCCCAGAGGAT
CGTCCCGTGGTCATCGTCACCGCTTCTTATGAGGGGCAGCCCCCGAGCAATGCTGCCCATTTCATCAAATGGATGGAGGACTT
GGATGGGAACGACATGGAAAAAGTATCTTACGCTGTCTTTGCCTGTGGTCATCACGACTGGGTGGAGACATTTCATCGGATCC
CGAAACTCGTCGACTCCACGCTGGAAAAGAGGGGCGGGACAAGACTAGTGCCAATGGGGTCTGCCGACGCCGCGACCAGCG
ACATGTTCTCCGACTTTGAGGCTTGGGAGGACATCGTTCTTTGGCCTGGGCTCAAAGAAAAGTATAAGATTTCCGACGAAGAG
AGCGGTGGCCAGAAGGGTCTGCTGGTTGAGGTTTCCACTCCGCGAAAGACCAGCTTGCGTCAGGATGTGGAGGAGGCCCTTG
TGGTCGCCGAAAAGACTTTGACGAAGTCCGGCCCAGCAAAGAAACATATAGAAATACAGCTGCCATCAGCGATGACTTACAA
GGCTGGAGATTATCTGGCGATCCTCCCCCTCAATCCTAAATCAACCGTCGCCAGGGTTTTTCGGCGGTTCAGTCTTGCCTGGG
ACAGTTTCCTTAAGATTCAATCCGAGGGCCCAACCACACTGCCCACAAATGTGGCCATAAGCGCTTTCGACGTATTCTCTGCA
TATGTCGAGCTCAGCCAGCCCGCAACCAAGCGCAATATCTTGGCCTTGGCCGAGGCTACAGAAGATAAGGACACCATACAGG
AGCTGGAACGACTTGCGGGGGACGCATACCAAGCTGAAATCTCGCCGAAGAGAGTATCGGTGCTAGACTTGCTGGAGAAGTT
CCCGGCAGTGGCTCTCCCTATCTCATCATATTTGGCTATGTTACCGCCAATGAGGGTCCGCCAGTACTCAATCTCGTCATCCCC
GTTTGCGGATCCTAGCAAACTGACGTTGACATACAGCCTGCTGGATGCACCTAGCTTAAGCGGTCAAGGCAGACACGTGGGA
GTAGCAACTAATTTCCTCTCTCACCTTACTGCGGGAGACAAGCTGCATGTGTCAGTTAGAGCCAGCTCCGAGGCTTTCCACCT
ACCCTCGGACGCTGAGAAAACTCCAATCATTTGTGTGGCTGCGGGCACAGGCTTAGCGCCCCTAAGGGGATTCATCCAAGAA
AGGGCCGCGATGCTCGCCGCCGGGAGGACACTTGCCCCCGCGCTCTTATTCTTCGGATGCCGGAACCCAGAGATCGATGACCT
TTACGCCGAGGAGTTCGAACGCTGGGAGAAGATGGGCGCCGTCGATGTCCGCCGAGCCTACTCTCGGGCCACCGATAAGTCC
GAGGGTTGTAAATACGTGCAGGACCGAGTGTATCACGACAGAGCTGATGTGTTCAAGGTCTGGGACCAGGGTGCAAAAGTGT
TCATATGCGGCAGCAGGGAGATCGGAAAGGCTGTTGAAGATGTGTGCGTCCGTTTGGCCATTGAAAAGGCTCAGCAGAACGG
ACGCGATGTCACAGAGGAGATGGCGCGCGCCTGGTTCGAACGTAGTAGGAACGAGAGATTCGCGACCGACGTGTTTGATTGA
TGAGCGGCCGCTCAAGAGGA

DNA sequence of CYP153A6-M1

N-terminal overhang to vector Start/End of P450 Start/End of Ferredoxin Reductase

Start/End of Ferredoxin C-terminal overhang to vector

GGTAAAAAATGACCGAAATGACGGTGGCCGCCAGCGACGCGACGAACGCGGCGTACGGGATGGCCTTGGAGGACATCGATG
TGAGCAATCCCGTGCTGTTCCGGGACAACACCTGGCATCCCTATTTCAAACGCCTGCGCGAAGAGGATCCGGTTCACTACTGC
AAGAGCAGCATGTTCGGCCCCTACTGGTCGGTGACCAAGTACCGCGACATCATGGCAGTCGAGACCAACCCGAAGGTGTTCT
CGTCGGAGGCTAAAAGTGGCGGCATCACCATCATGGACGACAACGCCGCAGCATCGCTTCCCATGTTCATCGCCATGGATCC
ACCGAAACACGATGTCCAGCGAAAGACCGTGAGCCCGATCGTGGCGCCCGAAAACCTTGCCACCATGGAATCGGTGATTCGC
CAGCGCACCGCGGACCTCCTCGACGGATTGCCGATCAATGAAGAGTTCGACTGGGTGCATCGGGTGTCGATCGAATTGACCA
CGAAGATGCTGGCGACGCTGTTCGATTTTCCCTGGGACGACCGCGCCAAGTTGACGCGCTGGTCGGACGTCACCACGGCGTTG
CCCGGTGGCGGGATCATCGATTCTGAAGAACAGCGCATGGCCGAGCTGATGGAGTGCGCGACGTATTTCACCGAGCTGTGGA
ACCAGCGCGTGAATGCCGAACCCAAGAACGATCTCATCTCGATGATGGCCCATTCGGAGTCAACACGACACATGGCGCCCGA
GGAATATCTCGGAAACATCGTGCTGCTGATCGTCGGCGGCAACGACACCACCCGCAACTCGATGACCGGCGGTGTGTTGGCC
CTGAACGAATTTCCCGACGAATACCGCAAACTGTCCGCCAACCCGGCGTTGATCAGCTCTATGGTGTCGGAGATCATCCGGTG
GCAAACACCTCTTTCGCACATGCGTCGTACCGCATTGGAAGACATCGAGTTCGGCGGCAAGCACATCCGCCAGGGCGACAAA
GTCGTGATGTGGTACGTGTCCGGCAACCGGGACCCCGAGGCCATCGACAATCCCGACACATTCATCATCGATCGCGCCAAGC
CCCGCCAGCACTTGTCCTTCGGGTTCGGCATCCACCGCTGCGTCGGCAACAGACTCGCCGAACTACAGCTCAACATCCTGTGG
GAAGAAATCCTCAAACGGTGGCCGGACCCACTGCAGATCCAGGTTCTTCAAGAACCGACCCGCGTGCTCTCACCGTTCGTCA
AGGGCTACGAATCGCTGCCCGTGCGCATCAACGCCTGATGATCCACACCGGCGTGACCGAAGCCGTTGTGGTGGTCGGTGCC
GGCCAGGCTGGCGCACAGACAGTCACCAGCCTTCGACAAAGAGGGTTCGAGGGGCAGATCACCCTGCTCGGCGACGAGCCG
GCGCTGCCCTATCAGCGCCCCCCACTGTCGAAAGCCTTCCTGGCCGGCACCCTCCCGCTGGACCGCCTGTACCTACGCCCTGC
GGCGTTCTACCAGCAAGCCCACGTCGATGTCATGGTCGACACTGGGGTGAGCGAGCTCGACACCGAAAACAGACGCATCCGG
CTCACCGACGGCCGCGCTATCAGCTTCGATCACCTAGTGCTGGCCACCGGCGGCCGCCCCCGCCCGCTGGCCTGCCCTGGTGC
CGATCACCCCCGCGTCCACTACCTGCGAACAGTGACCGACGTAGACAGGATCCGCTCCCAGTTCCATCCCGGGACACGGCTG
GTCCTGGTGGGCGGCGGTTACATCGGCCTCGAAATCGCCGCGGTAGCCGCAGAACTCGGGTTGACCGTGACCGTCCTCGAAG
CACAAACCACCGTCTTGGCACGGGTCACCTGTCCGACGGTGGCCCGCTTCTTCGAACACACCCACCGGCGAGCAGGAGTGAC
GATTCGGTGCGCAACCACAGTCACACGCATCCACGACAGCTCGTCCACCGCACGCATTGAACTCGATAGCGGCGAGTACATC
GACGCAGACCTCGTCATAGTTGGGATAGGATTGCTCCCCAACGTCGACTTAGCCTCAGCAGCTGGGCTGACATGCGAAAGCG
GCATCGTCGTGGACAGCCGTTGCCAGACAAGCGCACCTGGCATCTACGCAGCCGGTGACTGCACCCAGTACCCGAGCCCCAT
ATACGGCCGACCACTTCACCTCGAGTCGGTGCACAACGCCATCGAACAGGCCAAAACGGCCGCCGCAGCGATCCTCGGCAGA
GACGAGCCGTTCCGTCAAGTGCCCTGGTTCTGGTCAGACCAGTACAACATCAAACTACAGACGGCCGGCGTCAACGAAGGCT
ACGACGACGTGATCATCCGGGGTGATCCGGCCTCAGCATCGTTTGCAGCCTTCTACCTGCGCGCCGGGAAACTGCTGGCCGTC
GATGCAATCAACCGGCCGCGCGAATTCATGGCGTCGAAAACCCTTATCGCCGAACGCGCAGAGGTAGACCCGACGCAACTCG
CCGACGAGAGCCTCCCCCCCACAGCCCTTGCGGCGGCGGTCAACGGCCCTACCCGCGCAACGTCCCCAACCTCCCTCTAACCC
ACTGATAAAGGAATCGAAATGCCGAAGATCACCTACATCGACTACACCGGTACGAGCCGCTGCGTTGACGCCGAAAACGGCA
TGTCACTGATGGAAATCGCCATCAATAACAACGTGCCAGGCATCGACGGGGACTGCGGCGGGGAGTGCGCATGCGCGACATG
CCATGTGCACGTCGATGCAGACTGGTTGGACAAACTGCCGCCCAGCAGCGACCAAGAGGTGTCAATGCTGGAATTCTGTGAT
GGCGTAGACCACACATCCCGACTCGGCTGCCAAATCAAGATTTGCCCGACTTTGGATGGCATCGTCGTACGGACACCAGCTGC
ACAACATTAGGGTTGACCCC

Supplementary data

S 1: Gene CYP505X from *A. fumigatus* codon optimized for expression in *P. pastoris* in the vector pPpT4_S: *AOX1* promotor, CYP505 CDS: CYP505-hydroxylase coding DNA sequence, *AOX1* term: *AOX1* transcription terminator, *ILV5* promotor: eukaryotic promotor, *EM72* promotor: synthetic prokaryotic promotor, Zeocin CDS: Zeocin™ resistance gene, *AOD* term: *AOD* transcription terminator, pUC ORI: pUC origin of replication

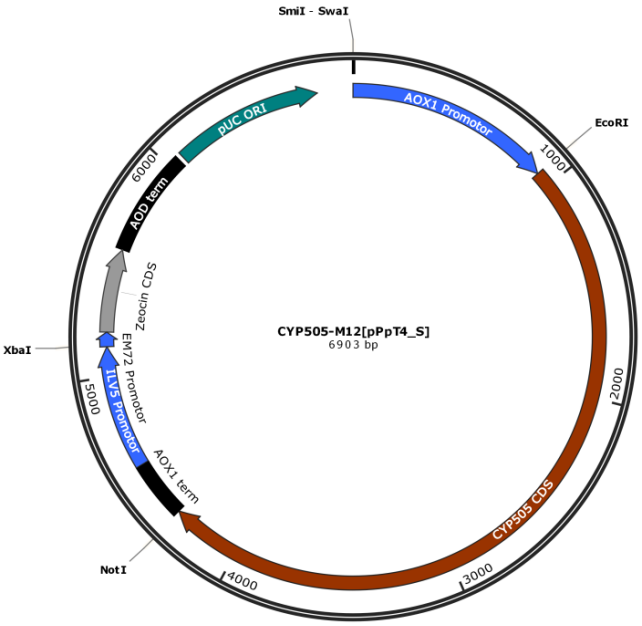

S 2: Gene CYP505A1 from *F. oxysporum* codon optimized for expression in *P. pastoris* in the vector pPpT4_S: *AOX1* promotor, CYP505A1 CDS: CYP505A1-hydroxylase coding DNA sequence, *AOX1* term: *AOX1* transcription terminator, *ILV5* promotor: eukaryotic promotor, *EM72* promotor: synthetic prokaryotic promotor, Zeocin CDS: Zeocin™ resistance gene *AOD* term: *AOD* transcription terminator, pUC ORI: pUC origin of replication

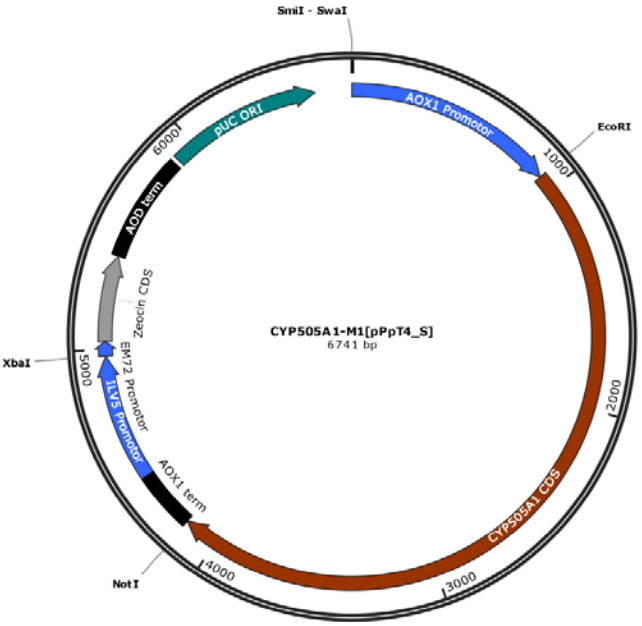

S 3: Illustration of a kinetic measurement of CYP505X variants expressed in *E. coli* BL21 or DH5α-T1 converting 7-benzyloxyreosrufin in a MTP. Formation of the fluorescent product was monitored over 15 minutes at 24°C on a SynergyMx plate reader (λex = 530nm, λem = 580nm). Column 1-11 are CYP505X M1-M11. Column 12 is CYP1536-M1. Lane 1-4 are CYP505X variants expressed in *E. coli* BL21. Lane 5-8 are CYP505X variants expressed in *E. coli* DH5α-T1.